

-64213-

**FABRICATION AND STUDY OF ZINC SULPHIDE
BASED ELECTROLUMINESCENT DEVICES**

M. K. JAYARAJ

THESIS SUBMITTED TO
COCHIN UNIVERSITY OF SCIENCE AND TECHNOLOGY
FOR THE AWARD OF THE DEGREE OF
DOCTOR OF PHILOSOPHY

DEPARTMENT OF PHYSICS
COCHIN UNIVERSITY OF SCIENCE AND TECHNOLOGY
COCHIN - 682 022

JUNE 1989

DEDICATED
To
MY PARENTS

DECLARATION

Certified that the work presented in this thesis is based on the original work done by me under the guidance of Prof. C.P. Girijavallabhan, in the Department of Physics, Cochin University of Science and Technology and has not been included in any thesis submitted previously for the award of any degree.



M.K. JAYARAJ

Cochin 682 022 ¶
June 20, 1989 ¶

CERTIFICATE

Certified that the work presented in this thesis is based on the original research done by Mr. M.K. Jayaraj, under my guidance in the Department of Physics, Cochin University of Science and Technology, and has not been included in any other thesis submitted previously for the award of any degree.



Dr. C.P. GIRIJAVALLABHAN
Professor of Physics
(Supervising Teacher)

Cochin 682 022 }
June 20, 1988 }
|

ACKNOWLEDGEMENTS

I wish to express my deep sense of gratitude to Professor Girjavallabhan for his able guidance, supervision and competent advice throughout the years of my research.

I am indebted to Professor Sathianandan, former Head of the Department of Physics, for his encouragement during the progress of this work.

I am thankful to Professor Krishna Pillai, former Head of the Department of Physics and Professor Babu Joseph for extending the facilities available in the Department.

I express my sincere thanks to all the research scholars of the Department of Physics, especially to Mr. Rajeev Kumar and Mr. Abraham for their wholehearted cooperation.

I would like to thank the University Grants Commission, New Delhi, for the award of a research fellowship which made this work possible.

Finally, I thank Mr. K.L. Joseph for neatly typing this manuscript.

M.K. JAYARAJ

PREFACE

Although the phenomenon of electroluminescence (EL) has been known for more than half a century, its utilization became a practical reality only after the development of conducting transparent electrode. Yellow emitting ZnS, still the best EL material known, is commonly used in flat panel displays which are now commercially available. The need for full colour devices has engaged the attention of scientists working in commercial, governmental as well as academic institutions and considerable efforts have been devoted in developing new efficient phosphor materials which can emit primary blue, green and red colours. This thesis contains the author's work in preparing efficient EL phosphors, the details of fabrication of low voltage operated thin film EL (TFEL) devices and DC TFEL devices, carried out in the past few years at the Physics Department of Cochin University of Science and Technology.

Some of the important work presented here are related to the white light emitting ZnS:Cu,Pr,Cl phosphor which can be colour tuned by changing the

excitation frequency, observation of energy transfer from Cu/Ag ions to rare earth ions in ZnS:(Cu/Ag), RE, Cl phosphors, development of TFEL device which can be operated below 50V, optimisation of the device parameters for long life, high brightness in terms of the active and insulating layer thicknesses, observation of dependence of threshold voltage for the onset of emission on frequency of excitation when a novel dielectric Eu_2O_3 film was used as insulator and the devices with multi-colour emission using ZnS doped with rare earth as active layer.

The results and observations, essentially based on the work carried out by the author are summarised in eight chapters. The reference to literature is made at the end of each chapter.

First chapter is the general introduction to the subject of electroluminescence with a comprehensive review of the phosphors together with a brief discussion of physical mechanism involved in electroluminescent process. A brief survey of different models to explain memory and non memory TFEL devices is also given.

Chapter two describes the experimental set up used for the various investigations. The phosphor preparation techniques are given in a detailed manner. The various measuring techniques used for recording EL spectra, brightness-voltage, brightness-frequency characteristics, recording of the brightness wave forms and measurement of brightness in absolute units are also outlined. This chapter also presents a concise description of various deposition techniques used for the fabrication of AC TFEL and DC TFEL devices.

The third chapter which is divided into two parts, is based on the preparation and characterisation of efficient EL powder phosphors using AC powder EL devices. Part A gives the details of preparation of white light emitting ZnS:Cu,Pr,Cl phosphor. The detailed investigation of Pr concentration dependence on EL emission spectra is presented. The frequency dependence of EL emission spectra of ZnS:Cu,Pr,Cl which makes it colour tunable by changing the excitation frequency is explained using Schön-Klasens model together with resonant energy transfer from Cu to Pr ions. The second part deals with the investigation of energy transfer from Cu/Ag ions to rare earth ions in ZnS doped rare earth phosphors.

Chapter IV presents the electrical conduction mechanisms, dielectric and optical properties of the insulator films used for TFEL devices. Detailed investigations of the dielectric properties of Eu_2O_3 films and its thickness, temperature and frequency dependence on dielectric constant and loss factor are given. This chapter also includes the dielectric studies of Sm_2O_3 , MgF_2 , CeO_2 , Na_3AlF_6 , BaTiO_3 and SiO insulator films. The Sm_2O_3 and Eu_2O_3 films are found to have large dielectric constant compared to other insulating material and these are found to be suitable for low voltage operated TFEL devices.

The fabrication of AC TFEL devices in MISIM and MIS structure using ZnS:Mn as active layer forms the subject of Chapter-V. This also demonstrates the frequency dependent threshold voltage for the onset of emission in the devices having MgF_2 and Eu_2O_3 as insulators, and this effect is explained on the basis of frequency dependent loss tangent of insulator materials. The optimisation of the device parameters for low voltage operation, high brightness and stability in terms of the insulator and active layer thickness are described.

The study on the effect of different insulators having different figure of merit on the EL emission brightness and on operating voltage shows that Sm_2O_3 and Eu_2O_3 films are best suited for low voltage operation. The study of aging of these devices is also presented.

Chapter-VI describes the fabrication of low voltage driven multicolour emitting AC TFEL devices using rare earth doped zinc sulphide (ZnS:RE) as active layers ($\text{RE} = \text{Pr, Nd, Sm, Eu, Tb, Dy, Er}$). The EL emission spectra and the probable transitions giving these emission are given here. The device with ZnS:TbCl_3 emitting blue green is found to be the most efficient one. The effect of halides on the EL emission spectra and B-V characteristics in the case of ZnS:Pr are also presented.

Chapter-VII deals with fabrication of DC powder EL cells using ZnS:Mn phosphor. The mechanism of EL emission and forming process are also described. In this chapter the fabrication of DC TFEL devices in $\text{SnO}_2\text{-ZnS-Cu}_x\text{S-ZnS:Mn-Al}$ structure is described in detail. The mechanism of light emission and forming process are explained to a certain extent from the electrical measurement data of these films. Characterisation of

other devices based on ZnS:Sm, ZnS:Pr, ZnS:Dy and their emission characteristics are also illustrated.

The concluding chapter gives the summary and evaluation of the investigations presented in the preceding chapters. The present status and the novel techniques adopted by the commercial and various R and D organisations are given in detail. The future possibilities of TFEL devices are also discussed in this chapter from an application point of view.

Part of the investigations presented in this thesis has been presented/published/communicated in the form of the following papers in Symposia/Journals:

- (1) "Spectral characteristics of EL emission from ZnS:Pr,Cl phosphor",
Proceedings of the National Conference on EOPS, March '87,
Paper 0016, Mithal Publications, Delhi.
- (2) "EL emission characteristics of $\text{SnO}_2\text{-ZnS-Cu}_x\text{S-ZnS:Mn-Al}$ structure thin film device", presented in the National Seminar on Crystallography, Changanachery, December 1987.
- (3) "Electroluminescence of ZnS:Cu,Tb,Cl, ZnS:Cu,Gd,Cl and ZnS:Cu,La,Cl phosphors", XVI OSI Symposium held at CGCRI, Calcutta 1988.

(4) "Observation of energy transfer from Cu and Ag centres to rare earth ions in ZnS(Cu/Ag), RE EL phosphors", National Seminar on Physics and applications of new materials, IACS, Calcutta 1988 Indian Journal of Physics 63A, 480 (1989)

(5) "AC electroluminescent thin film devices with ZnS:Dy,Cl and ZnS:Pr,Cl phosphors", National Conference on electrochemical materials science, CECRI, Karikudi, 1988. (Communicated to Bulletin of Electrochemistry).

(6) "Optical properties of vacuum evaporated Europium oxide films", National Conference on current trends in pure and applied physics, Department of Physics, CUSAT, 1988.

(7) "Red emitting low voltage-driven thin film electroluminescent devices", Proceedings of DAE Solid State Physics Symposium 1988, Bhopal University, 1988, p. 127.

- (8) " Dielectric properties of vacuum evaporated Europium oxide films", Proceedings of DAE Solid State Physics Symposium, Bhopal University, 1988, p.128.
- (9) " AC conductivity in Europium Oxide thin films", National Seminar on Crystallography, Banares Hindu University, Varanasi, 1988.
- (10) " Effect of Halides on the EL spectra and brightness of ZnS:Pr TEFL devices", National Seminar on Crystallography, Banares Hindu University, Varanasi, 1988.
- (11) " Thin film electroluminescent devices using ZnS:Tb,Cl and ZnS:Nd,Cl " IVS National Symposium 1988 on Vacuum Science and Technology, IIT, Bombay, December 1988, (Communicated to Bulletin of IVS).
- (12) " Dielectric and optical properties of Europium Oxide films", Thin Solid Films (In press).
- (13) " A study of white electroluminescence from ZnS:Cu,Pr,Cl Phosphors", Journal of Physics D: Applied Physics (In press).
- (14) " Low voltage driven ZnS:Mn thin film device with MIS structure", Communicated to Thin Solid Films.

CONTENTS

		Page No.
		--
Chapter I	ELECTROLUMINESCENCE - GENERAL INTRODUCTION	
	Abstract	.. 1
1.1	History	.. 2
1.2	Activators and coactivators	.. 5
1.3	Zinc sulphide and related phosphors	.. 6
1.4	Zinc sulphide: Rare earth systems	.. 10
1.5	Mechanism of EL	.. 12
1.6	Intrinsic EL	.. 13
1.7	Acceleration of charge carriers to optical energies	.. 15
1.8	Collision excitation	.. 19
1.9	Sensitized luminescence	.. 20
1.10	Operating characteristics of powder EL cells	.. 24
1.11	Injection EL	.. 29
1.12	AC thin film electroluminescent devices	.. 35
1.13	Device Physics (Non memory)	.. 38
1.14	Device Physics (Memory)	.. 39
1.15	Summary	.. 45
	References	.. 46
Chapter II	EXPERIMENTAL SETUP	
	Abstract	.. 53
2.1	Introduction	.. 54
2.2	Phosphor preparation	.. 55

Cont'd.

2.3	Vacuum furnace	..	56
2.4	AC powder EL cells	..	57
2.5	Setup for recording the EL spectra	..	61
2.6	Voltage brightness measurements	..	63
2.7	Brightness measurements in absolute units	..	64
2.8	DC powder EL cells	..	69
2.9	Requirements for fabrication of thin film EL devices	..	72
2.10	Vacuum systems for deposition of insulators: active layers and electrodes	..	78
2.11	Spray pyrolysis for conducting transparent electrodes	..	83
2.12	DC TFEL devices	..	87
	References	..	90
Chapter III	EL EMISSION CHARACTERISTICS OF ZnS:RE,Cl; ZnS:Cu,RE,Cl and ZnS:Ag,RE,Cl PHOSPHORS		
	Abstract	..	96
Part-A			
3.1	Introduction	..	97
3.2	Sample preparation	..	102
3.3	Experimental	..	103
3.4	Results	..	103
3.5	Discussion	..	106
Part-B			
3.6	Emission characteristics of ZnS:RE,Cl and ZnS:(Cu/Ag), RE,Cl phosphors	..	119
3.7	Results for ZnS:(Cu/Ag)RE,Cl phosphors	..	120
3.8	Discussion	..	126
	References	..	132

Cont'd.

Chapter IV	ELECTRICAL AND OPTICAL PROPERTIES OF INSULATOR FILMS USED IN THE TFEL DEVICES	
	Abstract	.. 135
4.1	Introduction	.. 136
4.2	Dielectric properties of Eu_2O_3 films	.. 138
4.3	Electrical properties	.. 152
4.4	Optical properties	.. 157
4.5	Dielectric properties of Sm_2O_3 films	.. 167
4.6	Dielectric properties of MgF_2 , CeO_2 , SiO_2 , Na_3AlF_6 and BaTiO_3	.. 173
	References	.. 178
Chapter V	AC THIN FILM EL DEVICE WITH ZnS:Mn ACTIVE LAYER	
	Abstract	.. 181
5.1	Introduction	.. 182
5.2	Fabrication of MISIM and MIS structure devices	.. 184
5.3	Frequency dependent threshold voltage of the devices	.. 188
5.4	Optimisation of device parameters	.. 192
5.5	Devices with insulators having different figure of merit	.. 198
5.6	Aging effects of TFEL devices	.. 207
	References	.. 212

Cont'd.

Chapter VI	MULTICOLOUR EMITTING ZnS:RE TFEL DEVICES	
	Abstract	.. 215
6.1	Introduction	.. 216
6.2	Device fabrication	.. 218
6.3	EL emission characteristics of the devices	.. 221
6.4	Brightness voltage characteristics	.. 230
6.5	Effect of halides on the emission spectra and brightness of ZnS:Pr TFEL devices	.. 233
	References	.. 240
Chapter VII	DC POWDER AND THIN FILM ELECTROLUMINESCENT DEVICES	
	Abstract	.. 243
7.1	Introduction	.. 244
7.2	DC powder EL cell fabrication	.. 246
7.3	Fabrication of ZnS:Cu,Mn PEL cells	.. 247
7.4	DC thin film electroluminescence	.. 257
7.5	Fabrication of ZnS:Mn,Cu,Cl DC TFEL devices	.. 258
7.6	DC electroluminescence in rare earth doped ZnS films	.. 268
	References	.. 273
Chapter VIII	CONCLUDING REMARKS	
	Abstract	.. 276
8.1	Summary of the work	.. 277
8.2	Present status of thin film EL devices	.. 279
8.3	EL Flat panel: applications	.. 286
8.4	Future possibilities	.. 288
	References	.. 290

Chapter-I

ELECTROLUMINESCENCE: GENERAL INTRODUCTION

Abstract

The field of electroluminescence is so vast and old making it difficult to give an exhaustive review, but a general introduction to the subject is presented in this chapter which gives the important developments and past discoveries which have taken place in this field. A concise review on the subject of EL giving special importance to high field EL is presented. The importance of ZnS based phosphor system, and the role of various activators and coactivators used for EL material preparation are discussed. A brief description of the basic phenomenon, and the mechanism of EL and energy transfer which help one to understand the physics behind the light emission is given. This is followed by comprehensive report on the ACTFEL devices along with essential physics of memory and non memory electroluminescent devices.

1.1 History

The phenomenon called luminescence in which light emission occurs from materials, was known to man for a long time. Probably the first observed luminescence phenomenon might have been bio-luminescence from fire flies and glow worms. The search for methods to produce luminescence by artificial means continued and a series of discoveries in basic sciences led to the understanding that a substance can be made to emit visible radiation in a multitude of ways. To mention a few, the emission of visible light from a substance can be produced by application of high energy radiation, pressure, heat, chemicals etc. Electroluminescence(EL), as the term indicates, involves the excitation of luminescence as a result of an applied electric potential difference in the phosphor material. The excitation, by an applied voltage, of light emission from silicon carbide crystals was first reported by Lossev [1] in 1923, though light appearing at one of the electrodes in an electrolytic solution, commonly called as galvanoluminescence, was known as early as 1898 [2]. In some cases such emission is undoubtedly electroluminescence resulting from fields produced across a poorly conducting film on the electrode. Lossev's observation was the first report on electroluminescence clearly indicating that emission is due to the

applied potential difference. Since then extensive research has been carried out by various workers [2]. It is worth enough to mention the name of G. Destriau who discovered EL emission from ZnS:Cu [13] which is the most important material even today. Though the field of electroluminescence is so old and so vast it took more than half a century for an EL flat panel display to become a reality. This itself is indicative of the complexities involved in the development of practical EL system. Despite these facts, the continued advances in materials and techniques in this field have led to the development of EL systems for specific application such as light sources, digital indicators, display devices, image amplifiers, etc. EL display devices can serve as the information linkage between complex electronic systems and their human users.

The EL phenomenon has been observed in a large number of materials especially in III-V and II-VI compound semiconductors. The efficiency of light production in most cases, however is very low compared to that of ZnS. The continued attempts to improve the performance and efficiency of EL devices have resulted in a large number of EL materials and new configurations for EL devices.

The III-V compound semiconductors are usually known as LED materials since they are widely used in the fabrication of light emitting diodes (LED) in which emission is due to the recombination of the injected minority carriers across a p-n junction. These display elements are commonly used in visual alpha-numeric information displays in many hand held and desk electronic calculators, as indicators in a wide variety of electronic instruments, as light modulators, optocouplers, etc. LED with emission near infrared (IR) region are used in fibre optic communication system [3,4]. The LED displays are not quite suitable for large area displays due to their high cost and much higher current density required for their excitation. Even the best device requires a current density of 0.25 mA/cm^2 [5]. This will need bulky excitation source making battery operation quite difficult.

The increasing need and range of applications of electronic systems and their man to machine interface have led to vigorous research for possible technologies for different kinds of panel displays namely, plasma, liquid crystal, gas-electron phosphor, flat CRTs and electroluminescent devices. Though each device has its own merits and demerits, EL displays appear to be a promising candidate in this context.

1.2 Activators and coactivators

Luminescent crystals usually exhibit broad, structureless, excitation bands near fundamental absorption edge and bell shaped, structureless emission bands at longer wavelengths. The excitation and emission bands are generally attributed to transitions between stages of an impurity system. Such a system is called an activator. In other words activators are certain acceptor type impurities introduced into the pure host crystal lattice to produce luminescence. There are numerous activators that cause luminescence in these materials as well as certain defect centers which can serve as if they were activators. Some of the common and most effective activators used in II-VI phosphors are copper, silver, aluminium, manganese and various lanthanides. A number of these, copper and silver in particular, can occupy various sites in crystalline lattice, thereby giving different emission colours and efficiencies. But for many activator elements to operate properly it is necessary to incorporate additional donor impurity usually called the coactivator. For example, the solubility of many activator elements except manganese, in the ZnS lattice is usually limited unless another element ie. coactivator is introduced at the same time. The coactivator

in the phosphors may be required to ensure physical incorporation of the activator or to create energy levels within the phosphor or band structures which helps the luminescence. In many of the ZnS phosphors with rare earth activator, coactivation with copper ensures both the functions of incorporation of activator and creation of energy levels in the band gap. Copper accomplishes this by performing two distinct functions viz., charge compensation and sensitization. The charge imbalance caused when a tripositive ion is substituted for a zinc ion must be compensated by adding a monovalent ion such as Cu^+ to the lattice. This is known as the charge compensation. Such a situation also arises when monovalent copper is present as an activator which can be compensated by a negative monovalent coactivator such as the halides, typically chlorine, bromine or iodine. Sensitization involves the presence of energy levels within the crystal which transfer excitation energy to certain activators [6,7]. This aspect is dealt in detail in the forthcoming section.

1.3 Zinc Sulphide and related phosphors

For many years wide band gap II-VI compounds of the Zn and Cd chalcogenides have been of great

interest to the scientific community as potential visible LED material since they possess excellent luminescent properties and have bandgaps which range throughout the visible spectrum into the near ultraviolet. These materials can also be produced in the form of mixed-crystal (alloy) combinations such as CdTe-ZnTe, ZnTe-ZnSe, ZnSe-ZnS and ZnS-CdS in varying proportions to achieve a continuous luminescence spectrum in the visible range. Further more, these are direct band gap materials and therefore, an efficient radiative recombination can be achieved in a straight forward manner.

However, in the past, much of this potential has not been realized due to the difficulty in achieving low resistivity amphoteric doping (p-n junctions) required for efficient carrier injection which in turn, causes efficient radiative recombination. One scheme [8] that has been proposed to overcome this difficulty is by introducing a wide band gap insulator between metal contact and the luminescent material which is a near-insulator like material.

In the 1950s and early 1960s several thousand papers in the field of EL were published [9]. These deal principally with panels based on powder ZnS and

related compounds with few exceptions. The work during these period has been reviewed and assessed by several books and articles [2, 9-12]. These studies suggested that EL panels of low power requirements can be developed with II-VI compound semiconductors. The first and most efficient EL material of this group is ZnS. Electroluminescence in ZnS was discovered by Destriau [13] in 1936. Compounds belonging to this class are comparatively less expensive and have good conversion efficiency. For example, Lehmann [14] in 1958 has prepared and optimised ZnS EL device activated with copper and chlorine (ZnS:Cu,Cl) which has an efficiency of 4.5×10^{-2} compared to the value of 1.7×10^{-1} of a 40W fluorescent white lamp which was the most efficient visible light source available. Though the defect chemistry and physical properties of narrow and medium band gap covalent semiconductors are relatively well known, this cannot be said of wide band gap semiconductors such as ZnS which tend to host various type of recombination centers creating energy levels within their band gaps. The efficiency of luminescence in such phosphors is determined by the nature of the band structure and various kinetic processes that occur at these centers. These centers interact and each type of centers plays a significant role in determining the overall efficiency and emission characteristics of luminescent materials.

Hence for all materials, in particular II-VI group of compounds the procedure adopted for preparation of the phosphors and the nature and amount of the additives called activators which create these centers are of great significance [6].

ZnS:Cu,Cl phosphor is the most extensively studied phosphor. With an activator such as Cu in ZnS, however, the situation is far from simple. Depending upon conditions of preparation and on the concentration of activator and coactivators it is found that this phosphor can emit blue, green or red or its combinations [15, 16, 17]. In addition, in some cases IR emission at 1.5 and 1.7 μm is observed [18]. There is also a very strong dependence of the emission colour on the excitation frequency and temperature. And it is not at all certain whether these two emission bands are due to two copper levels or due to the modification of the energy levels of sulphur ions located nearest to the copper ions, because of the difference in ionic charge associated with zinc or copper ion [2], although many models have been advanced to explain the occurrence of such a variety of emission bands arising from a single activator impurity [18-21].

At present in ZnS, the activator of practical importance, other than copper, is manganese. ZnS:Mn

has an yellow orange emission. Eventhough this is the one of the earliest EL phosphor system a complete picture of the physical phenomenon involved in the emission process is not yet well understood. Recently Skolnick et al. [74] have made an attempt to study the light emission mechanism with the aid of the time resolved spectroscopic approach and obtained evidence for the hot carrier impact excitation process in its EL emission. The ZnS:Mn devices have highest brightness and have emerged as practical EL systems. But the need for multi-colour display have led to the active search and interest in rare earth doped ZnS devices [22] as rare earth has got emission lines in the entire visible region. In this class ZnS:TbF₃ [23] is the most efficient one which gives a green emission colour.

1.4 Zinc Sulphide: Rare earth systems

A world wide interest exists in the development of multicolour thin film electroluminescent devices. The potential of the rare earth ions to provide the three basic colours (blue, green, red) needed in a full colour device has led to intensive study of the doping of II-VI compounds with rare earths during the past few years [24].

The EL studies on rare earth doped zinc sulphide began in the late 1960s and several colours typical for the rare earths were obtained from ZnS:RE F₃ thin films [25]. The rare earth ions were introduced into the ZnS lattice by various methods

- (i) by preparing RE³⁺ doped ZnS powder.
- (ii) by evaporating rare earth compounds together with ZnS.
- (iii) by evaporating rare earth metals with ZnS.
- (iv) by rf sputtering of sintered pellets containing ZnS and rare earth compound, and
- (v) by epitaxial growth of ZnS and sublimating rare earth chelates [26,27,28].

The most common method is electron beam evaporation of sintered mixed pellets.

The EL properties of the most trivalent lanthanides (Ce,Pr,Nd,Sm,Eu,Tb,Dy,Ho,Er,Tm) have now been characterised [22,25,29]. The work during the seventies was mostly basic research on topics such as the means of introducing of RE³⁺ into ZnS, excitation and electron injection mechanisms in ZnS:RE³⁺ and

relationship between brightness and doping level. The studies made by the author in ZnS:RE³⁺ phosphors and the resonant energy transfer mechanism are described in Chapter III. The multicolour devices produced with ZnS:RE thin film are also described in Chapter IV.

Kingsley et al. has observed that rare earth fluorescence can be efficiently excited by resonant energy transfer from copper and silver in ZnS, CdS and ZnSe [30]. Numerous reports on this aspect of the excitation of rare earth by resonant energy transfer from metal impurity, have appeared in literature[31-34].

1.5 Mechanism of EL

In order to convert the electrical energy from an applied potential difference in a crystal at ordinary temperatures into visible or near visible radiation, three distinct steps are involved:

(i) Excitation of crystals by the applied electric field to an energy state at least few electron volts above the ground state. The excited state can be an ordinary conduction state of the crystal, an excited state of an impurity system or a state of high kinetic energy within the conduction or valence band. The excitation process may be by means of injection of

minority carriers, valence electrons from field ionization of host atoms or impurities, or acceleration of charge carriers within a band to optical energies.

(ii) Transfer of the excitation energy through the crystals to a region where de-excitation can occur with large probability for radiative transition. The energy transport can be by charge carriers, excitation migration or by resonance transfer.

(iii) Radiative-de-excitation thus involves localized states of impurity systems, inter band transition or intraband transitions [35].

Various combination of these excitation, energy transport and emission processes can occur in actual crystals [36]. Depending upon the carrier generation process EL can be classified into two types (1) intrinsic EL and (2) injection EL.

1.6 Intrinsic EL

Electroluminescence of various crystalline phosphors and their mechanisms have been reported in the literature [18,36-38]. High field EL devices based on II-VI semiconducting compounds generally fall in intrinsic EL and Curie [18] has suggested a three step

process for such an EL emission. (1) Raising of electrons from donor levels for acceleration to the conduction band, (2) Acceleration of some of these electrons in the conduction band by the field and subsequent carrier multiplication or an avalanche effect, (3) Collision of these electrons with luminescent centers causing the excitation or ionization or with the basic crystal lattice itself followed by the production of electron hole pairs. Finally, the radiative or non-radiative transition or recombination of electrons takes place. The quantitative treatment of Piper and Williams differs from that of Curie and considers that the initial production of carriers can influence the EL emission. They have also assumed that the phosphor possesses deep donor levels lying perhaps ~ 0.5 eV below conduction band.

According to Frenkel [18] the field and the phonons mutually assist each other in producing ionization of the levels in the following way. If the depth of the level is ϵ in the absence of the field P the probability of ionization per second is

$$P = S \exp(-\epsilon/kT) \quad 1.1$$

where S is constant.

P is very small if ϵ is large. In the presence of the field E the depth is reduced to

$$\epsilon^* = \epsilon - f(E) \quad 1.2$$

and the probability of ionization becomes,

$$P = S \exp \left(- \frac{\epsilon - f(E)}{kT} \right) \quad 1.3$$

where $f(E)$ is the apparent change in trap depth due to the applied field. During the first few cycles of the applied field on the cell the brightness is very low. Gradually the electrons fall into the traps which at the beginning are empty, and the ionization of the latter by the same process as above soon plays a dominant role in supplying the electrons to the conduction band. This will naturally produce a buildup in the EL emission which is actually observed [33].

1.7 Acceleration of Charge Carriers to Optical Energies

The acceleration of charge carriers to optical energies can only be achieved by satisfying the following conditions. High fields capable of accelerating charge carriers to large kinetic energies must be produced and electrons or holes must be injected or

created in the high field region. The conduction electrons experience an accelerating force as a result of the field and retarding force resulting from interaction with the vibrational modes of the crystal lattice. When the applied field is strong the conduction electron which experience unusually few collisions with lattice phonons will attain sufficient energy to ionize impurities or valence electrons. A typical value of field intensity is $\sim 10^5$ V/cm. At a much higher field ($\sim 10^6$ V/cm) average conduction electrons acquire energy from the field faster than the rate at which energy is lost to the lattice phonons and will thereby attain sufficient energy to collision-ionize impurities or valence electrons. This may also lead to the condition for dielectric breakdown [35].

In facilitating the acceleration mechanism of excitation of electroluminescence, the catastrophic consequences of dielectric breakdown can be avoided by an inhomogeneous field distribution in the crystal. In other words, since this mechanism operates at field strengths approaching or equalling the field strength responsible for dielectric breakdown, field configurations yielding stability against breakdown are necessary. A narrow high-field region in series with an extensive low field region permits operation over a broad range

of applied voltages without creation of an unstable breakdown. A crystal which is partially stable against dielectric breakdown is one having nonlinear characteristics such that the width of the high field region as well as the magnitude of the field, increases with applied voltage.

Several types of barriers are feasible, each type having different characteristics for EL excitation by the carrier acceleration mechanism. The acceleration of charge carriers in EL phosphor occurs at Mott-Schottky exhaustion type barrier, as shown in Fig. 1. 1 which arises from the ionization of shallow donor levels [40, 41]. The concentration of deep donor is assumed to be much less than that of shallow donors so that the latter one alone determines the potential distribution in the barrier region. Most of the applied potential will appear across the barrier and hence a moderate applied electric field in the barrier region will be sufficient to produce ionization of these deep donors and subsequent acceleration and collision excitation can lead to luminescence. According to Zalm et al. [42] the donors responsible for positive space charge barriers are the ionized activator centers themselves and that the initial electrons are supplied by a surface layer of Cu_2S .

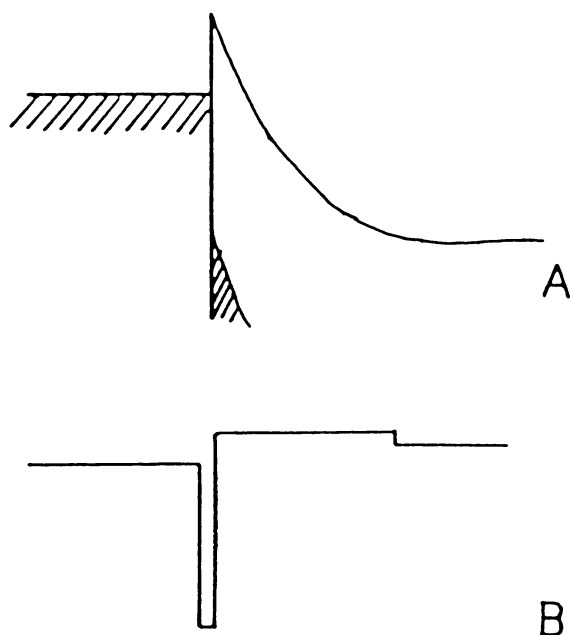


Fig.1.1. Mott-Schottky exhaustion layer
 (A) Potential configuration
 (B) Distribution of electrostatic charge density.

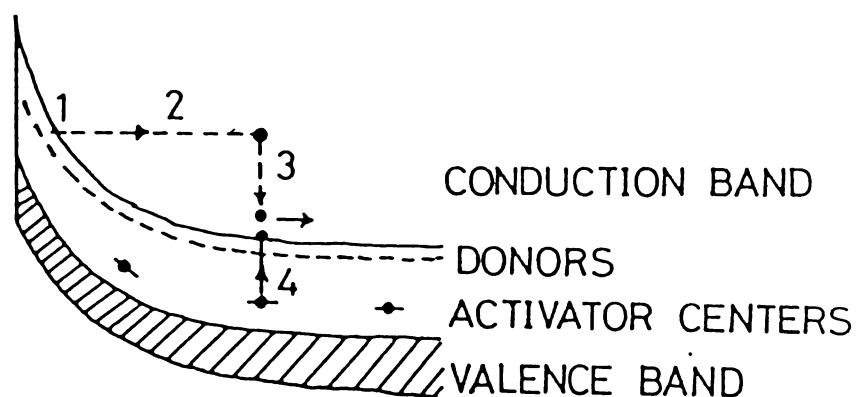


Fig.1.2. Schematic representation of acceleration collision mechanism of electroluminescence. Electron from traps in the localized high field region are liberated by the action of the field (1) or injected from a contact and then accelerated by the field (2) to acquire kinetic energy above the bottom of conduction band and collide with activator centres whereby they lose their energy (3) and the activator centre is ionised (4) or excited.

An intrinsic layer is another suitable type of barrier. This barrier remains constant in thickness with applied voltage, and the field which is independent of position in the barrier, varies linearly with applied voltage.

An additional possibility is p-n junction biased in the reverse direction. An idealized example is a junction in which the difference of donor and acceptor concentrations varies linearly with distance. With increasing applied voltage, the exhaustion region increases in width, and in this example, the field strength varies as two-thirds power of the applied voltage [35].

1.8 Collision excitation

The energy of accelerated electron in the band or hole in the valence band may create an electron-hole pair or to excite a localized impurity system by an inelastic collision (Fig. 1. 2) and further electrons are released from the centers to the conduction band. Both categories of electrons after impact possess some residual motion along the acceleration field direction and will be in the state they were before getting accelerated.

The other modes of energy transfer relevant to EL emission are the migration of minority charge carriers, exciton and resonance energy transfer processes [35].

1.9 Sensitized luminescence

The presence of more than one activator in a crystal affects the emission characteristics of the system due to interaction between the activator ions. The absorption spectra will be simple superposition of that of individual ions whereas the emission spectra may be superposition individual emission spectra, but other effects can also take place such as the following: (a) the luminescence spectral intensity of one ion can gain in strength at the expense of the other. (b) An ion not luminescent at a given concentration in a given crystal becomes luminescent in the presence of another ion when introduced in a different crystal. (c) If luminescence is not observed for an ion at a particular frequency it may be excited by introducing another ion having a strong absorption for that particular excitation. (d) In some cases the luminescence of one ion is intensified with complete quenching of the other.

These changes in luminescence of one ion in the presence of another are due to transfer of activation energy from one to another [18, 43]. Luminescence

of ions excited as a result of the energy transfer from another ion excited in the absorption band is termed as sensitised luminescence. In this phenomenon of sensitised luminescence, the energy absorbed in the absorption band of one ion can be re-emitted in the emission band of other ion. The transfer of energy from sensitizer to activator can happen by the following mechanisms, viz., (1) emission-reabsorption, (2) resonance radiationless energy transfer, and (3) non-resonance radiationless energy transfer.

The emission-reabsorption type of the energy transfer (Cascade luminescence) implies the emission of light by single ion called primary luminescence and its absorption and emission by other ion which is known as secondary luminescence. Both ions behave as independent systems and do not interact directly. The spectral distribution of the primary emission must overlap significantly with absorption spectrum of the secondary emitting ion. The strength of absorption band associated with the secondary emitting centers must have an appreciable intensity.

The resonance radiationless mechanism of the energy transfer is that there should be a coincidence or a close match between energy level pairs of the ion

sensitizer and the ion activator. An essential difference is that the transition in the level of sensitiser is not necessarily emissive, whereas the activator absorption corresponding to the pair of levels close to the first one may be of very low intensity. Then the emission of the activator does not necessarily occur as a result of transition between the pair of levels to which the energy of sensitiser is transferred.

In the above process energy transfer mostly results from dipole-dipole or dipole-quadrupole interaction between ions and the energy transfer probability depends on the type of interaction. With dipole-dipole interaction the probability of transfer is proportional to r^{-6} (where r is the mean distance between interacting ions, which, in this case should not exceed 30 \AA) and dipole-quadrupole interaction to r^{-8} (r not more than $10-12 \text{ \AA}$). Hence the process of luminescence is of an additive nature, and a reduced duration and decreased quantum yield of the luminescence of the sensitizer (partial or complete quenching) are compensated by a longer duration and greater quantum yield of the activator luminescence.

With interaction of ions the intensity of the entire luminescence spectrum of the sensitizer

decreases. Because of short critical distance between the sensitizer and the activator ions, the effectiveness of the sensitization does not depend either on the size or the shape of the samples.

The non resonance radiationless mechanism leads to the transfer of energy between the ions in the event of substantial non-concurrence of difference between the levels of an ion transferring the energy (upper) and the levels of an ion receiving energy (lower). The difference between these energies goes either to the lattice in the form of phonon or to a third ion which has a pair of levels supplementing the difference.

Among these, the resonant radiationless energy transfer mechanism is the most prevalent one. This type of sensitized luminescence involving such a process can be used to excite luminescent centers in crystals and phosphors which are, otherwise not possible to be excited directly at a particular excitation frequency. This technique is widely used to excite RE^{3+} doped laser crystals where the luminescent ions contain weak narrow absorption lines associated with the forbidden f-f transition. This is achieved by adding another RE^{3+} impurity ion which has an absorption at the excitation wavelength giving

rise to resonance excitation of the transition of interest.

1.10 Operating characteristics of Powder EL cells

1.10.1 Brightness-voltage characteristics

The brightness of a powder cell increases non linearly as excitation voltage is raised. If this characteristic is plotted on a log-log graph, the slope varies between 2 and 8. The same type of behaviour was reported for individual phosphor grains [42]. It is also known that depending on the type of barriers involved, the nature of field producing the acceleration of the carriers varies considerably. This causes variations in the number of carriers generated to produce luminescence and hence the brightness to vary with the type of barrier. In other words we can have an idea about the type of potential barrier involved in the process by studying the average brightness-voltage characteristics. Several analytic forms have been proposed to fit these data [42, 44-46]. Destriau has obtained an empirical relation which relates brightness (B) and applied voltage (V) as

$$B = B_0 \exp (-b/V) \quad 1.4$$

where B_0 and b are constants. This relation was later

modified by him to account the slight curvature of log B vs $1/V$ plot and wrote

$$B = B_0 V^n \exp (-b/V) \quad 1.5$$

The value n is found to depend on the phosphor used [41].

Alternate form of empirical relations were proposed by other workers [42,45]. Here the brightness follows the relation

$$B = B_0 \exp (-(V_0/V)^{\frac{1}{2}}) \quad 1.6$$

where B_0 and V_0 are parameters which depend on temperature and frequency of the alternating voltage, phosphor type and on details of construction of the test cell. The presence of square root of the voltage is normally explained on the basis of an electron acceleration mechanism together with the fact that the maximum field strength in a Mott-Schottky barrier varies as $V^{1/2}$. At very low voltages the brightness may vary as the 9th or 10th power of the applied voltage. At voltage approaching breakdown of the layer the dependence approximates V^2 or an even lower power of V and in some cases it is even less than unity. The phosphor contains particles of different sizes. For a given voltage the field experienced by each particle will be

different and hence the observed results will be only the average [47].

1.10.2 Effects of frequency and temperature.

ZnS:Cu phosphors generally show a shift in emission colour as frequency of the alternating exciting voltage is varied. This change is caused by excitation of the blue and green bands and their different combinations. Similar colour shift were also observed in (Zn,Cd,Hg)S:Cu phosphors. A simple explanation of such colour shifts has been given by Zalam et al. [48]. Lambe and Klick [81] has suggested another model which may be considered as the inverse case of Schön-Klasens model.

The interrelation between frequency and temperature in electroluminescence is a fundamental one. The release of electrons from traps or of holes from luminescence centers depends both on temperature and time. This necessitates consideration of the effects of both variables simultaneously and it has been shown that any combination of f and T which satisfies the relation [45,49,50]

$$f = C \exp (-E/kT)$$

produces essentially the same conditions in the phosphor; high frequency is equivalent to low temperature and therefore can be counteracted by increasing the temperature. The fact that the emission colour may change with changes in either variables viz., temperature or frequency.

1.10.3 Time dependence

There are different types of variation with time which are both of practical and fundamental interest in electroluminescence. These are: (1) The variation of output with time after application of voltage to a previously unexcited phosphor known as buildup processes, (2) variation output after removal of voltage, (3) dependence of brightness of emission with time during one cycle of the applied alternating voltage which is known as brightness waves.

Generally it is observed that for a sine wave excitation there exist two light peaks (known as brightness waves) per cycle of the applied voltage. The two peaks have different amplitudes [41]. Various workers have observed a phase shift between the brightness peak and the voltage maxima. Destriau [41] has attributed it to the phase shift of the field in the dielectric medium surrounding the phosphor particles. But

Zalam [42] has attributed it to the delayed recombination of the accelerated electrons. There occurs a secondary peak for green or blue emitting ZnS:Cu phosphors. The minor peaks are often not well resolved and occur near (and usually before) the instant the applied voltage passes through zero. The detailed characteristics of these peaks were studied by Destriau [51], Thornton [2] and Zalm [52].

Thornton [49] and later Georgobiani and Fok [53] assumed that the brightness wave is a kind of field controlled glow curve since the rate determining factor is the field controlled thermal release of trapped electrons. Thornton developed a model based on reduction of the trap depth by the field. This mechanism facilitated return of the electron to the excitation region, and hence an earlier primary peak, for high voltage and low frequency as well as for high temperature. Since it is known that trapping of charge carriers plays an important role in the temperature dependence of integrated output; secondary waves, EL build up etc., one can expect its effects on brightness frequency characteristics also. This is because of some sort of matching (or mismatching) between field frequency and trapping time which can effect release of electrons from traps and hence brightness.

1.11 Injection EL

1.11.1 p-n junction

In electroluminescence, the excitation is provided by supplying either potential or kinetic energy or both to free carriers. A forward bias at a p-n junction or electrode contact or at some other barrier gives an electron the necessary potential energy. All the commercially available LED's operate on the principle of forward biased p-n junction. At such a junction in the absence of an applied voltage there is a state of dynamic equilibrium between the process of thermal production and subsequent recombination of electron hole pairs. Some of the recombinations occur with the emission radiation, which contributes to normal thermal radiation of the material. When a voltage is applied in the forward direction and additional carriers are injected, however, this equilibrium is upset and the rate of recombination increased (Fig. 1.3). If some of these recombinations occur with the emission of radiation the result may be called injection electroluminescence [3, 54].

1.11.2 Heterojunction

Heterojunction is the generic name given to

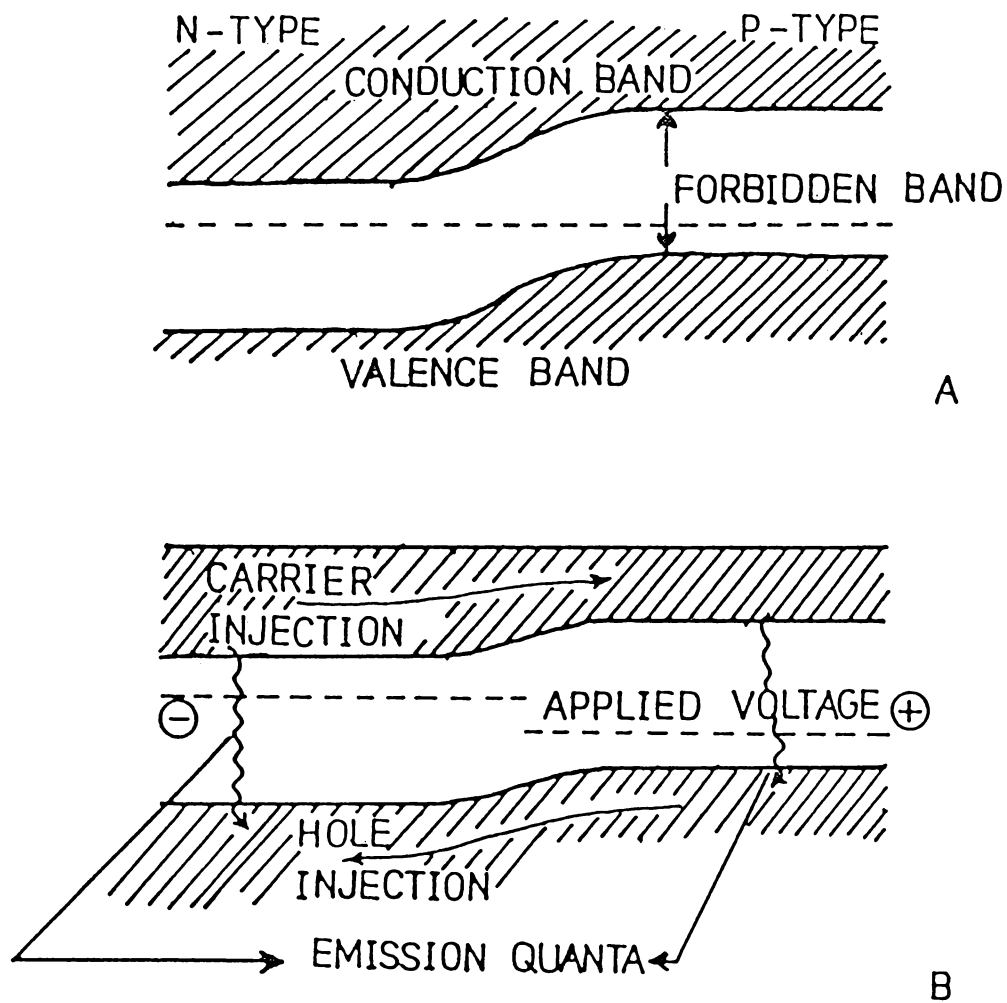


Fig.1.3. Energy level diagram for a p-n junction in the absence of an applied field (A) and for current flow in the forward direction with consequent injection of minority charge carriers (B)

the interface between two dissimilar materials. In the field of EL devices heterojunctions are currently being investigated as a means of making efficient large area emitters in materials which are poor amphoteric semiconductors. One can make use of a heterojunction (Fig. 1.4) to control as to which carrier is injected into the luminescent material. The source of injected carriers is a material having a wider gap than that of luminescent region. Then the asymmetry of the barriers seen by electrons and holes assures a high injection efficiency from the wider gap to the narrower gap layer [55, 56]. Although heterojunctions can be made between very different materials, the most successful devices are those made from different compositions of miscible alloys having similar lattice constants at fabrication temperature. $\text{Al}_{1-x}\text{Ga}_x\text{As}$ with two different values of x on either side of the junction is commonly used in LED's and diode layers [57].

1.11.3 Schottky barrier

When the surface of semiconductor is in contact with a metal there occurs a Schottky barrier which can act as p-n junction. Whenever surface states induce an inversion layer the surface has the opposite conductivity type compared with bulk. This is equivalent to

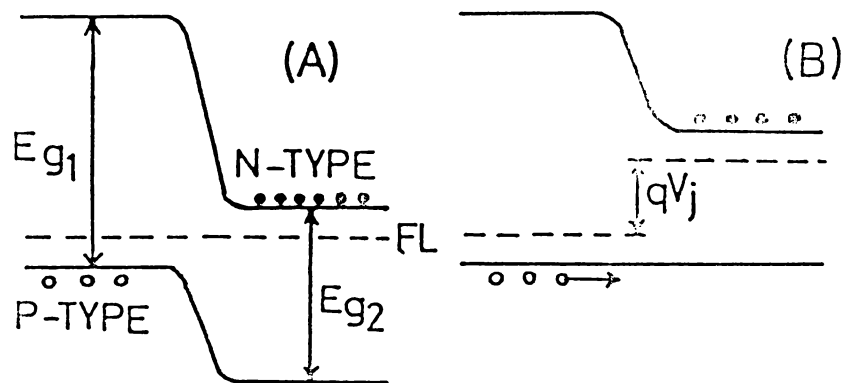


Fig.1.4. Diagram of heterojunction (A) at equilibrium (B) with a forward bias V_j .

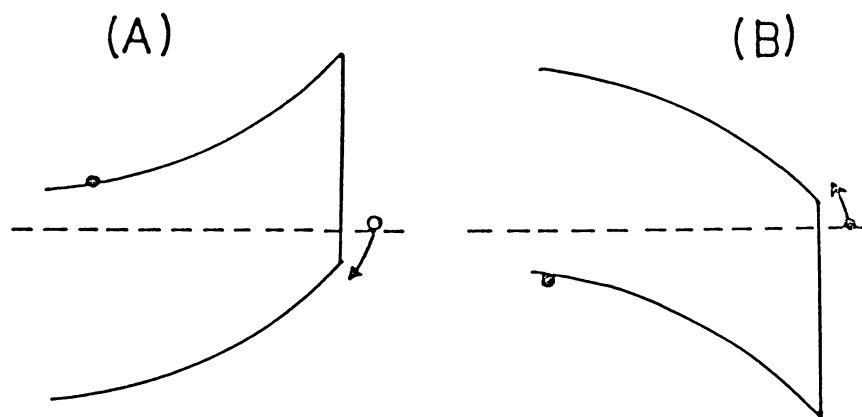


Fig.1.5. Diagram of Schottky barriers to n-type (A) and p-type (B) material. The arrows show the minority carrier injection during forward bias.

p-n junction immediately below the surface (Fig. 1.5). A forward bias tends to flatten the bands allowing the injection of minority carriers into the bulk. The minority carriers can then recombine radiatively just as they would in a p-n junction.

1.11.4 MIS Structure

When surface charges are insufficient to induce the desired inversion layer, one can induce surface charges by a capacitive coupling to the surface through an insulator. In a metal-insulator-semiconductor (MIS) structure, the surface charge on the semiconductor is determined by potential applied to the metal [54]. An immediate benefit of the MIS structure is that the band bending can be controlled by the applied voltage. Thus, an inversion layer can be induced by one polarity, then the carriers accumulated at the surface can be injected by reversing the polarity of the metal electrode (Fig. 1.6). This method has been used to obtain electroluminescence in GaAs without p-n junction [58]. When the insulator is made very thin (less than about 100 \AA), electrons can tunnel across the insulator [59].

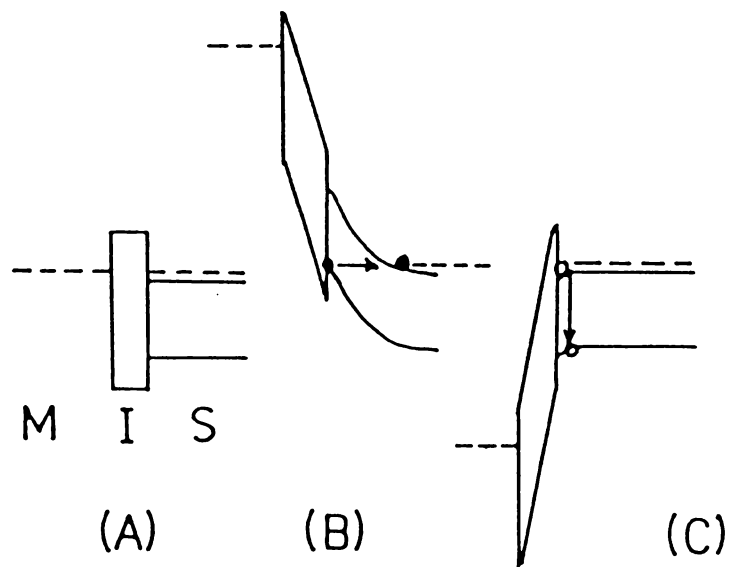


Fig.1.6. Band structure at MIS junction
(A) without bias (B) metal negatively biased for hole generation (C) metal positively biased for recombination.

Once the minority carriers are injected, a variety of recombination mechanisms are possible. Some of them, such as multiphoton emission, Auger effect and non-radiative trapping defects, etc. do not contribute to luminescence and thus contribute to low efficiency.

One of the most successful EL device is ZnS:Mn AC thin film EL device. These devices are essentially equivalent to two MIS structures in series.

1.12 AC Thin film electroluminescent devices

The study of electroluminescence in thin films dates back to many decades, and the striking nonlinearity of the phenomenon was emphasized by Halsted and Koller even in 1954 [60]. The importance of this nonlinear behaviour in B-V characteristics for application in information display was discussed by Thronton [61]. The principal drawback of thin film electroluminescent devices for practical application was their susceptibility to ageing and, more important, to catastrophic failure. Aging here refers to a simple loss of light output with time at constant voltage. It was soon realized the need of current limiting in order to have stable structure. Russ and Kennedy [62] introduced a double insulated AC coupled structure which by its

symmetry was designed to minimize any slow polarization effects and which also offered the protection of local current limiting, since the current flowing through the active film would charge up the interface with the dielectric and reduce the internal field. The most significant impetus to interest in thin film EL for displays came, however, with the report of Inoguchi et al. [63] of very high luminescence (> 1000 fL), coupled with very long life ($> 20,000$ hrs.), achieved through use of ZnS:Mn as active and Y_2O_3 as insulating layer.

The present status and current trends in the AC thin film electroluminescent devices are reviewed in the concluding chapter. The possibility for evolving flat panel displays and TV displays with many attractive features is also discussed in that chapter. Here in the following section the Device Physics of non memory and memory devices are explained.

One of the key characteristics of AC thin film devices is the steep non linearity of the threshold characteristic (Fig. 1.7) as well as the saturation often seen with ZnS:Mn devices. This curve implies that one can make refreshed X-Y matrix displays of good luminance and contrast where the elements are

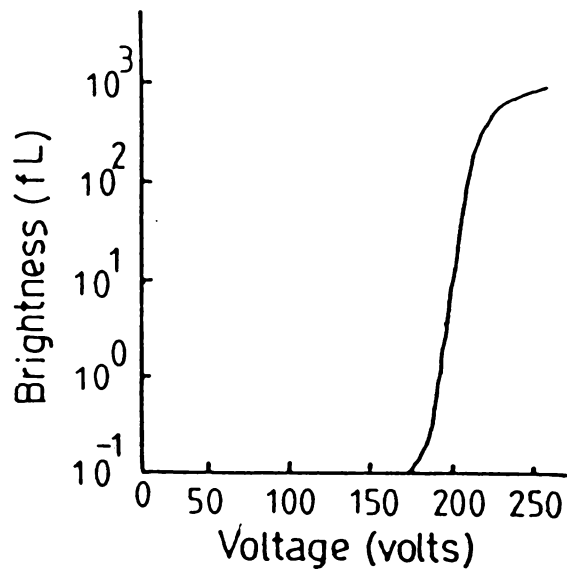


Fig.1.7. Typical B-V characteristic of AC TFEL device.

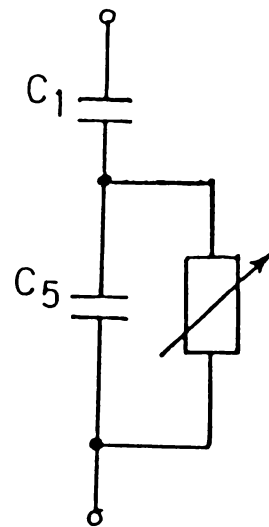


Fig.1.8(A) The equivalent circuit.

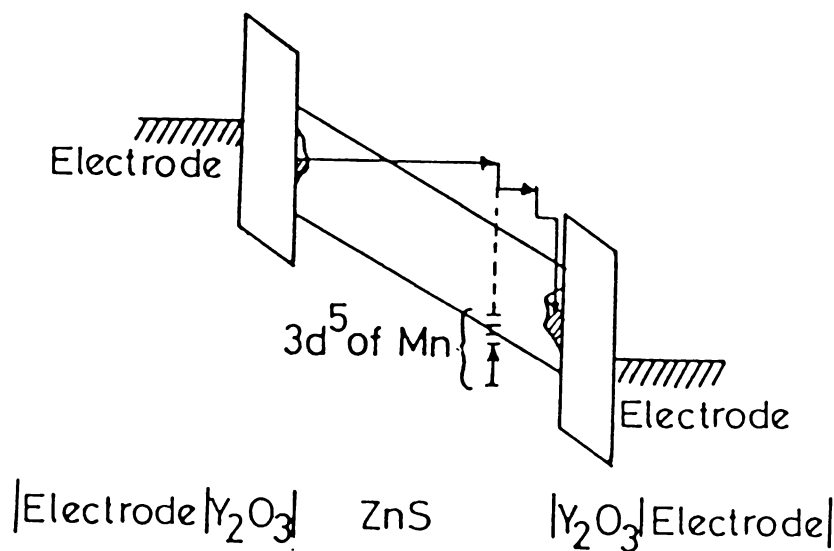


Fig.1.8(B) shows the main features of the field clamping model (1) high field induced tunneling from states near interface (2) collision excitation of Mn^{++} by electrons accelerated in the high field (3) retrapping near the opposite interface.

activated one line at time and whole scan process is repeated at a rate high enough that the display appears to be steady.

1.13 Device Physics (Non Memory)

Since one of the key characteristics of a non memory EL device for display application is the steep brightness-voltage variation and saturation of brightness at a high excitation field. (The typical B-V characteristic is shown in Fig. 1.7). It is important to consider what determines the shape of that curve. The analysis here involves two components viz., the equivalent circuit aspect and the internal mechanisms associated with the active layer. As shown in Fig. 1.8, the devices consist of a series capacitance made up of two dielectric layers and an active layer which has both capacitance and non linear conductance. That is, at low fields the active layer acts as an insulator but at higher internal field (1.5×10^6 V/cm in this case), it starts to breakdown and conduct, producing luminescence. The steep rise in brightness reflects the corresponding rise in current density as long as the voltage drop across the ZnS:Mn layer continues to increase. At higher intensity all the charge carriers produced do not recombine and as a result, a surface charge will be formed at the active

layer dielectric interface. This will effect the increased external voltage and is known as field clamping effect [64,65].

The internal efficiency of thin film EL devices depends upon: (a) the field at which current flows, (b) the fraction of electrons at such fields with sufficient energy to produce internal excitation of the activators, (c) the cross section and density of the activators, and finally (d) the luminescent probability of the activator. For example, Mn^{2+} shows strong concentration quenching, even in photoluminescence (PL) at concentrations greater than about 0.5 wt % in ZnS. It is clear that Mn^{2+} has more favourable cross section for excitation than the rare earths, which is probably related to the differences between d-electrons and f-electrons, but there are still efforts under way [66] to realize the 'lumocen' concept of Kahng [25] where a complex is impact excited, and then, via internal coupling, energy is transferred to the activator.

1.14 Device Physics (Memory)

An understanding of the memory behaviour (Fig.1.9) obviously requires the introduction of additional mechanisms. Yamauchi et al. [68] were the first to report

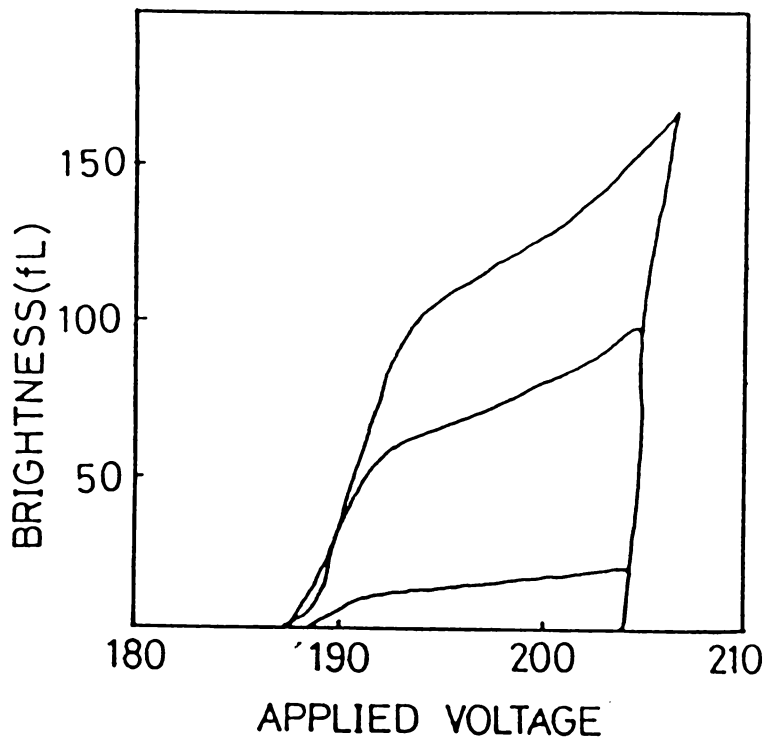


Fig.1.9. Typical B-V characteristic of a hysteretic thin film EL device.

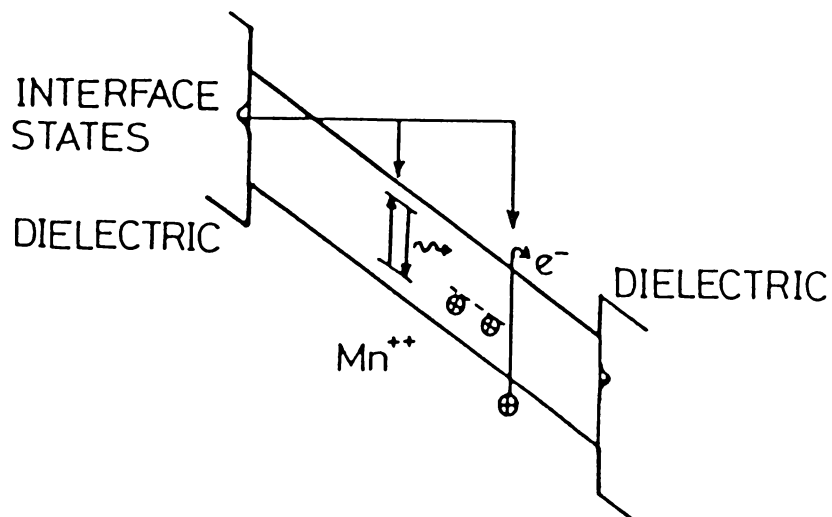


Fig.1.10. Band diagram of an EL memory device illustrating schematically some of the mechanisms involved such as tunnel injection, impact excitation, impact ionization and hole trapping.

the hysteresis behaviour in the brightness vs applied voltage curve of the thin film EL device with double insulating layer structure. The first important observation in this regard is that of Marello et al. [67] that B-V variation represents the aggregate behaviour of an ensemble of bistable localized emitting regions. The device physics problem is reduced, then to understanding the bistable behaviour of the localized regions.

One practical consequence of this characteristics is that in a matrix display all elements can be excited with a steady AC sustaining voltage within the range of hysteresis, at a relatively low frequency. Individual cells can then be switched on or off by transient waveform applied to the X-Y electrodes. The overall practical interest in the hysteresis behaviour was generated by the observation that the device can be switched by light [69] and electron beam [70], thus making them suitable for applications like image storage and in high content storage CRT tube displays [71]. Another important application of these devices are in the fabrication of image amplifiers [72].

Inoguchi et al. [63] have explained the occurrence of this hysteresis behaviour on the basis of charge storage and release of trapped electrons from

some deep levels and then subsequent detrapping at the removal of the field. They have also verified the existence of deep traps from the thermally stimulated current measurement across the active layer.

Howard et al. have proposed a model for this memory behaviour [64,73,75,76] which is based upon the equivalent circuit shown in Fig. 1.8 and the schematic band diagram of Figure 1.10. The observed bistability is explained by incorporating lattice ionization, or electron-hole pair production, as a further consequence to the electron heating which produces the impact luminescence.

For producing hysteretic behaviour there are several key empirical requirements: the active layer films must have good crystallinity, they must be thicker than $0.3 \mu\text{m}$, and they must be activated with Mn in concentrations greater than about 0.5 wt %. The former two conditions can be associated with the need in the model for deep traps in order to create and maintain space charge, as indicated in the Fig.1.10. Essentially, bistability is a consequence of an AC-coupled negative resistance, which arises because of space-charge induced by the trapping of holes, following impact ionization of the lattice. In order to

simulate the observed bistable behaviour of memory devices it is necessary to assume deep traps with a density in the range $10^{16} - 10^{17} \text{ cm}^{-3}$ and a very steep variation of ionization with electric field [64]. The model also allows for direct recombination of injected electrons with deeply trapped holes, which is important for erasing or switching off.

The observed maximum efficiency of high field EL device of the type discussed above is about one percent. One of the new concepts for thin film EL devices which has been proposed by Williams [77] is to separate the functions of acceleration and excitation, which in a ZnS:Mn device occur together in the active layer, into separate regions or separate materials, so that there can be a relaxation of simultaneous constraints on material properties. This is illustrated schematically in Fig. 1.11.

In this structure, electrons are injected into insulating layers, or even to active layer, at fields such that there is considerable electron heating. The hot electrons so produced can then be injected into a second material, where they produce impact excitation of activators or impact ionization followed by recombination at donor-acceptor pairs. The results of

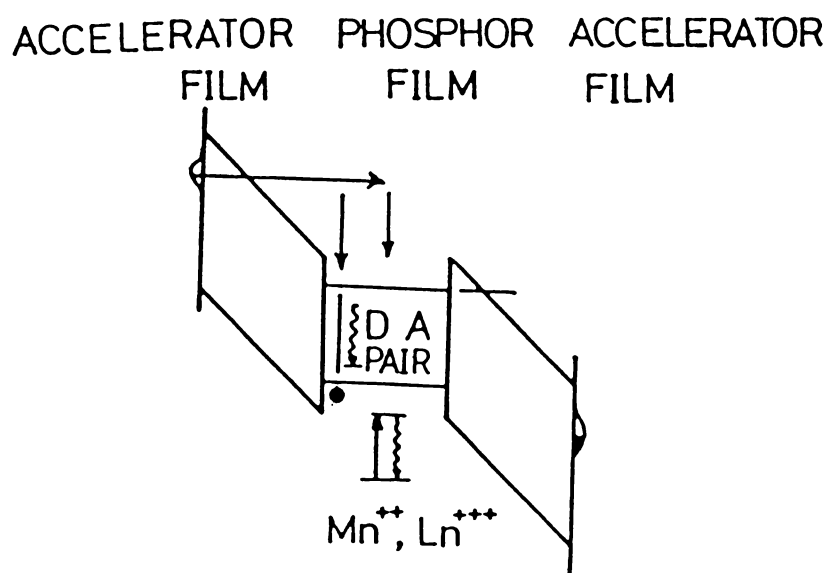


Fig.1.11. Schematic band diagram of the proposed structure to separate acceleration and excitation.

Okamoto et al.[78] can be considered as the implementation of this concept.

One of the drawbacks of AC thin film devices is their higher operating voltages. Attempts have been made to reduce the operating voltage by using insulators of high dielectric constant [79]. The details of a series of studies done by the author to reduce the driving voltage is given in Chapter V. By use of novel insulators having high dielectric constant, device in MIS structure is found to be driven by low voltage for light emission. One of the recent works by Nanto et al. [80] with BaTiO₃ Ceramic sheet as insulator reports a low threshold voltage.

The recent trends and investigations for other materials for multi colour display are reviewed in the concluding chapter.

1.15 Summary

In this chapter a detailed description of the basic phenomenon of electroluminescence is given. The fundamental process associated with EL emission are mentioned. The approach to fabricate EL devices and the fundamental features of such devices are summarised. Also the theoretical models for memory and non memory AC thin film devices are described.

REFERENCES

- [1] O W Lossew; *Telegrafia i Telefonía*, No.18(1923) 61.
- [2] H F Ivey; *Advances in Electronics and Electron Physics, Electroluminescence and related effects*, (Academic Press, London 1963).
- [3] A A Bergh and P J Dean; *Monographs in Electrical and Electronic Engineering, Light emitting diodes*, (Clarendon Press, Oxford, 1967).
- [4] F W Williams and R Hall; *International Series in the Science of Solid State Volume 13, Luminescence and light emitting diode*, (Pergamon Press, Oxford, 1978).
- [5] T Mishina, W Quan-Kun and Takahashi; *J. Appl. Phys.*, 59(1981) 5797.
- [6] Eilllott Schlam; *Proc. IEEE*. [7] 61(1973) 894.
- [7] M Aven and J S Parner; Eds. *Physics and Chemistry of II-VI compounds*, (North Holland, Amsterdam, Netherland, 1967).
- [8] A G Fischer and H I Moss; *J. Appl. Phys.*, 34(1963)2113.
- [9] P R Thornton; *The Physics of Electroluminescent Devices*, (E and F N Spon Limited, London, 1967).
- [10] H K Henisch; *Electroluminescence*, (Pergamon Press, Oxford, 1962).

- [11] A G Fisher; Luminescence of Inorganic Solids,
Ed. P Goldberg (Academic Press, New York, 1966) 541.
- [12] F F Morhead; Physics and Chemistry of II-VI compounds,
Eds. M S Aven and A Parner (North Holland,
Amsterdam, 1967) 613.
- [13] G Destriau; J. Chem. Phys., 33(1936) 587.
- [14] W Lehmann; J. Electrochem. Soc., 105(1958) 585.
- [15] S M Pillai and C P G Vallabhan; Solid State Commun.,
47(1983) 909.
- [16] H C Frelich; J. Electrochem. Soc., 100(1953) 280.
- [17] G F Garlick and M J Pableton; Proc. Phy. Soc.,
London, B. 67(1954) 442.
- [18] D Curie; Luminescence in Crystals, (Methun and Co.Ltd.,
London, 1963).
- [19] J S Prener and P.E Williams; Phys. Rev., 101(1956)1427.
- [20] M H Aven and R M Potter; J.Electrochem. Soc., 105(1958)
134.
- [21] H A Klasens; J. Electrochem. Soc., 100(1953) 72.
- [22] E W Chase, R T Hepplewhite, D C Krupka and D Kahng.,
J. Appl. Phys., 40(1969) 2512.

- [23] J Ohwaki, H Kozawaguchi and B Tsujiyama; Jpn. J. Appl. Phys., 22(1983) 1133.
- [24] C N King; Conference record of the 1985 International Display Conference, San Diego, (1985) p. 155.
- [25] D Kahng; Appl. Phys. Lett., 13(1968) 210.
- [26] D C Krupka and D M Mahoney; J. Appl. Phys., 43(1972) 2314.
- [27] H Kobayashi, S Tanaka, T Kunou, M Shiiki and H Sasakura; Proc.Int. SID Conf., 25/3(1984)187.
- [28] M Tammenmaa, T Koshinen, L Hiltanen, M Leskelä and L Niinisto; Thin Solid Films., 124(1985) 125.
- [29] H Kobayashi, S Tanaka, V Shanker, M Shiiki, T Kunou, J Mita and H Sasakura; Phys. Stat. Solidi.,(a) 88(1985) 713.
- [30] J D Kingsley, J S Parner and M Aven; Phys. Rev. Lett., 14(1965) 136.
- [31] B R Chaubey and L N Tripathi; Indian J. Pure and Appl. Phys., 25(1987) 47.
- [32] R C Maheshwari and K S Pathak; Indian J. Pure and Appl. Phys., 22(1984) 374.
- [33] R C Maheswari and R K Tripathi; Bull. Mater. Sci., 5(1983) 405.

- [34] S Bhushan, M Saleem and S Chandra; *Pramana*, 10(1978)1.
- [35] W W Piper and F E Williams; *Electroluminescence Solid State Physics*, Vol.6, Eds. Frederickseitz and David Turnbull (Academic Press Inc., New York, 1958)
- [36] W W Piper and F E Williams; *Phys. Rev.*, 98(1955) 180.
- [37] G Destriau; *Phil. Mag.*, 38(1947) 700.
- [38] J F Waymouth and F Bitter, *Phys. Rev.*, 95(1954) 941.
- [39] C H Haake; *J. Appl. Phys.*, 28(1957) 245.
- [40] W W Piper and F E Williams; *Brit. J. Appl. Phys.*, Suppl. 4, S 39(1955).
- [41] G Destriau and H F Ivey; *Proc. of IRE.*, 10(1955) 1911.
- [42] P Zalm, G Diemer and H A Klasens; *Philips Research Reports*, 10(1955) 205.
- [43] A S Marfunin; *Spectroscopy, Luminescence and Radiation centers in minerals*, Translated by V V Shiffer (Springer and Verlag, New York, 1979).
- [44] B T Howard, H F Ivey and W Lehmann; *Phys. Rev.*, 96(1954) 799.
- [45] J B Taylor and G F Alfrey; *Brit. J. Appl. Phys.*, Suppl. 4(1955) 44.

- [46] B T Howard; Phys. Rev., 98(1955) 1544.
- [47] W A Thornton; J. Appl. Phys., 32(1961) 2379.
- [48] P Zalm, G Diemer and H A Klasens; Philips Research Reports, 9(1954) 81.
- [49] W A Thornton; Phys. Rev., 102(1956) 38, 103(1956)158 5.
- [50] C H Haake; Phys. Rev., 101(1956) 490.
- [51] G Destriau; Brit. J. Appl. Phy. Suppl. No.4(1955) 49.
- [52] P Zalm; Philips Research Reports, [11] 353(1956) 417.
- [53] A N Geogobiani and M V Fok, Optics and Spectroscopy, 11(1961) 48.
- [54] J I Pankove; Electroluminescence. Topics in Applied Physics, Vol. 17, Ed. J I Pankove (Springer Verlag, Berlin, 1977).
- [55] H Kroemer; Proc. IRE., 45(1957) 1535.
- [56] A G Fisher, Luminescence of Inorganic Solids, Ed. P Goldberg (Academic Press, New York, 1966).
- [57] P J Dean; Electroluminescence. Topics in Applied Physics, Vol.17, Ed. J I Pankove, (Springer Verlag, Berlin, 1977).

- [58] C N Berglund; Appl.Phys. Lett., 9(1966) 441.
- [59] I Giaever, Phys. Rev. Lett., 5(1960) 147.
- [60] R E Halsted and L R Koller; Phys. Rev., 93(1954) 349.
- [61] W A Thornton; J. Appl. Phys., 33(1962) 3045.
- [62] M J Russ and D I Kennedy; J. Electrochem. Soc.,
114(1967) 1066.
- [63] T Inoguchi and S Mito; Electroluminescence. Topics
in Applied Physics, Vol.17, Ed. J I Pankove
(Springer Verlag, Berlin, 1977).
- [64] W E Howard; J. Lumin, 24/25(1981) 835.
- [65] R Törnquist; J.Cryst.Growth, 59(1982) 399.
- [66] J Benoit, P Benalloul and B Blanzat; J Lumin.,[1,2]
23(1981) 175.
- [67] V Marrello, W Rühle and A Onton; Appl. Phys. Lett.
31(1977) 452.
- [68] Y Yamauchi, H Kishishita, M Takeda, T Inoguchi and
S Mito; Digest. Int. Elect. Dev. Mtg. IEEE,
(New York, 1974) p. 352.
- [69] D H Smith; J. Lumin., 23(1981) 209.

- [70] W E Howard and P M Alt; Appl. Phys. Lett., 31(1977)399.
- [71] D Thesis; J. Lumin., [1,2] 23(1981) 191.
- [72] P K C Pillai and Nilonfee Shroff; National Conference on Instrumentation Proc., (1983) 285.
- [73] W E Howard; J. Lumin., [1,2] 23(1981) 155.
- [74] M S Skolnick and P J Dean; IEEE Trans. on Electron Devices, ED-28[4] (1981) 444.
- [75] P M Alt, W E Howard and O Sahni; IEEE Trans., ED-26(1979) 1850.
- [76] W E Howard, O Sahni and P M Alt; J. Appl. Phys., [1] 53(1982) 639.
- [77] F Williams; J. Lumin., 23(1981) 1.
- [78] K Okamoto and Y Hamakawa; Appl. Phys. Lett., 35(1978) 508.
- [79] J Ohwaki, H Kozawaguchi and B Tsujiyama; Jpn. J. Appl. Phys., 22(1983) 1133.
- [80] H Nanto, T Minami, S Murakami and S Takata; Thin Solid Films, 164(1988) 363.
- [81] J Lambe and C C Klich; Phys. Rev., 98(1955) 909.

Chapter-II

EXPERIMENTAL SETUP

Abstract

The most important phase in the development of EL display is the phosphor preparation and its characterisation. In this chapter a detailed description of phosphor preparation technique is given. To characterise the prepared phosphor various measuring techniques, viz., recording of EL emission spectra, brightness-voltage, brightness-frequency characteristics and brightness in absolute units are used and these are described here in detail. The present day interest is mainly in developing thin film EL devices. The various methods of deposition of thin films used for the present investigation are summarised at the end of this chapter.

2.1 Introduction

The development of efficient EL phosphor materials suitable for display applications is the most important step in the investigations for electroluminescence. During the last two decades there has been almost revolutionary changes in the materials and methods of preparation for EL panels. There has occurred the realization of extreme importance of preparative procedures for controlling the phosphor compositions. These factors indicate the need for a deeper understanding of the physical mechanism behind the process of light emission.

A world wide interest exists in the development of multicolour thin film electroluminescent devices. The objectives are quite challenging and require extensive and systematic investigations on both experimental as well as theoretical fronts. The need of three primary colours for full colour device has led to intensive trials on phosphors of different host materials doped with different activators and co-activators.

In order to carry out a systematic series of investigations a well equipped electroluminescent laboratory has been set up. This includes a chemical laboratory with facilities to handle high purity chemicals which is a must during the course of EL phosphor preparation.

The high temperature vacuum furnace, different type of powder and thin film EL cells, power supplies to excite the cells, detection and recording setups used for the study of the emission characteristics of the device etc. are the other requirements in this laboratory. Brief description of each of these items is given in this chapter. Details of the method of measurements of brightness voltage characteristics, life times and brightness wave forms are also given here. The method used to estimate EL brightness in absolute units is described in detail. The fabrication of thin film electroluminescent devices requires good understanding of the different aspects of vacuum technology. The last few sections give the details of various vacuum systems and techniques used for thin film preparation.

2.2 Phosphor preparation

Luminescent phosphors generally consists of a host material doped with an activator and also sometimes with a coactivator. The phosphor preparation technique can be classified into two viz., (1) slurring technique, (2) simultaneous activation. In the former method the activators and coactivators are added in a suitable chemical form to the prefired host material (eg. ZnS)

while, in the latter, the dopants are added during the precipitation of the host material [1]. The phosphors for the present investigations are prepared by slurring technique. For this, a weighed amount of the host material is mixed with appropriate weight percentage of activators and coactivators and a slurry is formed. This slurry is then dried by heating upto 80°C . During the preparation of the slurry a known weight percentage of flux is added. The dried powder is taken in quartz test tubes and introduced into the high temperature zone of a horizontal furnace which is kept at a specified high temperature. The firing can be done either in vacuum or in suitable atmosphere depending on the specific requirements.

The samples coated with Cu_2S conducting skin increases the efficiency of the phosphor [2]. This Cu_2S coating is done by slowly heating the formed samples in a suitable solution containing copper ions. The resulting phosphors which are black in colour may be washed with $\text{Na}_2\text{S}_2\text{O}_3$ solution or in KCN to reduce the thickness of the Cu_2S skin layer [3].

2.3 Vacuum furnace

The furnace used for firing process of the phosphor was constructed with a silca tube having 5 cm

internal diameter and 60 cm length. The two ends of the tubes are suitably adapted so that it can be evacuated or can maintain a suitable atmosphere of the desired gas in the tube. A Kanthal wire element of 18 gauge was wound closely over a length of 15 cm at the centre of the tube. The coil covered with fire clay formed the muffle of the furnace. The external heat insulation was produced by closing the muffle in a 25 cm x 20 cm cylindrical MS enclosure filled with silliminite gravel. The electrical leads are taken through synthanium insulators. The furnace is powered with a 15A autostat connected to a 5 KVA servocontrolled voltage stabiliser. For an input power of 1 KW (at 80V) it can attain a temperature 1000°C within 90 minutes. The constant temperature zone is 8 cms in length. It can be evacuated upto 10^{-3} torr. This system is used for preparing the phosphors presented in the present work.

2.4 AC Powder EL Cells

The electroluminescence emission from the phosphors can be excited by subjecting the phosphors to a fairly high electric field. In order to subject these phosphors to an intense electric field,

the phosphor powder dispersed in a suitable dielectric is sandwiched between two plane parallel electrodes. To observe the luminescence one of the electrodes must be transparent. For such a cell, assuming the phosphor particles are spheres of arbitrary diameter but of constant dielectric constant k_1 embedded in a medium of dielectric constant k_2 , which fills remaining volume between two plane parallel conductors separated by a distance d , the electric field strength acting on the spheres is given by Maxwell-Wagner formula [4,5].

$$E_1 = E_0 \frac{3k_2}{2k_2 + k_1 - f_v(k_1 - k_2)} \quad 2.1$$

where f_v is the fraction of the volume which is occupied by the spheres. But in practical EL cells the previous assumptions that phosphor particles are spheres and are in a homogeneous suspension are not always satisfied. The attempts made to arrive at a more general relation have resulted in complicated expressions and the results obtained based on these are found to differ very little from that obtained from equation (2.1) [6,7,8].

The brightness-voltage relation depends on various parameters and a number of relationship connecting brightness and voltage have been suggested [9,10,11]. It can be seen that generally the logarithm of brightness is a function of applied voltage which implies that higher brightness level can be obtained at much higher applied voltages. But it is observed that the electrical breakdown strength of a dielectric in which an electro-luminescent phosphor has been incorporated is normally much lower than that of the same material without phosphor particles [12]. Hence in order to protect the device from breakdown and to apply a higher field of excitation, a thin insulator of high breakdown strength may be introduced in between one of the electrodes and the phosphor layer. By choosing a material of higher dielectric constant the voltage drop across the insulator layer can be minimised.

Fig. 2.1 shows the experimental AC powder EL cell used for the present investigations. It is essentially a parallel plate condenser, with an aluminium block as the rear electrode and a transparent conducting glass plate as front electrode. The phosphor layer is in contact with one of the electrodes and is usually embedded in a liquid dielectric material with

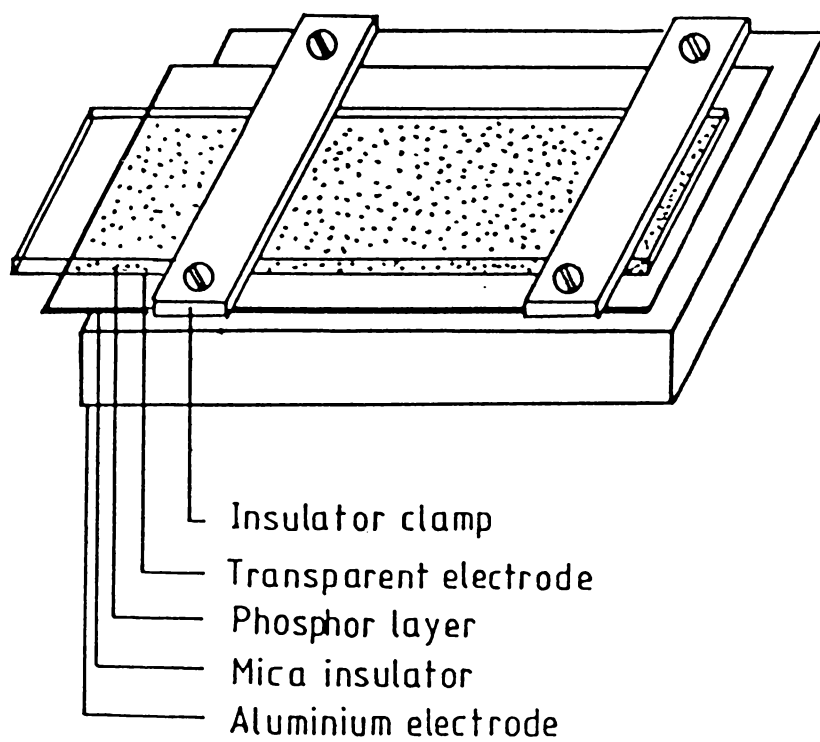


Fig.2.1. Experimental powder EL cell.

appropriate phosphor binder ratio to enhance the dielectric strength of the cell. This permits operation at higher voltages and suppresses any gas discharge which might be formed. A thin mica sheet introduced between the electrode and phosphor layer guard further the cell against dielectric breakdown. The conducting glass plate is fastened to the aluminium block with the phosphor layer in between.

2.5 Setup for recording the EL spectra

The EL spectra is recorded using the setup which is shown here with the aid of a block diagram (Fig.2.2). The emission from the EL cell is focussed at the entrance slit of scanning spectrometer. The spectrometer used is 0.5m Ebert Scanning Spectrometer (Jarrel Ash Model 82.00 series) [13]. The beam emerging out of the exist slit is detected with a high gain photomultiplier tube (PMT) (EMI 9683 KQB with S-20 cathode). The Preamplifier [14] helps in amplifying the PMT anode current and its output is recorded using strip chart recorder.

In order to subject the phosphors to an intense electric field, fairly high voltages are to be applied to the cell. For this a home made high voltage variable frequency sine/square wave power supply which gives a

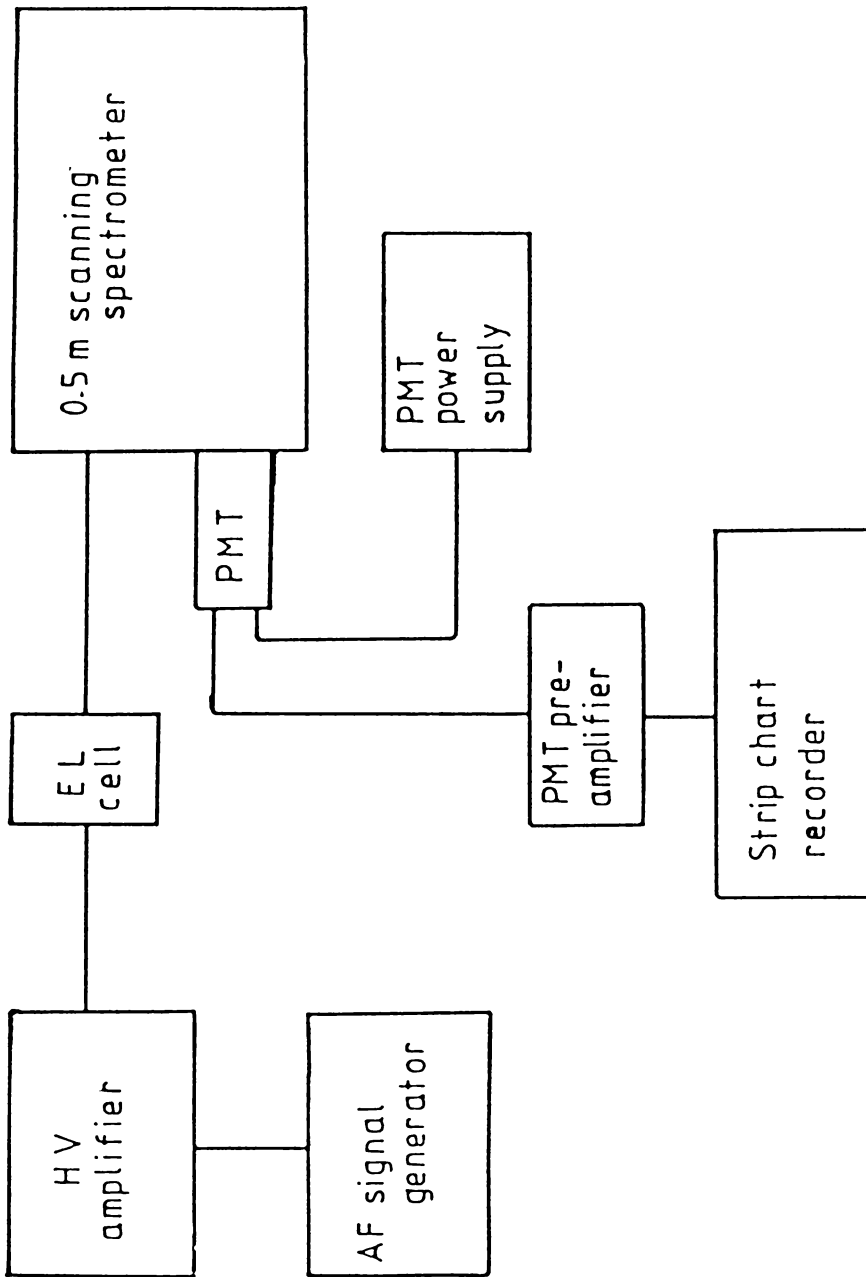


Fig.2.2. Block diagram of the experimental setup used for recording the EL spectra.

maximum of 2 KV is used. During the testing, it is found that electrical breakdown to the cell does occur very often. To safeguard the power supply from short circuiting during cell breakdown, protection measures are included in the circuit. A low frequency (upto 1 MHz) (Aplab model No.2004) signal generator having VCO external control has been used to obtain the audio signal at the required frequency. The low power output is fed to a 40W audio frequency amplifier. Thus final output of the high voltage variable frequency power supply has a maximum of 2 KV.

2.6 Voltage brightness measurements

The voltage brightness characteristics of the EL cells were measured using an EMI 9684 PMT with S-1 cathode along with a highly stabilized power supply. The EL emission is made to fall on the PMT kept in front of it. The PMT anode current and voltage across the cells were measured using digital multimeter of sensitivity 0.1 mV.

The brightness wave form as well as the decay studies were done by using the PMT in conjunction with Tektronix 466 Oscilloscope. For life time measurements the cells are excited using a current pulse of few micro

seconds duration. The permanent record of these observations were made by photographing the oscilloscope traces with a Tektronix oscilloscope camera.

2.7 Brightness measurements in absolute units

The brightness of EL cells is usually expressed in arbitrary units. This makes it difficult to compare with other results reported in literature. Hence for a meaningful description of the brightness of the EL cell can be had only by expressing it in terms of absolute units. This is done with a standard lamp in conjunction, with interference filters used to select the entire region where the eye is sensitive viz., the range 380–780 nm. A PMT having a spectral response matching the eye sensitivity is used as the detector. The following section gives the method for EL brightness measurement in absolute unit using PMT anode sensitivity curve. The Anode sensitivity of the PMT, which is expressed in A/lm is estimated by measuring the anode current obtained when the cathode is illuminated by a standard tungsten lamp kept at 2850°K. The emission spectrum of the standard tungsten lamp is shown in Fig. 2.3 denoted by $I(\lambda)$. The luminous flux from the

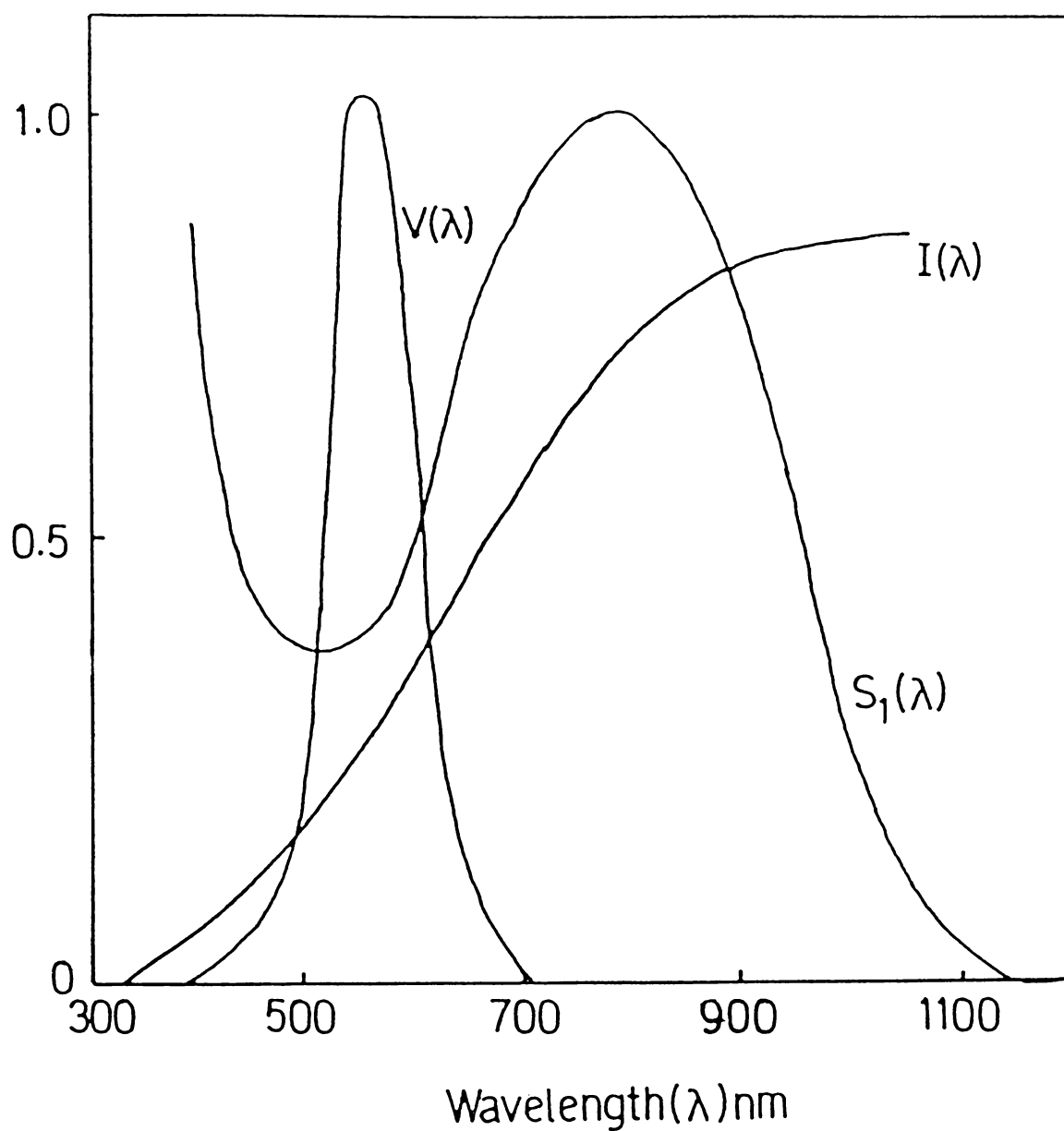


Fig.2.3. Relative response of the human eye $V(\lambda)$ the spectral distribution $I(\lambda)$ of light from a standard tungsten filament lamp and the sensitivity curve $S_1(\lambda)$ of a PMT with S_1 cathode.

source is given by

$$F = 680 \int I(\lambda) V(\lambda) d\lambda \text{ lm}$$

where $V(\lambda)$ is the relative response of human eye [15].

The shape of the $I(\lambda)$ curve will be modified as $I(\lambda) S_1(\lambda)$ (Fig. 2.4), if we are measuring the anode current of the PMT having a cathode response curve $S_1(\lambda)$. The anode current of the PMT when the cathode illuminated with the standard lamp such that the flux incident is 1 lm then the measured PMT anode current corresponds to the area under the curve $I(\lambda) S_1(\lambda)$ which will be equal to the anode sensitivity of the PMT at that operating voltage.

When the PMT is having a spectral response beyond the visible region, the term as expressed in the data sheet is meaningless [16]. In such cases for actual photometric measurements the specified value is to be corrected for the eye sensitivity. This can be done by plotting the $I(\lambda) S_1(\lambda) V(\lambda)$ curve as shown in Fig. 2.4. Then the current corresponding the area under this curve will be the correct value of the anode sensitivity which should be taken for photometric measurements.

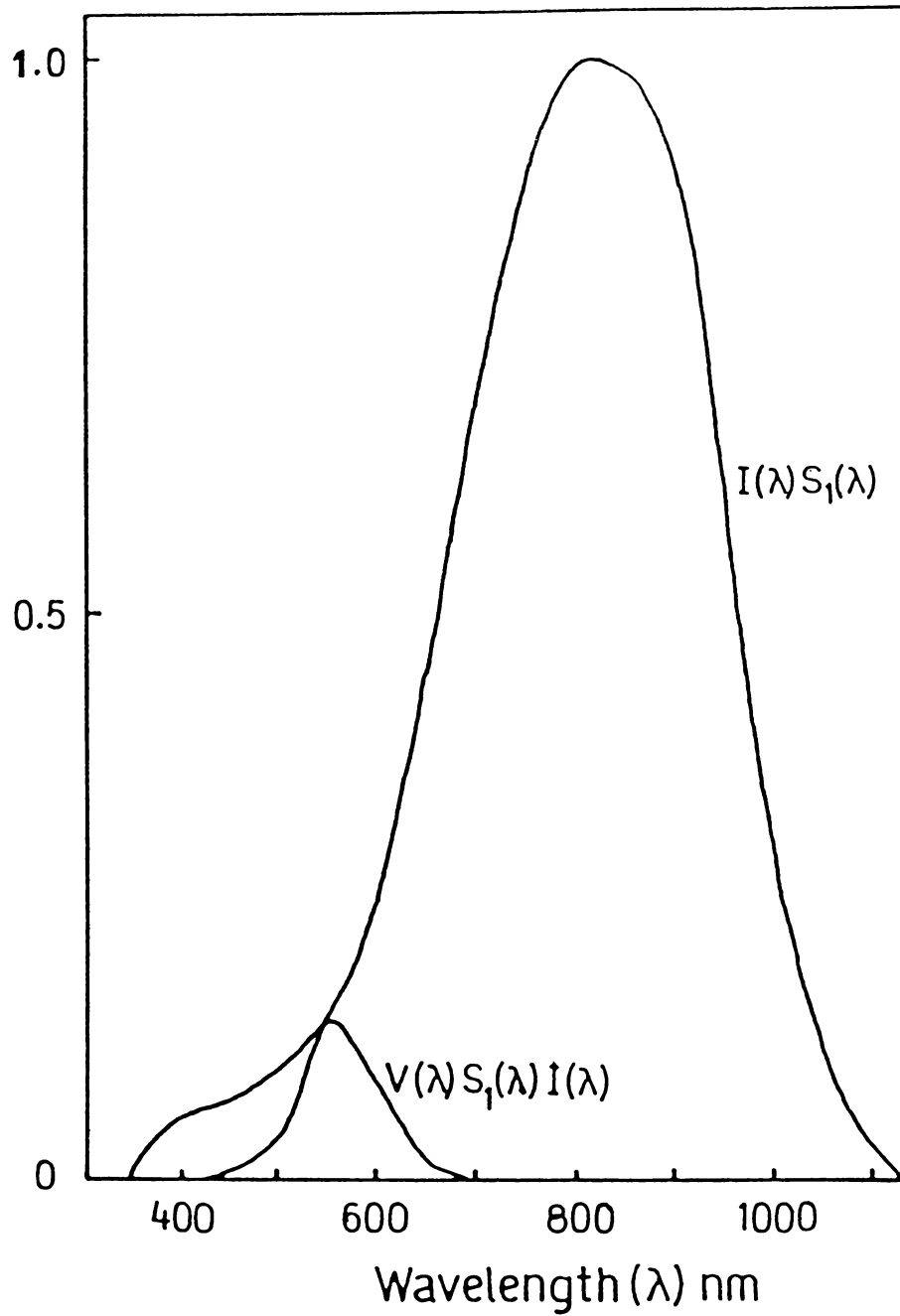


Fig.2.4. $I(\lambda) S_1(\lambda)$ curve is the $I(\lambda)$ curves corrected for the detector response $S_1(\lambda)$. $I(\lambda) S_1(\lambda) V(\lambda)$ curve incorporates the corrections for the detector sensitivity and relative response of the human eye.

The emission spectra $E(\lambda)$ of the source whose brightness is to be measured and is normalised with $I(\lambda) S_1(\lambda)$ curve. The area under the curve will corresponds to the measured PMT current. This value has to be corrected for the visual effectiveness. The area $S_1(\lambda) E(\lambda) V(\lambda) d\lambda$ corresponds to this corrected value of the PMT current. From this the amount of luminous flux incident on the detector can be calculated in lumens.

Assuming that the EL cell is illuminating uniformly the surface of hypothetical hemisphere of radius R , where R is the distance between source and detector. Then the luminance flux incident per unit area is

$$\frac{I}{2\pi R^2} = I_o$$

where I is the emitted luminance flux by the source. If I_D is the luminance flux measured by a detector having area D_A , then

$$\frac{I}{2\pi R^2} = I_o = I_D/D_A$$

so

$$I = \frac{2\pi R^2 I_D}{D_A}$$

If 1 sq. inch is the emitter area producing a luminous flux I, then the brightness B is given by

$$B = 144 I \text{ foot lamberts}$$

$$= 144 \frac{2\pi R^2 I_D}{D_A} \text{ fL}$$

2.8 DC powder EL cells

DC EL devices can be excited to higher levels in the pulsed excitation mode thus producing higher brightness level compared to the AC powder EL panels. Fig.2.5 gives the structure of typical DC powder EL cell. It consists of transparent conducting film deposited on a glass plate which acts as the positive electrode. The active layer which is $\sim 25 \mu\text{m}$ thick is spread on the transparent electrode. The structure is completed with the rear Al electrode. The whole assembly is then encapsulated with a proper dessicant to exclude water vapour from the atmosphere.

The phosphor for the preparation of DC powder EL cells can be prepared either by the conventional slurring technique or by the simultaneous activation; i.e., by precipitating the phosphor from solution containing appropriate amounts of activators and

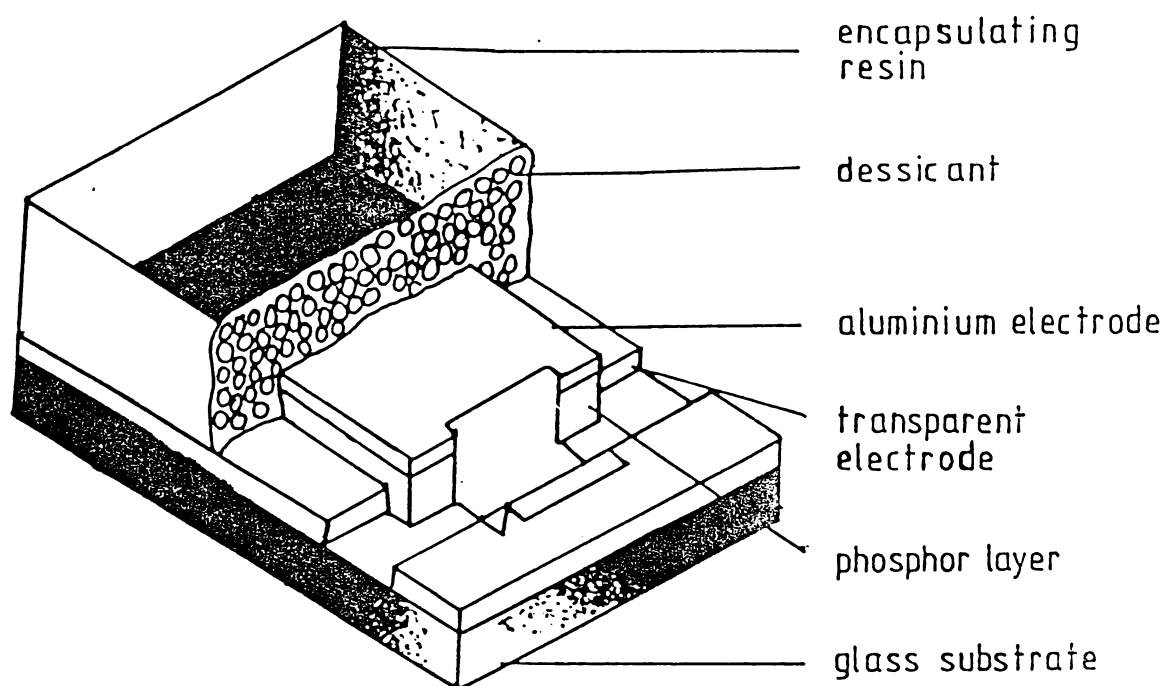


Fig.2.5. Structure of a DC PEL cell.

coactivators. The precipitation technique is found more suitable for DC EL cells because the phosphors thus obtained have virtually no particle size distribution unlike those obtained from the slurry technique[1]. The doped samples thus obtained is given a high conductive skin coating of Cu_xS by treating with cuprous or cupric salt solution. But the phosphors obtained by treating with cupric salt solution showed better reproducibility than phosphors treated with cuprous salt solution. The Cu_xS coating thus obtained is a p-type semiconducting layer. So, a heterojunction will be developed between the doped ZnS and Cu_xS suitable for the formation of high field region which facilitates the injection of charge carriers [18].

These Cu_xS coated phosphor particles were vigorously dispersed in a suitable binder (like nitrocellulose, polymethyl methacrylate solution in chloroform etc.) with appropriate phosphor-binder ratio. It was then spread on lithographed indium tin oxide coated glass by one of the following methods, viz., silk screen printing, doctor blading or spraying. Because of variation in thickness of large area, doctor blading has been used only for test areas and small display panels. The phosphor-binder mixture

is diluted with large volumes of solvents to obtain a solution useful for spraying. Silk screen printing gives controlled thickness layers of high packing density with little waste. The use of a minimum quantity of binder ensures the maximum particle packing density and therefore good interparticle contact which results in conducting phosphor/binder layers [19]. It is observed that devices of thickness in the range 30-100 μm have the same electrical characteristics and brightness [20]. Back electrode is usually provided with an evaporated aluminium or gold or with a graphite paint. The binder is used to hold the phosphor particles in contact with each other and to the glass substrate. It occupies less than 5 percent of the total volume [17]. The whole devices is encapsulated together with a molecular sieve.

2.9 Requirements for fabrication of thin film EL Devices

In recent years the advances in electronics and material science have helped each other in accumulating new knowledge as well as in developing new process technologies and device structures. The striking advent of the Lumocen device is worth mentioning in this context. The Lumocen device has the double

insulating layer structure [21,22,23] in which vacuum-deposited thin phosphor film act as the active layer. The vacuum-deposited thin film EL device with double insulating layer structure not only exhibits high brightness with exceptionally high stability and long life, but it can also be processed to possess inherent memory which lends itself to very useful applications. But generally these devices with double insulating structure require higher driving voltage [24] which makes it difficult to be compatible with compact IC based driving circuits. Metal-insulator-semiconductor (MIS) structure has been suggested one way of reducing the driving voltage. Another way is by incorporating films of high figure of merit as the insulators [25]. The cross sectional views of MISIM and MIS structure devices are shown in Figs.2.6 and 2.7 respectively. The main problem in developing high field EL structure is to find materials (electrodes, insulators, phosphors) that are transparent and at the same time can withstand the high electric field needed in the device. The materials and fabrication techniques of the various layers are given below.

Transparent electrode:

It is made of SnO_2 or In_2O_3 using conventional thermal evaporation-oxidation method (SnO_2) or vacuum

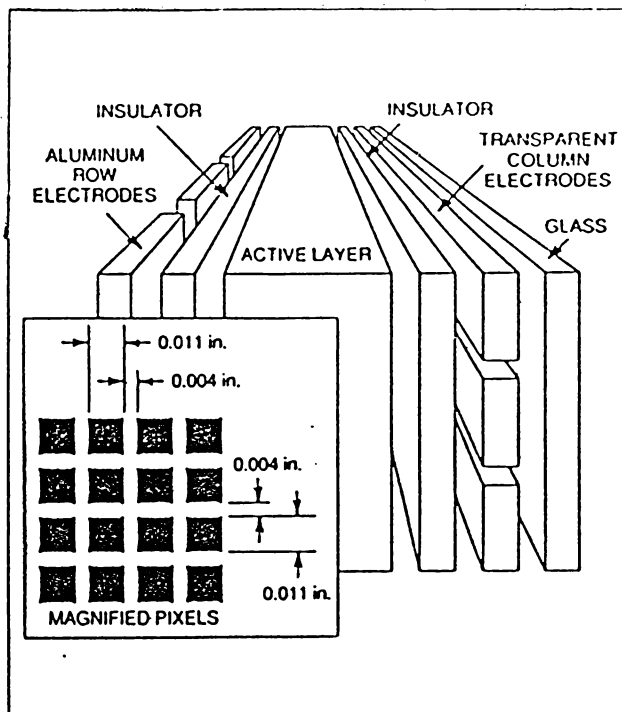


Fig.2.6. Structure of a MISIM TFEL device

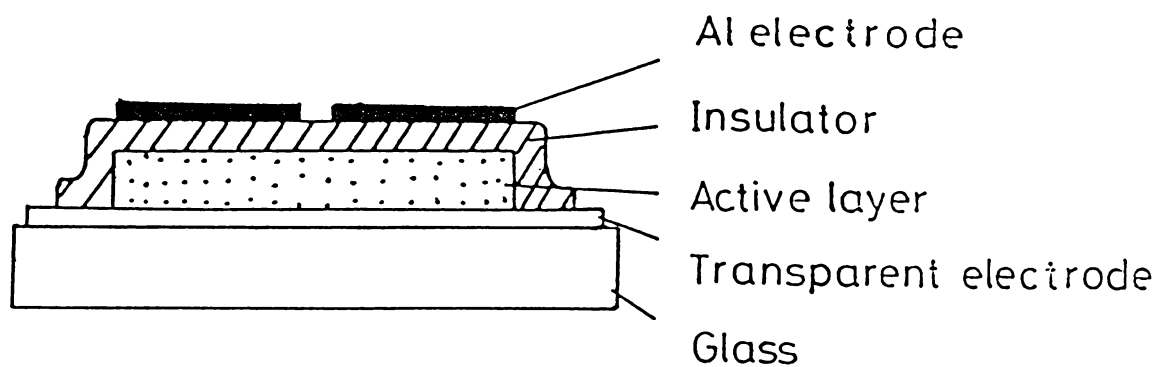


Fig.2.7. Structure of a MIS TFEL device

evaporation method In_2O_3 on glass substrates.

Insulating layer:

The range of suitable insulators is wider than that of electrodes extending from amorphous oxides and nitrides (Al_2O_3 , Y_2O_3 , Sm_2O_3 , TiO_2 , SiO_2 , ZrO_2 , $\text{Al}_x\text{Ti}_y\text{O}_z$, Ta_2O_5 , $\text{Ta}_x\text{Ti}_y\text{O}_z$, BaTa_2O_6 , Si_3N_4 and SiAlON) to ferroelectric materials (SrTiO_3 , BaTiO_3 , PbTiO_3) [25-29]. The main purpose of the insulator is to protect the phosphor layer from dielectric breakdown. Accordingly insulators must have high resistance and dielectric strength. In addition their dielectric-thickness ratio should be as high as possible. Other important properties of the insulator layer are adhesion, film stress, pinhole density, chemical stability, charge density and dielectric loss. The method for preparation of insulating films can be electron beam evaporation, reactive sputtering, radio frequency or laser heated sources.

Active layer:

The most widely used deposition method for the preparation of EL phosphor films and complete structures is sputtering in its various modifications [30,31]. Sputtering, roughly speaking, is a process where an

energetic stream of inert gas ions transfers its kinetic energy to a target material of appropriate chemical composition. Upon impact, atoms are ejected (sputtered) from the target surface on to a substrate, where they condense as thin film. Other common methods for thin film preparation are vacuum evaporation from resistance, electron beam, radio frequency or laser heated sources [25-29, 32]. The film materials can be evaporated from single or multiple sources [33,34]. The devices fabricated by the co-evaporation technique are required to undergo a current forming processes. The films prepared by evaporation or sputtering are usually annealed at 400-500°C in order to improve the crystallinity.

Chemical deposition methods in the growth of thin films are of most recent origin. One novel method in this is MOCVD (Metal Organic Chemical Vapour Deposition) [35,36], in which reactions of volatile organo-metallic compounds at atmospheric or reduced pressure are exploited. In commercial production of ACTFEL devices Atomic Layer Epitaxy (ALE) has been employed [26,37].

The preparation method critically affects several of the important properties of EL thin films. These

include crystal structure and orientation [38-40], the microstructure [38,40-44], optical properties and smoothness of the film thickness over the whole device area[45].

Rear electrode:

Usually formed by vacuum evaporated aluminium film.

Protection layer:

The device is protected from humidity usually with a Si_3N_4 over layer.

The basic structure of the device is essentially the same, but method of deposition of successive layers varies from manufacturers to manufacturers to improve the visibility under ambient illumination. Sharp Corporation (Japan) in their devices make use of metallic specular reflectors as the rear electrode but the ambient light reflection is eliminated by providing a circular polarizing filter at the front surface. A black absorbing layer in between the rear dielectric layer and the back electrode, which is a composite of Ag_2S_3 and BaTiO_3 is made use in the devices by Sigmatron Nova (USA). Oy Lohja Corporation (Sweden) devices have transparent rear electrode which makes the whole device transparent. A non critical black pigment may also be applied to the

rear surface [66]. For devices with long operating life time, different kinds of passivation layers are applied in between the successive films.

The various vacuum systems employed in the fabrication of TFEL devices are described in the following sections.

2.10 Vacuum systems for deposition of Insulators, active layers and electrodes

2.10.1 Deposition system for insulators and active layer films:

The deposition of insulator and active layers is done using a vacuum coating unit built in the laboratory. The 4 inch oil diffusion pump is connected to the coating chamber via a combined baffle and diaphragm valve which permits the diffusion pump to be kept under a vacuum and at operating temperature when the coating chamber is in atmospheric pressure. The diffusion pump is backed by a rotary vacuum pump of capacity 200 litre/minute. The diffusion pump was connected to the chamber through a liquid nitrogen trap which reduced the back streaming of the oil. The base plate has twelve feed throughs each for special purpose like current feed through, high tension for ion beam cleaning, substrate

heater, shutter, high current, thickness monitor, etc. The active layer, activator doped ZnS deposition was attempted by conventional thermal evaporation. For this an evaporation source of canoe type was made with molybdenum strip which was covered with molybdenum sheet with perforation. By passing high current through the strip fairly high evaporation rate was obtained without any spattering problem. For the evaporation of insulator tungsten baskets or molybdenum strips were used as sources. The metallic dome with cooling facility helps in the deposition of films at elevated temperatures.

2.10.2 Electron beam evaporation:

The films prepared by electron beam evaporation are smoother than films prepared by conventional thermal evaporation. A rough surface is unfavourable from the view point of EL emission stability, because clusters are considered to cause high electric fields. Moreover, conventional thermal evaporation could not be successfully used for good dielectric materials such as Y_2O_3 , Al_2O_3 , Sm_2O_3 , $BaTiO_3$, etc. The most logical approach is to use an electron beam evaporation system specially suited for the deposition of highly pure, stoichiometric films. Also, materials with extremely high evaporation temperature can be easily deposited by this technique.

In the present investigations a 3 KW electron beam evaporation unit supplied by M/s, Hind High Vacuum Company is fitted to the above home-made system. The electron bombardment heating arrangement consists of a heated tungsten filament to supply electrons. These electrons are accelerated by applying a positive potential to the material for evaporation. The electrons lose their energy in the material very rapidly, their range being determined by their energy and the atomic number of the material. Thus the surface of the material becomes molten and evaporation takes place.

The present system has a bend beam (180°) water cooled electron beam gun with four crucibles for evaporation of different materials by which sequential deposition on single substrate can be done in one vacuum cycle. A LT transformer 10V 30A is used for filament heating. The filament is kept at -6KV which can be varied from -5KV to -7KV by adjusting a potentiometer, this facilitates a 2mm shift in the striking point of the beam. The filament voltage and the beam current can be measured on the front panel meters on the power supply unit. The evaporation rate can be controlled by adjusting the beam current. With the remote control facility this can be done by visually

monitoring the source. The current and voltage stabilization in the circuit maintain the beam current and voltage irrespective of the line and load fluctuations.

The active layers are usually deposited at elevated temperature and a post deposition annealing is also required. For this, a radiant heater is fabricated which can uniformly heat the substrates. The substrate heater constructed with 1500 Watt coiled coil heater and the top of this is covered by stainless steel reflector. The heater can be clamped such that it does not come in direct contact with substrate but keeps a distance of 1 mm from the substrate. The electrical connections are taken through insulated feed throughs. The heater is powered through an auto-stat and it can be kept at any desired temperature by controlling the input power.

2.10.3 Evaporation unit for electrode deposition.

The rear electrode for the devices were metal films which were deposited by vacuum evaporation technique [46,47,48]. It consists of 2 inch diffusion pump, liquid nitrogen trap and a baffle valve connected in series to the coating chamber. Within the vacuum

chamber, filament holders, substrate heater, substrate holder, etc. are mounted on the base plate. The system can produce a pressure of 10^{-5} torr. The pressure in the system is monitored by penning and pirani gauges. A 100 $\overset{\circ}{\text{A}}$ transformer was used for resistive heating of the source. A high tension transformer is provided to power the ion beam cleaning set up in the system.

2.10.4 Thickness measurements

The film thickness were determined by two methods; viz., (i) determination from the evaporated mass, and (ii) multiple beam interferometry. The former method is used during trials and when accurate thickness are not necessary. But this will give an idea about the thickness of the film deposited by knowing the mass evaporated from the source and applying the formula for strip source $t = m/2\pi r^2 \rho$, where m is mass evaporated, ρ the density of the film, r distance between source and substrate and t the thickness of the film. For filament sources the thickness will be half of this value [49]. But for accurate measurement of film thickness multiple beam interferometric technique is used. The principle involved in this method is that, a partially reflecting surface is

placed on a totally reflecting surface forming an airwedge. Interference fringes are produced by a monochromatic parallel beam of light. The optical path difference between successive minima is λ which is the wavelength of monochromatic light used. If a step is formed by the thin film whose thickness is to be measured, the thickness of the film can be measured by knowing fringe shift and fringe separation as

$$\text{thickness} = \frac{\text{fringe shift}}{\text{fringe separation}} \frac{\lambda}{2}$$

This method was first used by Wiener [50] and further developed by Tolansky [51]. The experimental set up used for the measurement was the same as that described by Chopra [49].

2.11 Spray pyrolysis for conducting transparent electrodes

The simultaneous occurrence of high optical transparency in the visible region and high electrical conductivity is not possible in an intrinsic stoichiometric material. Partial transparency and fairly good conductivity may be obtained in thin films of variety of metals. But non stoichiometric and doped films

of oxides of tin, indium, cadmium, zinc and their various alloys, deposited by numerous techniques exhibit high transmittance in the visible region, high reflectance in the IR region and nearly metallic conductivity. The most prominent one is that of oxides of indium and tin doped with appropriate dopants. These transparent conductors have found major applications in a vast number of active and passive electronic and optoelectronic devices, as resistors, transparent heating elements for aircraft windows, antistatic coatings for instrument windows, heat reflecting mirror for glass windows and incandescent bulbs, antireflection coatings, electrodes for liquid crystal, electrochromic and ferroelectric photoconductor storage and display, selective absorber components in solar heat collectors, gas sensors, touch sensitive switches, solar cells, SIS heterojunctions, etc. [52].

With increasing sophistication of the active and passive devices based on transparent electrodes extensive investigations are being carried out especially in the preparation and characterisation of these films [52-55].

A variety of thin film deposition techniques

have been employed to deposit transparent conducting oxides. Since electrical and optical transport of these films depend strongly on their stoichiometry and the nature of impurities present, each deposition technique with its associated parameters yield films of different properties. The films have been prepared by almost all thin film deposition techniques such as oxidation of metal [56], reactive evaporation [57], direct evaporation by thermal [58] and EBE [59], sputtering [60], reactive ion plating [61], chemical vapour deposition [62], spray pyrolysis [63], dip technique [64], chemical solution growth [33].

The transparent electrodes for the present investigations were obtained by spray pyrolysis method. By this method high quality film with high transmittance and low resistivity can be got with much simple experimental set up.

Spray pyrolysis involves spraying a solution, usually aqueous, containing soluble salts of the constituent atoms of the desired compound on to heated substrates. The technique is very simple and is adaptable for mass production of large area coatings for industrial application. Important parameters are

the nature and temperature of the substrate, the solution composition, the gas solution flow rates, the deposition time and the nozzle to substrate distance. In the present case a number of trials were made to optimize these parameters. The glass plates to be coated was first thoroughly cleaned in detergent, chromic acid and distilled water. It was then placed on hot plate made of thick stainless steel which can be heated upto 500°C . The spray solution was prepared of $\text{SnCl}_4 \cdot 5\text{H}_2\text{O}$ which is saturated in isopropyl alcohol. The spray was produced by blowing compressed air into the sprayer and was controlled by adjusting the valve. Spraying was done such that it hits the hot substrate at about 45° and the substrate to nozzle distance was about 30 cms. The substrate temperature was maintained at 450°C . The films prepared under these conditions show a sheet resistance of $\sim 80 \Omega/\square$ and transmittance above 85 percent. In order to make pattern, selective removal of SnO_2 films was done by etching the film with nascent hydrogen. These films have got good adhesion to the substrate and can be subjected to ordinary cleaning procedures.

2.12 DC TFEL Devices

In the field of EL devices heterojunctions are currently being investigated as a means of making, efficient large area emitters in materials which are poor amphoteric semiconductors, i.e., which cannot be made with both n-type and p-type conductivities. Heterojunction is the generic name given to the interface between two dissimilar materials. For example the interface between a metal and an insulator or between two semiconductors can be termed as heterojunction. Heterojunctions can be abrupt or graded rather like p-n junctions. Often the intermediate layer in graded heterojunctions is intrinsic layer of one of the bulk material so that the structure is essentially p-i-n structure used for double injection studies [65]. The versatility of design is that i region can be designed for maximum recombination properties while n and p region can be designed independently to give good current carrying properties. Basically there are two methods of forming heterojunction, (i) Alloying, in which the two solids are cleaned and heated so that the lower melting point one is melted and alloyed with material of higher

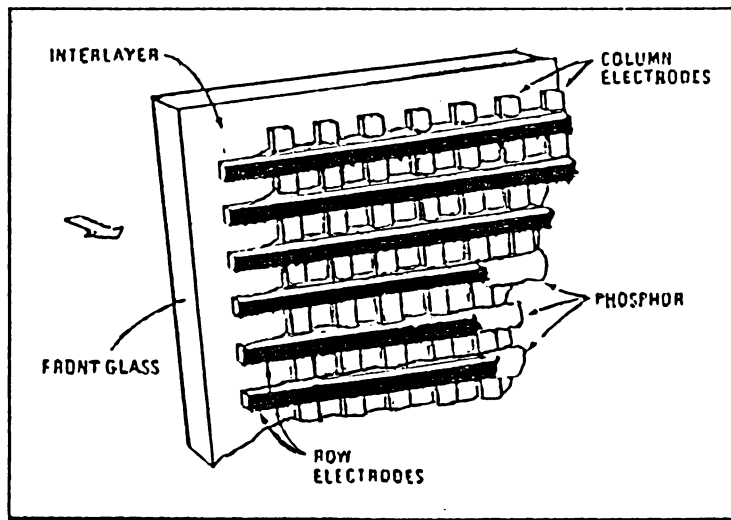


Fig.2.8. Structure of a DC TFEL device

melting point on subsequent cooling, (ii) Deposition, in which the second material is grown by conventional vapour or liquid transportation techniques on the surface of the other. Fig. 2.8 shows the cross-sectional view of a typical DC TFEL device. A thin ZnS film was evaporated onto glass substrate coated with SnO₂ film. The p-layer is formed over this usually by Cu_xS layer formed by alloying or deposition by conventional vapour or liquid transportation techniques. The doped ZnS and outer electrodes were evaporated by vacuum evaporation. The device is encapsulated and sealing is done in the presence of an activated molecular sieve.

REFERENCES

- [1] A Vecht, N J Werring, R Eillis and P J F Smith;
Brit.J.Appl.Phys. (J.Phys.D), 2(1969) 953.
- [2] A Vecht and N J Werring; J.Phys.D. Appl.Phys.,
3(1970) 105.
- [3] W Froelich and A P Cleiron; J.Electrochem.Soc.,
106(1959) 672.
- [4] K W Wagner; Archiv fur Electrotechnik, 2(1914) 371.
- [5] S Roberts; J.Opt.Soc. Am., 42(1952) 850.
- [6] W F Brown Jr; J.Appl.Phys., 23(1955) 1514.
- [7] R S Smith; J.Appl.Phys., 27(1956) 824.
- [8] J A Reynolds and M J Hough; Proc.Phys.Soc.London,
B 70(1957) 764.
- [9] G Destriau and H F Ivey; Proc. IRE, 43(1955) 1911.
- [10] G F Alfrey and J B Taylor; J.Appl.Phys., Suppl.No.4(1955)44.
- [11] P Zalm, G Diemer and H A Klassens; Philips Research Repts.,
10(1955) 205; for further reference see H F Ivey,
Advances in Electronics and Electron Phys. Suppl.1.
Electroluminescence and related effects, (Academic
Press, New York, 1963).

- [12] H F Ivey; Advances in Electronics and Electron Physics. Suppl.1. Electroluminescence and related effects (Academic Press, New York, 1963) p. 122.
- [13] Jarrel Ash Instruction Manual, Engineering Publication, No.82.00/IMRW 7(1971).
- [14] S M Pillai and C P G Vallabhan, J.Instru.Soc.India, 12(1982) 7.
- [15] EMI Photomultiplier tubes, (1979).
- [16] Hewlett Packard Photomultiplier Tube Catalogue, (1983).
- [17] A Vecht; J.Cryst.Growth, 59(1982) 81.
- [18] Hiroshi Kawanada and Nobumasa Ohshima; Proc. IEEE,[7] 61(1973) 907.
- [19] C J Alder, A F Cattell, K F Dexter, M Dixon, J Kirton and M S Skolnick; IEEE Trans on Electron devices, Ed. 28(1981) 680.
- [20] A Vecht, N J Werring, A Ellis and P J F Smith; Proc. IEEE, [7] 61(1973) 902.
- [21] D Kahng; Appl. Phys. Lett., 13(1980) 210.
- [22] M J Russ, D I Kennedy; J.Electrochem.Soc., 114(1967)1066.

- [23] T Inoguchi, M Takeda, Y Kakihara, Y Nakata and M Yoshida;
74 SID Intern. Symp. Digest, (1974) pp.84-85.
- [24] J Ohwaki, B Tsujiyama and H Kozawaguchi; Jpn.J.Appl.Phys.,
23(1984) 699.
- [25] M G Clark; Proc. 9th Int. Vacuum Congr. and 5th Int.
Conf. Solid Surfaces, Madrid 1983, p. 499.
- [26] T Sutola, J Antson, A Pakkala and S Lindfors; SID 80
Digest, 11(1980) 108.
- [27] K Okamoto, M Wakitami, S Sata, S Miura, S Andoh and
S Umeda; SID 83 Digest, 14(1983) 16.
- [28] S K Tikku, G C Smith and M R Johnson; SID 83 Digest,
14(1983) 140.
- [29] K Okamoto, Y Nasu, Y Hamakawa; IEEE Trans. on electron
devices, Ed. 28[6] (1981) 698.
- [30] H Onishi, N Sakuma, K Ieyasu and Y Hamakawa; J.Electro-
chem. Soc., 130(1983) 2115.
- [31] H Onishi, K Yamamoto and Y Katayama; Conference Record
of the 1985 International Display Conference,
San Diego, (1985) p.159.
- [32] H Kobayashi, S Tanaka, V Shanker, M Shiiki and H Deguchi;
J.Cryst.Growth, 72(1985) 559.

- [33] Z Porada, E Schabowska and T Piech; Acta Physica Polonica, A 57(1980) 267.
- [34] M Abdalla, J Thomas, A Brenac and J P Noblanc; IEEE Trans., ED 28[6] (1981) 694.
- [35] P J Wright and B Cockayne; J.Cryst.Growth, 59(1982)148.
- [36] P J Wright, B Cockayne, A F Cattel, P J Oean, A D Pitt and G W Blackmore; J.Cryst.Growth, 59(1982) 155.
- [37] U Storm; Information Display, (1984) 6.
- [38] V P Tanninen, M Oikkonen and T Tuomi; Thin Solid Films, 109(1983) 283.
- [39] J A Lahtinan, A Lu, T Tuomi and M Tammenmaa; J.Appl.Phys., 58(1985) 1851.
- [40] P J Oean; Phys.Stat.Solidi., A 81(1984) 625.
- [41] M Oikkonen, M Blomberg, T Tuomi and M Tammenmaa; Thin Solid Films, 124(1985) 317.
- [42] D Thesis, H Oppalzer, G Ebbinghaus and S Schild; J. Cryst.Growth., 63(1983) 47.
- [43] D Thesis; Phys.Stat.Solidi., A 81(1984) 647.
- [44] R Menn, R J Tueta, A Izrael and M Braguier; IEEE Trans. Electron Devices, 30(1983) 460.

- [45] T R N Kutty; Thin Solid Films, 127(1985) 223.
- [46] Leon I. Maissel and Reinhard Glang; Handbook of Thin film technology, (McGraw Hill, New York, 1970).
- [47] L Holland; Vacuum deposition of thin films, (Chapman and Hall, New Fetter lane, London, 1970).
- [48] A Roth; Vacuum Technology, (North Holland Publishing Co., Amsterdam, New York, 1976).
- [49] K L Chopra; Thin film phenomena, (McGraw Hill, New York, 1969).
- [50] O Wiener, Wied. Ann., 31(1887) 629.
- [51] S Tolansky; Surface Microtopography, (John Wiley and Sons, New York, 1960).
- [52] K L Chopra, S Major and D K Pandya; Thin Solid Films, 102(1983) 1.
- [53] J L Vossen; Phys. Thin Films, 9(1977) 1.
- [54] G Haacke; Annu. Rev. Mater. Sci., 7(1977) 1.
- [55] J C Manificier; Thin Solid Films, 90(1982) 297.

- [56] T Nishino and Y Hamakawa; Jpn.J.Appl.Phys., 9(1970) 1085.
- [57] A Hjorlsberg, I Hamberg and C G Granqvist; Thin Solid Films, 90(1982) 323.
- [58] M Mizuhashi; Thin Solid Films, 70(1980) 91.
- [59] A Balasubramanian, M Radhakrishnan and C Balasubramanian, Thin Solid Films, 91(1982) 71.
- [60] R R Mohota and S F Vogel; J.Electrochem Soc., 121(1974) 394.
- [61] R P Howson, J N Avaritsiotis, M I Ridge and C A Bishop; Thin Solid Films, 58(1979) 379.
- [62] T Muranoi and M Furukoshi, Thin Solid Films, 48(1978)309.
- [63] H S Soni, S D Sathaya and A P B Sinha; Indian J.Pure and Appl. Phys., 21[4] (1983) 197.
- [64] H Dislich and E Hussman; Thin Solid Films, 77(1981) 129.
- [65] M A Lampert; Proc. IRE, 50(1962) 1781.
- [66] W E Howard; J.Lumin., 24/25(1981) 835.

Chapter-III

EL EMISSION CHARACTERISTICS OF ZnS:RE,Cl; ZnS:Cu,RE,Cl AND ZnS:Ag,RE,Cl PHOSPHORS

Abstract

Rare earth ions have got emissions in the entire visible spectrum caused by their internal momentum change. This chapter which is divided into two parts, deals with the study of EL emission characteristics of RE doped ZnS phosphors. The first part gives the preparation of white light emitting ZnS:Cu,Pr,Cl phosphor. The EL emission of these phosphors is found to depend on the frequency of excitation which make the EL device colour tunable. This effect is explained on the basis of Schön-Klasens model together with resonant energy transfer from Cu to Pr ions. The second part essentially deals with the effect of Cu and Ag ions on the EL emission spectra of rare earth ions. Some of the rare earth doped ZnS phosphors which showed spotty luminescence give good luminescence when coactivated with Cu and Ag. It is concluded that this is due to the resonant energy transfer from Cu and Ag ions to rare earth ions. In the phosphors studied efficient energy transfer appear to be taking place between Cu and Sm³⁺ ions.

PART-A

3.1 Introduction

Even today, the most important material used for photoluminescence, cathodoluminescence and electroluminescence is zinc sulphide which was first described by Destriáu [1]. Not only has ZnS held an important place in the historical development of electroluminescence, but it still figures prominently in current research and very much retains its importance in applications field. The light emitting properties of ZnS are still not fully understood. The reasons for this can briefly be summarised by saying that the macroscopic light emitting properties depend strongly on the microscopic properties of the materials employed and these microscopic variables are neither completely under control nor do they lend themselves easily to experimental study. These facts, together with the number of complexity of the microscopic properties which affect electroluminescence have led to some contradictions in apparently identical materials.

At low temperature ZnS exists in the cubic (sphalerite or zincblende) structure and at high temperature in hexagonal (wurtzite) structure. The situation,

however is far from simple because of the fact that difference in energy of the two structures is small. ZnS in common with SiC, exists in many poly types numbering at least 10[2]. In order to produce luminescence, ZnS host material should be activated by suitable impurities. Photoluminescent emission in ZnS may be activated by a variety of elements [3] such as Cu, Ag, Au, P, As, Sb, Sn, Pb, Mn, V, Fe, Na, Li, Ga, In, Tl, Sc and rare earths. The zinc vacancies in the lattice are assumed to be responsible for self activated emission [4,5].

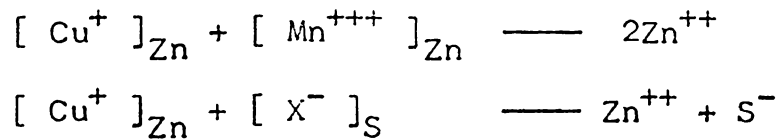
The introduction of coactivator in the ZnS lattice helps in increasing the solubility of the activator in the ZnS lattice which is usually limited except in the case of manganese. The coactivator is usually a halide (Cl, Br, I) or a trivalent element (Al, Ga, In, etc.) and its action is usually explained on the basis of charge compensation as described by Kröger [4].

The best estimate seems to be that ZnS is about 75% ionic [6,7] that is actual charges are near Zn^+ , and S^- rather than Zn^{++} and S^- (completely ionic) or Zn^{--} and S^{++} (completely covalent). Thus if ionic model is assumed

T

535.376:549.32

JAY



The symbol $[\text{Cu}^+]_{\text{Zn}}$ denotes a Cu^+ ion at a normal Zn lattice site. In the above model Mn is divalent and can readily substitute itself directly for Zn and hence no charge compensation (coactivator) is needed.

Vacant zinc lattice sites may serve as self activator centers and vacant sulphur sites may act as self coactivator centers [8,9]. When an activator is introduced into the lattice simultaneously with a coactivator an electron from the coactivator is transferred to activator atom thus affecting the charge compensation and thus increases the solubility of the activator. The presence of coactivators can influence many properties (thermoluminescence, phosphorescence, etc.) in addition to electroluminescence because, when the phosphor is excited the electrons appearing in the conduction band can be captured by coactivator centers and release them under thermal action or some other stimulation. Thus they can act as electron traps or donors just like activator center acting as hole traps or acceptors.

Various types of luminescent centers such as transition metal ions, rare earth ions and donor-acceptor pair type impurities have been studied in ZnS luminescent phosphors to achieve multicolour emission [10,11]. Rare earth ions which offer wide variety of emission wavelengths in the visible spectrum have been extensively studied in recent years. The rare earth ions in II-VI semiconductor lattices form an interesting system to study because of the energy transport and transfer mechanisms which come into play. The common feature of all the investigations on ZnS doped with rare earth phosphors is that they exhibit emission lines corresponding to $(4f)^n$ configuration of trivalent ions. Usually the emissions are superposed on strong background emission due to Cu and Mn which are added to make the phosphors luminescent. In all these systems host lattice plays an important role in the excitation of the rare earth luminescence. Since we are dealing with semiconductors, energy transport can take place via hole and electron motion. The lattice can give up large amount of energy in hole-electron recombinations which determine the emission properties.

It is found that rare earth fluorescence can be excited by energy transfer from copper or silver in ZnS.

The properties of copper doped ZnS [12,13] and silver doped ZnS [12,14] have been extensively discussed in literature. There are a few reports on rare earth doped ZnS systems [15,16]. But the effect of copper and silver ions on the emission of rare earth is still not completely clear. Also the important point of current controversial discussion is whether the rare earth ions are excited directly or by hot or ballistic electrons or indirectly by resonance transfer of energy [17,18] from electron hole pair to luminescent centers. Thus there exist sufficient reasons for making further investigations on these phosphors directed towards clarifying the various physical processes involved in its EL emission. Here the method of preparation and the emission characteristics of the white emitting ZnS:Cu, Pr,Cl phosphor whose emission wave length changes with the change of excitation frequency are outlined. The spectral characteristics and its dependence on activator concentration, frequency of applied voltage and excitation voltage are investigated in detail. Investigations are also made on another set of phosphors viz., ZnS:RE,Cl; ZnS:Cu,RE,Cl and ZnS:Ag,RE,Cl. RE(Pr,Nd,Sm,Eu,Gd,Tb,Dy,Er,La) whose spectral characteristics indicate that the rare earth luminescent centers can be excited by the

energy transfer from copper and silver centers.

3.2 Sample preparation

The electroluminescent phosphors were prepared by mixing a weighed amount of ZnS (luminescent grade) with known percentage of rare earth chloride (99.99% pure) and NH_4Cl which acts as flux. A slurry of the mixture was prepared in aqueous medium and this was slowly heated and dried. The resulting mass was crushed and mixed with equal amount of sulphur taken in quartz tube, and introduced into the high-temperature zone of the horizontal furnace maintained at 1050°C . One end of the furnace was closed while the other end was fitted with a small bore stopper to allow the gases evolved during the solid state reaction to escape. Firing was done at 1050° for 90 minutes. The white emitting phosphors were prepared by adding cupric acetate solution containing 0.5 wt % of copper and PrCl_3 solution containing 0.5 wt % Pr to weighed amount of ZnS along with 5 wt % of NH_4Cl added as flux. This slurry was dried and fired in the same manner as described earlier.

Another set of phosphors was prepared under the same conditions described above coactivated with copper or silver. In the case of copper or silver coactivated

ZnS:RE,Cl phosphors, the metal ions were added as cupric acetate or silver nitrate.

3.3 Experimental

The experimental investigations were carried out by preparing AC powder test cells as described in Chapter II. The spectra were recorded with 0.5 meter Jarrel Ash Scanning Spectrometer having an EMI 9683 KQB PMT with S-20 cathode as detector along with highly stabilised power supply. An EMI 9684 PMT with S-1 cathode together with a dual beam storage oscilloscope provided the instantaneous brightness measurements and wave form studies.

3.4 Results

The EL spectrum of ZnS:Pr,Cl phosphors consists of two emission bands-- one at 470 nm and the other at 570 nm. The emission intensities of these bands are found to depend both on activator (Praseodymium) concentration (Fig. 3.1) and also on frequency of excitation voltage (Fig. 3.2). An important feature of the experimental results obtained here is that EL emission shows a colour shift towards red in a striking manner as frequency of excitation voltage is increased. This

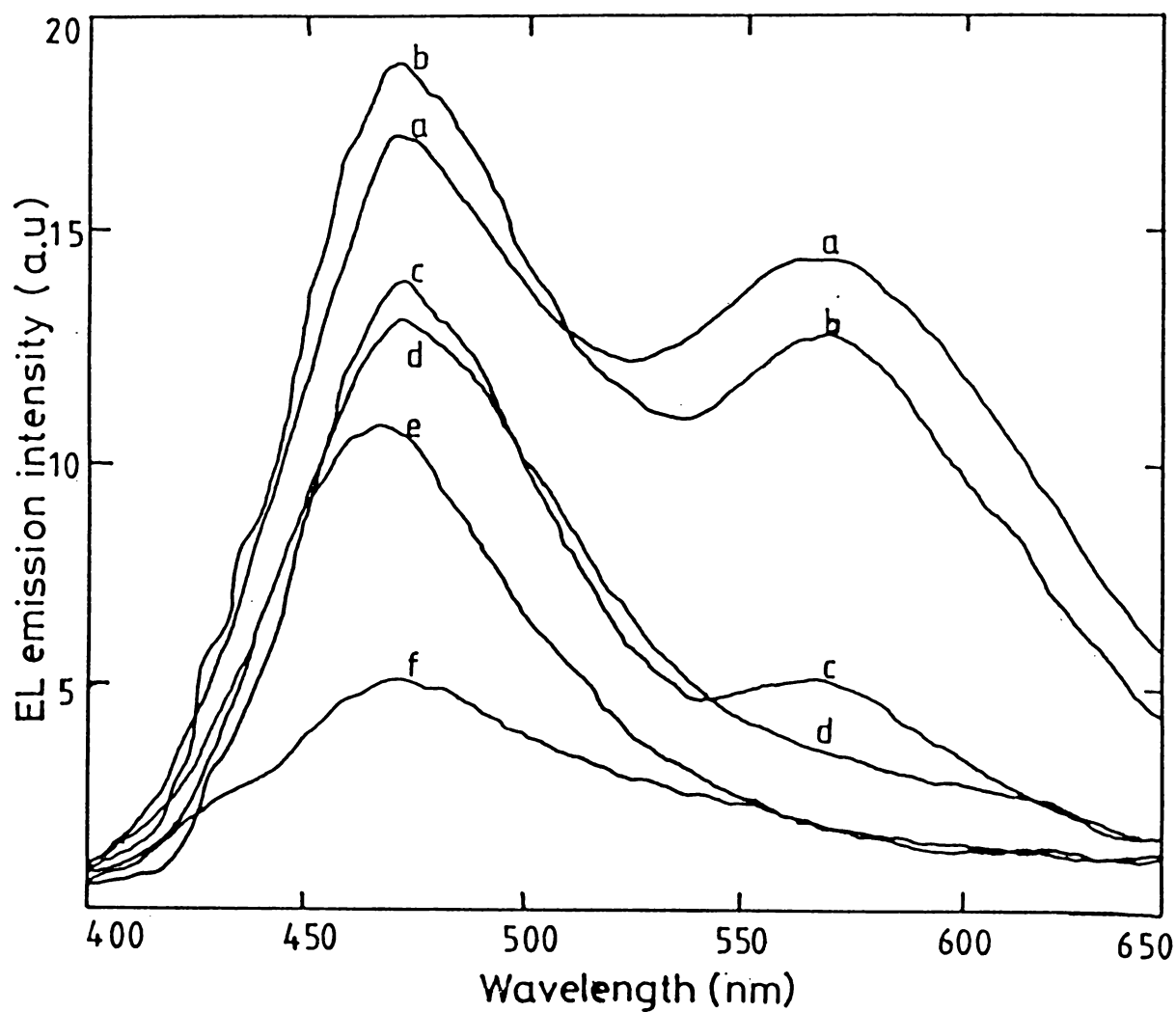


Fig.3.1. EL spectrum of ZnS:Pr,Cl phosphor containing various concentrations of Pr. a,b,c,d,e and f are phosphors containing 1.0, 0.5, 0.25, 0.1, 0.02 and 0.01 wt % of Pr respectively in the preferred mixture under 1 KHz excitation frequency and 400 volts peak to peak.

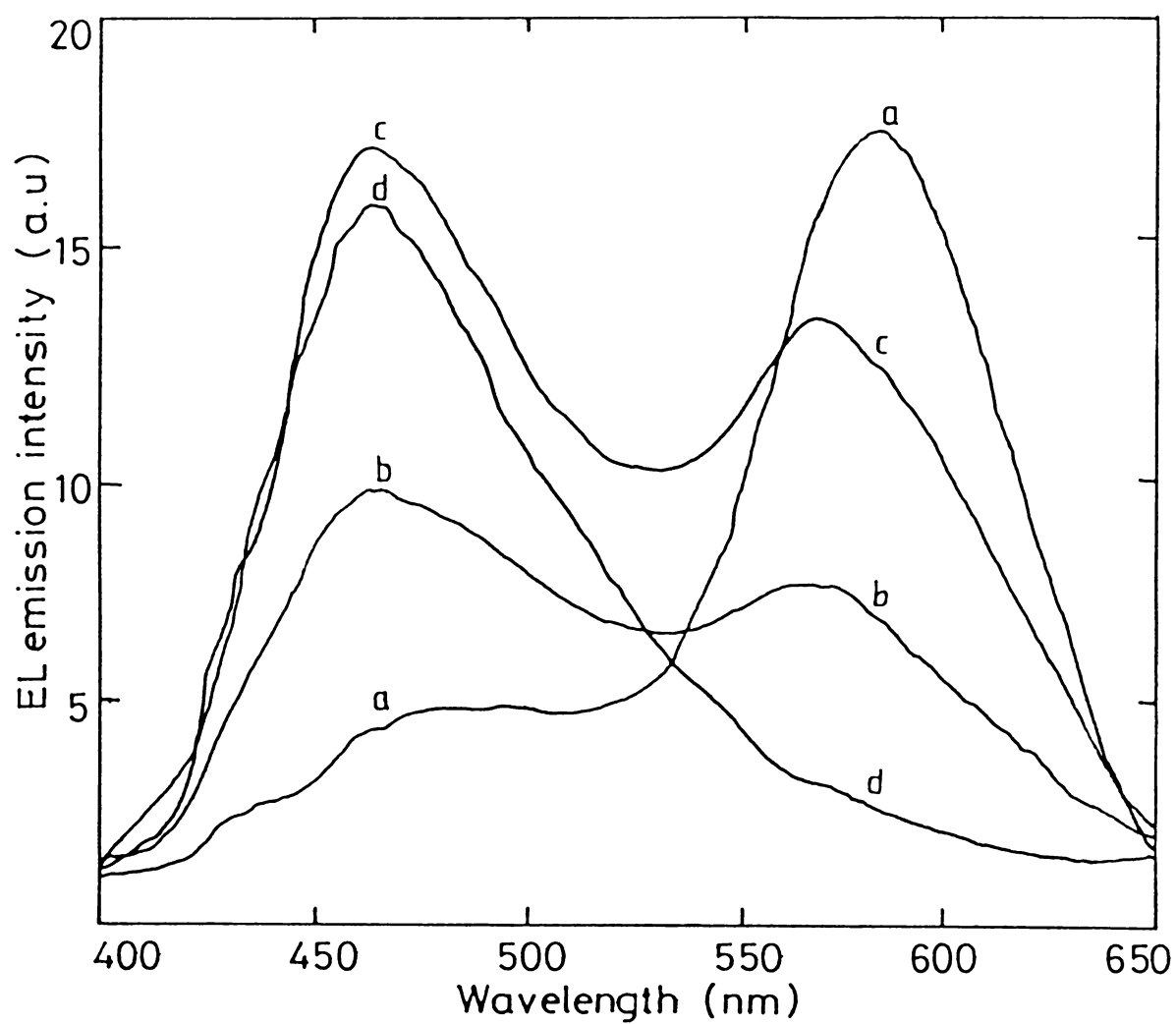


Fig.3.2. EL emission spectrum of ZnS:Pr,Cl (Pr 0.5 wt %) at various excitation frequencies under 400 volts peak to peak.
a - 100 Hz, b - 400 Hz, c - 1 kHz and d - 4 kHz.

apparently is caused by a change in relative intensities of bands rather than by a major shift in emission wavelengths. Figure 3.3 gives the variation of ratio of intensities (I_{470}/I_{570}) with excitation frequency. In the case of the EL spectrum of ZnS:Cu,Pr,Cl it has been found that emission peaks occur at 470 nm, 520 nm and 570 nm in addition to a shoulder peak at 640 nm. These phosphors also exhibit a shift in overall emission colour as the frequency of excitation is varied (Fig.3.4). Keeping the Pr doping concentration at 0.5 wt %, when Cu concentration is increased, the emission intensities of all the bands are found to increase. For a concentration of 0.5 wt % of copper at a frequency of 1 KHz for the applied voltage, the emission bands have more or less equal intensities and emission has overall white appearance (Fig. 3.5).

3.5 Discussion

The transitions giving rise to 470 nm and 570 nm can be attributed to ${}^3P_0 \longrightarrow {}^3H_4$ and ${}^3P_0 \longrightarrow {}^3H_5$ transitions of Pr^{3+} ions basing the assignment made by Magno et al. and Chase et al. [10,19]. Recombination of conduction band electron with Cu^{2+} and Cu^+ ions also may give rise to emission in these regions. But the observed proportionate increase of intensity clearly

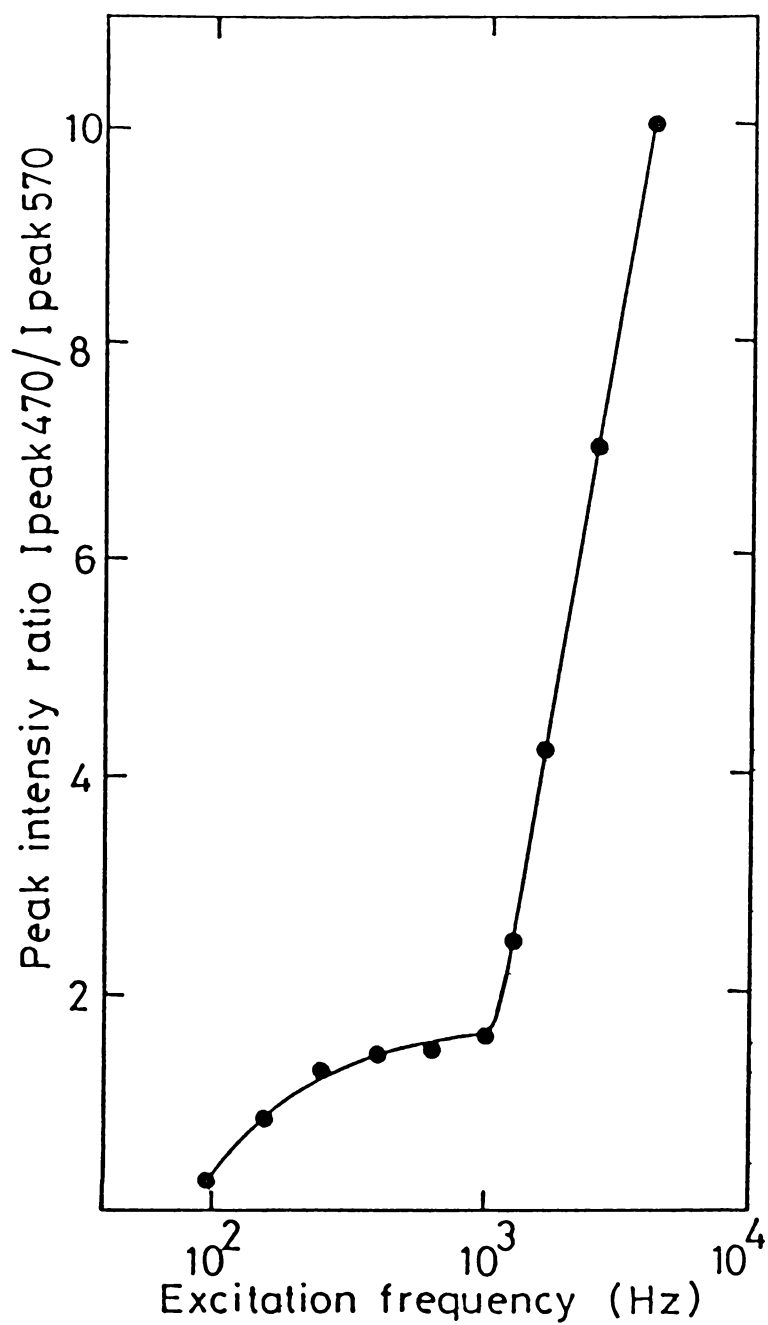


Fig.3.3. Variation of ratio of peak intensities of 470 nm and 570 nm bands with frequency of excitation voltage.

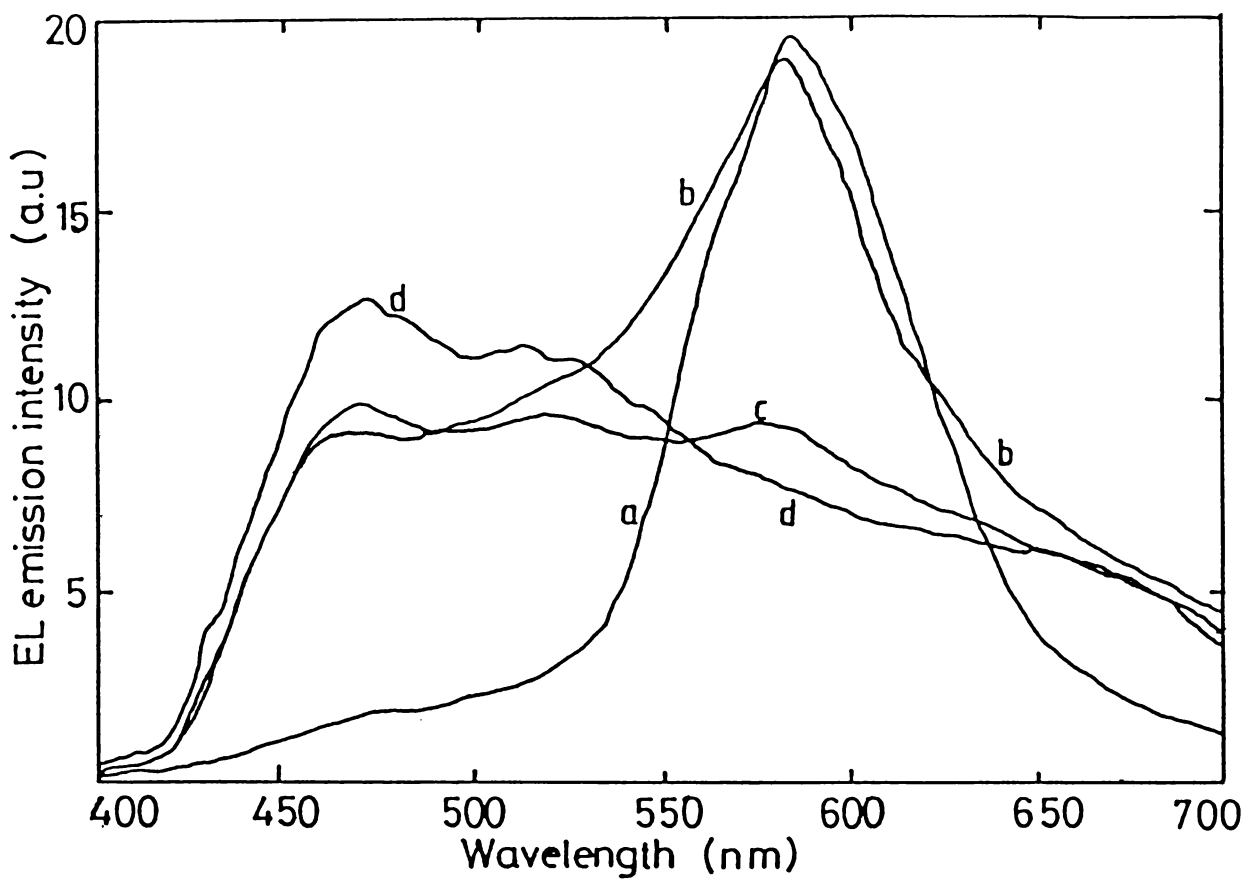


Fig.3.4. EL spectrum of ZnS:Cu,Pr,Cl (Cu 0.5 and Pr 0.5 wt %) phosphor at various excitation frequencies.
a - 100 Hz, b - 500 Hz, c - 1 KHz and d - 2 KHz.

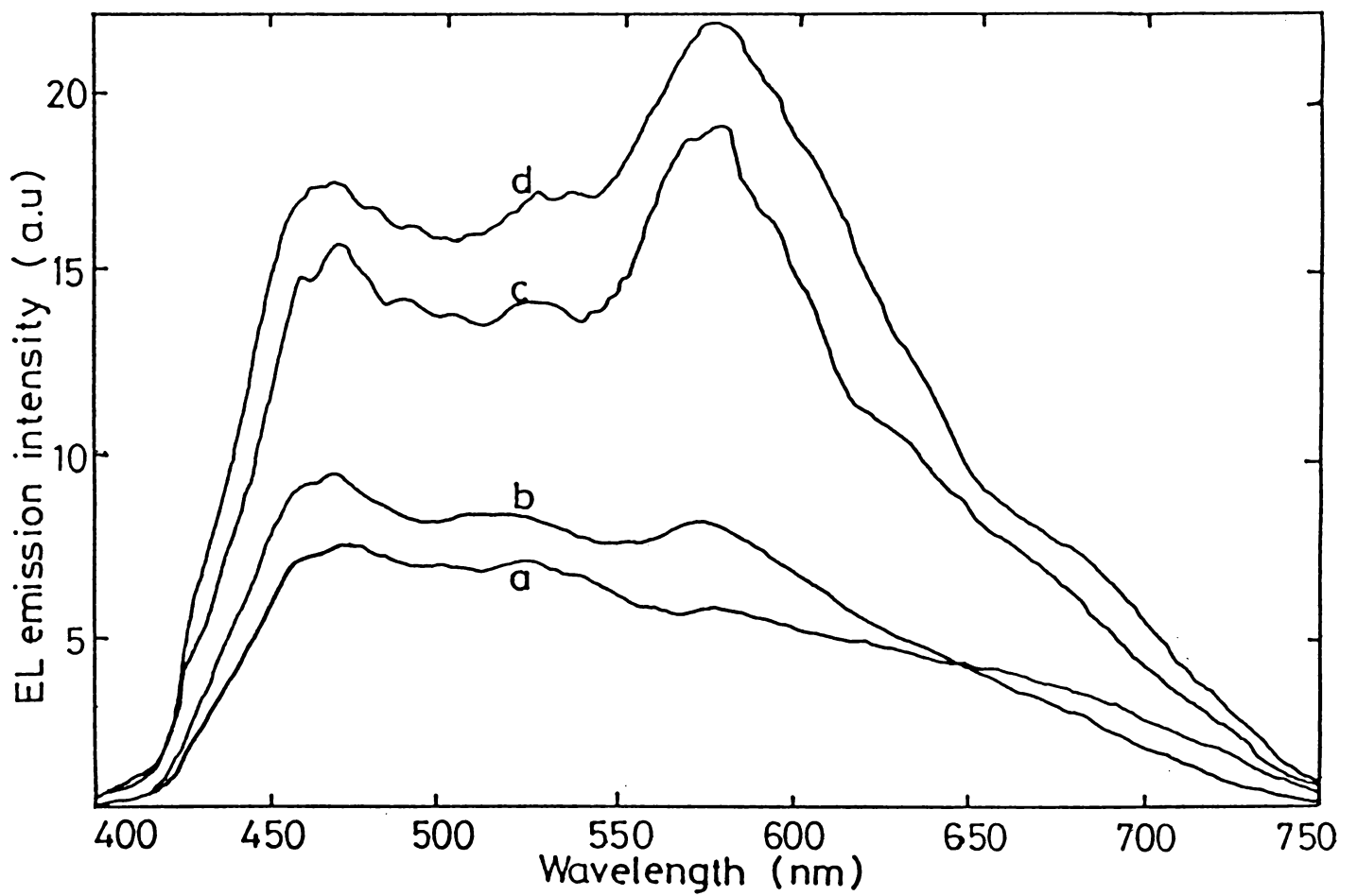


Fig.3.5. EL spectrum of ZnS:Cu,Pr,Cl phosphor at 1 KHz excitation frequency.
a - 400 V, b - 500 V, c - 600 V and d- 800 V peak to peak.

indicates that these bands originate from the transitions occurring in Pr^{3+} ions.

Figure 3.6 shows the EL emission spectra of ZnS phosphor prepared without any dopants but with 5 wt % NH_4Cl with same firing conditions of the above said phosphors. The emission spectra of this phosphor are found to be broad band centered around 500 nm which though very weak also shows a frequency dependent emission profile. The atomic absorption analysis shows that the luminescent grade ZnS used as starting material contains about 80 ppm by weight of copper. Hence the emission in this phosphor apparently arises from the presence of levels due to Cu centers in the ZnS band gap. The emission colour of ZnS:Cu,Cl phosphor depends on the amount of copper and chlorine present in the sample [20]. Also it is possible to identify three different type of centers viz., Cu^{2+} , Cu^+ and Cl^- introduced into ZnS lattice as a result of firing process [21]. It has been shown that the recombination of conduction electron with Cu^{2+} gives rise to 460 nm emission and Cu^+ gives rise to 520 nm emission [13,22].

In ZnS phosphor containing copper and chlorine the relative concentration of Cu^{2+} , Cu^+ and Cl^- ions in the

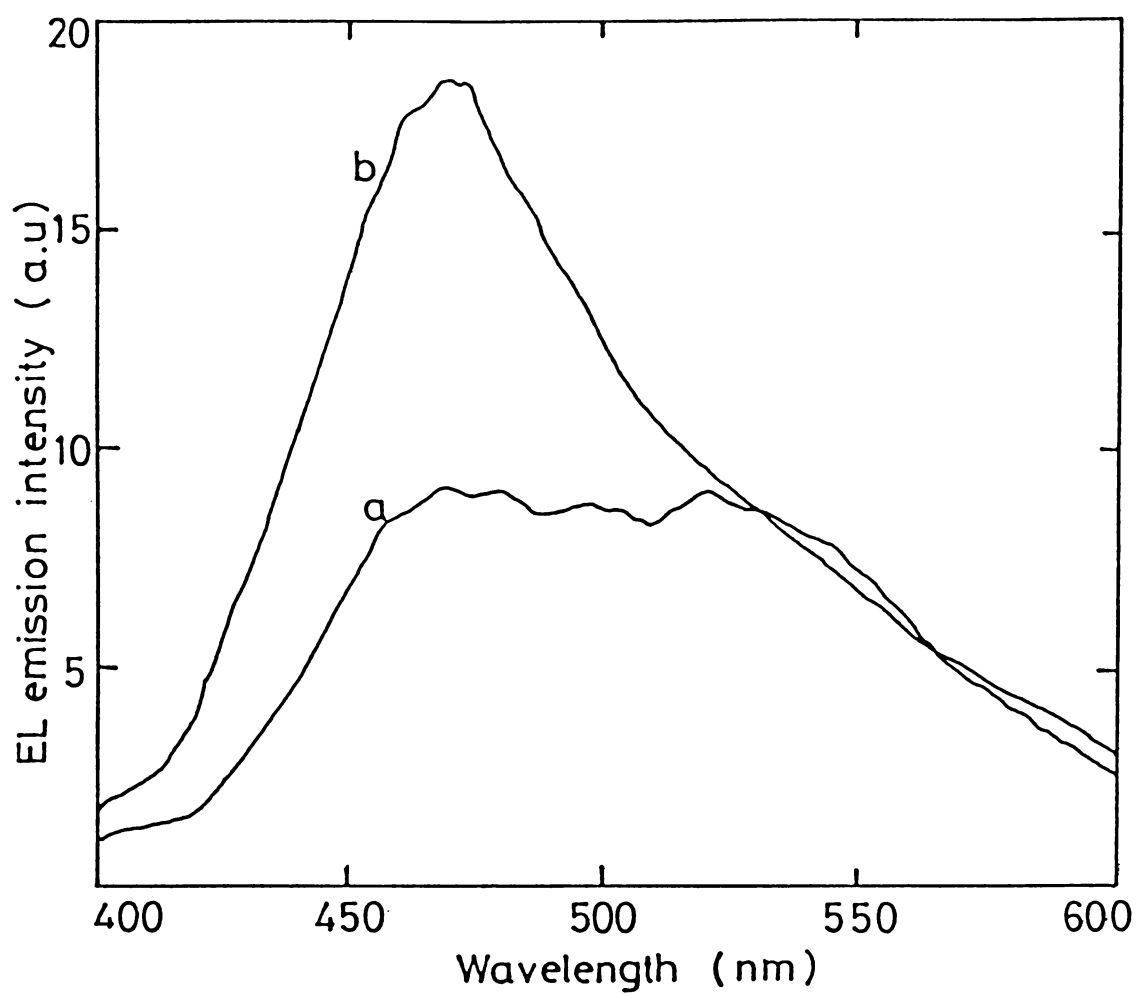


Fig.3.6. EL spectrum of ZnS phosphor without any activators at various excitation frequencies under 400 V peak to peak.
a - 100 Hz, b - 2.5 KHz.

phosphor has been found to depend on the amount of chlorine in the initial mixture [13]. Therefore in ZnS:Pr,Cl phosphors, as the amount of PrCl₃ which is the starting material for Pr doping is increased there is a good possibility of having more number of Cu⁺ centers as the original luminescent ZnS powder has been found to contain copper. Also the tendency for all Lanthanides in ZnS is to emit from levels near 20,000cm⁻¹ indicating that sensitization may involve energy transfer from Cu defects at or slightly above 20,000 cm⁻¹ [16]. In the present case the $^3P_0 \longrightarrow ^3H_4$ and $^3P_0 \longrightarrow ^3H_5$ transitions can be considered to be excited by the resonant energy transfer from Cu²⁺ and Cu⁺ levels respectively. As observed earlier [13] when the concentration of chlorine in the starting material becomes higher due to addition of higher amount of PrCl₃, the number of Cu⁺ centers may also increase. Thus intensity of 570 nm band increases at higher Pr concentration due to the possibility that this band due to $^3P_0 \longrightarrow ^3H_5$ transition of Pr³⁺ ions is excited via Cu⁺ level. The energy transfer from Cu to Pr is a resonant one, and this can be further demonstrated by substituting Ag instead of Cu as the sensitizing impurity. The ZnS:Ag, Pr,Cl has an emission band centered at 520 nm which

indicates energy transfer take place to a higher lying level compared with ZnS:Cu,Pr,Cl as observed by Kingsley et al. [16] in ZnS:Ag,Ln.

In the case of ZnS:Cu,Pr,Cl phosphors as Cu concentration is high, in addition to the transitions of Pr^{3+} ions, the chlorine levels below the conduction band get field ionized and these electrons are either raised to conduction band or they can recombine with near by Cu^+ centre with emission at 640 nm, while recombination of conduction electron with Cu^+ and Cu^{2+} centers give emissions also at 520 nm and 460 nm [13] respectively. This makes the EL emission white in appearance.

The apparant colour shift in the emission from these EL phosphors can be accounted for within the framework of the Schön-Klasens theory concerning temperature quenching of luminescence which was adopted by Waymouth et al. [23] to explain field induced colour shift in electroluminescent ZnS phosphor [24,25]. The presence of copper in the present case creates two energy levels within the band of ZnS due to Cu^{2+} and Cu^+ centers below the conduction band. An empty low lying centre will be filled by an electron

from filled higher centre, if sufficient time and activation energies are available. Thus at lower excitation frequencies, time required to transfer the electron from higher centre is available hence more frequent recombination takes place at higher centre in which emission at longer wavelength predominates. At higher excitation frequencies the case is different and there will be no transfer of electron from higher centre to lower centre which favours shorter wavelength emission. The mechanism of transport of energy from lower centre to higher centre by hole migration is as shown in Fig.3.7. But in the case of ZnS:Pr,Cl and ZnS:Cu,Pr,Cl phosphors the emissions are mainly due to ${}^3P_0 \longrightarrow {}^3H_4$ and ${}^3P_0 \longrightarrow {}^3H_5$ transitions of Pr^{3+} ions. These levels which have energies closely matching those of Cu^{2+} and Cu^+ can now be excited due to resonant energy transfer from the Cu defects to Pr^{3+} levels. Since the excitation of Cu levels is a frequency dependent process the energy transfer from Cu to Pr^{3+} ions also thus becomes frequency dependent. This evidently explains the phenomenon of frequency dependent emission colour in ZnS:Pr,Cl and ZnS:Cu,Pr,Cl phosphors.

The log B vs log V plot (Fig. 3.8) shows that brightness-voltage relation follows $B = bV^n$ where b and n

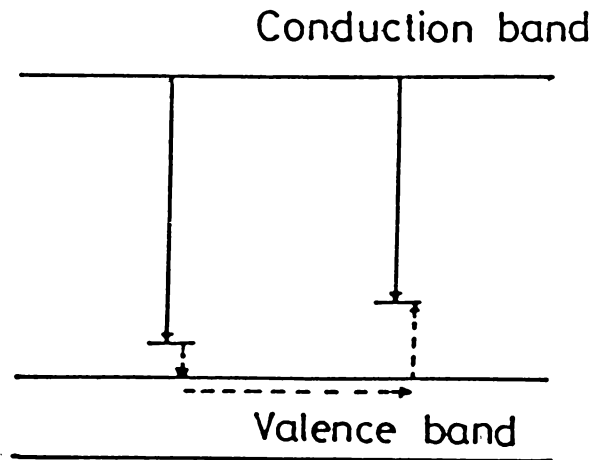


Fig.3.7. Schon-Klasens scheme. The transport of energy from lower to higher centers by hole migration is shown by the dotted arrows.

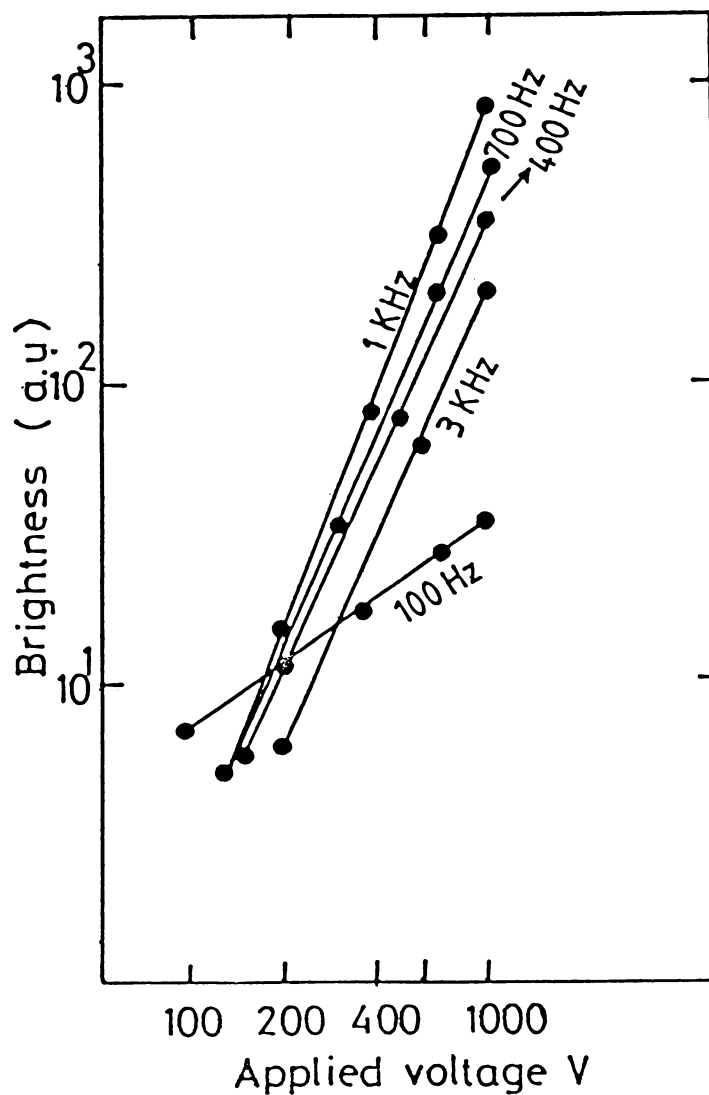
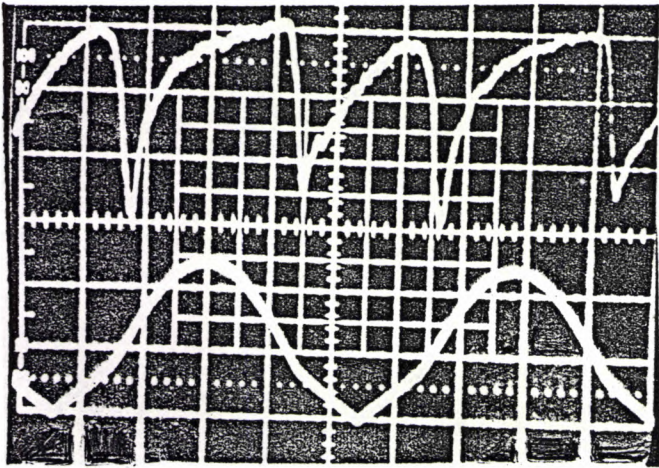


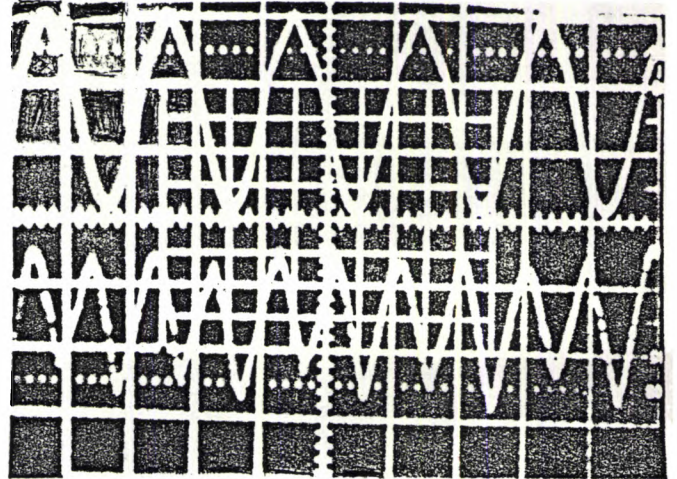
Fig.3.8. Log B vs log V plot of a typical ZnS:Pr,Cl EL cell excited at different frequencies.

are constants. This can be considered as a special case of Destriau relation [26] given by $B = B_0 V^n \exp(-b/V)$. Such characteristics arise when carrier acceleration is occurring at a Mott-Schottky barrier. Mott-Schottky barrier is assumed to exist giving rise to a high field region, where carriers are accelerated to energies necessary for the ionization of luminescent centers. The width of the barrier is proportional to \sqrt{V} . But if width of barrier becomes equal to the length of crystal, then barrier width cannot increase any more by the field and width changes proportional to the voltage and we have the above relation $B = B_0 V^n \exp(-b/V)$. Such a transition has been interpreted by many workers in terms of size of the particles or length of the comets [27,28].

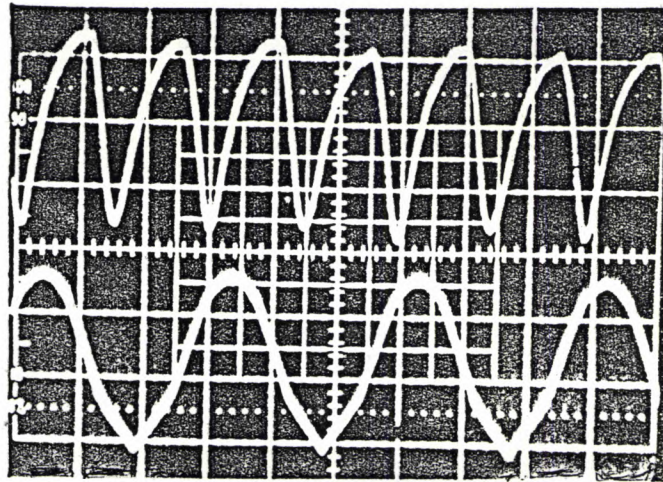
Figure 3.9 shows the brightness waves of ZnS:Pr,Cl phosphors at different frequencies. From the figure it is clear that the emission maxima are not in phase with the applied voltage maxima, and the two peaks are not identical but one is slightly higher than the other. The observed phase change according to Destriau [26] is due to the fact that the field acting on the crystals is out of phase with field in the insulator. When a voltage is applied to the cell, within the cell, the



(a)



(b)



(c)

Fig.3.9. The brightness waves of ZnS:Pr,C1 EL cell at 400 volts.
a - 50 Hz, b - 2.5 KHz and c - 700 Hz.

field experienced by the phosphor particles will be out of phase with the field in the insulator and the crystal, the former leading the latter by an angle \mathcal{A} such that [26]

$$\tan \mathcal{A} = 2/k_1 \rho f \quad 3.1$$

where k_1 is the dielectric constant of the crystal, ρ is the specific resistance and f is the frequency. But the field in the insulator also lags with respect to the potential applied to the EL cell by an angle γ such that

$$\tan \gamma = \frac{2k_2 \rho f}{4b/a + k_1 \rho^2 f^2 (k_2 + k_1 b/a)} \quad 3.2$$

where k_2 is the dielectric constant of the insulator, a is the thickness of the phosphor layer and b is the thickness of the insulating layer. Thus

$$\begin{aligned} \phi &= \mathcal{A} - \gamma \\ \text{and } \tan \phi &= \frac{\tan \mathcal{A}}{1+kx} \end{aligned} \quad 3.3$$

with $k = k_2/k_1$ and $x = a/b$

Thus total phase change ϕ becomes zero if there is no insulator ($b = 0$ ie. electrodes in contact with the crystal) and it increases upto \mathcal{A} when a/b is decreased to a very small value.

The asymmetry in the brightness waves results from the asymmetric structure of the EL cell due to the introduction of the mica sheet.

PART B

3.6 Emission characteristics of ZnS:RE,Cl and ZnS:(Cu/Ag),RE,Cl Phosphors

Sensitized luminescence from ZnS phosphors activated with rare earth ions has been subjected to a series of investigations by earlier workers [16,29,30]. But recent developments of efficient electroluminescent devices which emit basic primary colours [31] and observation of lasing phenomena in ZnS:Cu,Nd,Cl thin film direct current electroluminescent devices [32] have renewed the interest in rare earth activated ZnS phosphors. But no such phosphors, ZnS doped with rare earth ions other than Nd have been subjected to detailed investigations in spite of their great technological importance. Sensitized luminescence of rare earth ions in ZnS host lattice by Ag ions appear to be least studied. These facts prompted the investigation of spectral characteristics of ZnS:Cu,RE,Cl and ZnS:Ag,RE,Cl (RE=Pr,Nd,Sm,Eu,Gd,Tb,Dy,Er and La) phosphor systems.

The EL phosphors were prepared by mixing weighed amount of ZnS with rare earth chloride containing 1.0% RE ions and 5 wt % of NH_4Cl (added as flux). In the case of copper and silver containing phosphors metal ions are added as cupric acetate and silver nitrate. The mixture was dried. The powder thus obtained was fired at 1050°C for 90 minutes in vacuum furnace at 10^{-2} torr. The EL emission spectra are found to be the same in the case of vacuum fired samples as well as samples fired in sulphur atmosphere. AC powder EL cells were fabricated using these phosphors and the emission characteristics were studied using the same set up described in the case of ZnS:Pr,Cl phosphors.

3.7 Results for $\text{ZnS:(Cu/Ag), RE,Cl}$ Phosphors

Figure 3.10 shows the EL spectrum of ZnS:RE,Cl phosphors with 1 wt % RE recorded at 1 KHz excitation frequency. Figures 3.11 and 3.12 are the EL spectra of ZnS:Cu,RE,Cl and ZnS:Ag,RE,Cl phosphors containing RE 1 wt % and metal ions 0.5 wt % recorded at 1 KHz excitation frequency. The various emission bands recorded in the present case can be assigned to rare earth transitions by comparison with data available in the literature [37] for these ions as dopants in LaCl_3 [Table 3. 1] [10].

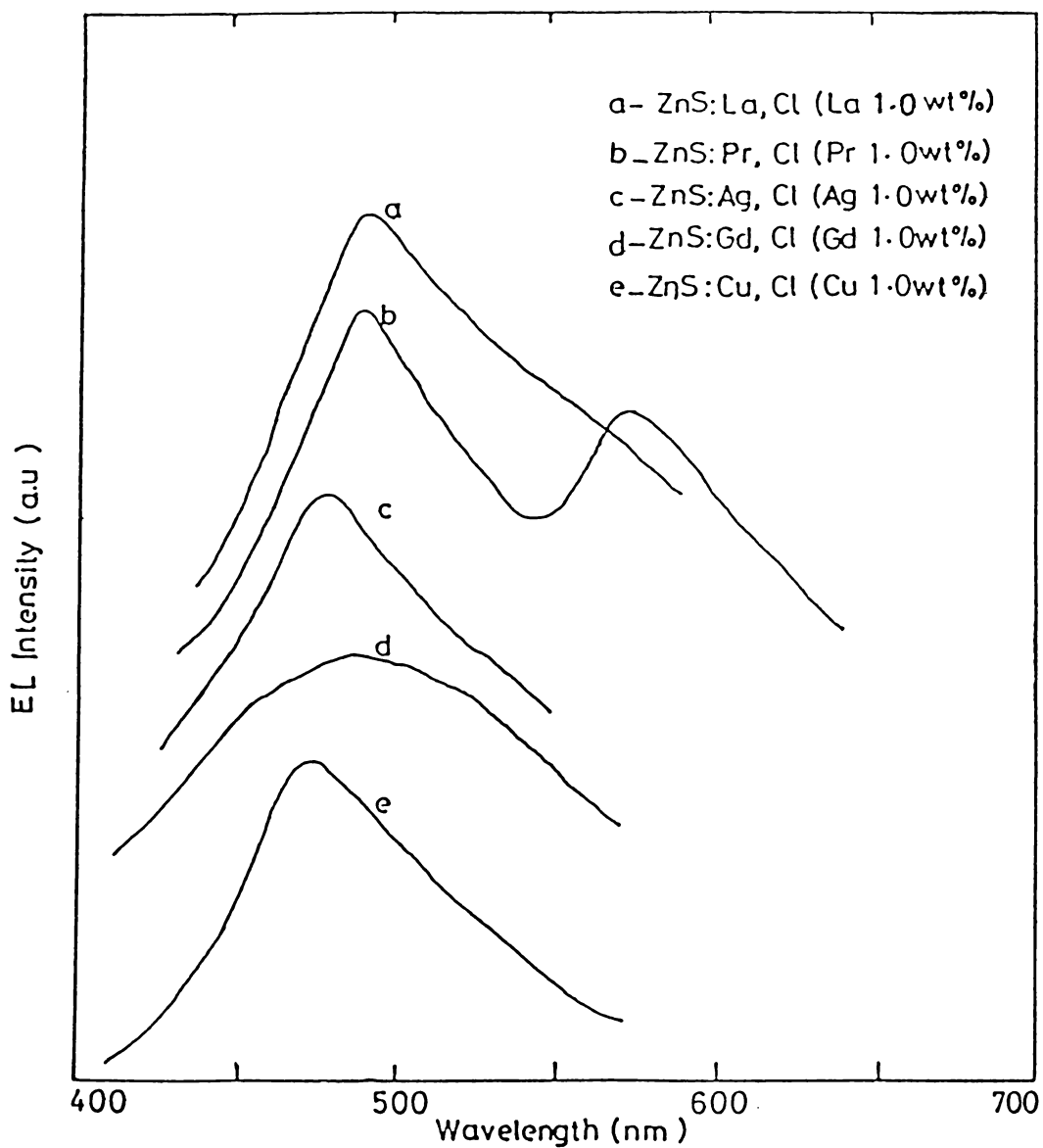


Fig.3.10. EL spectra of ZnS:RE,Cl; ZnS:Ag,Cl and ZnS:Cu,Cl phosphors at 1 KHz excitation frequency.

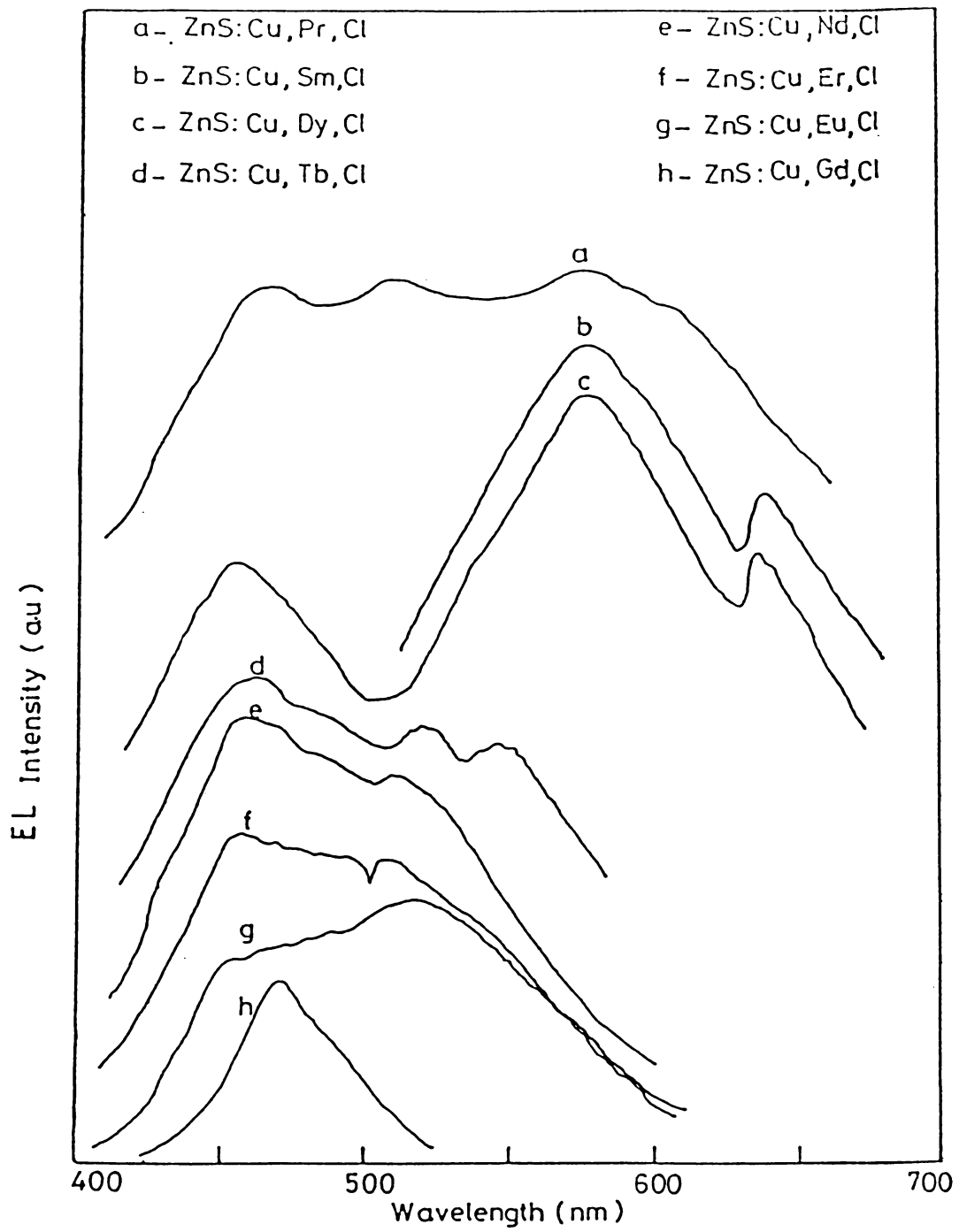


Fig.3.11. EL spectra of ZnS:Cu,RE,Cl phosphors at 1 KHz excitation frequency.

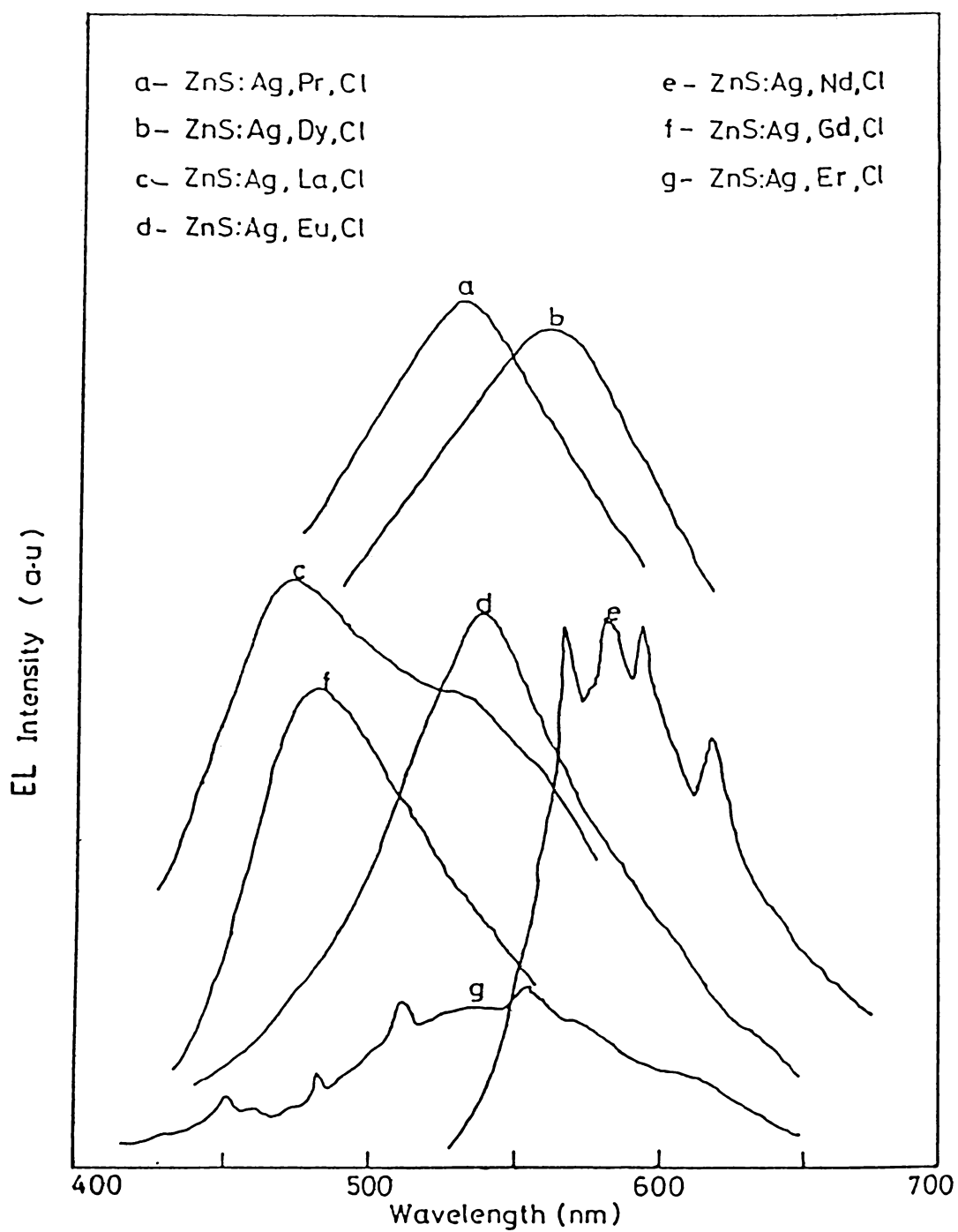


Fig.3.12. EL spectra of ZnS:Ag,RE,Cl phosphors at 1 KHz excitation frequency.

TABLE 3. 1. ASSIGNMENT FOR RARE-EARTH TRANSITIONS

Molecule	Wavelength (nm)	Assignment		
PrCl ₃	470	3P_0	→	3H_4
	500 540	3P_0	→	3H_5
	570	3P_0	→	3H_6
NdCl ₃	470	$^2P_{1/2}$	→	$^4I_{9/2}$
	520	$^4G_{7/2}$	→	$^4I_{7/2}$
	550	$^4G_{9/2}$	→	$^4I_{9/2}$
	580	$^4G_{7/2}$	→	$^4I_{9/2}$
	600	$^4G_{7/2}$	→	$^4I_{9/2}$
SmCl ₃	570	$^4G_{5/2}$	→	$^6H_{5/2}$
	620	$^4G_{5/2}$	→	$^6H_{7/2}$

Cont'd.

EuCl ₃	470	Eu ²⁺ ions	
	520	5D_0	\longrightarrow 7F_0
TbCl ₃	460	5D_4	\longrightarrow 7F_6
	520 540	5D_4	\longrightarrow 7F_5
DyCl ₃	460	$^4F_{9/2}$	\longrightarrow $^6H_{15/2}$
	540 570	$^4F_{9/12}$	\longrightarrow $^6H_{13/2}$
	620	$^4F_{9/2}$	\longrightarrow $^6H_{11/2}$
ErCl ₃	470	$^2P_{3/2}$	\longrightarrow $^4I_{9/2}$
	520	$^2H_{11/2}$	\longrightarrow $^4I_{15/2}$
	555	$^4S_{3/2}$	\longrightarrow $^4I_{15/2}$

The emission from ZnS activated with Cu or Ag is around 460 nm which is in accordance with that reported in literature [22,33].

3.8 Discussion

In the absence of metal coactivators the ZnS:RE,Cl generally shows spotty luminescence. Addition of copper or silver gives significant enhancement of EL emission intensity. Line emission has been observed in certain ZnS:(Cu/Ag) RE,Cl phosphors. The EL emission spectra of ZnS:Pr,Cl consists of two emission bands, the relative intensity of which strongly depends on excitation frequency. The dependence of the concentration and frequency dependent colour shift of emission are explained in the previous section of this chapter. In the case of ZnS:Cu,Gd,Cl phosphor no direct energy transfer from carrier collision can occur to Gadolinium since its lowest excited state lies at 4.0 eV which is well above the band gap of ZnS. The emission of ZnS:Cu,Gd,Cl is thus likely to be characteristic of the copper centers.

By substituting Ag instead of Cu as the sensitizing impurity it can be shown that the energy transfer is a resonant one. It is known that all the group 1-b elements introduce analogous defects in II-VI compounds [16].

For ZnS:Cu,Al has emission band at 440 nm (2.82 eV) and ZnS:Ag,Al has emission at 390 nm (3.2 eV) [16] due to similar defect. Thus there is reason to believe that energy transfer should occur to higher lying states in ZnS:Ag,RE,Cl than in ZnS:Cu,RE,Cl and it is found to be so in most of the cases.

Though firm conclusions cannot be drawn regarding the microscopic nature of the sensitizer and activator centers of these systems there is some evidence that the copper or silver ions and rare earth ions are close enough to mutually alter their optical spectra. For example ZnS:Pr,Cl; ZnS:Cu,Pr,Cl and ZnS:Ag,Pr,Cl each has a distinct emission spectrum. The transition of ${}^4F_{9/2} \longrightarrow {}^6H_{13/2}$ of Dy^{3+} ions lies about 30 nm lower in emission wavelength for ZnS:Ag,Dy,Cl than for ZnS:Cu,Dy,Cl. This sensitivity of the rare earth spectrum to specific group 1b element used implies that two ions are closely associated.

Except for ZnS:Cu,Sm,Cl generally ZnS:Cu,RE,Cl phosphors have emission peaks around 470 nm in addition to other peaks. However, in the case of ZnS:Cu,Sm,Cl it has been observed that the emission due to copper

centers (470 nm) is completely suppressed. This suggests that there is very efficient energy transfer to Sm^{3+} centre from copper in the case of $\text{ZnS}:\text{Cu},\text{Sm},\text{Cl}$ phosphor. The EL emission intensities were studied keeping rare earth concentration (RE = 1 wt %) while the concentration of sensitizer (Cu) is varied. The results show a clear enhancement of rare earth emission bands, with increase of sensitizer concentration to a greater degree in comparison with the band due to sensitizer (470 nm). This gives direct evidence that RE rare earth luminescent centers are excited by energy transfer from the sensitizing centers.

A plot of $\log B$ vs $\log V$ in all these phosphors at different frequencies of excitation is found to be straight lines [Fig. 3.13]. It implies that brightness (B), voltage (V) relation is of the form

$$B = bV^n \quad 3.4$$

where b and n are constants. This may be a special case of Destriau relation [26]. Such characteristics arise when the carrier acceleration is occurring at a Mott-Schottky barrier. The dependence of integrated EL output with frequency of excitation voltage has also been studied. EL emission increases linearly with

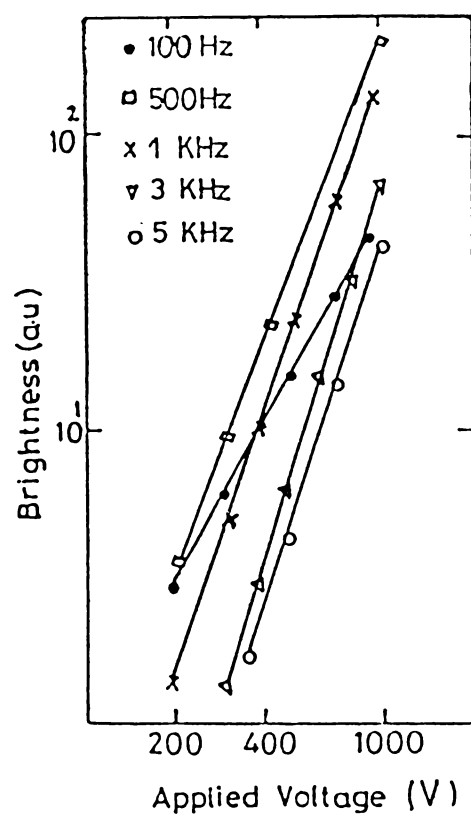


Fig.3.13. Log B vs log V plot of a typical ZnS:Cu,Dy,Cl cell excited at different frequencies.

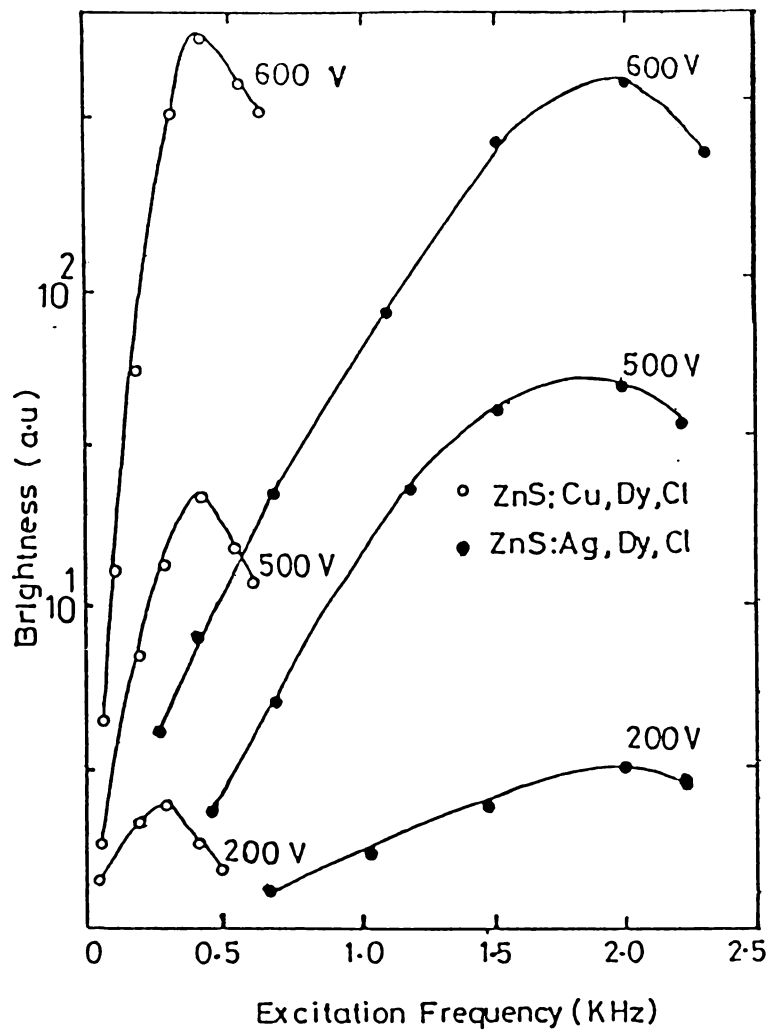


Fig.3.14. B-f plot of the ZnS:Cu,Dy,Cl and ZnS:Ag,Dy,Cl at different voltages.

frequency until saturation begins to occur [34,35]. The characteristic frequency of saturation varies from cell to cell. However, in general it is found that in ZnS:Ag, RE,Cl phosphors the saturation begins at higher frequency [Fig. 3.14] than that for ZnS:Cu,RE,Cl phosphors. These observations can be explained by assuming the bimolecular law of recombination of electrons with luminescent centers [6]. We have the relation

$$B = K n_0^2 \alpha / 1 + (n_0 / 2f) \quad 3.5$$

where B denotes EL brightness, K is a constant of proportionality, n_0 is the initial electron concentration, α is the recombination coefficient and f frequency of applied voltage. If α is large compared to f, the EL brightness will grow with frequency. When excitation frequency is sufficiently high ($n_0 / 2f \ll 1$) a state of saturation results. Decrease in EL brightness at still higher frequencies and voltage may be mainly due to the dielectric heating of the samples [36] or due to finite recombination time for carriers in the phosphor.

REFERENCES

- [1] G Destriau; J.Chem.Phys., 33(1936) 887.
- [2] P Zalm, G Diemir and H A Klasens; Philips Research Reports, 9(1954) 81.
- [3] S Rothschild; Solid State Physics in Electronics and telecommunications, Ed. M Desirant and J L Michiels (Academic Press, New York), Vol.4 (1960) p. 705.
- [4] F A Kröger and J E Hellingman; J.Electrochem Soc., 93(1948) 156, 95(1949) 68.
- [5] J S Perner and D J Weil; J.Electro Chem. Soc., 106(1959) 409.
- [6] D Curie; Luminescence in Crystals, (Methuen, London, 1963).
- [7] R F Potter, Phys. and Chem. Solids, 3(1957) 223.
- [8] M H Aven and R M Potter, J.Electrochem.Soc., 105(1958) 134.
- [9] J S Perner and F E Williams; J.Chem.Phys., 25(1956) 361.
- [10] E W Chase, R T Hepplewhite, D C Krupka and D Kahng; J.Appl.Phys., 40(1969) 2512

- [11] H Kobayashi, S Tanaka, V Shanker, M Shiiki,
T Kunou, J Mita and H Sasakuara; Phys.
Stat.Sol., (a) 88(1985) 713.
- [12] H F Ivey, Electroluminescence and related effects,
(Academic Press, New York, 1963).
- [13] S M Pillai and C P G Vallabhan; Solid State Commn.,
47(1983) 909.
- [14] P Zalm; Philip Research Repts., 11(1956)353, 417.
- [15] R C Maheswari and R K Tripathi; Indian J.Pure and
Appl.Phys., 22(1984) 102.
- [16] J D Kingsley, J S Perner and M Avens; Phys.Rev.Lett.
14(1965) 136.
- [17] D L Dexter; J.Chem.Phys. 21(1963) 836.
- [18] J Shatter and F E Williams; Phys.Stat.Solidi,
38(1970) 657.
- [19] M S Magno and G H Dieke; J.Chem.Phys., 37(1962) 2354.
- [20] W A Thornton; J Electrochem.Soc., 107(1960) 895.
- [21] M Godlewski, W E Lamb and B C Cavenett;
J.Phys.C.Solid State Phys., 15(1982) 3925.
- [22] S M Pillai, Ph.D. Thesis, (Cochin University, 1984).

- [23] J F Waymouth and F Bitter; Phys.Rev., 102(1956) 686.
- [24] H A Klasens; J.Electrochem.Soc., 100(1953) 72.
- [25] M Schon; Z-Physik, 119(1942) 463.
- [26] G Destriau and H F Ivey; Proc. IRE, 43(1953) 1911.
- [27] W Lehmann; J.Electrochem.Soc., 105(1958) 585.
- [28] A G Fisher; J.Electrochem.Soc., 109(1962) 1043.
- [29] W W Anderson; Phys.Rev., 136(1964) 556.
- [30] S Ibaki and B W Langer; Appl.Phys.Lett., 2(1963) 95.
- [31] J Benoit, B Benalloul and B Blankzat; J.Lumin.,
23(1980) 175.
- [32] G Z Zhong and F J Bryant; Solid State Commn.,
39(1981) 907.
- [33] R H Bube; Phys.Rev., 90(1953) 70.
- [34] W Lehmann; Phys.Rev., 101(1956) 489.
- [35] G H Haake; Phys.Rev., 101(1956) 490.
- [36] W W Pipper and F E Williams; Br.J.Appl.Phys.,
54(1955) 39.
- [37] A S Marfunin; Spectroscopy, Luminescence and
radiation centers in minerals, translated by
V V Shiffer(Springer Verlag, New York,1979).

Chapter-IV
ELECTRICAL AND OPTICAL PROPERTIES OF INSULATOR
FILMS USED IN THE TFEL DEVICES

Abstract:

Most of the thin film electroluminescent devices have Metal-Insulator-Semiconductor-Insulator-Metal (MISIM) structure or Metal-Insulator-Semiconductor-Metal (MISM) structure. Hence the study of electrical and optical properties of each layer of film is necessary to have a deeper understanding of the mechanism behind the light emission. In this chapter the investigations on dielectric and optical properties of Eu_2O_3 and Sm_2O_3 are given in detail. The dielectric properties of other insulators such as Na_3AlF_6 , CeO_2 , MgF_2 and SiO are also presented. From these studies it is concluded that Eu_2O_3 and Sm_2O_3 act as stable dielectric films having high dielectric constant, high breakdown strength and higher transmittance, suitable for the fabrication of low voltage operated AC TFEL devices. Also it is concluded that higher substrate temperature results in better quality dielectric films in the case of rare earth oxide films.

4.1 Introduction

The increasing requirements and complexity of electronic systems have stimulated the development of thin film microelectronics. Thin film insulators are used in a wide variety of components such as resistors, capacitors, MOSFET, etc. [1,2]. These films are usually amorphous or near amorphous, since polycrystalline films are generally found to be less insulating and single-crystal insulating films are difficult to prepare. A second virtue of amorphous films is their remarkable insensitivity to impurity, a property shared with bulk glass. However, these dielectric films are of interest only for application which are thermally and chemically stable. In thin film circuits dielectrics serve two purposes. They are used as insulating layer between crossing or superimposed conductor patterns and as capacitor dielectrics. In both cases, uniform adhesion to substrates and other materials, high dielectric breakdown strength, low dielectric constant and variation of these parameters with temperature, frequency, film thickness and applied field are also of importance to merit serious consideration in many situations.

The requirement regarding permittivity, however differs to certain extent; a low dielectric constant is preferable for insulator films, a high dielectric constant for capacitor dielectrics. The main purpose of the insulator in thin film electroluminescent device is to protect the phosphor layer from dielectric breakdown. Accordingly, insulators must have high resistance and dielectric strength. In addition, their capacitance, ie., dielectric constant, thickness ratio should be as high as possible. Other important properties of the insulating layer are adhesion, film stress, pinhole density, chemical stability, charge density and dielectric loss.

The EL structures that are commonly used are MISIM (Metal-Insulator-Semiconductor-Insulator-Metal) structure. So the insulator must be highly transparent to the radiation emitted from the phosphor layer. For films to be used in integrated optical circuits the most important characteristics are the optical attenuation and the refractive index of the films.

In this chapter the detailed investigation on dielectric properties viz., dielectric constant and loss factor and their dependence on film thickness, frequency

and temperature of Eu_2O_3 and Sm_2O_3 film are presented. It also deals with the electrical conduction mechanisms and optical properties of these films. The dielectric properties and electrical breakdown strength of other insulating materials such as MgF_2 , CeO_2 , SiO_2 , Na_3AlF_6 and BaTiO_3 are also presented at the end of this chapter.

4.2 Dielectric properties of Eu_2O_3 films

Rare earth oxide films have been studied recently [3-7] with a view to use them in thin film capacitors in which required degree of perfection varies according to specific application. Rare earth oxide films are also increasingly being used now as insulating layer in TFEL devices [8]. Dielectric constant 7-30 and relatively low dissipation factors of 0.55-2.5% are reported for oxides of lanthanum [9], cerium [10], dysprosium [5] and erbium [3]. Studies on Eu_2O_3 [7], Pr_2O_3 [11], Nd_2O_3 [6] and Dy_2O_3 [5] thin films, which forms useful capacitors showed a thickness dependent dielectric constant. The dielectric properties of rare earth oxide films are found to change with annealing or aging and they required an annealing of ~ 200 hrs to have a stable

dielectric properties [7]. But in the present case films prepared at higher substrate temperature showed better dielectric properties.

Eu_2O_3 dielectric films were prepared by vacuum evaporation of high purity (99.99%) Eu_2O_3 pellets using tungsten baskets. The electron beam evaporated films showed better surface smoothness. However, the present studies were carried out using vacuum evaporated films using tungsten baskets. The glass substrates were thoroughly cleaned first in soap solution, then in acid and distilled water. These plates were ultrasonically cleaned and dried and loaded into the coating chamber and finally they are subjected to ion bombardment cleaning. Thick aluminium (99.99%) was vacuum evaporated and this ($\sim 0.2 \mu\text{m}$) forms the rear and front electrodes in metal-insulator-metal structure. During the deposition of Eu_2O_3 film the substrate temperature was maintained at 150°C .

The dielectric and electrical measurements were carried out under vacuum of 10^{-2} torr in specially designed metallic cell in which temperature can be varied from -160°C to $+200^\circ\text{C}$. The capacitance and

loss factor were measured over a range of frequencies 1 KHz to 1 MHz using a O.1% Universal Bridge at 1 KHz and HP LCZ Bridge (Hewlett Packard Model 4277 A) in the range 10 KHz and above. The dielectric constant ϵ was evaluated from the capacitance measurement data knowing the area and thickness of the film which were measured by Tolansky's interference method. The DC current voltage characteristics and breakdown voltage were measured with the help of a highly stabilised DC power supply, ECIL Electrometer and $4\frac{1}{2}$ auto-ranging digital multimeter. The optical constants were calculated from the transmittance spectra in the UV-Visible-near IR region obtained using a Hitachi (Model 330) Spectrophotometer.

4.2.1. Dependence of ϵ and $\tan\delta$ on film thickness.

Figure 4.1 shows the variation of dielectric constant ϵ and loss factor $\tan\delta$ as a function of dielectric film thickness. The dielectric constant evaluated from the measured capacitance, effective area and film thickness, increases with increase of dielectric film thickness and attains a constant value of ~ 20.4 for insulator thickness greater than 1000 \AA .

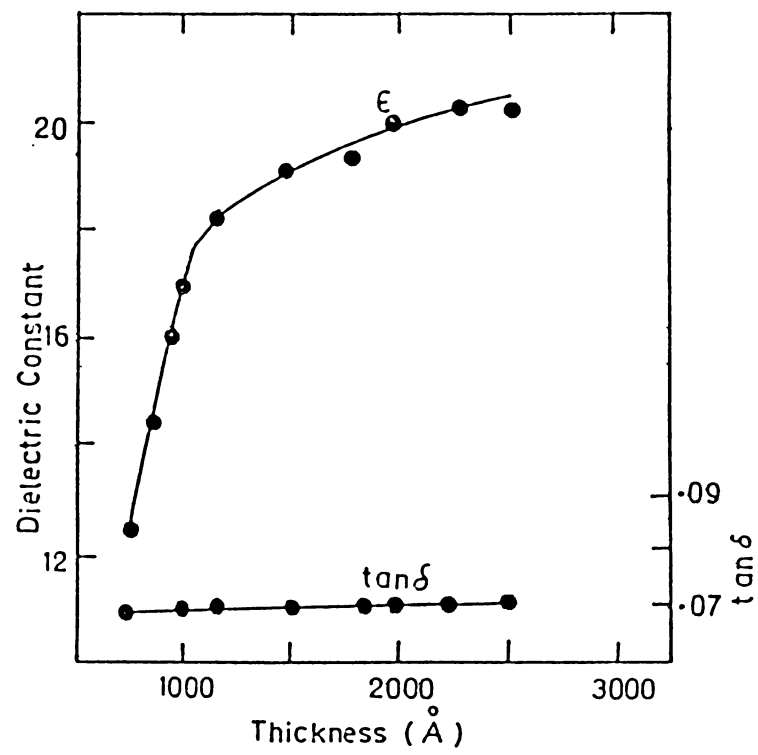


Fig.4.1. Variation of dielectric constant and loss factor with Eu_2O_3 film thickness.

The loss factor of .07 evidently is independent of film thickness. A similar thickness dependence of ϵ has been observed for films of other rare earth oxides [5-7]. The observed thickness dependence of dielectric constant on the dielectric film thickness for films less than 1000 \AA is apparently due to defects such as voids, stress, inhomogeneity etc. which are normally present in vacuum deposited thin films rather than non-stoichiometry of the deposits resulting from excess oxygen or metal ions. As films become thicker, the density of voids decreases [12] resulting in higher value of dielectric constant and eventually ϵ becomes thickness independent. A theoretical analysis by Kornyshev [30] suggests that the observed effect was too large to be ascribed to the non-local nature of the dielectric response alone and the presence of voids and other inhomogeneity contributes to the observed anomaly in rare earth oxide films.

4.2.2 Frequency and temperature dependence.

The dielectric constant (ϵ) of the Eu_2O_3 films is found to increase with increase of frequency. The variation of ϵ with frequency is small at room temperature

while at higher temperatures ϵ increases drastically with increase and decrease of frequency, i.e., the dielectric constant show a minimum at a particular frequency. The typical plot of variation of ϵ with frequency at different temperatures for a dielectric film of thickness 1200 \AA is shown in Fig.4.2. From the plot of capacitance versus temperature at different frequencies (Fig. 4.3) it is observed that at low temperature the curves merge to a single curve and below room temperature capacitance varies only slightly with temperature. On extrapolating, the static dielectric constant ϵ_s is obtained. It has a value $\epsilon_s = 16.4$. The temperature coefficient of capacitance γ_c was obtained from the graph $\gamma_c = \frac{1}{C} \frac{dC}{dt}$. The temperature coefficient of capacitance γ_c is 234 ppm K^{-1} at room temperature at 1 KHz. This value is comparable with that of other kind of dielectric materials reported in literature [5,13,14]. The loss factor $\tan\delta$ value is found to decrease with increase of frequency and attains a minimum value and again increases with increase of frequency. The variation of $\tan\delta$ with frequency is more prominent at higher temperature while at low temperature the decrease of $\tan\delta$ with frequency is less marked. Figure 4.4 shows the variation of $\tan\delta$ with frequency at different temperatures. The observed dependence of dielectric

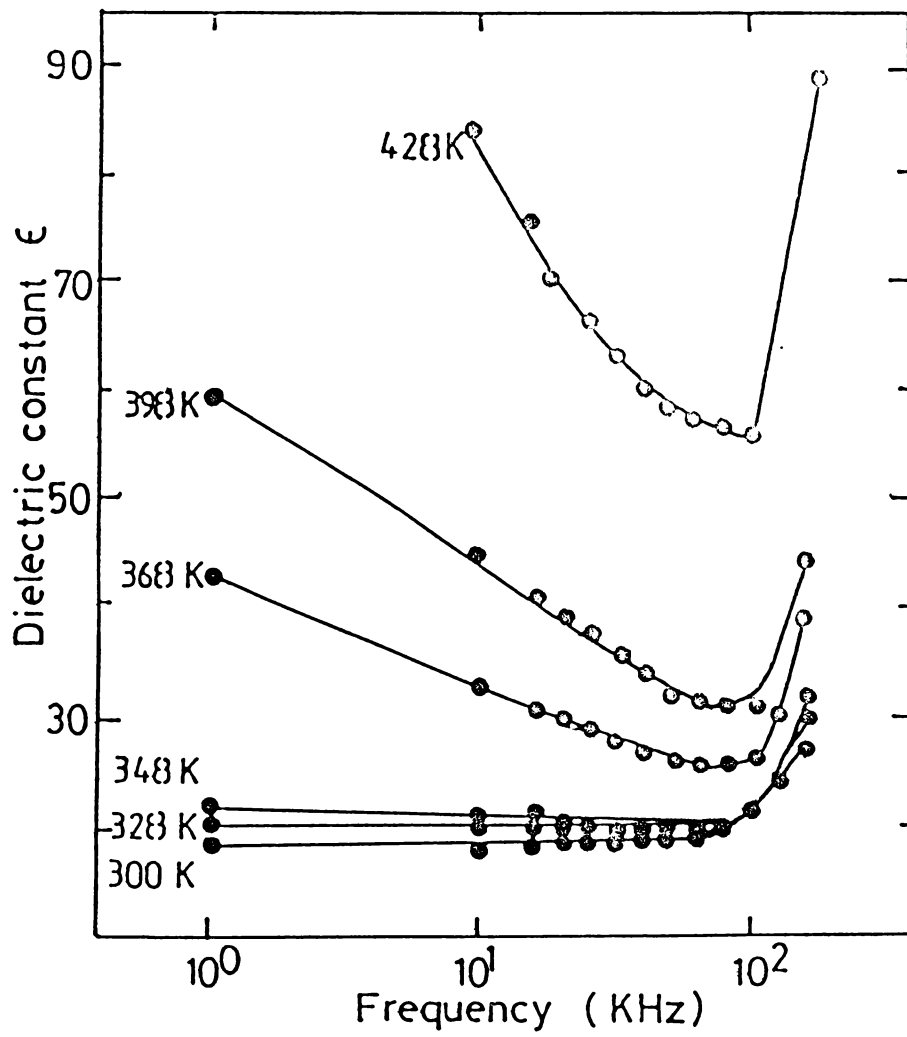


Fig.4.2. Variation of dielectric constant of Eu_2O_3 film with frequency at different temperatures (film thickness -1200 Å).

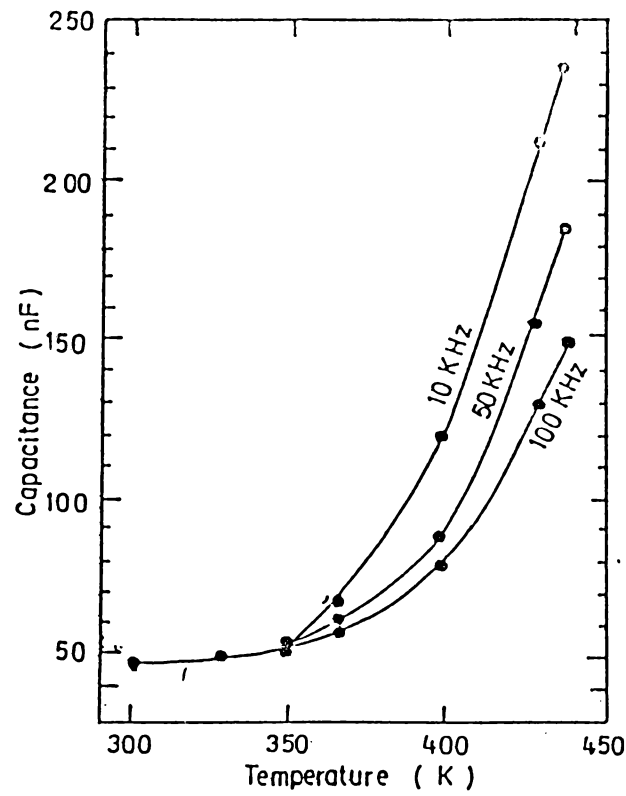


Fig.4.3. Capacitance vs temperature at different fixed frequencies (Eu_2O_3 film thickness - 1200 \AA).

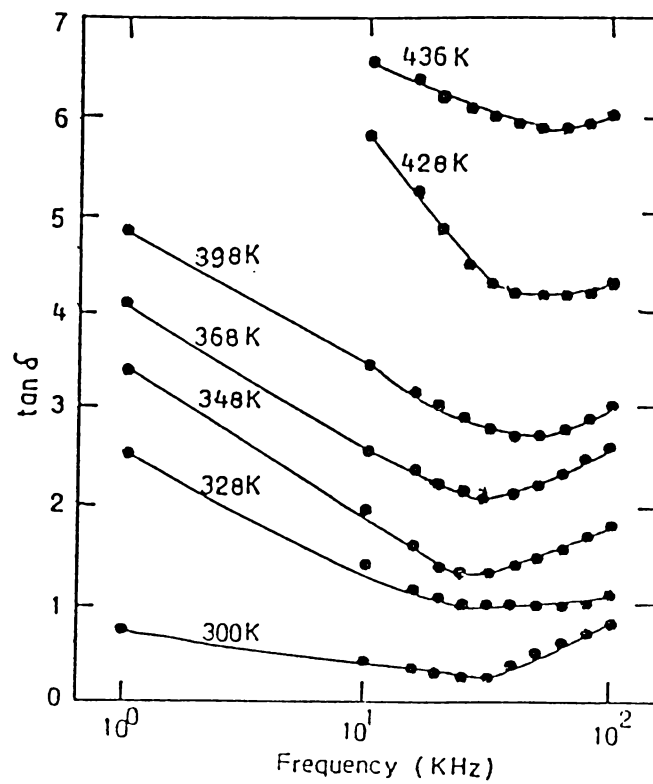


Fig.4.4. Variation of $\tan \delta$ with frequency at different temperatures (Eu_2O_3 film thickness - 1200 \AA).

constant ϵ and loss factor $\tan\delta$ on frequency and temperature may be accounted for by considering each capacitor [11] system to comprise 1) an inherent capacity element, (C) unaffected by frequency (f) and temperature, a discrete resistance element R due to the dielectric film in parallel with C and a series resistance (r) due to lead lengths, etc. The equivalent circuit is as shown in Fig.4.5. It is assumed that R will be affected by temperature as $R = R_0 \exp(\Delta E/KT)$ while lead resistance etc. will be more or less a constant and generally $R \gg r$. From Fig. 4.5a the impedance Z in terms C,R,r and ω is given by

$$Z = \frac{R}{1+j\omega RC} + r = R + \frac{r(1+\omega^2 R^2 C^2)}{1+\omega^2 R^2 C^2} - \frac{j\omega CR^2}{1+\omega^2 R^2 C^2} \quad 4.1$$

This in simpler equivalent series circuits can be represented by

$$R_s + \frac{1}{j\omega C_s} \quad \text{or} \quad R_s - j \frac{1}{\omega C_s} \quad 4.2$$

where R_s and C_s are equivalent series resistance and equivalent series capacitance.

From real and imaginary part of (4.1) and (4.2)

$$C_s = \frac{1 + \omega^2 R^2 C^2}{\omega^2 R^2 C^2} = (1 + D^2) C \quad 4.3$$

and

$$R_s = \frac{R + r(1 + \omega^2 R^2 C^2)}{(1 + \omega^2 R^2 C^2)} = r + \frac{D^2}{1 + D^2} R \quad 4.4$$

where $D = \frac{1}{\omega RC}$ since loss factor $\tan \delta$ is given by $\omega C_s R_s$

$$\begin{aligned} \tan \delta &= \frac{\omega(1 + \omega^2 R^2 C^2) [R + r(1 + \omega^2 R^2 C^2)]}{(\omega^2 R^2 C^2)(1 + \omega^2 R^2 C^2)} \\ &= \frac{1}{\omega RC} + \frac{r}{\omega R^2 C} + \omega r C = D(1 + \frac{r}{R}) + \omega r C \quad 4.5 \end{aligned}$$

This is expressed in terms of r, ω, C and R . Now differentiating $\tan \delta$ with respect to ω equation (4.5) becomes

$$\tan' \delta \omega = \frac{-r}{\omega^2 R^2 C} - \frac{1}{\omega^2 RC} + rC \quad 4.6$$

$$\tan'' \delta \omega = \frac{2r}{\omega^3 R^2 C} + \frac{2}{\omega^3 RC} \quad 4.7$$

which is positive for all values of ω, R, C and r . Hence $\tan \delta$ must pass through a minimum value and this will occur only when equation (4.6) is zero, i.e., when

$$rC = \frac{r}{\omega^2 R^2 C} + \frac{1}{\omega^2 RC} = \frac{1}{\omega^2 RC} \left(1 + \frac{r}{R}\right) \quad 4.8$$

Since $R \gg r$ in all cases we have $rC = \frac{1}{\omega^2 RC}$

Hence loss minimum will be observed at a frequency

$$\omega_{\min} = \sqrt{\frac{1}{rRC^2}} \quad 4.9$$

Again when $\omega R^2 C \gg 1$ or $\frac{r}{R} \ll 1$ which is true for all case, equation (4.5) becomes

$$\tan \delta = -\frac{1}{\omega RC} + \omega rC = D + \omega rC \quad 4.10$$

When ω is small $\frac{1}{\omega RC} \gg \omega rC$ then

$$\tan \delta = \frac{1}{\omega RC} = D \quad 4.11$$

when ω is large $\frac{1}{\omega RC}$ is generally $\ll \omega rC$ and hence

$$\tan \delta = \omega rC \quad 4.12$$

The equations (4.11) and (4.12) predict conditions when the loss factor will be inversely or directly proportional to ω . From equation (4.9) it can be seen that ω_{\min} is determined by $(\frac{1}{rRC^2})^{1/2}$ since R which is temperature dependent increases with the lowering of temperature, while r is practically a constant. ω_{\min} will also be lower at lower temperatures. Thus a shift of ω_{\min} would be to a lower frequency at lower temperatures and vice versa. The variation of $\tan\delta$ can also be explained in a similar way.

4.2.3 Breakdown field strength

The knowledge of the dielectric strength is very important for the design of thin film capacitors because it determines the voltage at which destructive breakdown of the dielectric occurs. In the case of thin film electroluminescent devices, according to Howard [15] in order to obtain high brightness and high efficiency for these devices, the insulator film used must satisfy the condition that the product of its dielectric constant (ϵ) and breakdown voltage (F_b) must at least be three times higher than the corresponding value for the active layer. For most of the dielectric film

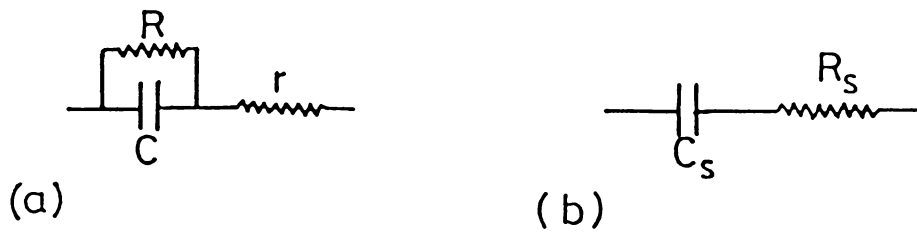


Fig.4.5. (a) Capacitor elements (C, R and r)
 (b) Equivalent circuit

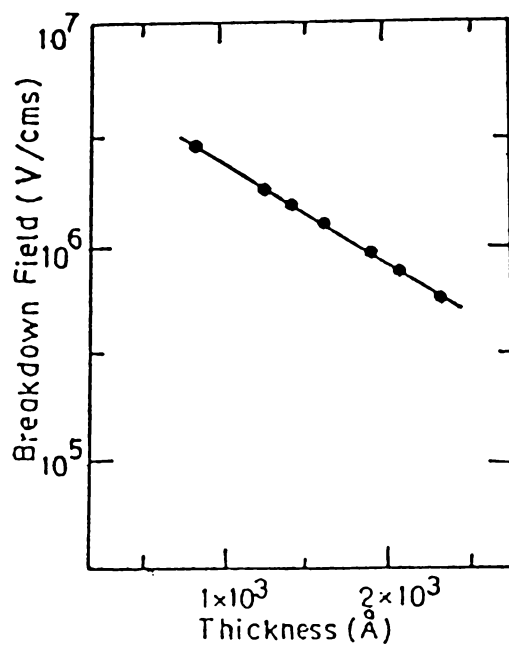


Fig.4.6. Breakdown field strength vs dielectric film thickness

materials the dielectric breakdown strength is between 10^5 and 10^7V cm^{-1} . In the present case, the Eu_2O_3 film have dielectric breakdown strength of the order 10^6V cm^{-1} . The electrical breakdown occurs either on generation of carriers or the transfer of excess energy from existing carriers to phonons. But in thin film dielectrics the breakdown due to flows in the dielectric layer is much more typical [16,17] than intrinsic breakdown, while the maximum dielectric strength in a thin film capacitor structure is often characterized by breakdown due to thermal instability [16]. The dielectric breakdown field strength F_b in the case of Eu_2O_3 film is of the order of 10^6V cm^{-1} . The dielectric breakdown field strength F_b is found to decrease with increase of film thickness. The plot of dielectric breakdown strength versus film thickness on a log scale (Fig.4.6) is a straightline having a negative slope of 0.518. Thus the breakdown field strength follows closely the Forlani-Minnaja relation [18] $F_b \propto d^{-1/2}$. Among the various kinds of mechanisms which are suggested to be responsible for breakdown [19] impact ionization can be considered as the most important reason for initiating the breakdown process. The initial electrons are injected by field emission at the cathode and the electron

current grows by collision ionization of the initial electrons. This build up of electron current finally results in breakdown.

4.3 Electrical properties

4.3.1 DC conduction.

In this section the conduction mechanisms in Eu_2O_3 thin films sandwiched between metal electrodes, i.e., conduction through the film rather than along the plane of the film is discussed. Since the films are generally of the order 1000 \AA thick, a bias voltage as low as few volts will induce fields of the order of 10^4 to 10^6 V cm^{-1} in the film. From the current-voltage (I-V) measurements of Eu_2O_3 films, it is found that $I \propto V$ in the first region, i.e., at low fields and at higher fields $I \propto V^2$ (Fig.4.7).

Though an insulator material which contains very few volume generated carriers and hence virtually no conductivity, in actual case the electrical properties of thin film insulators are determined not by intrinsic properties of the insulator but by other properties, such as the nature of the electrode-insulator contact. In the present case at low fields $I \propto V$ implies that the conduction is ohmic. A ohmic contact is capable of injecting additional

carriers into the insulator, far in excess of the bulk [20]. At higher fields when the injected free carrier density exceeds the volume generated free carrier density, space charge effects will be observed. That is, when insulator does not contain donor and film is sufficiently thick to inhibit tunneling, it will not normally conduct significant current. However, if an ohmic contact is made to insulator, the space charge injected into the conduction band of the insulator is capable of carrying current. This process is termed as Space Charge Limited (SCL) conduction. In the present case aluminium is an ohmic contact to Eu_2O_3 film and at high fields $I \propto V^2$ implies the conduction is space charge limited. The DC conductivity is calculated from the I-V measurements knowing area and thickness of the film. The temperature dependence of conductivity is given by the relation

$$\sigma = \sigma_0 \exp - E_a/kT$$

where σ_0 is pre-exponential factor, E_a activation energy, k Boltzman constant and T temperature. From the plot of $10^3/T$ versus $\ln \sigma$ (Fig.4.8) the activation energy is calculated to be 0.86 eV. The space charge limited current and low activation energy suggests the presence of shallow traps in the films. Consequently the observed

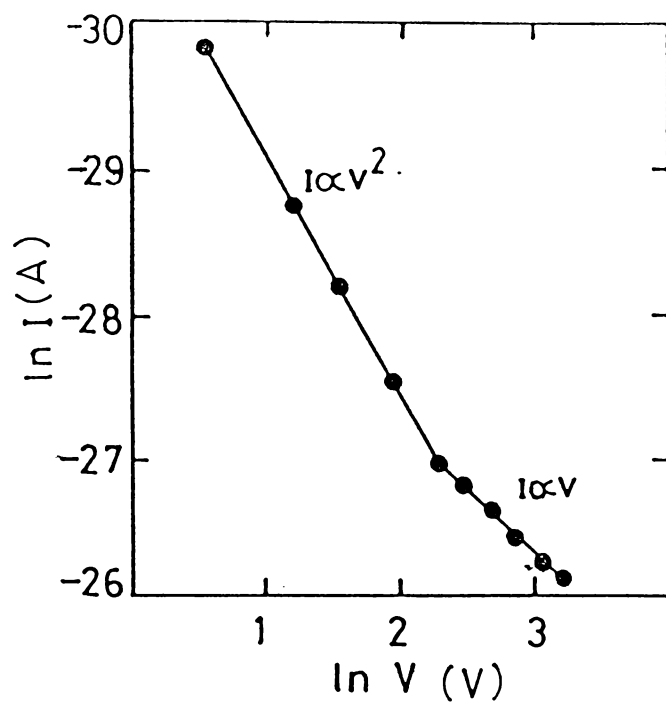


Fig.4.7. Current-voltage plot of Eu_2O_3 film

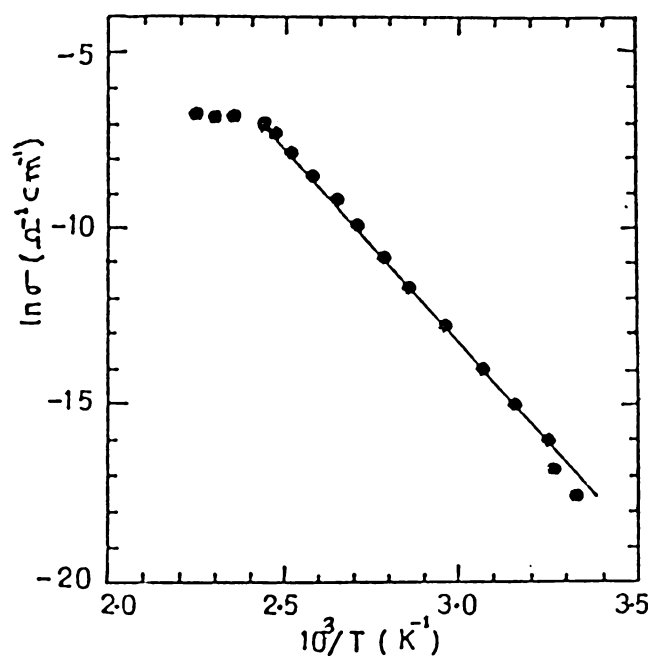


Fig.4.8. $\ln \sigma$ vs $10^3/T \text{ K}^{-1}$.

activation energy is less than the value of band gap expected.

4.3.2 AC conduction

The main advantages of A.C measurements are (i) it permits measurements in the region of low conductivity, (ii) the AC bias voltage needs only a few hundred milli volts. Thus the maximum field within the insulator film is kept minimum and there is little danger of more than one conduction process being active. Various theories were put forward by Mott and Davis [21] and these were modified by Elliot [22]. But these theories deal with AC conductivity having frequency dependence such that $\sigma_{ac} \propto \omega^s$, where $s < 1$. In practice it is observed that the AC conductivity is proportional to first power frequency or slightly less and also there exist regions where conductivity proportional to ω^2 . Such cases are discussed by Pollak [23].

AC conductivity of Eu_2O_3 films varies with frequency as shown in Fig.4.9. It can be seen that the conductivity shows two distinct dispersive regions, one below 40 KHz and the other above it. The conductivity

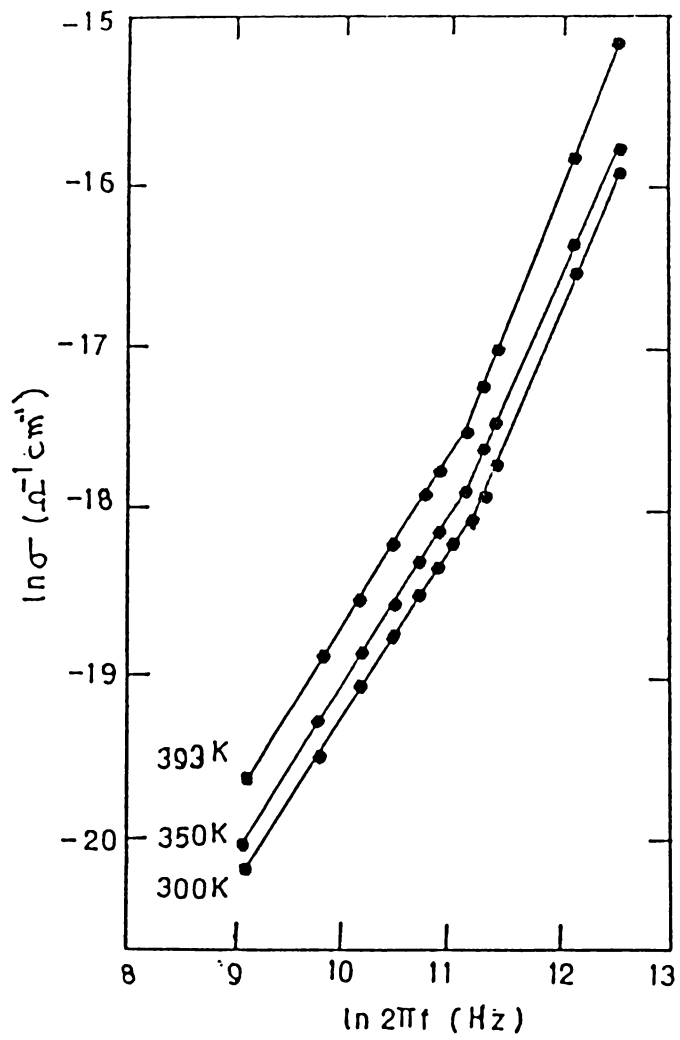


Fig.4.9. AC conductivity vs frequency at different temperatures (Eu_2O_3 film thickness - 1200 Å)

is proportional to ω in the first region and to ω^2 in the second region at room temperature. The same trend is observed at higher temperatures also. The second region of conductivity follows a square law dependence on frequency. From the plot of $\ln\sigma$ vs $10^3/T$ the activation energy is calculated to be 0.13 eV in the temperature range 300-365 K (Fig.4.10). X-ray diffraction studies show that (Fig.4.11) the film is amorphous in nature. No crystallinity was observed for films coated at higher substrate temperatures also. The low activation energy coupled with square law dependence of conductivity on frequency suggests the prevalence of electronic hopping conduction mechanism as observed in amorphous materials [23,24].

4.4 Optical properties

Optical properties of thin films become very important when they are made use of in interference filters, integrated optical circuits, etc. There are different methods to measure n and k such as spectroscopic ellipsometry, simultaneous measurement of transmission and reflection, and the measurement of reflection or transmission only. Each method has its own merits and demerits.

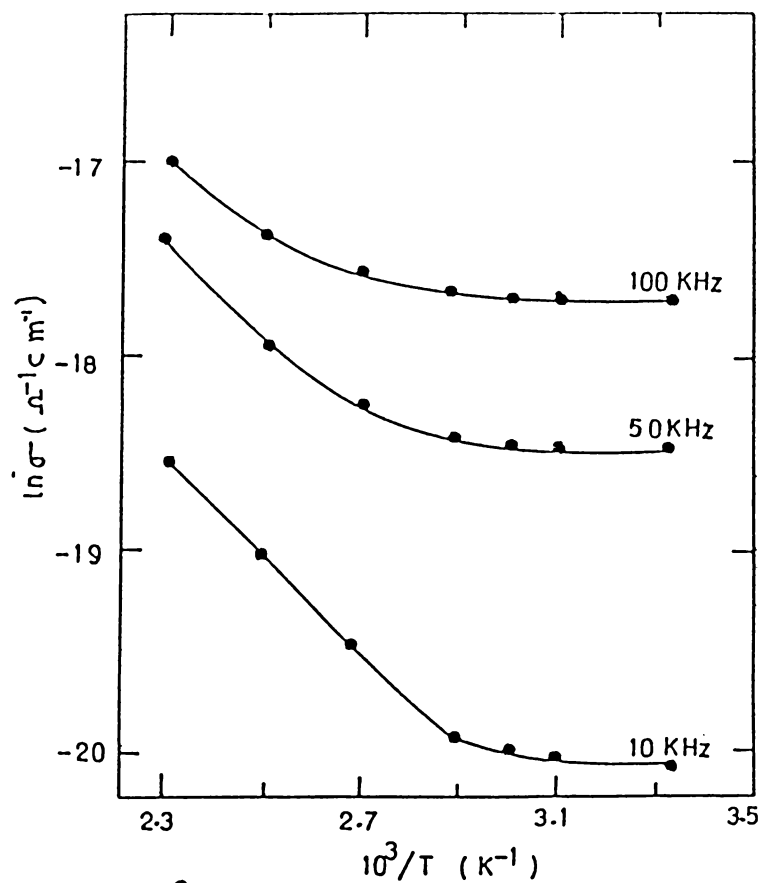


Fig.4.10. $\ln \sigma$ vs $10^3/T \text{ K}^{-1}$ at different fixed frequencies (film thickness - 1200 \AA)

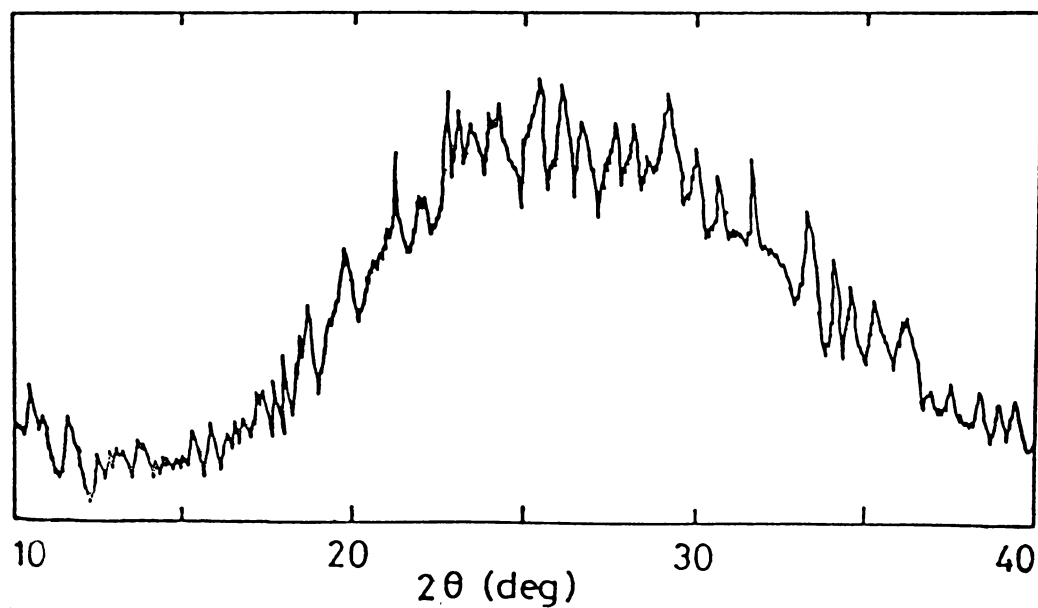


Fig.4.11. X-ray diffraction pattern of Eu_2O_3 film (Substrate temperature 150°C)

In the present case to deduce optical constant, the method proposed by Manifacier et al. [25] is used. This method is much simpler and the accuracy is of the same order as for the other conventional methods.

The thin film with complex refractive index $\eta=n-ik$ can be considered to be bounded by two transparent media with refractive indices n_0 and n_1 (Fig. 4.12). Considering a unit amplitude for incident light (in this case normal incidence) the amplitude of the transmitted wave is given by

$$A = \frac{t_1 t_2 \exp(-2\pi i \eta t / \lambda)}{1 + r_1 r_2 \exp(-4\pi i \eta t / \lambda)} \quad 4.13$$

in which t_1, t_2, r_1, r_2 are the transmission and reflection coefficients from front and rear faces. The transmission of the layer is given by

$$T = n_1 / n_0 |A|^2 \quad 4.14$$

In the case of weak absorption $k^2 \ll (n-n_0)^2$ and $k^2 \ll (n-n_1)^2$. Hence

$$T = \frac{16n_0 n_1 n^2 \alpha_1}{C_1^2 + C_2^2 + 2C_1 C_2 \alpha_1 \cos(4\pi t/\lambda)} \quad 4.15$$

where

$$C_1 = (n+n_0)(n+n_1), \quad C_2 = (n-n_0)(n_1-n)$$

and

$$\alpha_1 = \exp(-4\pi kt/\lambda) = \exp(-\alpha t) \quad 4.16$$

α is the absorption coefficient of thin film.

Generally $n > n_1$ corresponding to a semiconducting film on a transparent non-absorbing medium $C_2 < 0$. Then extreme values of transmission is given by

$$T_{\max} = 16 n_0 n_1 n^2 \alpha / (C_1 + C_2 \alpha)^2 \quad 4.17$$

$$T_{\min} = 16 n_0 n_1 n^2 \alpha / (C_1 - C_2 \alpha)^2 \quad 4.18$$

considering T_{\max} and T_{\min} as continuous functions of λ through $n(\lambda)$ and $\alpha(\lambda)$. These functions which are the envelopes of the maxima $T_{\max}(\lambda)$ and minima $T_{\min}(\lambda)$ in the transmission spectrum as shown in Figure 4.13.

The equations 4.17 and 4.18 gives

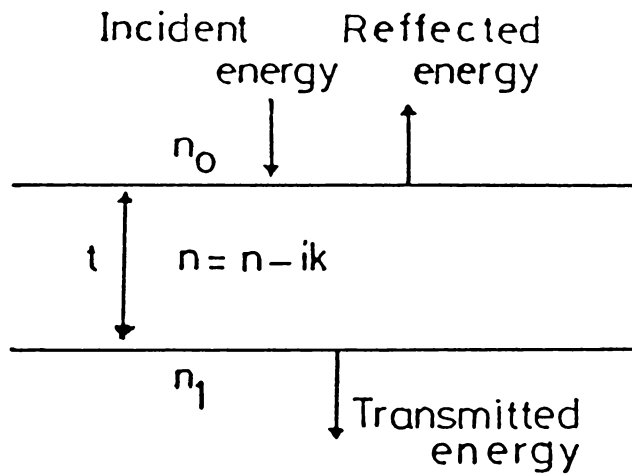


Fig.4.12. Reflection and transmission of light by a single film.

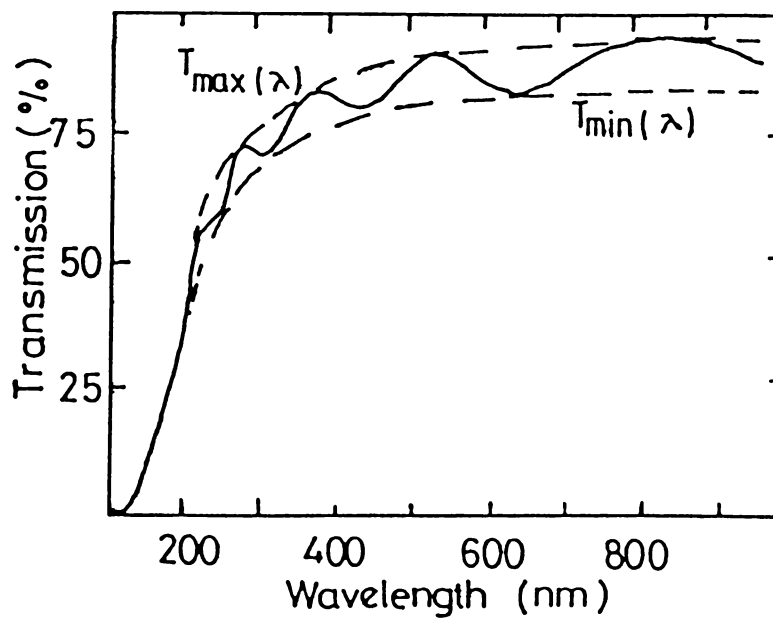


Fig.4.13. Typical transmission spectrum of a thin Eu_2O_3 film of uniform thickness of 860 Å.

$$\alpha_1 = \frac{C_1 [1 - (T_{\max}/T_{\min})^{1/2}]}{C_2 [1 + (T_{\max}/T_{\min})^{1/2}]} \quad 4.19$$

Then from 4.17

$$n = [N + (N^2 - n_0^2 n_1^2)^{1/2}]^{1/2} \quad 4.20$$

where

$$N = \frac{n_0^2 + n_1^2}{2} + 2n_0 n_1 \frac{T_{\max} - T_{\min}}{T_{\max} T_{\min}}$$

From equation 4.20 n can be determined knowing T_{\max} , T_{\min} , n_1 and n_0 at the same wavelength. Knowing n and t we can determine α from equation 4.19. Outside the region of fundamental absorption for higher wavelengths, this dispersion of n and k is not very large. The maxima and minima of T in equation 4.15 occur for

$$4 \pi n t / \lambda = m \pi \quad 4.21$$

The thickness t of the layer can be calculated from two maxima or minima using the above equation

$$t = \frac{M \lambda_1 \lambda_2}{2[n(\lambda_1) \lambda_2 - n(\lambda_2) \lambda_1]} \quad 4.22$$

where M is number of oscillations between the two extrema.

λ_1 , $n(\lambda_1)$ and λ_2 , $n(\lambda_2)$ are the corresponding wavelengths and indices of refraction. Knowing t and α_1 the extinction coefficient k can be calculated from equation 4.16. Some experimental care should be taken in the application of this method. (1) To obtain good fringe pattern, the difference between film refractive index n and substrate refractive index n_1 should be great as possible. (2) The effective bandwidth of the spectrometer should be kept smaller than the half width of the interference maximum. (3) The sample must be homogeneous and parallel faced. The variation of n and k with the wavelength should be small. This condition fails in the vicinity of the fundamental absorption in the short wavelength region.

The value of n , k and α were calculated from the transmission spectra of Eu_2O_3 films. Figure 4.14 gives the variation of n and k with wavelength. The value of refractive index is a constant (~ 1.64) in the visible and near IR regions. Outside the fundamental absorption, the dispersion of n and k are not very large. The absorption coefficient α and the extinction coefficient k

evaluated from the transmission data were found to be almost zero for higher wavelengths, i.e., above fundamental absorption. Figure 4.15 shows the dependence of absorption coefficient on photon energy. The optical absorption data of Eu_2O_3 films were investigated for evidence of either indirect or direct transitions in accordance with the theory of Bardeen et al. [26]. For such transitions

$$\alpha = \frac{A(h\nu - E_g' \pm E_p)^r}{h\nu} \quad 4.23$$

where $r=3$ for forbidden indirect transitions and $r=2$ for allowed indirect transitions. E_g' is the indirect band gap and E_p the absorbed or emitted phonon energy. The plot of $(\alpha h\nu)^2$ vs photon energy $h\nu$ (Fig. 4.16) gives a straight line portion and on extrapolating, its intercept gives a band gap of 3.38 eV. From this, conclusion may be drawn that the transition leading to fundamental absorption take place at 3.38 eV and the transition is an indirect one. The lack of long range order in a amorphous material causes smearing of the conduction and valence band edges so that the energy gap is not well defined. So the band gap determined in Eu_2O_3 film is the average of the smeared out energy gap.

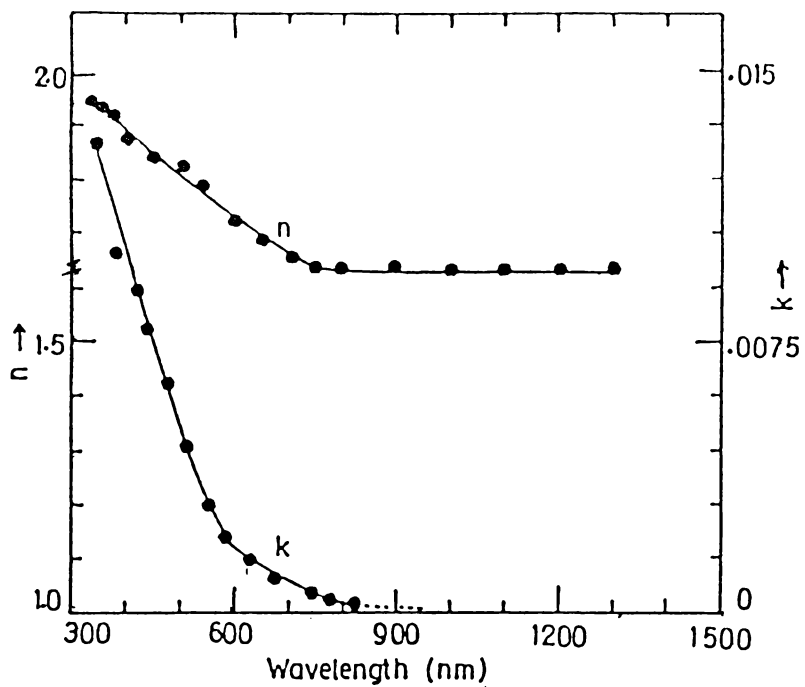


Fig.4.14. Variation of refractive index and extinction coefficient of the dielectric film with wavelength.

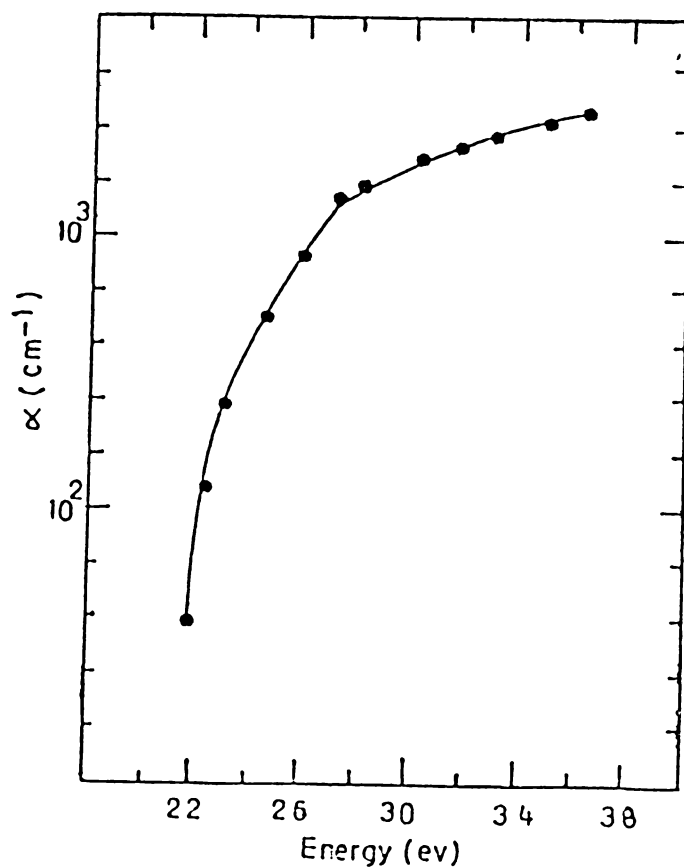


Fig.4.15. Absorption coefficient α vs photon energy $h\nu$.

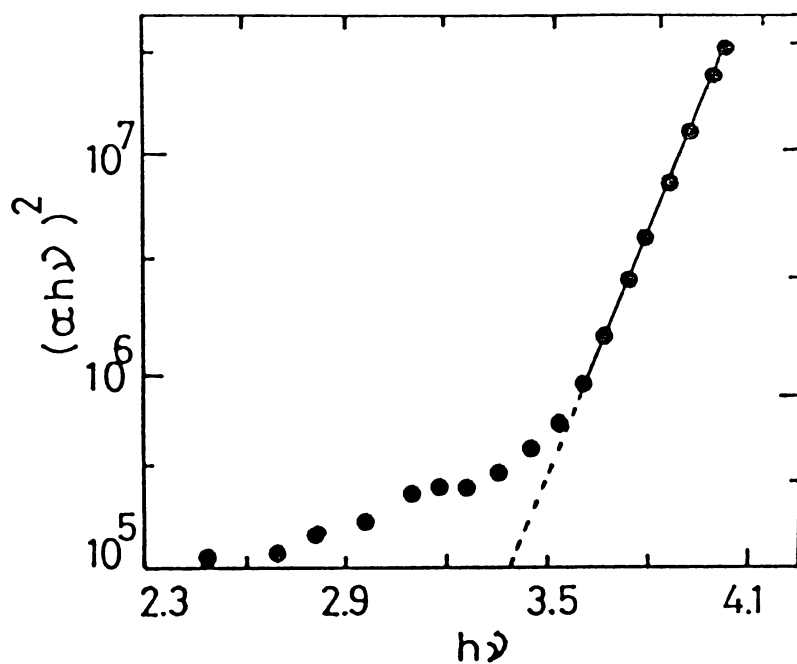


Fig.4.16. Plot of $(\alpha h\nu)^2$ vs photon energy $h\nu$.

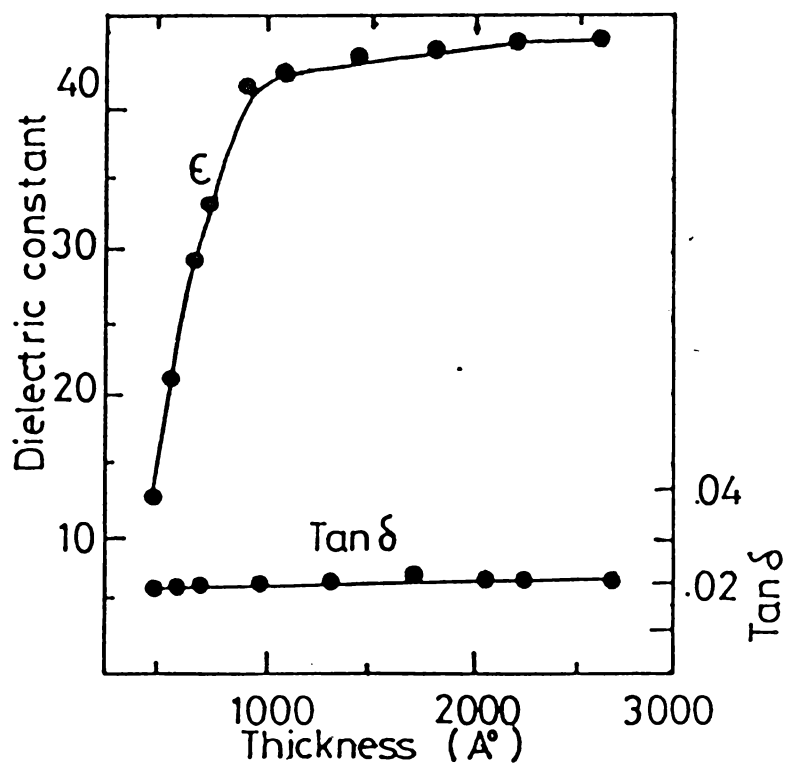


Fig.4.17. Variation of dielectric constant and loss factor with dielectric film (Sm_2O_3) thickness.

4.5 Dielectric properties of Sm_2O_3 thin films

Sm_2O_3 films were prepared by vacuum evaporation of high purity (99.99%) Sm_2O_3 powder using electron beam gun. The glass substrates were thoroughly cleaned and dried and loaded into the coating chamber and subjected to ion bombardment cleaning. Thick aluminium forms the front and rear electrodes in the MIM structure. During the deposition the substrate temperature was maintained at 150°C and kept at that temperature for 1 hour. The dielectric measurements were carried out as described in Section 4.2.

Figure 4.17 shows the variation of dielectric constant ϵ and $\tan\delta$ as a function of dielectric film thickness. The dielectric constant evaluated from the measured capacitance, effective area and film thickness, increases with increase of dielectric film thickness and attains a constant value of 43 for insulator thickness greater than 1000 \AA . The loss factor is 0.02 and is independent of film thickness. Similar thickness dependence have been observed [5,7] in the case of rare earth oxide films. The reasons for this can be given as explained in the case of Eu_2O_3 films.

Figure 4.18 shows the variation of dielectric constant and loss factor of Sm_2O_3 film with time. It is found that films prepared at room temperature (300 K) show large variation in dielectric constant with time. While the films prepared at (423 K) show less variation in dielectric constant, the films prepared at higher substrate temperature show better dielectric properties owing to improved stoichiometry of the films.

The dielectric constant (ϵ) of the Sm_2O_3 films is found to increase with increase of frequency. The variation of ϵ is small and it shows a minimum at particular frequency which is prominent only at higher temperatures (Fig. 4.18b).

The temperature coefficient of capacitance γ_c is an important practical parameter for assessing the expected behaviour of thin film circuits. γ_c is defined as $\frac{1}{C} \frac{dC}{dt}$. Figure 4.19a shows the variation of capacitance with temperature. Using the given equation [27] γ_c is given by

$$\gamma_c = A \tan\delta - \alpha\epsilon$$

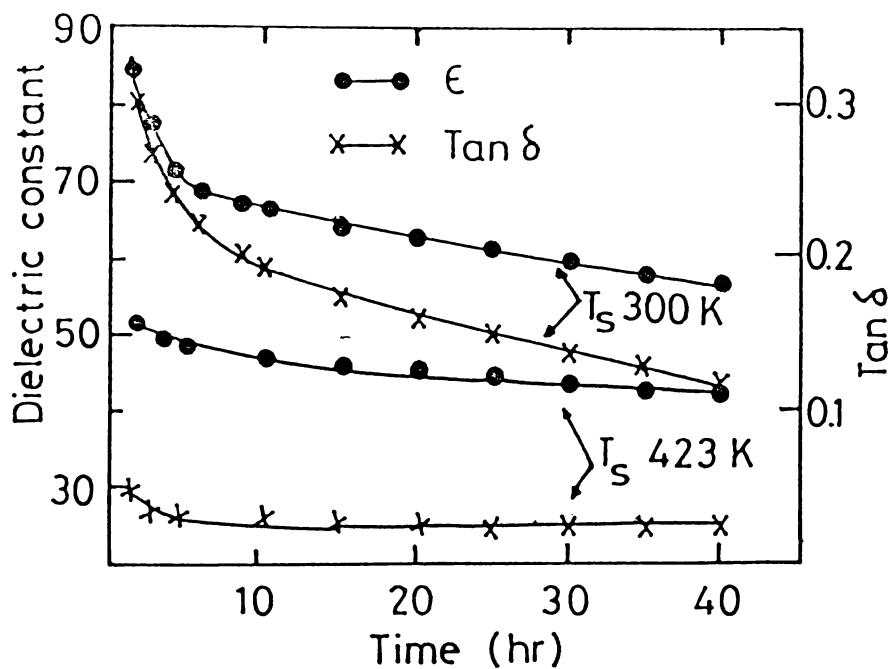


Fig.4.18 A. Variation of dielectric constant and loss factor of Sm_2O_3 films prepared at different substrate temperature with aging time.

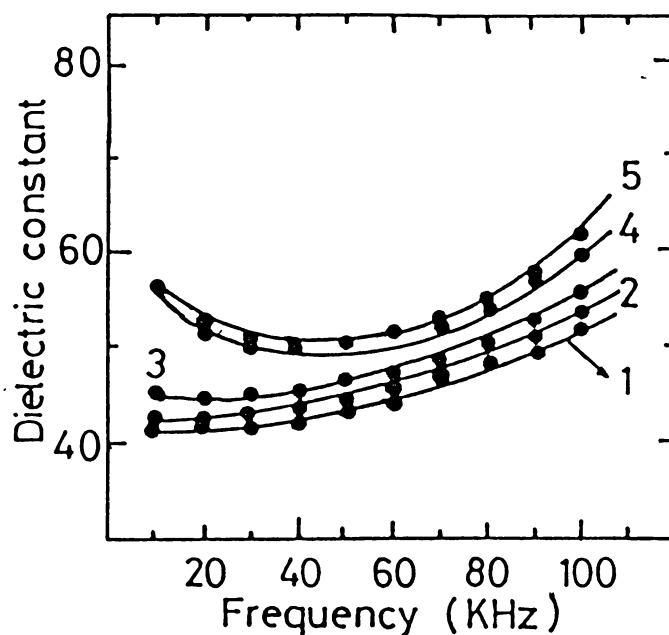


Fig.4.18 B. Dependence of dielectric constant on frequency for Sm_2O_3 film.
(1- 300 K, 2 - 338 K, 3 - 370 K, 4 - 415 K and 5- 438 K)

where A is constant for practical purposes it can be taken as $.05 \pm .01$ K and $\alpha\epsilon$ is the linear expansion coefficient. Typical values of the product $\alpha\epsilon$ lies in the range 10-60 ppm K^{-1} which may be neglected in comparison with the error in the coefficient A. Calculated value gives γ_c (minimum) 1000 ppm K^{-1} at room temperature and 10 KHz. From the graph the value of γ_c is obtained as 1300 ppm K^{-1} . The loss factor $\tan\delta$ is found to increase with increase of frequency at room temperature (Fig.4.19b). At higher temperature the variation is more prominent and also show a minimum, i.e., $\tan\delta$ first decreases with frequency and on further increase of frequency $\tan\delta$ again increases. The observed dependence of dielectric constant and loss factor $\tan\delta$ on frequency and temperature can be attributed to the same reasons as in the case of Eu_2O_3 films.

The conduction mechanism in Sm_2O_3 thin film is investigated by sandwiching the film between metal electrodes. The current voltage (I-V) measurements of Sm_2O_3 films (Fig. 4.20a) show three distinct regions viz., $I \propto v^{1/2}$, $I \propto v$ and $I \propto v^4$. At low very low fields the conduction is ohmic and at high fields it become trap filled SCL process. From the plot of

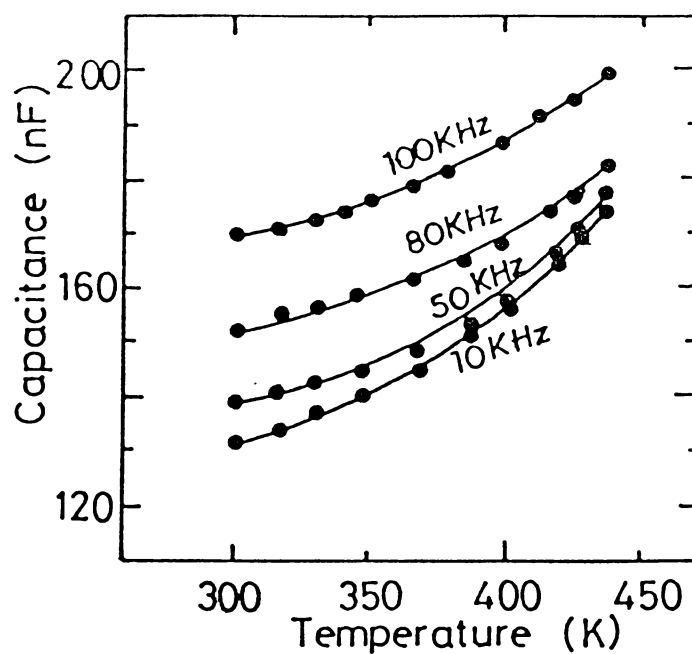


Fig.4.19 A. Capacitance vs temperature at different fixed frequencies (Sm_2O_3 film)

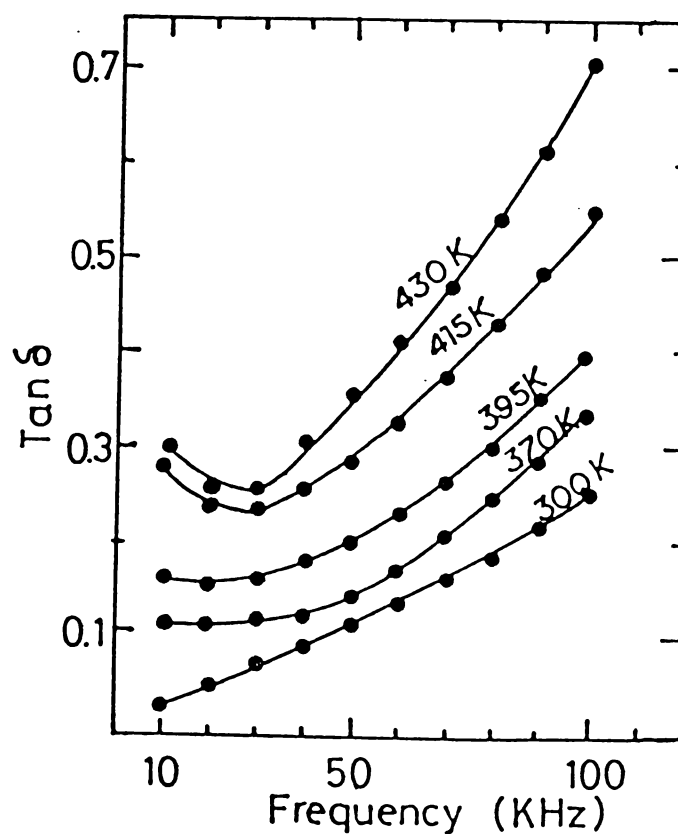


Fig.4.19 B. Variation of $\tan \delta$ with frequency at different temperatures (Sm_2O_3 film thickness - 1100 Å).

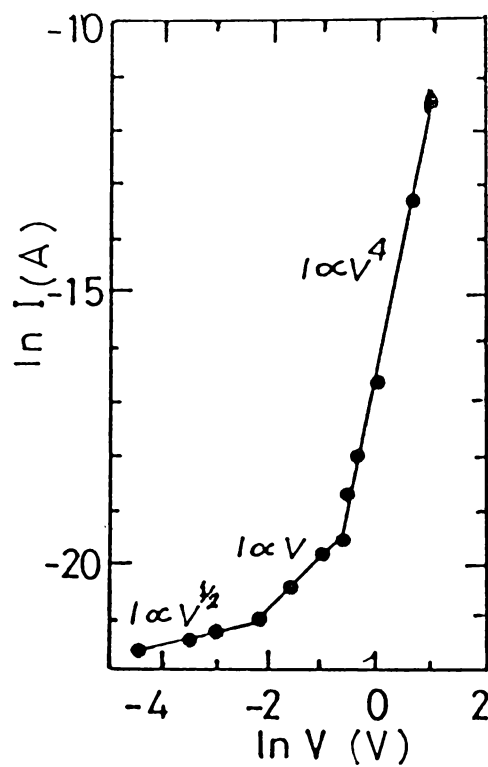


Fig.4.20 A. Current-voltage plot of Sm_2O_3 film of thickness 1050 Å.

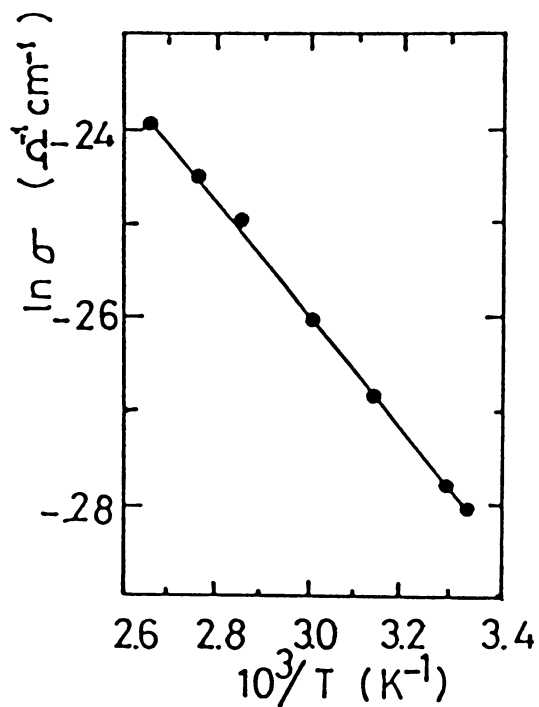


Fig.4.20 B. $\ln \sigma$ vs $10^3/T$ K^{-1} plot for Sm_2O_3 film of thickness 1050 Å.

$\ln \sigma$ vs $\frac{1}{T}$ (Fig. 4.20b) the activation energy is calculated to be 0.054 eV. This may be due to the presence of shallow traps. The Sm_2O_3 films has got high transmittance above 95% in the visible and IR regions.

4.6 Dielectric properties of MgF_2 , CeO_2 , SiO , Na_3AlF_6 and BaTiO_3

Though the insulating films such as MgF_2 , CeO_2 , SiO , Na_3AlF_6 and BaTiO_3 are well studied and reported in literature, the dielectric properties of these materials are investigated because it is an important factor for application in TFEL devices.

The dielectric films were deposited by vacuum evaporation of high purity materials using electron beam gun. The glass substrates were thoroughly cleaned by usual cleaning procedure described earlier and loaded into the coating chamber which were subjected to a final ion bombardment cleaning. Thick aluminium was vacuum evaporated ($\sim 0.2 \mu\text{m}$) forms the rear and front electrodes in metal-insulator-metal structure. During the deposition of the films the substrate temperature was maintained at 150°C . In the case CeO_2 films it was subjected to prolonged annealing before taking measurements, because rare earth

oxide films are found to improve the dielectric properties due to prolonged annealing [7].

The dielectric and electrical measurements were carried out under vacuum of 10^{-2} torr in a specially designed metallic cell. The capacitance and loss factors were measured over a frequency range of 1 KHz to 1 MHz using a 0.1% Universal Bridge and HP LCZ Bridge (Model 4277 A). The dielectric constant ϵ was evaluated from the capacitance measurement data knowing the area and thickness of the film.

Table 4.1 gives the dielectric properties of thin insulating films of the materials having thickness of 0.2 μm .

Material	Dielectric constant at 1 KHz	$\tan\delta$ at 1 KHz	Break-down strength
--	--	--	--
Na_3AlF_6	6.6	0.4	2.5×10^6 V/cm
MgF_2	4.9	0.1	2×10^6 V/cm
SiO	4.2	0.02	2×10^6 V/cm
CeO_2	4.8	0.05	3×10^6 V/cm
BaTiO_3	10-15	0.05	---

The variation of $\tan\delta$ with frequency is given in Fig.4.21. Generally all materials show an initial decrease with increase of frequency and attains a minimum, then increase drastically with increase of frequency. The apparent high loss at higher frequencies is due to the uncorrected electrode resistance. This effect can be explained by the same arguments as in the case of Eu_2O_3 film. Except in the case of BaTiO_3 film it is observed that the dielectric constant and loss behaviour are comparable with values reported in literature. Bickley et al. [12] has reported evaporated films of BaTiO_3 have a dielectric constant of ~ 200 . But in the present case BaTiO_3 films do not exhibit stable values for dielectric constant and it is around 10. This may be due to the pinholes or non stoichiometry of the deposits resulting from excess oxygen or metal ions.

The observed values of dielectric constants and loss factor of MgF_2 , CeO_2 and SiO are in good agreement with the values reported earlier in literature [4,12,19, 28,29].

The silicon monoxide films has got low loss .02% though the actual composition of the dielectric layer is uncertain and the loss factor SiO is much less than that

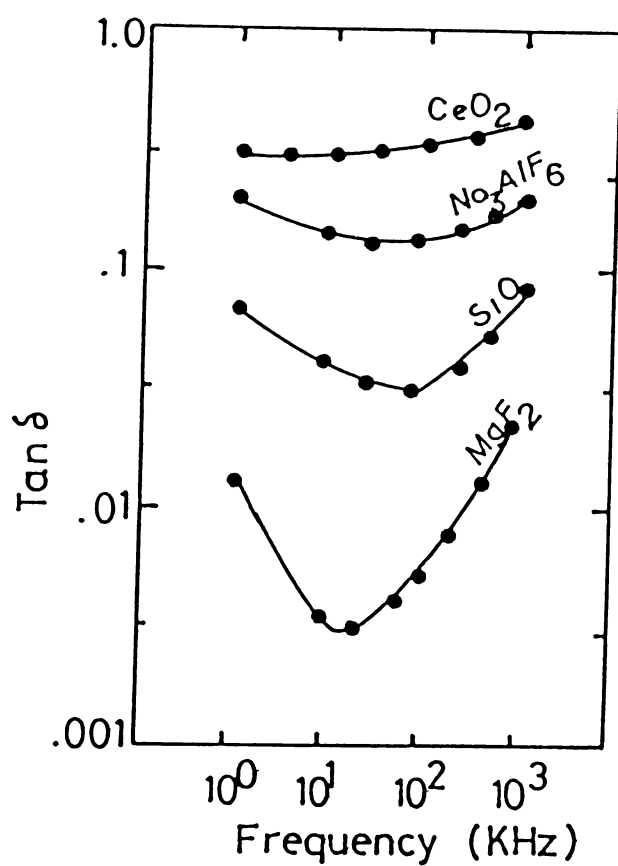


Fig.4.21. The variation of loss factor $\tan \delta$ with frequency of certain insulating films at room temperature.

of electron beam evaporated silicon dioxide. The dielectric breakdown strength of CeO_2 is found to be very high. It is also observed that the dielectric loss of CeO_2 film though high compared to other films, the variation of loss factor with frequency is negligible. MgF_2 and Na_3AlF_6 films are found to be sensitive to moisture and it affects its dielectric properties. These films were used as insulators in the electro-luminescent devices. The operating characteristics of the devices were found to depend on the dielectric constant and loss factor. When films with high dielectric constant were used as insulators the devices have a low threshold voltage. The dependence of dielectric properties on device performance is described in Chapter V.

REFERENCES

- [1] P K Weimer; Proc. IRE, 50 (1962) 1462.
- [2] F V Shallcross; Proc. IEEE, 51(1963) 851.
- [3] U Saxena and O N Srivastava; Thin Solid Films, 33(1976) 185.
- [4] V M Koleshko and N V Babushkina; Thin Solid Films, 62(1979) 1.
- [5] A Goswami and R Ramesh Varma; Thin Solid Films, 28(1975) 157.
- [6] V S Dharmadhirari and A Goswami; Thin Solid Films, 87(1982) 119.
- [7] H Nakane, A Noya, S Kuriki and G Matsumoto; Thin Solid Films, 59(1979) 291.
- [8] J Ohwaki, H Kozawaguchi and B Tsujiyama; J. . J. Appl.Phys., 22(1983) 1133.
- [9] R M Goldstein and F W Leonhard; Proc. Electronic Components Conf. Washington 1967, IEEE New York, 1967, p. 312.
- [10] G Has, J B Ramsey and R Thun, J.Opt.Soc.Am., 48(1988) 324.

- [11] A Goswami and A P Goswami; Thin Solid Films, 20(1974) 53.
- [12] K L Chopra, Thin film phenomena, Mc Graw-Hill, New York, 1969 pp. 189, 466-467.
- [13] C K Campbell; Thin Solid Films, 6(1970) 197.
- [14] T Wiktorczyk and C Wesolowska; Thin Solid Films, 71(1980) 15.
- [15] W E Howard; Proc. SID, 18(1977) 119.
- [16] W Klein and H Gafni, IEEE Trans. Electron Devices, ED-13(1966) 281.
- [17] W W Axelrod, J.Electrochem.Soc., 116(1969) 460.
- [18] F Forlani and N Minnaja; Phys.Stat.Soldi., 4(1964) 311.
- [19] L I Maissel and R Glang; 'Handbook of Thin Film Technology' Mc Graw-Hill, New York, 1983.
- [20] A Rose; Phys. Rev., 97(1955) 1538.
- [21] N F Mott and E A Davis; Electronic Processes in Non-Crystalline Materials, Oxford, Clarendon Press, 1971.
- [22] S R Elliott; Philosophical Magazine, 36(1977) 1291.

- [23] M Pollak; Philosophical Magazine, 23(1971) 519.
- [24] K Bhal and K L Chopra, J.Appl.Phys., 41(1970) 2196.
- [25] J C Manificier, J Gasiot and J P Fillard;
J.Phys.E.Scientific Instru., 9(1976) 1002.
- [26] J Bardeen, F J Blott and L M Hall; Proc. Photo-
conductivity Conference, Athlantic City Wiley,
1956, p. 146.
- [27] M Gevers; Philips Res. Rept., 1(1946) 279.
- [28] C Weaver; Advan. Phys., 11(1962) 85.
- [29] H G Manfield, Micro Elec. Reliability, 3(1964) 5.
- [30] A A Kornyshev, M A Vorotyntsev and J Vistrup;
Thin Solid Films, 75(1981) 105.

Chapter-V

AC THIN FILM EL DEVICE WITH ZnS:Mn ACTIVE LAYER

Abstract:

ZnS:Mn is the most efficient EL material known to date. Though ZnS based EL devices have long life and high brightness it requires a high driving voltage. In this chapter the fabrication of low voltage operated thin film EL device with novel dielectric Eu_2O_3 in MIS structure is described. TFEL devices with ZnS:Mn as active layer and Eu_2O_3 or MgF_2 as insulator have been found to possess a frequency dependent threshold voltage for onset of EL emission. This effect is explained on the basis of frequency dependent loss tangent of the insulating material. The device parameters of TFEL device with Eu_2O_3 as insulator is optimised in terms of thicknesses of active and insulator layers. It is observed that a thickness ratio of 1 and 2 between active and insulator is suitable for low voltage operation. TFEL devices with insulators of different figure of merit are fabricated. From the EL emission characteristics it is concluded that films with high figure of merit is suitable for low voltage operation.

5.1 Introduction

AC thin film EL (ACTFEL) devices with double insulated structure [1] are known for their long life and high brightness. They are emerging as practical flat panel display systems because of a number of attractive properties. These include low power dissipation and the possibility of fabricating large area solid state multicolour flat panel displays with integrated driving circuits. The most popular double insulated ZnS:Mn TFEL device consist of an active layer of ZnS:Mn sandwiched between two insulating layers of Y_2O_3 . Eventhough they have high brightness level (~ 1500 fL) and long life[2,3] ($> 20,000$ hours) they require a fairly high driving voltage of about 200 V. This makes it difficult to use them with a compact driving circuit composed of available ICs. In some practical systems this problem is solved to some extent by adding an external inductor to the device which is capacitive in nature, thereby forming an LC resonant circuit. Devices with Metal-Insulator-Semiconductor (MIS) structure have been suggested as one way of reducing the driving voltage requirements of TFEL devices [4]. Another possible approach is by incorporating dielectrics of high figure

of merit for the insulating layer. According to Howard [5] in order to obtain high brightness and high efficiency for these devices, the insulator film must satisfy the condition that the product of its dielectric constant (ϵ) and breakdown voltage (F_b) must be at least three times higher than the corresponding value for the active ZnS:Mn layer. This implies that low voltage operation can be obtained without sacrificing the brightness or efficiency by using insulators of high dielectric constant, and preferably, with high breakdown voltage. Based on this idea Okamoto et al. [6] have prepared a device using piezoelectric PbTiO_3 ($\epsilon = 150$) insulating layer and found that they can operate at ~ 50 Volts. Attempts are also being made to use SrTiO_3 and BaTa_2O_3 films in such devices [7]. Another innovative idea on this type of devices is due to Yoshiro Oishi et al. [8] and Y.A Ono et al. [9] who have very recently fabricated tunable colour EL devices.

Quite different from these attempts, as described in this chapter, the author has prepared an AC thin film EL device of ZnS:Mn having an insulator with a frequency dependent characteristics which modifies the device performance in such a way that it can be switched on and off, by changing frequency while keeping its amplitude constant.

This makes the high voltage switching unnecessary and hence minimises capacitive loading. Eu_2O_3 insulator has been used and the choice of Eu_2O_3 as insulator was motivated by the fact that it has got a dielectric constant [10] of 22 and breakdown strength 2×10^6 V/cm. However, the loss factor and hence the effective impedance vary with the applied frequency [10]. The devices were prepared in both MIS as well as MISIM structure using ZnS:Mn active layer and Eu_2O_3 as insulator. Optimisation of device parameters in terms of thickness of active and insulating layers is also dealt with in some detail in the present chapter.

The following sections of this chapter also give the details of fabrication and study of MIS and MISIM structure devices with ZnS:Mn and insulators having different figure of merit such as MgF_2 , Sm_2O_3 , CeO_2 , SiO_2 , Na_3AlF_6 , BaTiO_3 .

5.2 Fabrication of MISIM and MIS structure devices

The AC TFEL device with MISIM and MIS structure fabricated for the present studies is as shown in Fig. 5.1 a,b. The substrates used were 1 mm ordinary glass substrates of 7.5 cm x 2.5 cm size. All the layers

except the transparent conducting electrode were deposited by thermal evaporation. The detailed procedure for deposition of each film is given below.

The SnO_2 conducting films on the glass substrates were deposited by the chemical spray pyrolysis method which is described in detail in Chapter-II. For the fabrication of thin film devices, films of sheet resistance $80 \Omega/\square$ and of transparency 85 percent were used. The deposited electrodes were then suitably etched by a chemical method. These transparent electrodes were then cleaned with soap solution and washed with water, then rinsed in distilled water, xylene and acetone successively. The plates were subjected to an ultrasonic cleaning procedure. The plates were then dried and loaded into the coating chamber.

For the deposition of the layers in the device of the type $\text{SnO}_2\text{-Eu}_2\text{O}_3\text{-ZnS:Mn-Eu}_2\text{O}_3\text{-Al}$ and $\text{SnO}_2\text{-ZnS:Mn-Eu}_2\text{O}_3\text{-Al}$, weighed amounts of Eu_2O_3 and ZnS:An which are slightly in excess needed for the deposition of required thickness were taken in the respective source heater. For Eu_2O_3 a tungsten basket was used as source heater which was powered by a 200A, 10V transformer. The ZnS:Mn was taken in the form of pressed pellets and the source used was a molybdenum box type heater. The active layer

was obtained in the present case by evaporating electro-luminescent ZnS:Mn phosphor having 3 wt percent of Mn prepared in the laboratory by the slurring technique as described in Chapter-II. During the deposition the substrate temperature was maintained at 423 K. The device fabrication was completed by the deposition of the final aluminium back electrode. This was done by the usual vacuum evaporation method. The aluminium film was deposited through a mica mask suitably prepared so that on each substrate 5 electrode strips of size 1 cm x 0.5 cm were formed. This resulted in five identical devices each of emitting area 0.5 cm.

On the first application of electric field to a newly built cell, there occur spurious arcing and momentary rupturing of the metal electrode followed by the emission of light. Due to the self healing, pin hole burn-out occurs in small isolated regions. Even-though there exist burnt-out portions, they are not visible when the device is switched on as the entire area is uniformly illuminated. The cells were then operated for several hours continuously without any observable deterioration. To ensure reliability, device operated for long a time duration only have been subjected to detailed investigation. Also

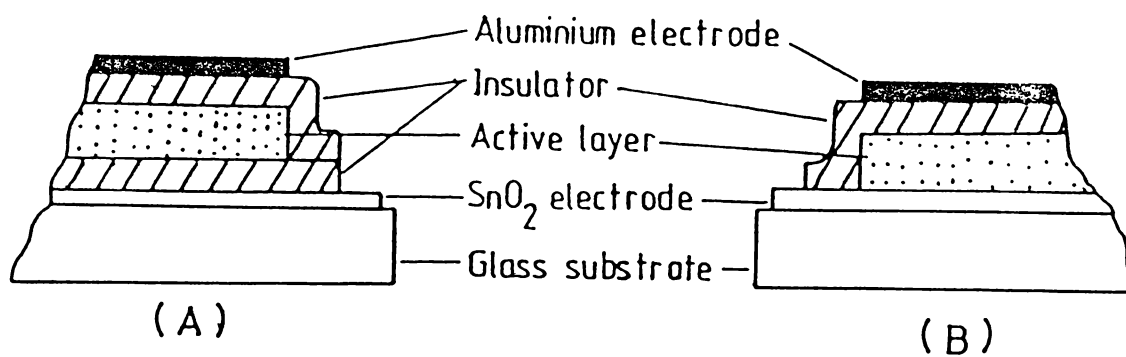


Fig.5.1. Schematic structure of (A) MISIM TFEL, and (B) MIS TFEL devices used for present investigations.

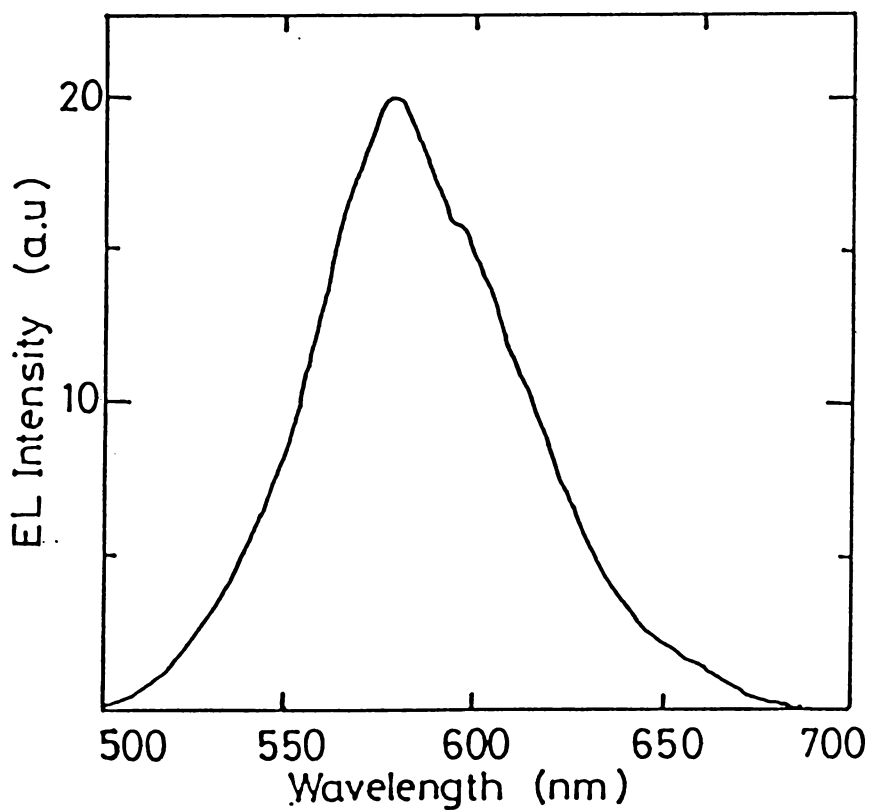


Fig.5.2. EL emission spectra of ZnS:Mn TFEL device.

these devices even without any protection layers, can operate for months without any sign of deterioration.

The EL spectrum of TFEL cell was recorded with the set up described earlier (Chapter-II). The excitation set up and the arrangement for the voltage-brightness measurements are the same as used for the study of powder cells described in Section 2.6 of Chapter-II.

5.3 Frequency dependent threshold voltage of the devices

The EL emission spectrum recorded for both MISIM and MIS cells are the same and typical spectrum is shown in Fig. 5.2. The emission has its maximum at 585 nm and the width at half maximum is 40 nm. This is due to the well known intra-atomic transition of the Mn^{2+} ion from ${}^4\text{T}_1$ to ${}^6\text{A}_1$ state [11]. The B-V characteristic obtained for the present devices was found to depend strongly on the excitation frequency as can be seen in Fig. 5.3 for MISIM device. The brightness is found to be zero upto a threshold voltage (V_{th}), beyond this value of the applied voltage the brightness increases steeply and after attaining a certain brightness value it levels off indicating saturation. Such a saturation effect has been observed for all type of AC thin film EL

devices as well as in some DC powder EL devices [12]. Tornquist [13] has attributed this apparent brightness saturation to two cases: (1) Due to the dissipative current in the ZnS:Mn layer that is directly related to the excitation of Mn^{2+} ion (This is because at higher fields the conductivity of ZnS:Mn layer will increase and hence the internal field will be limited by the capacitance of the insulating layers), (2) Due to the internal quenching of Mn^{2+} emission.

The device is found to have frequency dependent threshold voltage, that is the voltage for onset of EL emission increases with excitation frequency. This observation, though anomalous at first sight, can be explained on the basis of the physical properties of materials used in the fabrication of the device.

In order to understand the usual B-V characteristic of the TFEL devices an equivalent circuit as shown in Fig. 5.4 adapted by Tornqvist [13] is made use of. But in the present equivalent circuit an additional parallel resistance R_i is included. The resistance R_i included in the circuit accounts for the leakage currents. The voltage appearing across the active layer can be

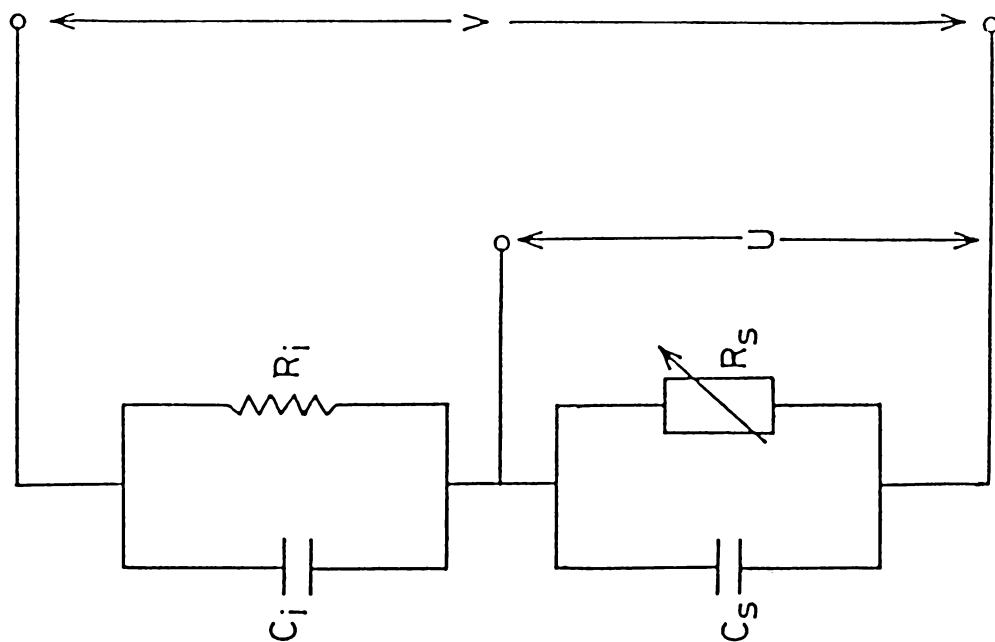


Fig.5.4. The equivalent circuit for the TFEL device.

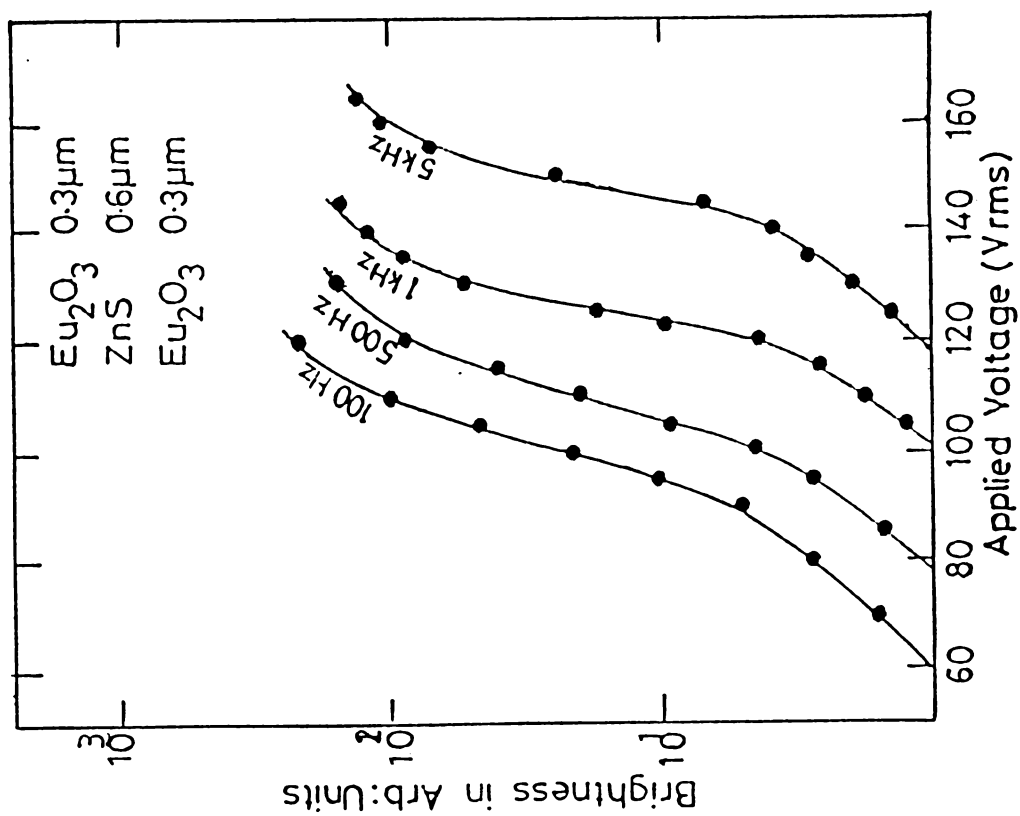


Fig.5.3. B-V characteristic of ZnS:Mn MISIM structure TFEL device with Eu_2O_3 insulator at different excitation frequency.

expressed as

$$U = \frac{Z_s}{Z_i + Z_s} V \quad 5.1$$

where V is the applied voltage, Z_i is the total impedance offered by the insulating layers and Z_s that of the active layer. C_i and C_s are the equivalent capacitance of the insulator and active layers. If U_{th} is the threshold voltage for the onset of emission and V_{th} is the corresponding applied voltage having a particular frequency ω then

$$U_{th} = \frac{Z_s(\omega)}{Z_i(\omega) + Z_s(\omega)} V_{th} \quad 5.2$$

U_{th} is the threshold voltage to be applied across the active layer for the onset of light emission and V_{th} the corresponding applied voltage. But $Z_i(\omega)$ will be proportional to $R_i / \sqrt{1 + \tan^2 \delta}$ which means that the voltage drop across the insulator layer is a function of $\tan \delta$ and higher the $\tan \delta$ value the lower the $Z_i(\omega)$ value or drop across the insulator. So for higher $\tan \delta$ value the U_{th} can be attained for a much lower applied voltage as is evident from equation 5.2. In the case of Eu_2O_3 its $\tan \delta$ value is strongly dependent function of frequency and it goes on decreasing as the frequency

is increased [10]. The variation of $\tan\delta$ with frequency is given in Fig. 4.4. This leads to the result that by increasing the excitation frequency the $\tan\delta$ value is increased thereby increasing the value of the applied voltage required to produce emission from ZnS:Mn. Thus one can conclude that the threshold voltage should depend on the excitation frequency and the nature of this dependence must be as shown in Fig. 5.3.

5.4 Optimisation of device parameters

To fulfil the potential needs, a number of approaches for lowering threshold voltage have been attempted. For example, the use of lower band gap host material such as ZnSe [14], low energy Mn ion implantation into the ZnS [15], thin active and insulating layers [16], etc. have been tried so far. MIS structure devices [4] and use of dielectrics [5] of high figure of merit are also possible ways of reducing the driving voltage. Although many interesting results have been obtained, no definite practically available solution has been found.

In order to fabricate legible low-voltage driven, high brightness yellow-orange emitting ZnS:Mn TFEL devices, MIS structure as shown in Fig. 5.1b have been investigated.

The following section gives the detailed emission characteristics of ZnS:Mn MIS TFEL devices and information on the optimal conditions of the active and the insulator film thickness ratio in low-voltage driven MIS TFEL devices.

The devices in MIS structure (Fig. 5.1b) were fabricated with different active layer thickness keeping the insulator layer thickness and devices having different insulator thickness but keeping active layer thickness constant. The deposition procedure and conditions are the same as described in the case of MISIM structure devices as in Section 5.2.

Figure 5.5 shows the dependence of brightness on the thickness of the active layer in ZnS:Mn MIS TFEL device with constant insulator thickness of 0.2 μm . The brightness is found to decrease as thickness of the ZnS:Mn active layer is reduced. The threshold voltage of the device also decreased with the decrease of active layer thickness. Fig. 5.6 shows the dependence of the brightness on insulator thickness with a constant thickness of 0.3 μm for active layer. The threshold voltage again decreases with decrease of insulator layer thickness.

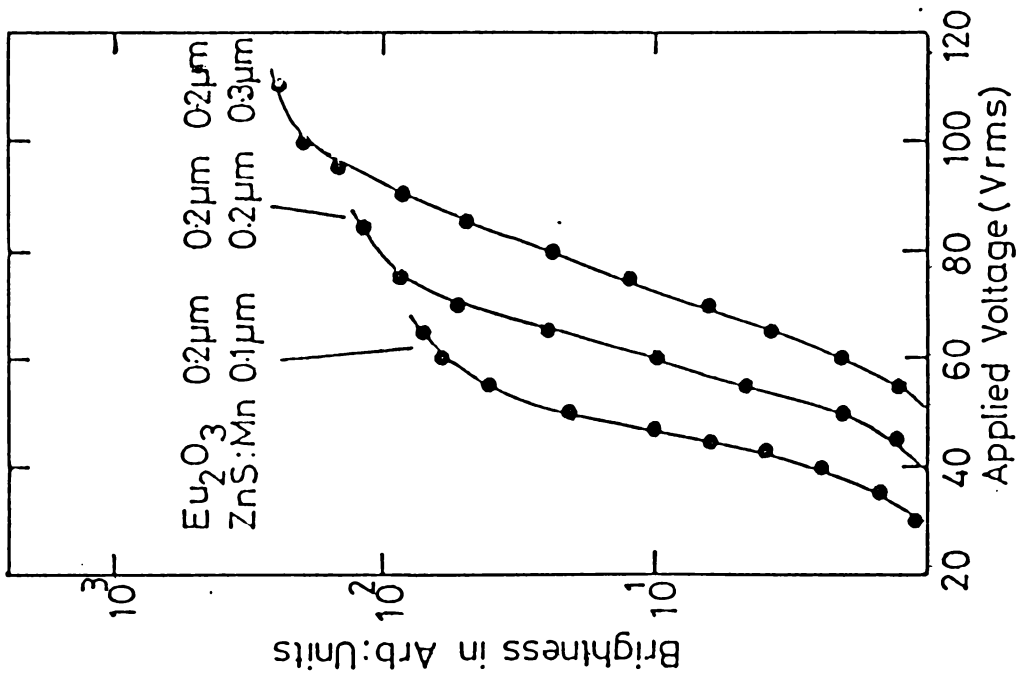


Fig.5.5. Dependence of brightness on thickness of active layer in MIS structure device under 1 KHz excitation frequency.

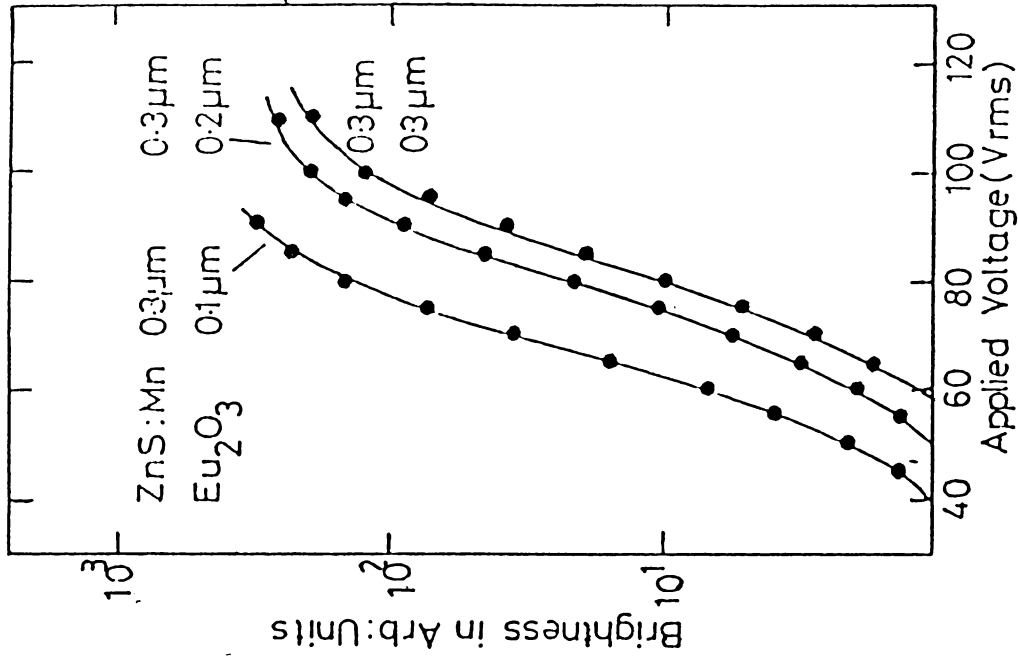


Fig.5.6. Dependence of brightness on insulator layer thickness in MIS structure device under 1 KHz excitation frequency.

In MIS, TFEL devices the mechanism of EL evidently is the impact excitation of the emission centers by accelerated charge carriers injected into the active layer. These carriers can originate from the electrode, ZnS-insulator interfaces, ZnS-SnO₂ interface states and also from trapping levels in ZnS layer. When ZnS (active layer) thickness is reduced, the number of emission centers correspondingly decreases and acceleration efficiency is reduced owing to low crystal quality [17,18]. This may reduce the maximum brightness with the decrease of ZnS layer thickness. Further in the case of MIS structure electron leakage to SnO₂ side is smaller, for thick layers of ZnS owing to grain boundary barriers [19] than for thin ZnS layer. On reducing the insulator thickness the number of electrons injected from the insulator side is increased. Thus reduction of insulator layer thickness helps in increasing the EL emission intensity. For thicker layer of insulator, voltage drop across the insulator is high, necessitating higher applied voltage for the onset of emission.

Figure 5.7 shows the variation of maximum brightness with ratio of active layer (ZnS) to insulator thickness (t_z/t_I). It is found that brightness increases upto a value of 1.5 for (t_z/t_I) and then begins to saturate. Curve B shows the variation of threshold voltage with t_z/t_I . The

threshold voltage is found to increase with increase of either t_z or t_I . From Fig. 5.7 it is clear that a thickness ratio of t_z/t_I between 1 and 2 is best for low voltage operation and maximum brightness.

The driving voltage of TFEL devices can be reduced either by reducing the thickness of the active layer (ZnS) or the insulator (Eu_2O_3) or both. For a thicker insulator layer $Z_i(\omega)$ is high causing a decrease in the maximum brightness. When the insulator is too thin there is a possibility for breakdown. The optimal condition for high stability as well as brightness is found to be for a thickness ratio lying between one to two for the ZnS- Eu_2O_3 layers

The MIS structure device also shows a frequency dependent threshold voltage for onset of emission as in the case of MISIM device. Figure 5.8 gives the variation of threshold voltage for the onset of emission for a typical cell of MIS structure with active layer (ZnS) thickness $0.3 \mu\text{m}$ and insulator (Eu_2O_3) thickness $0.2 \mu\text{m}$. This can be explained in similar manner as in the case of double insulating devices.

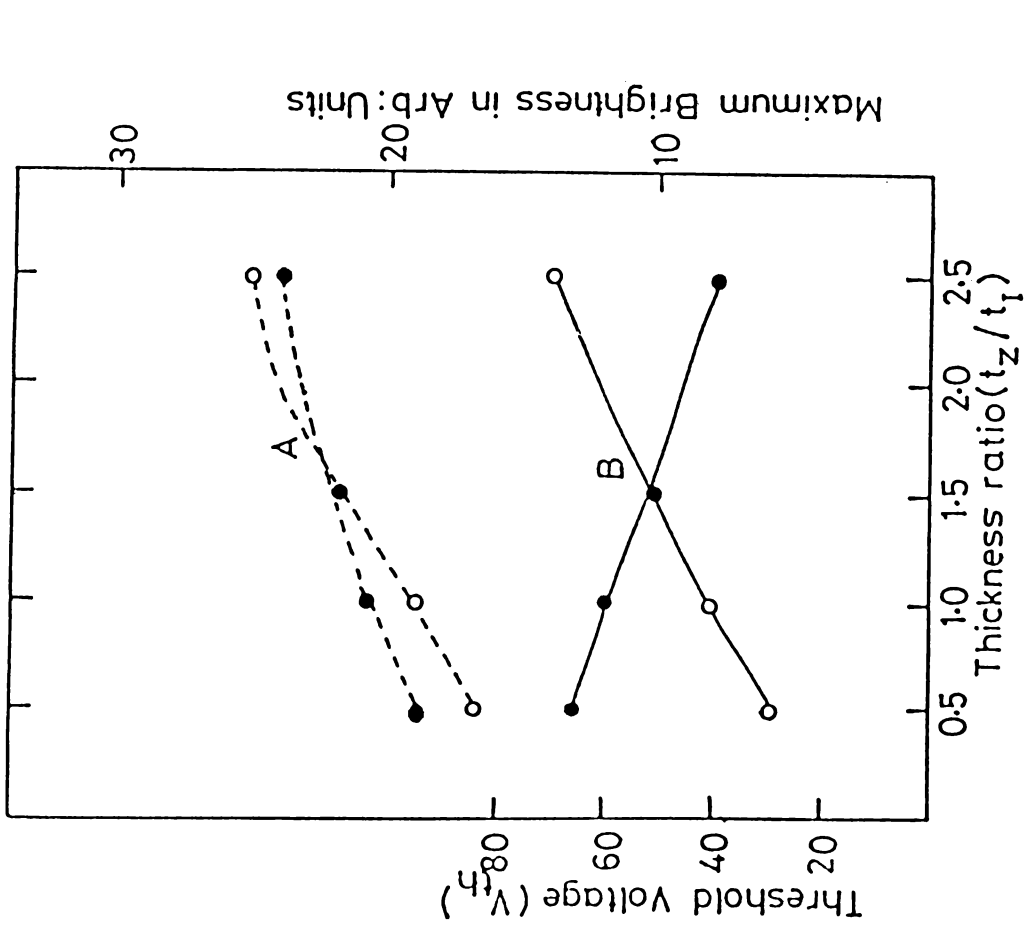


Fig.5.7. Variation of maximum brightness with t_z/t_I -curve A (o ... o for $t_I=0.2\mu\text{m}$, $\bullet\cdots\bullet$ for $t_z=0.3\mu\text{m}$) and variation of V_{th} with t_z/t_I -curve B (o—o for $t_I=0.2\mu\text{m}$, $\bullet\text{---}\bullet$ for $t_z=0.3\mu\text{m}$)

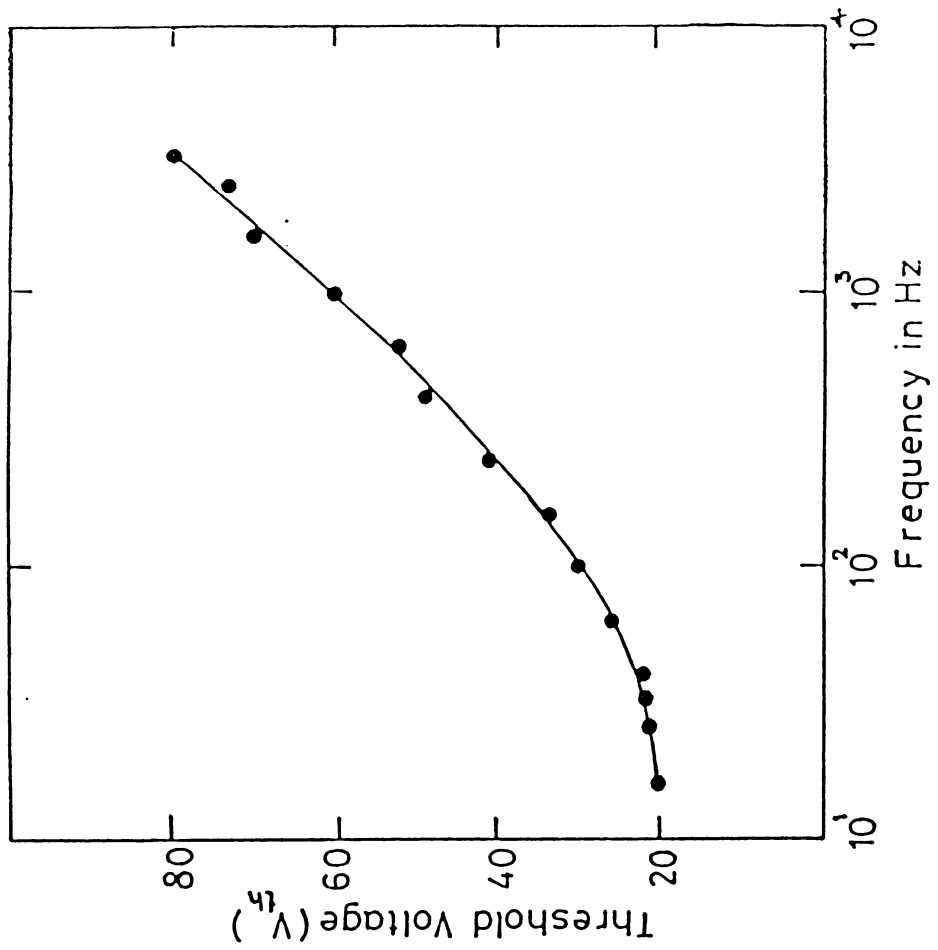


Fig.5.8. Variation of V_{th} excitation frequency of a typical MIS TFEL device with active layer $0.3\mu\text{m}$ and insulator $0.2\mu\text{m}$ thickness.

5.5 Devices with insulators having different figure of merit

A number of approaches to lower the driving voltage have been attempted; such as using small band gap semiconductor materials, the use of insulators with high dielectric constant, etc. Although the driving voltage was reduced by such attempts, the brightness also was reduced simultaneously. The reason for this is considered to be the low resistance and the deviation from stoichiometry in the semiconducting as well as the insulating films.

Insulators with a high dielectric constant and low dielectric loss factor should be used as the TFEL insulator in order to achieve a low voltage driven high brightness TFEL device. Hence TFEL devices were fabricated in MISIM and MIS structure with ZnS:Mn active layer and insulating layers of different figure of merit such as Sm_2O_3 , Eu_2O_3 , MgF_2 , Na_3AlF_6 and CeO_2 . In the following section the details of fabrication and emission characteristics of the devices are given.

All the devices prepared have the same emitting area of 0.5 cm^2 . In the case of MISIM structure devices (Fig. 5.1a) the thickness of insulator was $0.3 \mu\text{m}$ and

that of ZnS:Mn was 0.6 μm ; whereas in the case of MIS structure (Fig. 5.2b) the thickness of insulator was 0.2 μm and that of the active layer was 0.3 μm . All the devices were prepared by vacuum evaporation of each layer sequentially using electron beam gun in single pump down cycle. During the deposition of the insulator and active layer the substrate temperature was maintained at 150°C. and annealed for 1 hour after each layer deposition. But in the case of devices with MgF_2 and Na_3AlF_6 the higher substrate temperature and the subsequent annealing actually diminished the emission. However, in the case of Eu_2O_3 and Sm_2O_3 , CeO_2 , SiO insulating devices, the annealing and higher substrate temperature improved the device quality. This is mainly because of the improvement of dielectric properties of insulating film as we have seen in Chapter-IV, and not contributed by ZnS:Mn active layer. This observation is supported by the recent studies on Y_2O_3 insulator devices by Theis et al. [20] with the aid of transmission electron microscopy. However, during deposition of ZnS:Mn the substrate temperature is found to increase. So in the case of MgF_2 and Na_3AlF_6 insulating devices the substrate temperature was maintained at about 80°C. Compared to other insulators MgF_2 and Na_3AlF_6 are highly sensitive to moisture. Hence protection layer is necessary for these

devices.

The TFEL device with MgF_2 and Eu_2O_3 as insulating layer are found to exhibit a frequency dependent threshold voltage for onset of emission. The B-V characteristic of Eu_2O_3 device is shown in Fig.5.3. and that of MgF_2 insulating device is given in Fig. 5.9. The reason for this can be explained in terms of frequency dependent loss factor of the insulating film (see Section 5.3). The loss factor of MgF_2 film is found to decrease with increase of frequency [21] as shown in Fig. 4.21. The explanation given for Eu_2O_3 insulating film holds good in the case of MgF_2 insulating devices also.

The EL emission spectrum of all the devices are the same as those of conventional ITO- Y_2O_3 -ZnS:Mn- Y_2O_3 -Al. The typical EL emission spectrum is given in Fig. 5.2.

Figure 5.10 shows the brightness-voltage (B-V) characteristic of MISIM devices having an active layer thickness $0.6 \mu\text{m}$ and insulator layer thickness of $0.3 \mu\text{m}$ excited under 1 KHz excitation frequency. Fig. 5.11 gives the B-V characteristic of the MIS devices with active layer thickness of $0.3 \mu\text{m}$ and an insulator thickness of $0.2 \mu\text{m}$. It is observed that the threshold voltage for onset of emission is minimum for devices

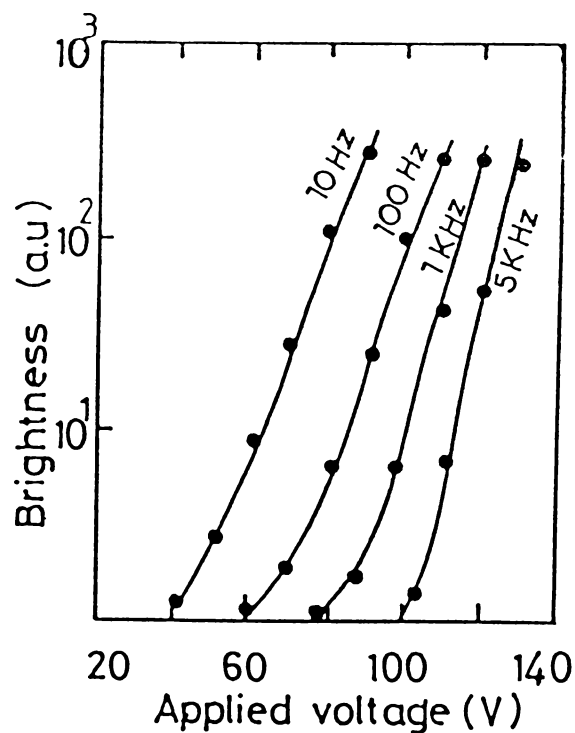


Fig.5.9. B-V characteristic of ZnS:Mn MIS TFEL device with MgF_2 as insulator at different excitation frequency.

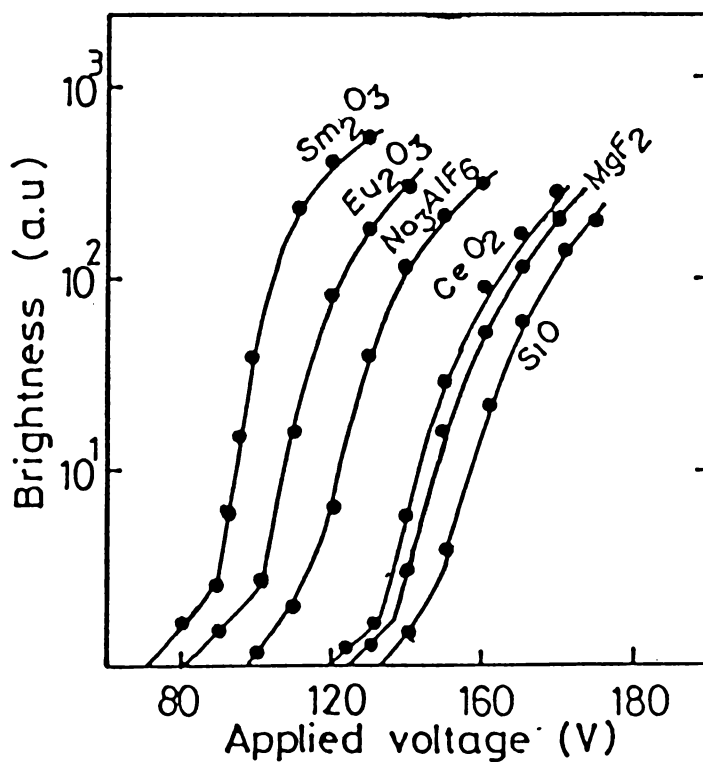


Fig.5.10. B-V characteristic of MISIM TFEL device under 1 kHz excitation frequency.
(ZnS: Mn - $0.6\mu\text{m}$ and insulator $0.3\mu\text{m}$)

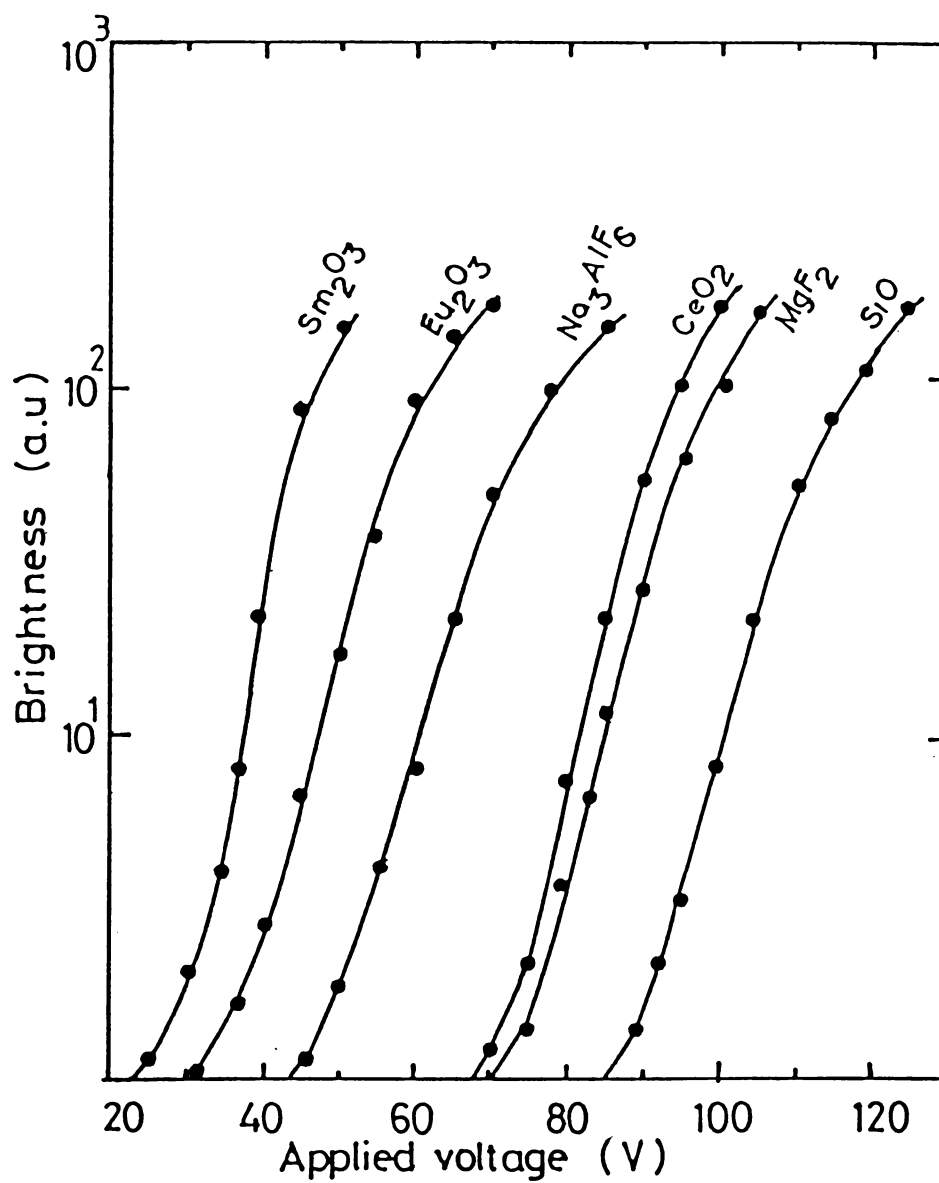


Fig.5.11. B-V characteristics of MIS TFEL devices under 1 KHz excitation (ZnS:Mn - 0.3 μm and insulator 0.2 μm).

with Sm_2O_3 insulator. Table 5.1 illustrates the insulator material used in TFEL device with the value of its dielectric constant and loss factor (at 1 KHz) at room temperature. It also gives the breakdown strength of the insulator material and the threshold voltage for onset of emission for MISIM and MIS structure based devices at 1 KHz excitation frequency. The threshold voltage for onset of emission is minimum for the device with insulator Sm_2O_3 and it can be driven with a voltage below 50 volts. Also from the table it is clear that the device employing insulator having high dielectric constant has low threshold voltage. When dielectric constant of the insulating layer is low, then the threshold voltage for onset of emission is high. This can be accounted using the equivalent circuit of the device employed for explaining B-V characteristic, as shown in Fig. 5.4. We have the relation between the threshold voltage for onset of emission and applied voltage given by 5.2 as

$$U_{\text{th}} = \frac{Z_s(\omega)}{Z_i(\omega) + Z_s(\omega)} V_{\text{th}} \quad 5.3$$

The impedance offered by the insulating layer

$$Z_i = \left(R_i^2 + \frac{1}{C_i^2 \omega^2} \right)^{1/2} \quad 5.4$$

Table 5.1

Insulating Material	Dielectric constant	$\tan\delta$	Breakdown Strength	V_{th} of MISIM device (volts)	V_{th} of MIS device (volts)
Sm_2O_3	35-40	.02	$2.2 \times 10^6 \text{V/cm}$	80	25
Eu_2O_3	15-21	.05	$2 \times 10^6 \text{V/cm}$	90	30
Na_3AlF_6	6.6	0.40	$2.5 \times 10^6 \text{V/cm}$	100	45
MgF_2	4.9	0.1	$2 \times 10^6 \text{V/cm}$	120	65
SiO	3.2-5.2	.004-0.2	$2 \times 10^6 \text{V/cm}$	125	70
CeO_2	4.8	5.5	$3 \times 10^6 \text{V/cm}$	130	80

The capacitance C_i is directly proportional to the dielectric constant of insulating film. Hence for devices having insulating film with high dielectric constant will have smaller Z_i value, i.e., drop across the insulating layer is less. So the U_{th} can be obtained at lower applied voltage. Whereas in the case of devices employing insulating films with low dielectric constant, the impedance (Z_i) offered by insulating film will be high and hence U_{th} can be obtained only at higher applied voltages. Thus dielectric films with high dielectric constant is found to be suitable for TFEL devices for low voltage operation.

The B-V characteristic curve shows that (Figs 5.10, 11) the driving voltage for MIS structure is less than that for MISIM structure. In the latter case the effective field for acceleration of charge carriers injected from electrodes or generated in the insulating layers across ZnS layer will be greater compared with the same in device having MISIM structure. The doubly insulated TFEL device shows a remarkable increase in brightness when the applied voltage exceeds a certain value. The MIS TFEL device has no insulator layer between the electrode and ZnS layer. Thus carriers could be

readily injected from the electrode or released from the ZnS layer with the result that no carriers will accumulate near the ZnS-electrode interface, where as in MISIM TFEL device the charges will be stored in ZnS-insulator interface. As a consequence electric field induced by space charge at ZnS insulator layer is strong and it will superpose with electric field due to the applied voltage [22]. The trapped holes inside the ZnS layer can generate an internal field which increases the probability of electrons tunneling through the ZnS-insulator barrier. Moreover, the TFEL device being a capacitive load, conduction current which contributes to luminescence is different at high voltages [22]. These factors can account for the sudden increase in brightness observed for MISIM structure devices.

The brightness of these devices were measured in absolute unit as described in Chapter-II using a PMT having spectral response closely matching that of human eye as defector. Thus the brightness of the present devices with ZnS:Mn active layer is found to be 1450fL which is comparable with the reported values.

5.6 Aging effects of TFEL devices

It is well known that the threshold voltage for the TFEL devices increases with operating time and then gradually becomes constant [2]. Aging for more than 100 hrs. has been found to be required to stabilize the device characteristics [23]. The substrate temperature and deposition conditions are also critical for TFEL devices as they affect the maximum brightness. In the case of Y_2O_3 TFEL devices deposition of insulator layer at 473 K or annealing 723 K is found to be effective for higher brightness and it is attributed to the improvement of crystallinity of Y_2O_3 films [24].

Figures 5.12 and 5.13 shows the variation of threshold voltage with aging time for devices with Eu_2O_3 and Sm_2O_3 as insulating layers. It can be seen that devices prepared at higher substrate temperature (453 K) and subsequent annealing show little variation in the threshold voltage whereas devices prepared with cold substrate (300 K) show marked deviation in threshold voltage with operating time. It is observed that annealing can enhance the stabilization of the device more quickly. From the plot of dielectric constant and loss factors of Eu_2O_3 and Sm_2O_3 films prepared at

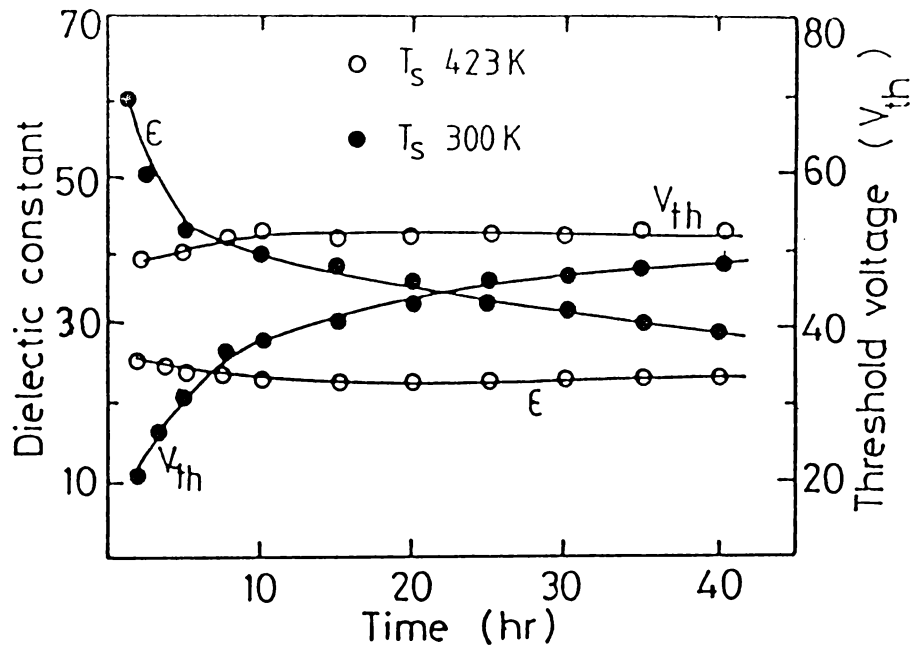


Fig.5.12. Variation of threshold voltage with aging time at 1 KHz for MIS TFEL device with Eu_2O_3 as insulator.

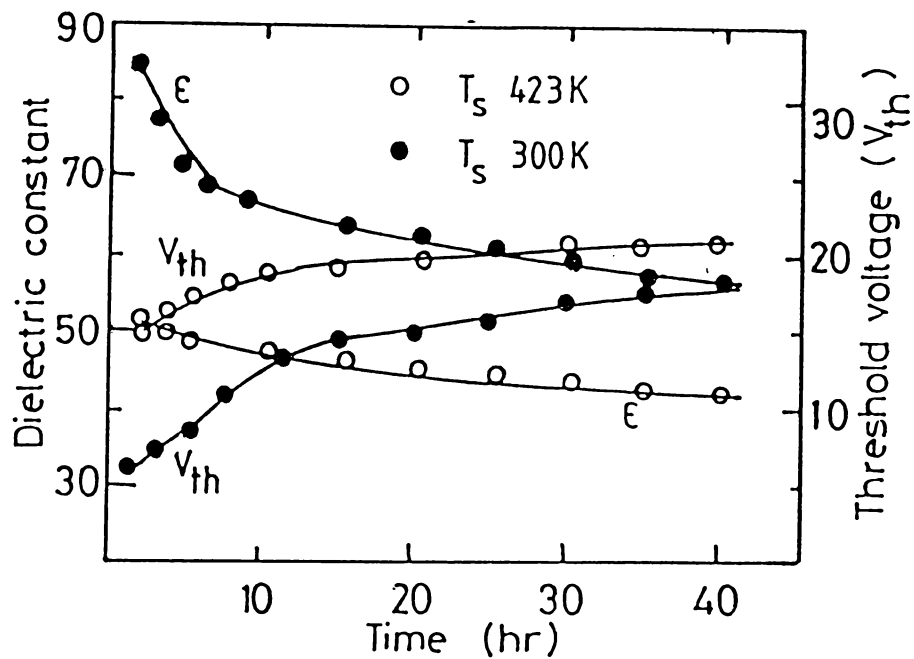


Fig.5.13. Variation of V_{th} at 1 KHz with aging time for MIS TFEL device with Sm_2O_3 as insulator.

substrate temperature of 453 K show stable dielectric properties i.e., the variation of dielectric constant and loss factor are negligible with aging time. But in the case of these films prepared at 300 K show drastic variation in their dielectric properties with aging time. It is found that the repeated annealing of these films at 150°C enhances the stabilization of dielectric properties fairly rapidly.

The shift in B-V characteristics with time of operation (Fig. 5.14) until a final curve is achieved is considered by Inoguchi and Mito [3] to be a stabilization or aging process rather than degradation. The effect of deposition conditions on the aging behaviour of AC TFEL devices may be due to variations in the characteristics of the ZnS:Mn or insulator layers. But ZnS deposited on cold substrate (300 K) is predominantly amorphous in nature whereas films deposited at 473 K are more polycrystalline [24]. On annealing at 723 ZnS:Mn films acquire more content with hexagonal phase.

Sasakura et al. [18] have reported that electron-beam evaporated ZnS:Mn is predominantly cubic, while Willoughly and Tuen [25] obtained a mixture of cubic and hexagonal phases in ZnS thin films prepared using

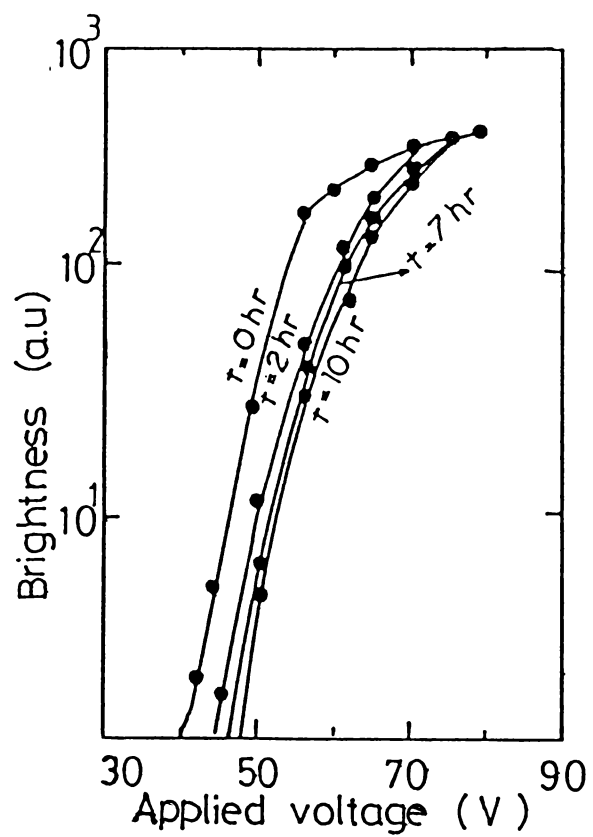


Fig.5.14. Aging characteristic of a typical AC TFEL device with Eu_2O_3 as insulator at 1 KHz excitation frequency ($T_{\text{substrate}} = 423 \text{ K}$).

same technique. ZnS:Mn deposited by Atomic Layer Epitaxy (ALE) method in sulphur atmosphere is purely hexagonal[26]. Hence the phase content of the ZnS film may not be critical for EL emission from manganese centers. Therefore the change in B-V characteristics and threshold voltage would depend on variations in the characteristics of the insulating layers.

Rare earth oxide films are amorphous in nature and no crystallinity was observed for films deposited at higher temperature. But the dielectric constant is found to show a constant value when prepared at higher substrate temperature. Hence the variation of the threshold voltage can be accounted using the equivalent circuits and U_{th} is given by equation 5.2. From 5.2 and 5.4 it is clear that as dielectric constant decreases with time the impedance offered by the dielectric film Z_i increases and hence voltage drops across the insulator. Thus a higher voltage is required for onset of emission. This explains why the threshold voltage for onset of emission increases with aging time. Thus the variation in threshold voltage is due to the variation in the dielectric properties of rare earth oxide films rather than in phase content of ZnS:Mn film.

REFERENCES

- [1] M S Russ and D I Kennedy; J.Electrochem Soc., 114(1967) 1066.
- [2] T Inoguchi, M Takeda, Y Kakihara, Y Nakata and M Yoshida; 1974 SID Int.Symp.Dig., Tech. Pap. V, Diego C A, (Society for Information Display, Los Angeles, CA, 1974), p.84.
- [3] T Inoguchi and S Mito; Topics in Applied Physics, Vol.17, Electroluminescence Ed. J I Pankove, Springer Verlag, Berlin, 1977, p.197.
- [4] H Kozawaguchi, J Ohwaki, B Tsujiyama and K Murase; 1982 SID Symp.Diego., Tech. Pap. XIII, San Diego, CA (Society for Information Display, Los Angeles, CA 1982) p.126.
- [5] W E Howard; Proc. SID, 18(1977) 119.
- [6] K Okamoto, Y Nasu and Y Hamakawa; IEEE Trans., ED 28[6] (1981) 698.
- [7] Y Fujita, J Kuwata, M Nishikawa, T Tohda, T Matsuoka, A Abe and T Nitta; Japan Display '83, Paper 4.1, October 3-5, Kobe, Japan.
- [8] Y Oishi, T Kato, Y Hamakawa; Japan Display '83, Paper 3.2, October 3-5, Kobe, Japan.
- [9] Y A Ono and M Fujama; J.Lumin., 40(1988) 796.
- [10] H Nakane, A Noya, S Kuriki and G Matsumoto; Thin Solid Films, 59(1979) 291.

- [11] H E Gumlich; J.Lumin.,23(1981) 73.
- [12] P J Dean; J.Lumin., 23(1981) 17.
- [13] R Törnquist; J.Cryst.Growth, 59(1982) 399.
- [14] J Shah and A E Di Giovanni; Appl.Phy.Lett.,
33(1978) 995.
- [15] T Takagi, I Yamada, A Sasaki and T Ishibashi;
IEEE Trans.Electron Devices, ED.20(1973) 1110.
- [16] K O Fugate; IEEE Trans. Electron Devices, ED.24
(1977) 909.
- [17] T Suyama, N Sawara, K Okamoto and Y Hamakawa;
Proc. 13th Conf.Solid State Devices, Tokyo,
Jpn.J.Appl.Phys., 21(1982) 383.
- [18] H Sasakura, H Kobayashi, S Tanaka, J Mita,
T Tanaka and H Nakayama; J.Appl.Phys.,
52(1981) 6901.
- [19] D Theis; Phy.Stat.Solidi, A.81(1984) 647.
- [20] D Theis, H Venghaus, H Oppolzer and S Schild;
Proc. First Europ. Display Res. Conf.
SID/NTG, (1981) 152.
- [21] K L Chopra; Thin Film Phenomena, (Mc Graw Hill
Book Co., New York, 1969) 475.

- [22] M Ogawa, S Nakada, M Sakurai and T Yoshida;
J. Lumin., 29(1984) 11.
- [23] H Kozawaguchi, B Tsujiyama, K Murase;
J. Appl. Phys., 21(1982) 1028.
- [24] T R N Kutty; Thin Solid Films, 127(1985) 223.
- [25] A F W Willoughly and F C Yuen; Thin Solid Films,
13(1972) 199.
- [26] N P Tanninen and T O Tuomi; Thin Solid Films,
90(1982) 339.

MULTICOLOUR EMITTING ZnS:RE TFEL DEVICES

Abstract:

ZnS:Mn TFEL devices emitting yellow light are now commercially available. But, still multicolour emitting devices are lacking in luminescence output. This chapter gives the fabrication details of ZnS:RE,Cl TFEL devices. The various emission bands obtained are assigned to the transitions of RE³⁺ ions. The blue green emitting ZnS:Tb,Cl is found to be the best device among them. The operating voltage of the device has been brought down below 50V using MIS structure for the device with Sm₂O₃ as insulator. The effect of halides (F⁻, Cl⁻, Br⁻) and oxygen O₂⁻ on the EL emission spectra ZnS:Pr TFEL device is presented. The device with fluoride dopant has been found to have the maximum efficiency. The halogen compounds of rare earth elements offering efficient luminescent centers are explained to some extent. The PrF₃ dopant appears as a promising candidate for EL devices because of its capacity for producing white light emission from single luminescent centre.

6.1 Introduction

TFEL displays are generally recognized as the most aesthetically pleasing among the flat display systems. A TFEL display is an active light emitter, has clearly defined uniformly illuminated pixels and has high contrast because of its low reflectivity yet specular like surface. The TFEL display has become a viable, producible flat-panel display for wide range of applications. In spite of these advantages, these devices require still higher luminescence output and contrast for use in high ambients upto sunlight and for multi-colour displays.

Various types of luminescent centers such as transition ions, rare earth (RE) ions and donor acceptor pair impurities have been employed in ZnS TFEL devices to obtain multicolour emission [1,2]. Due to a wide variety of emission wave lengths possible with rare earth ions in the visible spectrum, extensive investigations have been carried out in recent years in this direction [2,3,4]. Earlier workers have noted that in the case of samples doped with RE metals, one obtains bright spots but where halide coactivation (F, Cl) was used, the EL emission

was uniform over the entire surface [5,6].

It is difficult to introduce substitutionally RE ions into ZnS with relatively high concentration because of the mismatch in ion size and charge valance between Zn^{2+} and RE^{3+} ions. A new type of emission centre was proposed by Chase et al. [1] who introduced rare earth fluoride in ZnS. This molecular centre offer several advantages such as possibility of high doping levels and weak coupling with the lattice vibration. Among RE luminescent centers TbF_3 dopant is identified as the most efficient emitter (green). The best reported value for TbF_3 device is 2400 cd/m^2 by Hale et al. [7]. But in literature very few reports on luminescent centers with RE other than Tb exist. Inspite of all efforts, the maximum brightness achieved with these activators is relatively low [8]. These factors motivated the study of ZnS:RE,Cl TFEL devices. The following section gives the fabrication and study of ZnS:RE:Cl (RE = Tb,Sm,Dy,Nd,Er,Eu,Pr) in devices with MISIM and MIS structure. The Sm_2O_3 insulator layer is found to be effective for low voltage operation and the device parameters are optimised in terms of thickness of active and insulator layer. The last section

of this chapter gives the effect of halide and oxide coactivators on the device performance and emission spectra.

6.2 Device Fabrication

The EL devices with thin film structure of $\text{SnO}_2\text{-Sm}_2\text{O}_3\text{-ZnS:RE,Cl-Sm}_2\text{O}_2\text{-Al}$ (MISIM) and $\text{SnO}_2\text{-ZnS:RE,Cl-Sm}_2\text{O}_3\text{-Al}$ (MIS) (shown in Fig. 5.1) were fabricated as described below. The transparent conducting glass plates were prepared by spray pyrolysis of an aqueous solution of SnCl_4 onto a glass substrate kept at 450°C as described in Chapter-II. The SnO_2 coated glass plate having a transmittance above 80% and sheet resistance below $120 \Omega/\square$ cm were selected for the fabrication of the devices. The active layer of ZnS:RE,Cl was evaporated onto SnO_2 coated glass substrate using an electron beam gun from ZnS:RE,Cl phosphors prepared in the laboratory by the slurring technique described in Chapter-II. The starting material of ZnS was luminescent grade material from Koch light, England. The Sm_2O_3 insulating layer was evaporated onto this followed by the aluminium back electrode. During the deposition of the insulator and active layer the substrate temperature was maintained at 150°C . After the deposition of insulator layer the

film was annealed at 150°C for one hour. The experimental investigations were carried out using AC TFEL cells having a rectangular area of 0.5 cm². The EL emission and brightness voltage characteristics were studied using the experimental set up described in Chapter-II.

The device performance such as brightness and threshold voltage depends not only on the type of insulating material but also on the film thickness of ZnS layer and insulator thickness. In the case of device with Sm₂O₃ as insulator, the device having an active layer to insulator thickness ratio, t_z/t_I lying between 1 and 2 is found to be the optimal condition for the low voltage operation of the MIS TFEL device. Figure 6.1 gives the B-V characteristic of the device with ZnS:Pr,Cl as active layer and Sm₂O₃ as the insulator with different insulator thicknesses keeping the thickness of active layer fixed and also for different active layer thicknesses with insulator thickness constant. It is found that the threshold voltage for onset of emission can be reduced by reducing the thickness of ZnS layer thickness or insulator or both. But reduction of ZnS layer thickness causes reduction in brightness which can be compensated by reducing insulator thickness. The reasons for dependence of brightness and threshold voltage on the

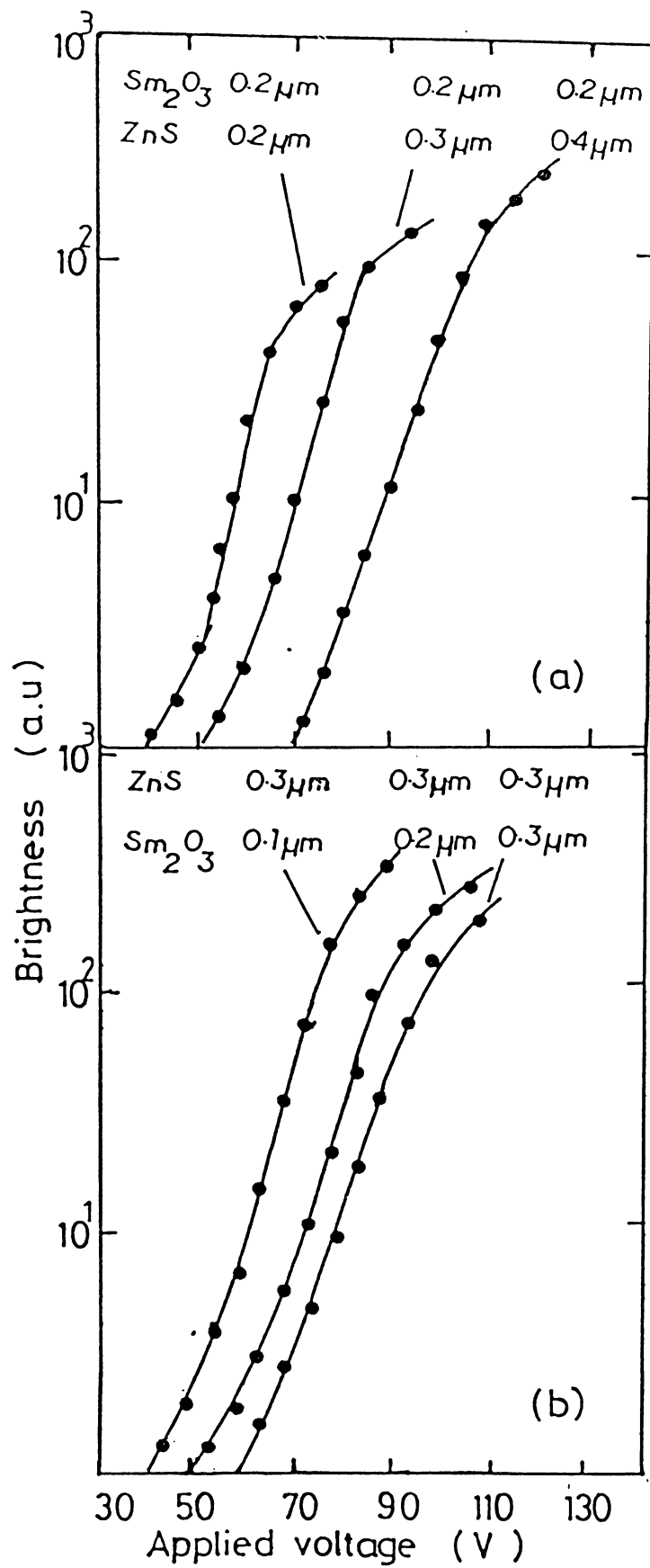


Fig.6.1. B-V characteristic of the ZnS:Pr,Cl MIS TFEL device with Sm_2O_3 as insulator (a) varying active layer, and (b) varying insulator layer thickness.

active and insulator film thickness in case of device with Eu_2O_3 as described in Chapter-V holds good in this case also. Taking into account of the maximum brightness and low threshold voltage optimal condition is found to be for an active layer to insulator thickness ratio in the range 1-2. Consequently the TFEL devices with MIS structure were prepared with active layer thickness $0.3 \mu\text{m}$ and an insulator thickness of $0.2 \mu\text{m}$.

Sm_2O_3 has been selected as the insulator layer because it has got high dielectric constant of 43 and low loss factor. The film has a transmittance above 90%. The detailed study on dielectric properties of Sm_2O_3 is given in Chapter-IV.

6.3 EL emission characteristics of the devices

6.3.1 ZnS:Pr,Cl.

The EL emission spectra of a typical TFEL device with ZnS:Pr,Cl active layer under 1 KHz excitation frequency is as shown in Figure 6.2. These devices give emission at 450, 500, 580, 615, 680 and 700 nm. The emission spectral characteristics of these devices are found to be more or less independent of excitation frequency. Blue green (500 nm) ${}^3\text{P}_0 \longrightarrow {}^3\text{H}_4$ and orange (580 nm, 615 nm) ${}^3\text{P}_0 \longrightarrow {}^3\text{H}_5$,

${}^3P_0 \rightarrow {}^3H_6$ transitions dominate this spectrum and the overall emission colour is yellow-orange in appearance. The assignments are based on those of Dieke and Sarup [9]. Unlike the ZnS:PrF₃ system [1,10], the PrCl₃ doped device has emission at slightly higher wavelength. Luminescence characteristics such as emission and brightness are strongly dependent on the environmental effects. It is expected that emission properties depend on the number of halide ions linked to Pr³⁺ ion, which result in different strength and symmetry of crystal field [11]. In order to have clear picture, further studies on Pr³⁺ emission on halide concentration are necessary.

6.3.2. ZnS:Nd,Cl.

The distinguishing feature of this system is the IR output, which is largest among the Lumocen devices. Though very few reports on ZnS:Nd system are available, Zhong et al. [12] have reported that stimulated emission at 1080 nm can be achieved in DCEL of ZnS:Cu,Nd,Cl thin films by population inversion involving ${}^4F_{3/2}$ and ${}^4I_{11/2}$ energy levels.

Figure 6.3 shows the EL emission spectra of the device with ZnS:Nd,Cl as active layer. Because of the

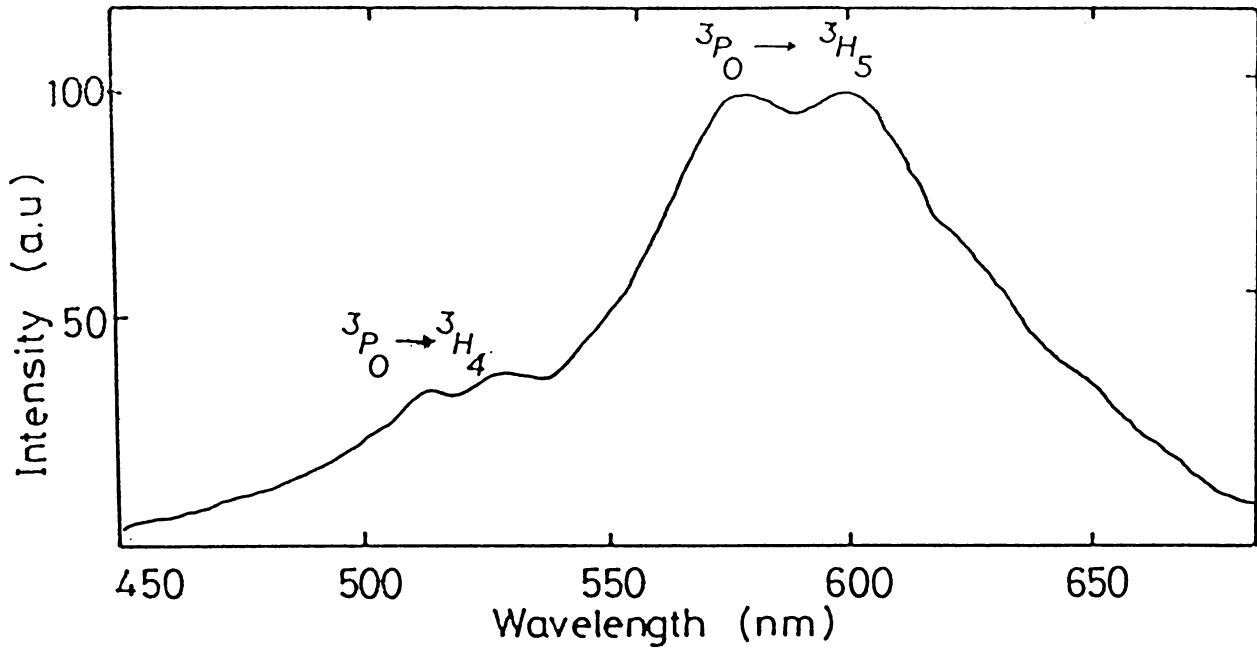


Fig.6.2. EL emission spectra of ZnS:Pr,Cl TFEL device with 1 KHz excitation frequency.

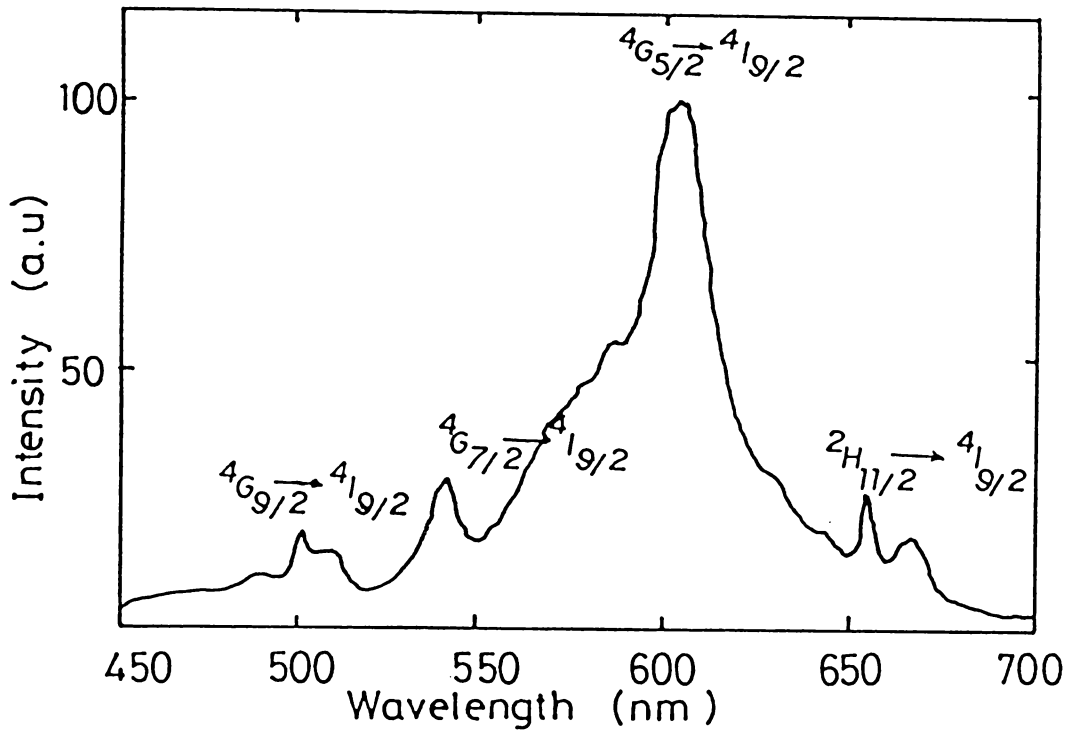


Fig.6.3. EL emission spectra of ZnS:Nd,Cl TFEL device under 1 KHz excitation frequency.

limitation of monochromator and PMT sensitivity the EL emission spectra is recorded only in the visible region. The device has an orange emission colour which results due to the following transitions of Nd^{3+} ions

$${}^4\text{G}_{7/2} \longrightarrow {}^4\text{I}_{9/2} \text{ (606 nm and 586 nm), } {}^4\text{G}_{9/2} \longrightarrow {}^4\text{I}_{9/2}$$

$$\text{(488 and 500 nm) and } {}^2\text{H}_{11/2} \longrightarrow {}^4\text{I}_{9/2} \text{ (656, 686 nm).}$$

6.3.3. ZnS:Sm,Cl.

Samarium is a significant luminescent centre which are of interest for full colour display. ZnS:SmF₃ has orange-red emission [2]. The EL emission of the present device with ZnS:Sm,Cl as active layer appears orange-red. The dominant transitions are occurring at 600 nm (${}^4\text{G}_{5/2} \longrightarrow {}^6\text{H}_{7/2}$) and 650 nm (${}^4\text{G}_{5/2} \longrightarrow {}^6\text{H}_{9/2}$). Weak emission line at 570 nm (${}^4\text{G}_{5/2} \longrightarrow {}^6\text{H}_{7/2}$) is also observed. The EL emission spectra of the device is shown in Fig. 6.4.

6.3.4. ZnS:Eu,Cl.

Unlike other rare earth system ZnS:Eu,Cl device is found to have broad band emission. The ${}^5\text{D}_0 \longrightarrow {}^7\text{F}_2$ transition [13] at 610 nm is the dominant one (Fig. 6.5). In addition, there are transitions from the ${}^5\text{D}_0$ to some other

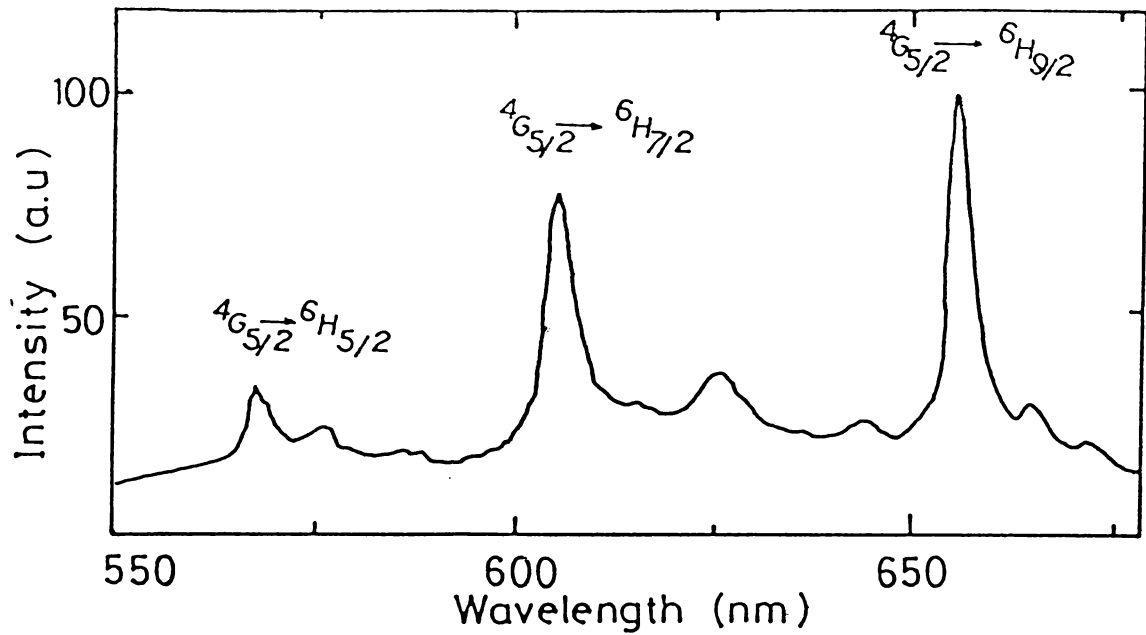


Fig.6.4. EL emission spectra of ZnS:Sm,Cl TFEL device under 1 KHz excitation frequency.

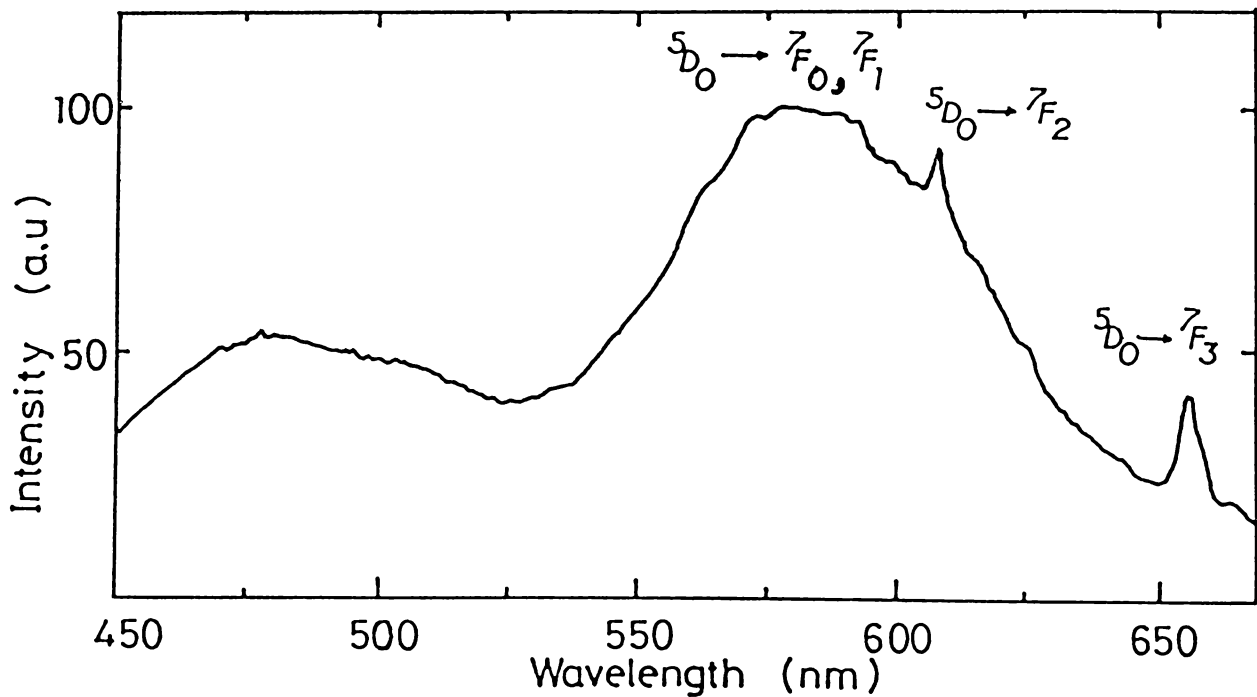


Fig.6.5. EL emission spectra of ZnS:Eu,Cl TFEL device under 1 KHz excitation frequency.

levels of the 7F multiplet viz., ${}^5D_0 \longrightarrow {}^7F_0$ (650 nms). The broad band on the lower wavelength side centered around 480 nm is probably due to presence of some Eu^{2+} impurity [14].

6.3.5. ZnS:Tb,Cl.

Among the localised emission centers, such as rare earth elements, terbium (Tb) doped zinc sulphide shows the brightest green electroluminescence. All ZnS:Tb devices give rise to transitions which originate in the 5D_3 and 5D_4 and terminate in the 7F manifold [15]. Emission from 5D_3 level is generally weaker and has been shown to decrease with concentration [16]. Figure 6.6 shows the EL emission spectra of ZnS:Tb,Cl device. As can be seen from the EL spectra of the device, it has emissions corresponding to ${}^5D_4 \longrightarrow {}^7F_j$ ($j = 3,4,5,6$) transition of Tb^{3+} ion. The emission corresponding to the transition ${}^5D_4 \longrightarrow {}^7F_5$ occurring at 505 nm in bluish-green is the most prominent one. The present device with ZnS:Tb,Cl has emission at slightly shorter wavelength than that in the case of ZnS:TbF₃ systems [2]. There are marked difference between spectra of ZnS:RE and ZnS:RE F₃. It appears the spectral details depend sensitively on sample preparation, concentration of rare earth activator and coactivators.

6.3.6. ZnS:Dy,Cl.

Figure 6.7 shows the EL spectra of a typical ZnS:Dy,Cl TFEL device at 1 KHz excitation frequency. The yellow output of these devices arises from the strong emission from ${}^4F_{9/2} \longrightarrow {}^6H_{13/2}$ transition [17]. In the present case ZnS doped DyCl₃ TFEL cells, the type of transitions of Dy ions observed are similar to those appearing in DyF₃ doped ZnS TFEL device [1] and Dy doped CaS phosphors [18].

6.3.7. ZnS:Er,Cl.

Among the ZnS:RE system ZnS:Er seems to be very little studied. Xu-mou Xu et al. [19] have calculated the input cross section of Er³⁺ ions in ZnS and this comes to the value about $2 \times 10^{-16} \text{ cm}^2$. The EL emission spectra of the present device with ZnS:Er active layer is as given in Figure 6.8. The faint green light emitted by this system is the result of the transitions at 530 nm (${}^2P_{3/2} \longrightarrow {}^4I_{9/2}$ or ${}^2H_{11/2} \longrightarrow {}^4I_{15/2}$) and 550 nm (${}^4S_{3/2} \longrightarrow {}^4I_{15/2}$). In addition there are other transitions at 650 nm (${}^4F_{9/2} \longrightarrow {}^4I_{15/2}$) [20]. The spectra observed in the case of ZnS:RE Cl₃ differ generally in relative intensity of the lines from those observed for

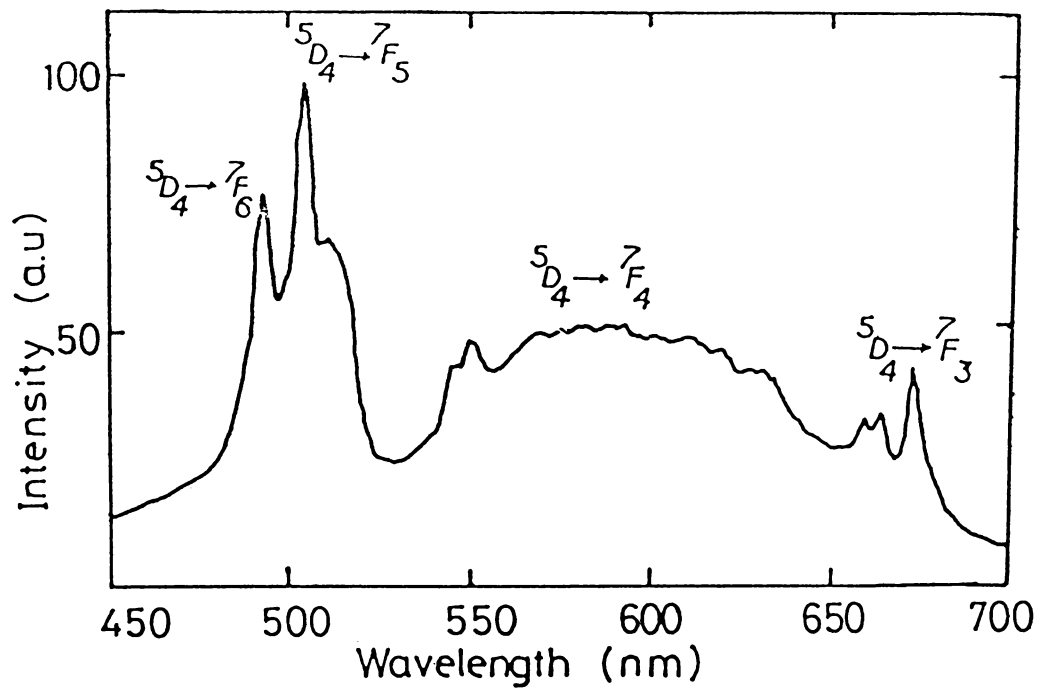


Fig.6.6. EL emission spectra of ZnS:Tb,Cl TFEL device under 1 KHz excitation frequency.

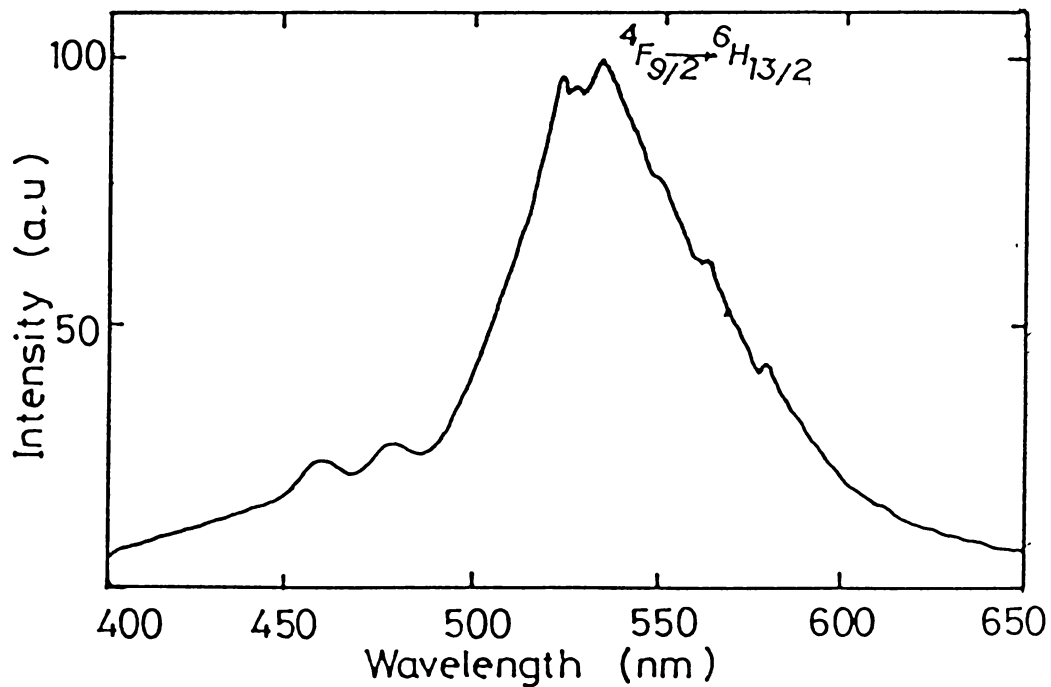


Fig.6.7. EL emission spectra of ZnS:Dy,Cl TFEL device under 1 KHz excitation frequency.

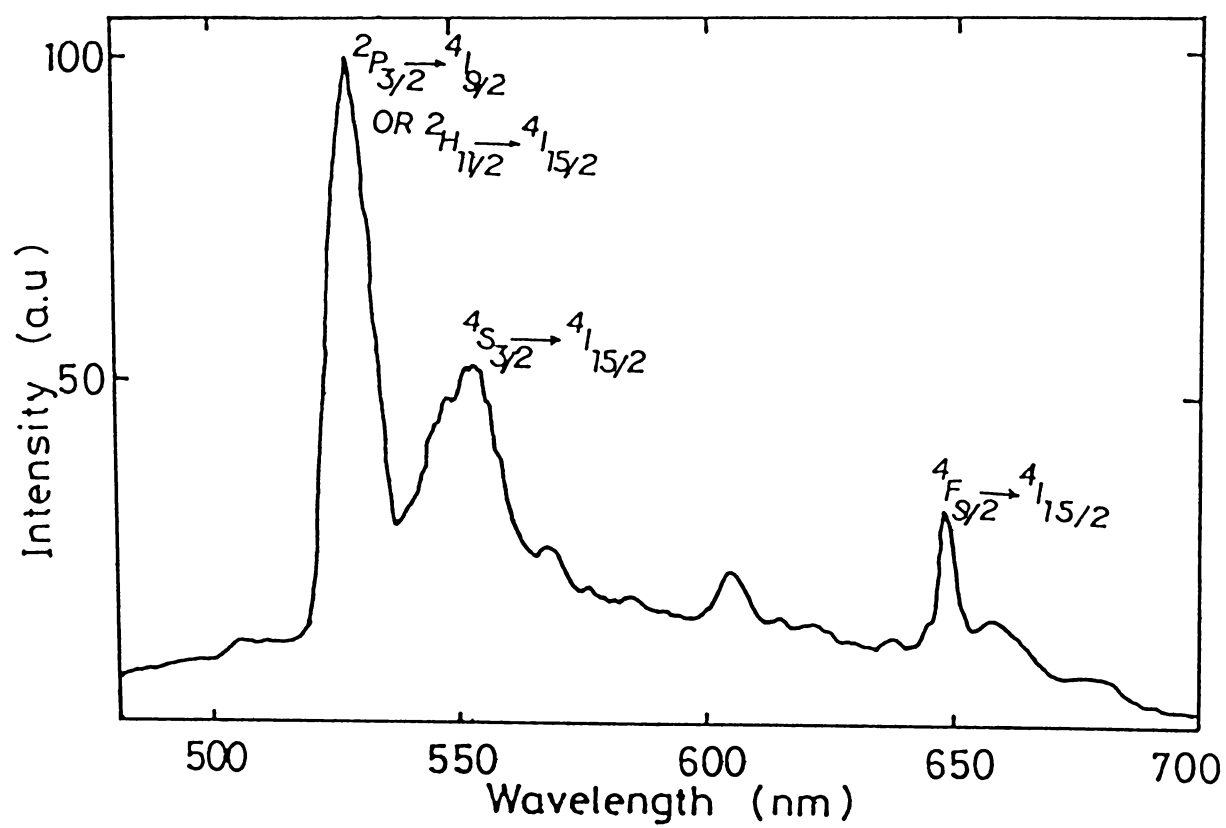


Fig.6.8. EL emission spectra of ZnS:Er,Cl TFEL device under 1 KHz excitation frequency.

bare ions in ZnS [21, 22] and also in some cases from RE F₃ dopants systems [1]. If one makes the assumption that the dominant contribution to the crystal field at the central ion arises from the neighbouring chlorine, it is reasonable to expect that this field will vary from site to site as the molecule distorts to achieve the minimum energy in its cavity within ZnS lattice. On this model, it is possible to account for the large breadth of the lines without invoking strong coupling to the lattice. The effect of halides and oxide coactivation on the emission characteristic of ZnS:Pr system is described at the end of this chapter.

6.4 Brightness voltage characteristics

The brightness-voltage (B-V) characteristics of these devices with ZnS:RE,Cl as active layers and Sm₂O₃ as insulator having MISIM and MIS structure under 1 KHz excitation frequency are shown in Figure 6.9 and Figure 6.10 respectively. Figure 6.11 shows the B-V characteristic of devices with ZnS:Sm,Cl as active layer and MgF₂, Eu₂O₃, Sm₂O₃ and BaTiO₃ as insulators in the MIS and MISIM structure. It is observed that device with insulator having high dielectric constant has low threshold voltage for onset of emission. In the present case the device with Sm₂O₃ as

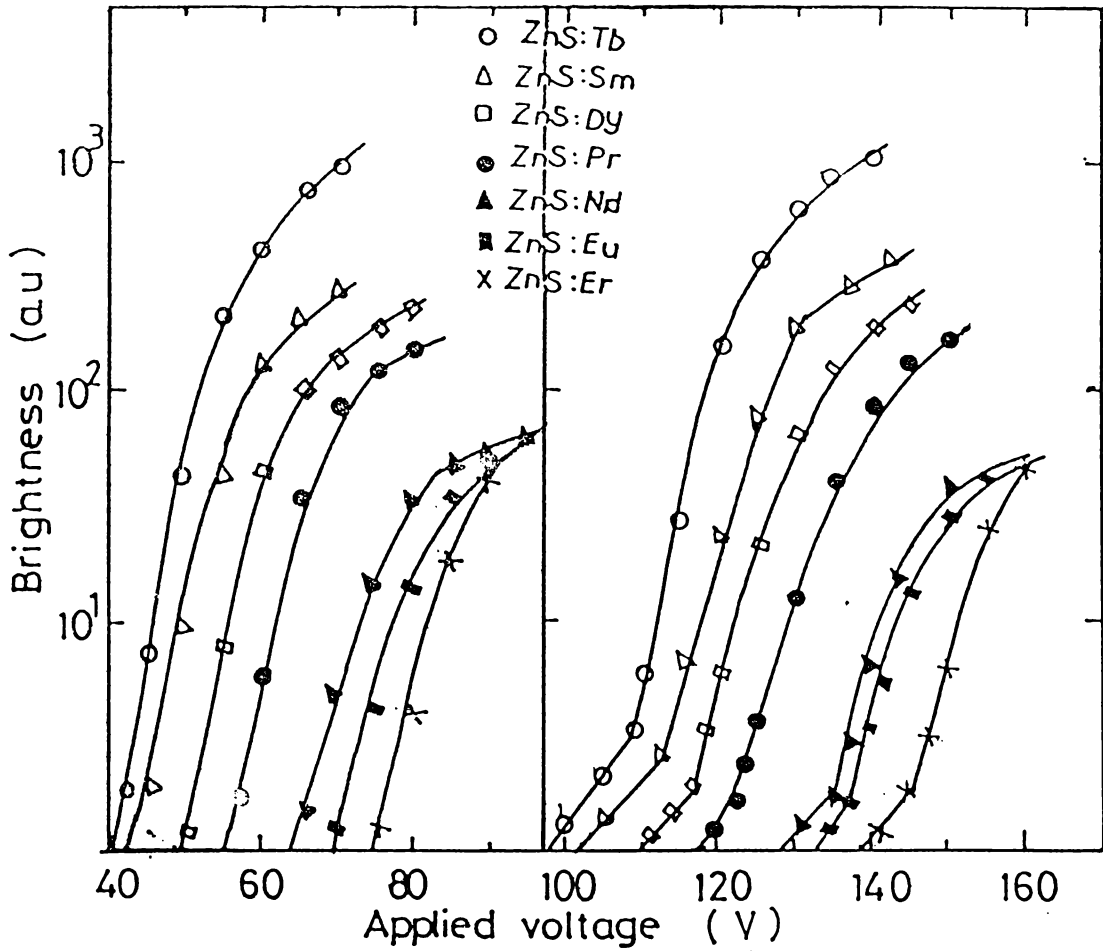


Fig.6.9. B-V characteristic of ZnS:RE,Cl MIS TFEL device with Sm_2O_3 as insulator at 1 KHz.

Fig.6.10. B-V characteristic of ZnS:RE,Cl MISIM TFEL device with Sm_2O_3 as insulator at 1 KHz

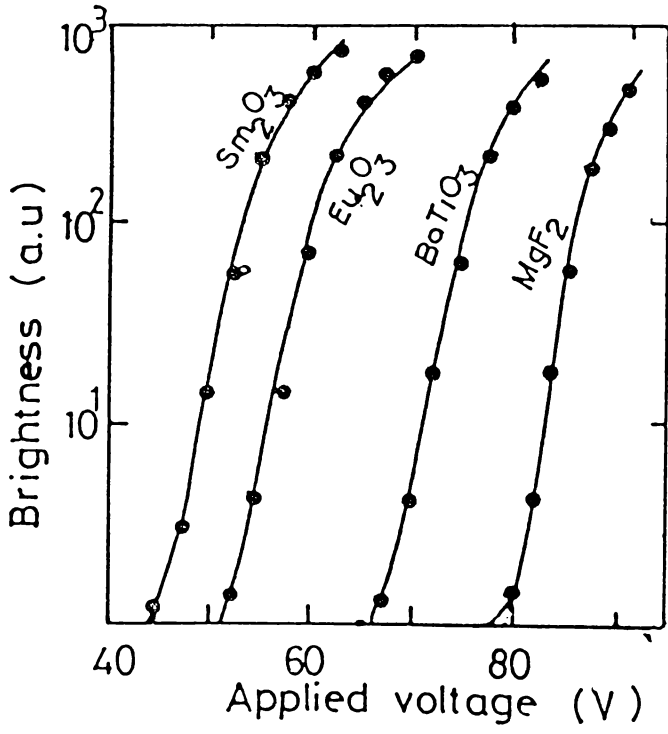


Fig.6.11. B-V characteristic of ZnS:Sm,Cl MIS and MISIM TFEL devices with different insulating layers at 1 KHz excitation frequency.

insulating layer in MIS structure has the lowest threshold voltage. The reasons for this can be explained in terms of the dielectric constant of the insulating material as described in Chapter-V. Nanto et al. [23] have reported low voltage TFEL device with BaTiO_3 ceramic sheet as insulator which has very high dielectric constant. However, in the present case the BaTiO_3 films show very low dielectric constant. This may be due to impurities and defects and perforation in the film.

The experimental results shown in Figures 6.9 and 6.10 indicate that brightness of rare earth doped ZnS devices could not compete with that of Mn doped devices. The brightness of ZnS:Tb,Cl device, although the best among the rare earth doped devices is still only about 60% of that ZnS:Mn. The devices with ZnS:Eu,Cl and ZnS:Er,Cl are least efficient. But for ZnS:RE,Cl devices there is an optimum concentration and its value is found to depend upon the kind of the activator.

From the B-V characteristics (Figures 6.10, 11) it can be seen that the doubly insulated TFEL device shows a remarkable increase in brightness when the applied voltage exceeds a certain value, whereas in MIS TFEL device the brightness is found to increase steeply and after attaining

a certain brightness value it levels off indicating saturation. The MIS TFEL device has no insulator in between the electrode and ZnS layer. Thus carriers could be readily injected from the electrode or released from the ZnS layer with the result that no carriers will accumulate near the ZnS-electrode interface, whereas in MISIM TFEL device the charge will be stored in ZnS-insulator interface. As a consequence electric field induced by space charge at ZnS-insulator layer is strong as it will superpose with electric field due to the applied voltage [24]. The trapped holes inside the ZnS layer can generate an internal field which increases the probability of electrons tunnelling through the ZnS-insulator barrier. Moreover, the TFEL device being a capacitive load, conduction current which contributes to luminescence is different at high voltages [24]. These factors account for the sudden increase in brightness observed for MISIM structure devices.

6.5 Effect of halides on the EL emission spectra and brightness of ZnS:Pr TFEL devices

Thin film EL devices, though have a number of advantages there are applications that require higher luminescence and contrast for use in high ambience upto

sunlight and for multicolour displays. Thus practical application calls for other colours of emitted light, especially white. In view of this Praseodymium was chosen as dopant in ZnS matrix. The brightness of TFEL structures strongly depends on particular rare earth compound used in the doping [5,6]. Also it is difficult to introduce rare earth ions into ZnS with relatively high concentration because of the mismatch in ion size and charge valance between Zn^{2+} and RE^{3+} ions. A new type of emission centre was proposed by Chase et al. [1] who introduced rare earth fluoride in ZnS. This molecular centre offers several advantages such as possibility of high doping and weak coupling with lattice vibration. The present investigation are on the effect of coactivation of halides on the EL spectra of ZnS:Pr. It is well known fact that emission spectra and brightness depend critically on preparation conditions [25]. Thin film electroluminescent devices having low threshold voltage and white like emission have been developed using ZnS:PrF₃ as active layer and Sm₂O₃ as insulator. The effect of F⁻, Cl⁻, Br⁻ and O₂⁻ coactivation of ZnS:Pr TFEL devices on the EL spectra and brightness are investigated here.

The TFEL devices were prepared with SnO₂-ZnS:Pr-Sm₂O₃-Al

having MIS structure. The conducting transparent electrodes were prepared by spray pyrolysis method. The active layer ($\sim 0.3 \mu\text{m}$) was evaporated by electron beam gun from the phosphors prepared in the laboratory. Then the insulator layer ($0.2 \mu\text{m}$) Sm_2O_3 was evaporated by electron beam gun. Evaporated aluminium acts as the back electrode. The phosphors for active layer was prepared using luminescent grade ZnS with 3 wt % of Pr, which was introduced in the form of PrF_3 , PrCl_3 , PrBr_3 and Pr_3O_{11} . $\text{Na}_2\text{S}_2\text{O}_3$ was used as flux. The phosphor was prepared by slurring technique and vacuum firing process as described in Chapter-II.

Figure 6.12 shows the EL emission spectra of ZnS:Pr TFEL devices coactivated with F^- , Cl^- , Br^- and O^{2-} . The EL spectra of ZnS: PrF_3 shows two emissive groups that are centered around 500 nm and 650 nm. The former corresponds to ${}^3\text{P}_0 \longrightarrow {}^3\text{H}_4$ and the latter to ${}^3\text{P}_0 \longrightarrow {}^3\text{F}_2$ of Pr^{3+} ions. These two groups of spectral emission roughly satisfy the complementary colour relationship. The comparative intensity relationship is such that these combination results in a white appearance. The emission colour is independent of driving voltage and excitation frequency.

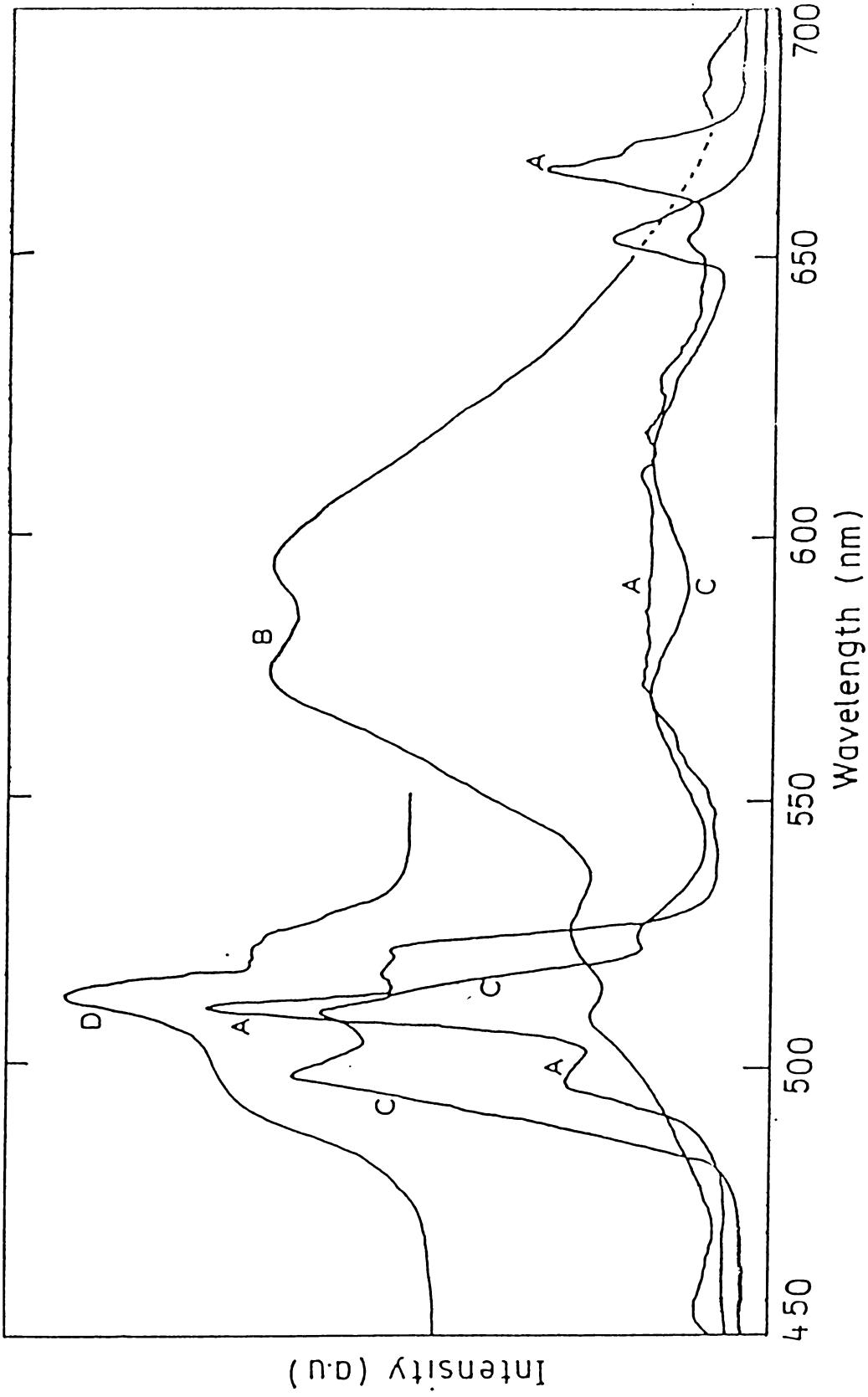


Fig.6.12. EL emission spectra of ZnS:Pr TFEL devices coactivated with F^- , Cl^- , Br^- and O_2^- under 1 KHz excitation frequency
 A- ZnS:PrF₃, B- ZnS:PrCl₃, C- ZnS:PrBr₃, D- ZnS:PrO₁₁

In the case of ZnS:PrBr₃ and ZnS:Pr₆O₁₁ also the emission shows transition corresponding to $^3P_0 \longrightarrow ^3H_4$ at 500 nm and $^3P_0 \longrightarrow ^3F_2$ at 650 nms. But in the case of ZnS:PrCl₃ system the transition corresponding to $^3P_0 \longrightarrow ^3H_5$ and $^3P_0 \longrightarrow ^3H_6$ (580 nm and 600 nm) are prominent.

Luminescence characteristics such as emission and brightness are strongly dependent on the environmental effects. It is expected that emission properties depend on the number of halide ion linked to Pr³⁺ ion which result in different strength and symmetry of crystal field [3].

Figure 6.13 shows the brightness voltage (B-V) characteristics of these devices. The device with ZnS:PrF₃ have maximum brightness while ZnS:Pr₆O₁₁ is least efficient. Thus Halogen compounds of rare earth elements offer efficient luminescent centre in TFEL device and this may be due to the following facts: (i) The low solubility of trivalent rare earth ions in ZnS which would prevent one from introducing these ions in concentrations sufficiently large to optimise electroluminescence efficiency. This could be circumvated by the introduction of a neutral entity, (ii) the valance of rare earth ion could be controlled by choosing an appropriate rare earth compound which does not dissociate during evaporation, (iii) since

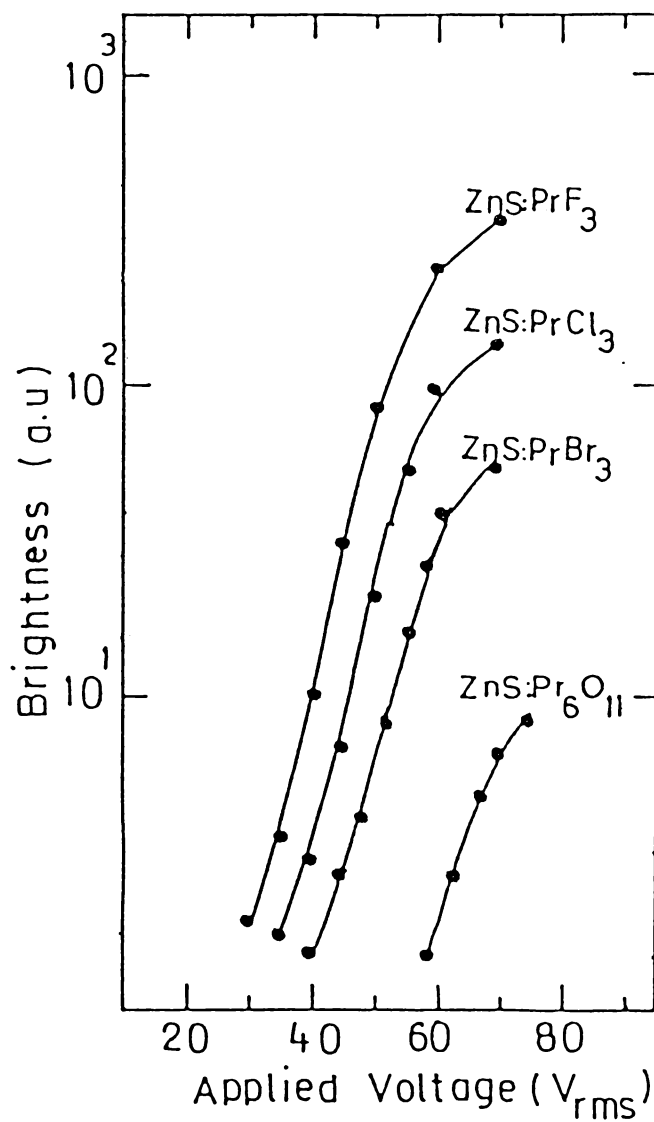


Fig.6.13. B-V characteristics of ZnS:Pr TFEL devices coactivated with F^- , Cl^- , Br^- and O_2^- under 3 KHz excitation frequency.

the excitation of the active ions was assumed to proceed by direct electron impact, the large size of molecular system could serve to increase the excitation cross sections, (iv) in a molecular center weakly coupled to the surroundings, non radiative decay of the fluorescing ion could be reduced in comparison with a system where the ion enters substitutionally. From the above studies, the PrF_3 appears to be a promising candidate for application of EL devices because of its capacity of producing white light from a single luminescent centre.

REFERENCES

- [1] E W Chase, R T Hepplewhite, D C Krupka and D Kahng;
J.Appl.Phys., 40(1969) 2512.
- [2] H Kobayashi, S Tanaka, V Shanker, M Shiiki, T Kunou,
J Mita and H Sasakura; Phys.Stat.Sol.,(a)
88(1985) 713.
- [3] A Mikami, T Ogura, K Tanaka, K Taniguchi, M Yoshida
and S Nakajima; J.Appl.Phys., 61(1987) 3028.
- [4] J Ohwaki, B Tsujiyama and H Kozawaguchi; Jpn.J.Appl.
Phys., 23(1984) 669.
- [5] E C Freeman, D H Baird and J R Weaver; Proc.Int.
SID Conf., 25/3 (1984) 183.
- [6] H Kobayashi, S Tanaka, T Kunou, M Shiiki and
H Sasakura; Proc.Int. SID Conf., 25/3(1984) 187.
- [7] L G Hale, B Garcia, R D Ketchpel and T C Lim;
Digest 1980 Internat.Elect.Dev.Mtg. IEEE,
New York, (1980) p. 719.
- [8] T Suyama, W Sawara, K Okamoto and Y Hamakawa; Proc.
13th Conf. Solid State Devices, Tokyo 1981,
Jpn.J.Appl.Phys. 21, Sept., 21-1(1982) 383.
- [9] G H Dieke and R Sarup; J.Chem.Phys., 29(1958) 741.

- [10] M Yoshida, K Tanaka, K Taniguchi, T Yamashita,
Y Kakiyama and T Inoguchi; SID '80, Digest, p.106.
- [11] A Mikami, T Ogura, K Tanaka, K Taniguchi, M Yoshida
and S Nakajima; J.Appl.Phys., 61(1987) 3028.
- [12] G Z Zhong and F J Bryant; Solid State Commun.,
39(1981) 907.
- [13] L G de Shazer and G H Dieke; J.Chem.Phys., 38(1963) 2195.
- [14] M V Hobden; Phys.Lett., 15(1965) 10.
- [15] K S Thomas, S Singh and G H Dieke; J.Chem.Phys.,
38(1963) 2180.
- [16] A D Pearson, G E Peterson and W R Northover;
J.Appl.Phys. 37(1966) 729.
- [17] H M Crosswhite and G H Dieke; J.Chem.Phys., 35(1961)
1535.
- [18] S M Pillai and C P G Vallabhan; Phys.Stat.Sol.,
(b) 134 (1986) 383.
- [19] Xu-mou XU, Jia-gi YU and Guo-Zhu Zhong; J.Lumin.,
36(1986) 101.
- [20] G H Dieke and S Singh; J.Chem.Phys., 35(1961) 555.

- [21] W W Anderson and D J Walsh; *J.Chem.Phys.*,
43(1965) 1153.
- [22] H C Froelich; *J.Electrochem.Soc.*, 100(1953) 496.
- [23] H Nanto, T Minami, S Murakami and S Takata;
Thin Solid Films, 164(1988) 363.
- [24] M Ogawa, S Nakada, M Sakurai and T Yoshioka;
J.Lumin., 29(1984) 11.
- [25] P Benalloul, J Benoit and A Geoffrey; *J.Cryst.*
Growth, 72(1985) 713.

Chapter-VII

DC POWDER AND THIN FILM ELECTROLUMINESCENT DEVICES

Abstract:

DC powder and thin film EL devices can be excited more efficiently in the pulsed excitation mode thus producing higher brightness level. In this chapter the fabrication techniques of DC powder EL and DC TFEL devices are given. From the current voltage and brightness voltage measurements, the forming process and degradation of the devices are explained. The EL spectra of ZnS:Mn DC TFEL device is found to contain some shorter wave length emission due to Cu centers. This is explained in terms of the Cu migration from Cu_xS layer to ZnS:Mn layer. The active layer of the device can be considered as ZnS:Cu, Mn,Cl layer. This conclusion is supported from the additional experimental observation on the electrical conductivity studies of each layer. DC TFEL devices with multicolour emission using ZnS:RE and their spectroscopic transitions are also included in this chapter.

7.1 Introduction

Electroluminescent devices based on ZnS doped with Mn with various device structures prepared by different methods are still being investigated because of their efficient luminescent output. It is reported that, compared to the AC panels, DC devices can be excited more efficiently in the pulsed excitation mode thus producing higher brightness level. Cross talk effect is less in this type of panels because of their highly nonlinear brightness-voltage characteristics. Moreover, the scanning circuit of these devices will be simpler in the DC mode of operation. Presently available DC EL devices are of two types, (i) DC Powder EL cells [1], (ii) DC TFEL cells [2].

The ZnS:Mn,Cu DC electroluminescent (DCEL) powder panels have become reasonably successful as displays despite a lack of detailed knowledge of the mechanisms involved in their operation. These are essentially Destriau type cells which consists of the electroluminescent phosphor suspended in a dielectric sandwiched between two electrodes. An efficient DC powder EL device was first reported by Vecht et al. [3] which aroused the interest

of many workers in this field. Using ZnS:Mn,Cu [4] and CaS:Ce [5] phosphors information display panels have been developed. Yashiyama et al. [6] and Hiroshi Kawarda et al. [4] have fabricated TV display panels based on DC powder technology.

Direct current electroluminescence in thin films is of considerable importance for two reasons. Firstly, it involves an understanding of the fundamental physics of the electronic and optical processes that occur in solids. In particular, it gives information about hot electron energy distributions and their involvement with optical centers and also about luminescence centre excitations and energy transfer processes. Secondly, the development of a DC EL system in thin films is of considerable potential for display devices generally. Furthermore, these devices require only low excitation voltages. When rare earth ions are incorporated by coevaporation or by ion implantation there arises the possibility of making various colour display devices. DC EL thin film technology devoted to the preparation of practical displays has not yet reached the stage where any large area panels with a limited maintenance can be produced, although fairly low voltage, high brightness DC TFEL devices have been

described [8,9,10]. But this chapter describes the attempts made to fabricate DC powder EL devices using ZnS:Cu,Mn. It essentially contains the detailed preparation technique of DC TFEL devices, emission characteristics of ZnS:Cu,Mn,Cl and ZnS:Cu,RE,Cl DC TFEL devices.

7.2 DC Powder EL cell fabrication

The phosphors for the fabrication of DC powder cells of ZnS:Cu,Mn can be prepared either by the conventional slurring technique or by the simultaneous activation, i.e., by precipitating the phosphor from solution containing appropriate amounts of Cu and Mn. The latter method is found to be more suitable for DC EL cells. This is because the phosphors thus obtained have virtually no particle size distribution unlike those obtained from slurry technique [11]. Moreover, these samples will have an even spreading of Cu and Mn, which will improve the visual appearance of the devices. The doped samples obtained were then treated with cuprous or cupric salt solution to form a high conductive skin of Cu_xS . The Cu_xS thus obtained is a P-type semiconducting layer. So a heterojunction will be developed between the doped ZnS and Cu_xS suitable for the formation of high field

region for the injection of charge carriers [7].

These Cu_xS coated phosphor particles were then dispersed in a suitable binder with appropriate phosphor-binder ratio. It was then spread on a suitably etched transparent electrode by one of the following methods, viz., silk screen printing, doctor blading or spraying. Because of variation in thickness of large area glass substrates doctor blading has been used only for test areas and small display panels. For spraying the phosphor should be diluted with large volumes of solvents. Silk screen printing gives controlled thickness layers of high packing density with little waste. It is observed that devices of thickness in the range of 30–100 μm have same electrical characteristics and brightness [4]. The back electrode is usually provided with an evaporated aluminium or with graphite paint. The binder is used to hold the phosphor particles in contact with each other and to the glass substrate. It occupies less than 5% of the total volume of the layer [11].

7.3 Fabrication of ZnS:Cu,Mn PEL cells

In the present case powder phosphors required for DC PEL of ZnS:Cu,Mn were prepared by slurring technique.

For this a weighed amount of ZnS of luminescent grade was mixed with cupric acetate containing 0.5 wt % copper and manganese acetate containing 1 wt % of Mn. A slurry of the mixture was then prepared in aqueous solution. It was then slowly dried and fired at 1000°C for 90 minutes at 10^{-2} torr, by introducing the phosphors into the high temperature zone of a horizontal furnace. The phosphor was then treated with cupric acetate solution containing 2 wt % copper. The powder thus obtained was then mixed with a polymethyl methacrylate solution prepared in chloroform. The mixture was then agitated ultrasonically by suspending the mixture container in an ultrasonic cleaning tank. This uniformly disperses the powder particles in the binder.

Phosphor binder mixture thus obtained was dispersed on a suitably etched transparent conducting electrode. For this a mica mask of 100 μm thick with a groove $4 \times 2 \text{ cm}^2$ was cut, and placed on the transparent electrode. Then the phosphor mixture was poured in the groove, carefully filling it with a flat glass. Then the solvent was allowed to evaporate from the mixture. When the solidification was complete the mask was removed and a thin phosphor layer embedded in the polymer matrix resulted. The thickness of

the layer can be changed by altering the phosphor-binder solvent ratio. It was observed that fast evaporation resulted in a foggy phosphor layer. So the whole preparation procedure was done in an atmosphere which favoured slow evaporation of the solvent. After evaporation of the solvent the device was introduced into the vacuum chamber and an aluminium metal electrode was deposited as the rear electrode through proper mask. The device thus fabricated is of the type as shown in Figure 7.1.

The spectrum of DC PEL device with ZnS:Cu,Mn is the same as those of AC TFEL with emission peak at 585 nm as shown in Figure 7.3. Typical brightness voltage characteristics is as shown in Figure 7.4. The brightness of the device is found to decrease with time under constant voltage drive.

On the initial application of a DC voltage a high current flows and no light emission is observed. This is because the high conductivity of the phosphor surface and interparticles themselves. At a critical power density the current falls and light emission appears at the electrode. For a cell of area $0.5 \times 2 \text{ cm}^2$ this transition occurred at 100 mA. An increase in applied

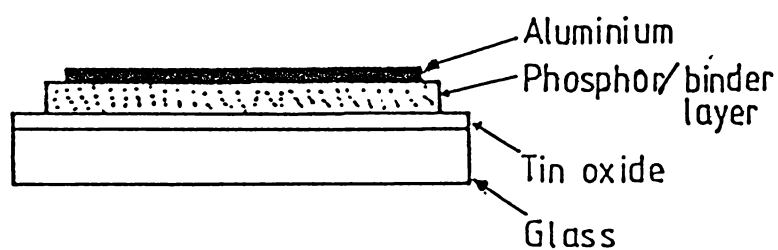


Fig.7.1. Schematic structure of ZnS:Cu,Mn DC PEL cell.

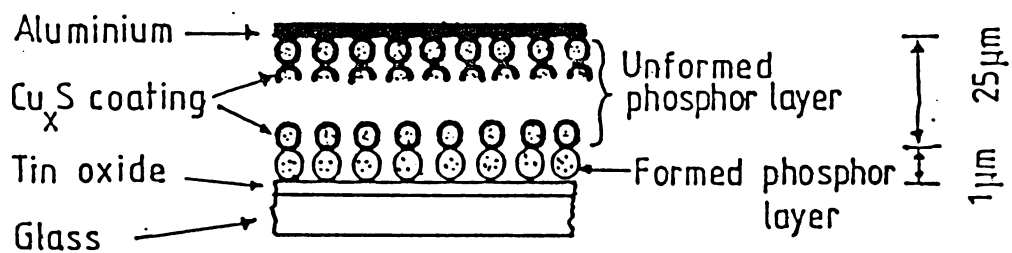


Fig.7.2. Depicts of the formed and unformed regions.

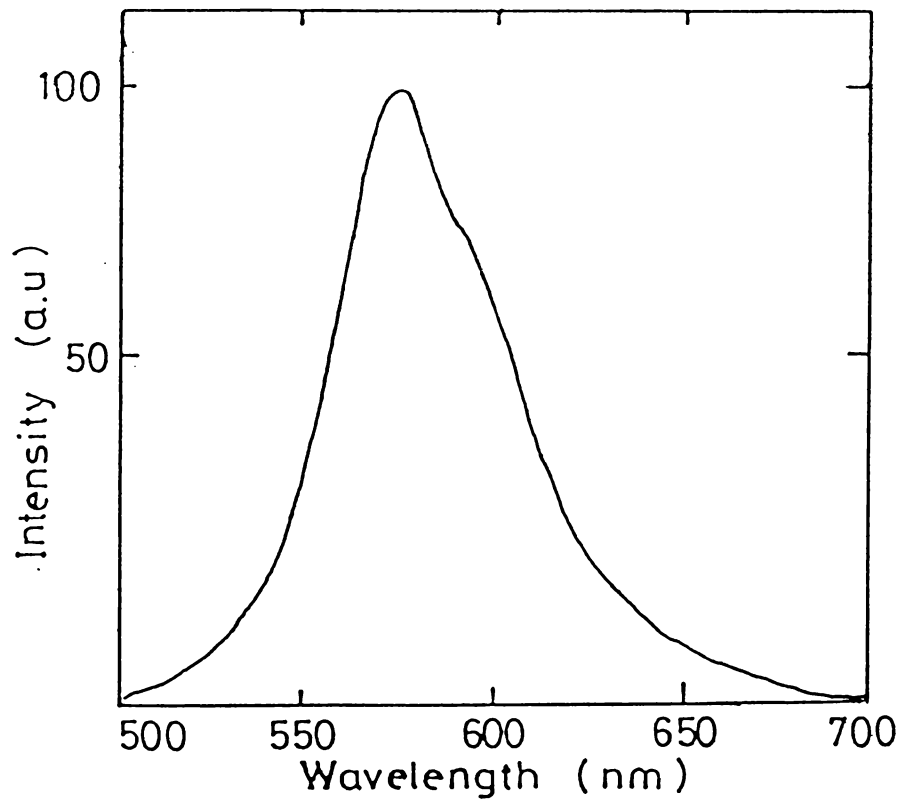


Fig.7.3. The EL emission spectra of ZnS:Cu,Mn DC PEL cell

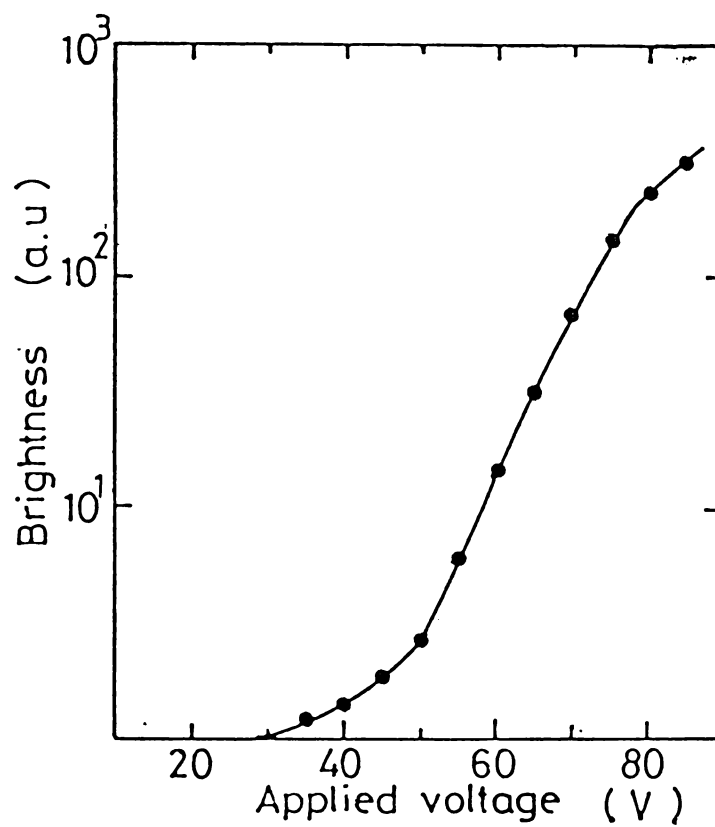


Fig.7.4. The B-V characteristic of ZnS:Mn DC PEL cell.

voltage produces a temporary rise in current density but this falls rapidly and panel brightness increases. This is termed as 'forming process'. The forming process does not occur simultaneously over the whole of the panel area but usually begins where the shortest current path that exists between the electrodes. This represents the region of higher current density. When forming takes place, the resistance of the phosphor increases and current density falls. This increases the current density in adjacent unformed areas and forming will take place at this region. Thus the formed region will spread across the panel until a complete plane of high resistance phosphor develops between the electrodes. The forming process results from the diffusion of copper from the copper sulphide surface coating into the bulk of zinc sulphide particle. Considerable heating of the panel takes place during the forming process and a phase change in the copper sulphide coating seems to contribute the development of a high resistance region [12]. Since the EL emission is field dependent, the localization of the applied field in the formed layer gives an important advantage in these devices. High fields can be generated at relatively small applied voltage provided the applied

voltage has reached a value where current drops by an order of magnitude or more. The forming process is irreversible as the high resistance of the phosphor permanently reduces the power density.

The reduction in brightness with time under constant voltage drive can be related to the following reasons. The increase in resistance of the unformed layer, the broadening of the formed layer termed as further forming, and decrease in resistivity of the formed region usually known as softening. Physically, the phosphor layer in the formed devices consists of at least two regions, the formed and unformed (Fig. 7.2). It has been shown that the unformed layer is quite conducting while the formed region is far more resistive [11]. Abdalla et al. [13] have assumed that a multi-hetero structure exists for each powder particle. The assembled device can be considered to have a configuration

Anode (ITO) - (Σ P.Cu_xS ... n. ZnS:Mn ... P.Cu_xS)-cathode

where the n-ZnS:Mn is known to be an insulator. When voltage is applied to the device, a high current termed as forming current is found to pass through the device. This current has been attributed to the high surface

conductivity of Cu_xS surrounding each particle. The current voltage characteristics of the device during the initial forming stage resemble that of pure resistance. The configuration of the luminescing device can always be regarded as reverse biased diode, and have current-voltage characteristics of a leaky diode [14].

The current-voltage measurements of the device gives some idea about degradation process taking place in the panel. Figure 7.5a gives the dependence of current on voltage for freshly prepared devices in the voltage range below the onset of electroluminescent emission. Figure 7.6 shows the dependence of current on voltage in a degraded device. Thus the devices exhibit two type of conduction process before and after onset of light emission. Below the voltage required for emergence of electroluminescence the logarithm of current is found to increase in proportion to the square root of applied electric field. Such a behaviour can be interpreted as either due to Poole-Frankel effect or Schottky effect [15]. This conduction process is due to Poole-Frankel effect because the plot of $\ln I$ vs $1/T$ gives a straight line. If it were Schottky effect the linear dependence is between $\ln 1/T$ and $1/T^2$ [14]. The second process occurs in the applied voltage region between

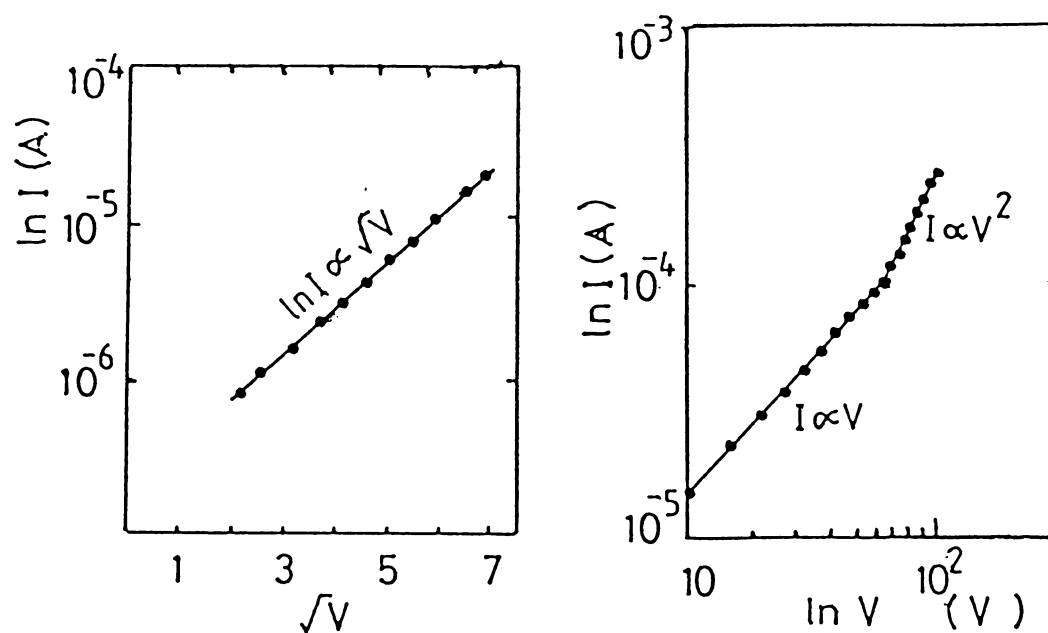


Fig.7.5a. Dependence of current on voltage for freshly prepared device. The voltage range below the onset of emission.

Fig.7.5b. Dependence of current on voltage for freshly prepared device. The voltage range above onset of light emission, indicating zener tunneling mechanisms.

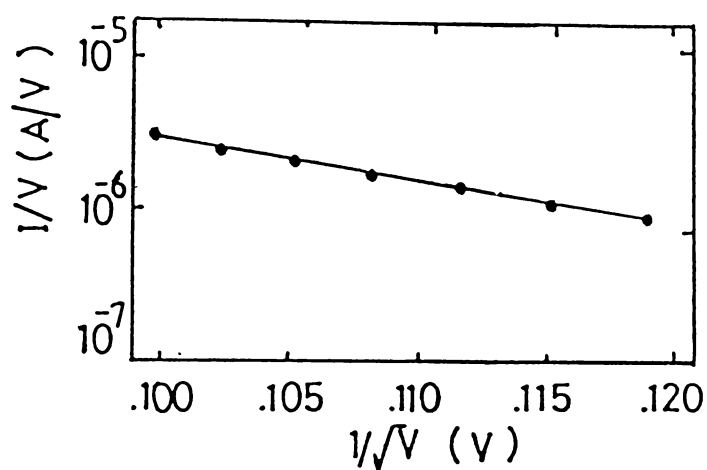


Fig.7.6. Dependence of current on voltage of a degraded device.

onset of EL and above that. In this case the plot of $\ln 1/V$ vs $1/\sqrt{V}$ is a straight line. Such behaviour is found in the case of reverse-biased heterojunction devices [16] which can be explained by means of Zener tunnelling model where $I \propto AV \exp BV^{-1/2}$ where A and B are constants. Figure 7.5b shows that the above equation is obeyed by the present devices. Therefore the device can be considered to be between the thin luminescing region (n-type) and the extended cathode (globally p-type). Hence freshly prepared devices can be considered as reverse-biased heterojunction [13] as

Anode-ZnS- Σ (P-Cu_xS ... n-ZnS:Mn-P Cu_xS)- Cathode

which is responsible for the observed conduction mechanism [13].

The devices which are operated for long time with a driving voltage above emergence of luminescence i.e., degraded devices show ohmic conductivity at lower fields and at high fields space charge limited conductivity ($I \propto V^2$) predominates (Fig. 7.6). This indicates the conduction mechanism has undergone modification due to degradation. Abdalla et al. [14] have shown that under degradation, copper is completely depleted from the degraded region and a nonuniform composition exists

across the device. The electroluminescence mechanism for devices which are not degraded is based on heterojunction in which the electrons are tunnel-injected in the reverse biased heterojunction from the valence band of Cu_xS into the conduction band ZnS. These electrons are accelerated to sufficient kinetic energy to cause impact excitation of the luminescent centers. In the degraded devices, the junction resistance is much lower than the resistance of non degraded region. This causes a voltage drop across the degraded region. Therefore, in order to have a field necessary for impact excitation a higher applied voltage is necessary.

7.4 DC Thin film electroluminescence

Investigations on DC EL properties of ZnS thin films have, in general, proved more fruitful than studies on powder layers. Geometrically thin films can more readily be subjected to high uniform fields, since they can be prepared with uniform thickness down to fractions of a micrometre. The absence of dielectric binder material enables one to make direct electrode contact to the phosphor. It may be assumed that the burn-out/pin hold problem is far more acute here than in AC thin film devices. Clearly no

protective insulating layers can be interposed between the electrodes.

An excellent review on the development of DC EL is given by Vecht et al. [17]. The recent observation of laser action in DC EL ZnS:Cu,Nd,Cl thin films at low temperature [18] has aroused great interest in this field. The low voltage DC EL devices incorporating rare earth activators [19] indicate the possibility of colour display. For the fabrication of DC TFEL devices various methods have been used viz., chemical vapour reaction method [20], simultaneous evaporation of previously doped samples [19] and coevaporation [2]. The following section gives the detailed account of fabrication of DC EL thin film device using ZnS:Cu,Mn,Cl and ZnS:Cu,RE,Cl and its emission characteristics. In order to obtain some information accompanying electroluminescence the electrical measurements of the device are carried out, and this gives some information about aging and forming process.

7.5 Fabrication of ZnS:Mn,Cu,Cl DC TFEL device

Thin ZnS:Mn,Cu,Cl films exhibiting DC electroluminescence of Mn²⁺ prepared by one step process based on evaporation of ZnS containing Mn and Cu as activators, copper being

in excess of solubility limit [21,22]. Some authors have concluded Cu could migrate under influence of an electric field [23] and the excess copper forms a Cu_2S phase which is P-type semiconductor with a high concentration of holes. The main feature of EL devices is that the existence of P- Cu_5S n-ZnS heterojunction. In the present investigations, a related technology was employed to develop P- Cu_2S n-ZnS heterojunction, in which a Cu_xS layer is produced by chemical exchange of previously deposited ZnS into Cu_xS . This method is a three step process viz., evaporation of ZnS with no activator, chemical exchange of ZnS into Cu_xS and evaporation ZnS:Mn layer. The structure of a typical DC thin film EL device is as shown in Figure 7.7. The transparent conducting electrode is prepared by spray pyrolysis of an aqueous solution SnCl_4 in isopropyl alcohol onto a glass substrate kept at 450°C . This SnO_2 electrode is suitably etched and thoroughly cleaned by the usual cleaning procedure and loaded into the vacuum chamber. The ZnS without any activators is deposited by vacuum evaporation of ZnS pellet using electron beam gun at substrate temperature 150°C . The thickness of the layer is about $0.3\ \mu\text{m}$. The Cu_xS layer was formed by chemical exchange of ZnS into Cu_xS . For this the ZnS film is dipped in

0.02 Molar solution of copper chloride. The CuCl solution is mixed with NH_4OH , HCl and KCl and pH value of the solution is maintained between 2 and 3. During dipping the temperature of the solution is maintained at about 80°C . The films were dried at about 80°C and loaded and annealed at 250°C for 10 to 15 minutes. Depending upon the dipping time the concentration of Cu is found to change. For ZnS film of $0.3\ \mu\text{m}$ a dipping time of 10 seconds is likely to change ZnS layer to Cu_xS . The experiments performed on CdS layers [24], a dipping time 5 seconds in hot CuCl resulted in the formation of Cu_xS layer of $0.2\ \mu\text{m}$ over this ZnS:Mn,Cl films of about $1.5\ \mu\text{m}$ were deposited at a substrate temperature of 150°C . The ZnS:Mn,Cl phosphor was prepared in the laboratory with 3 wt % Mn by a slurring technique and firing process as described in Chapter-II. The back electrode was provided by an evaporated aluminium film. Figure 7.8 shows the EL emission spectra of the DC ZnS:Cu,Mn,Cl thin film device excited under DC voltage. It is observed that emission has broad peak at 585 nm. This is due to the well known intra-atomic transition of Mn^{2+} ion from $^4\text{T}_1$ to $^6\text{A}_1$ state [25, 26]. It is also observed that when devices were prepared with longer dipping time in CuCl solution to

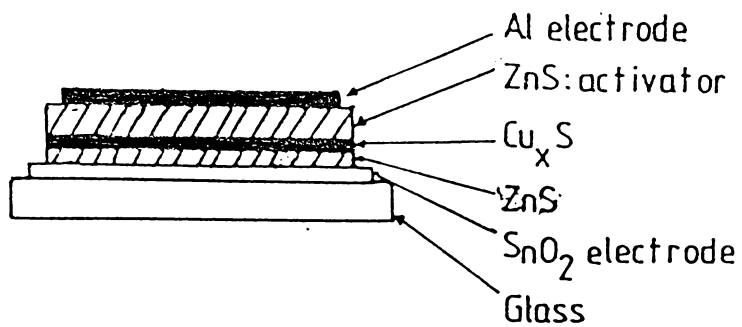


Fig.7.7. Schematic structure of a typical DC TFEL device.

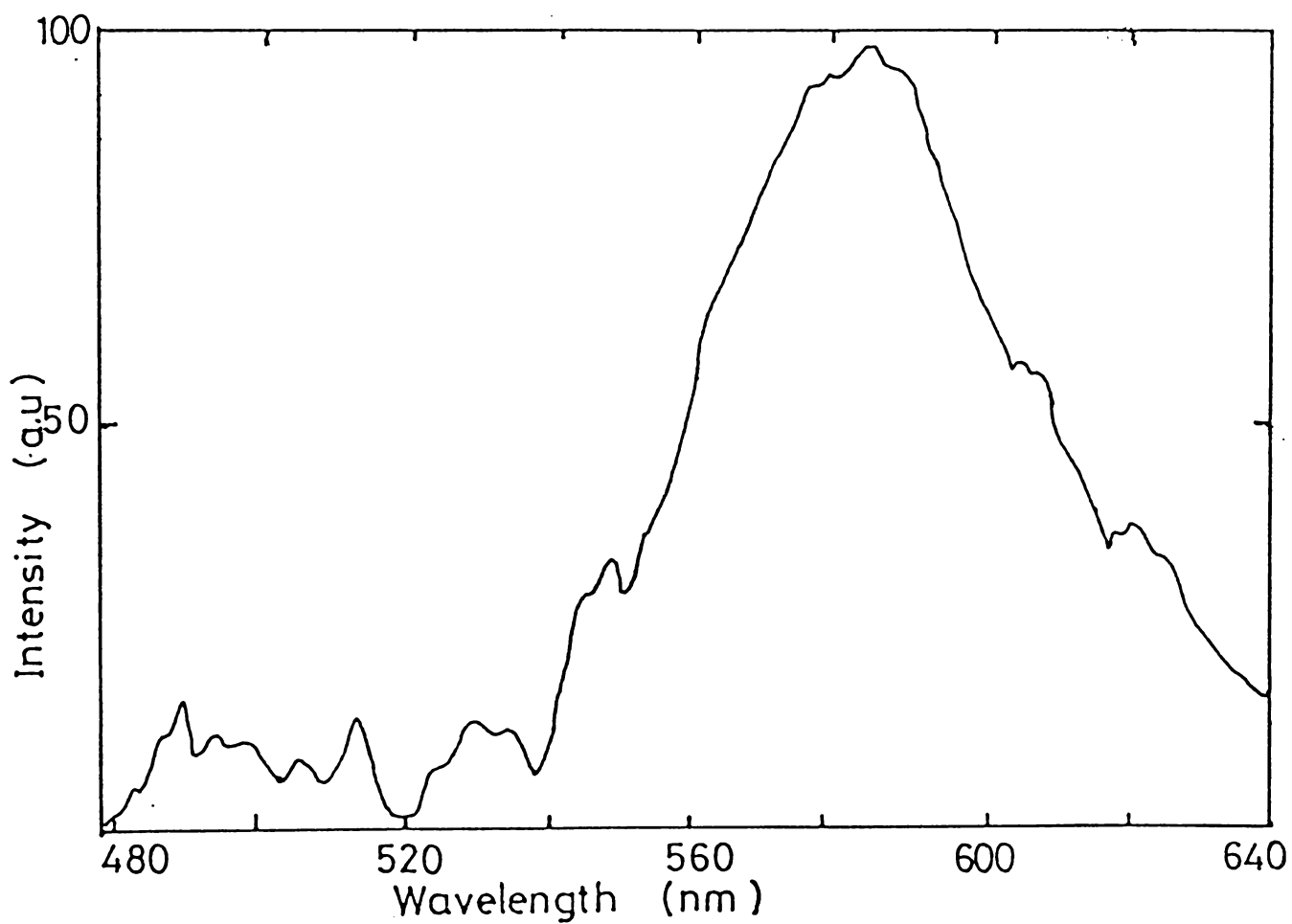


Fig.7.8. EL emission of ZnS:Cu,Mn,Cl DC TFEL device.

form a Cu_xS layer, a ZnS:Mn layer of 0.3 μm showed some shorter wavelength emission in addition to the emission due to Mn^{2+} ion. Similar observations, i.e., emission in the blue or bluish green region with short decay time was observed in thin film EL devices and ZnS:Mn Schottky diodes [27]. Skolnick [28] found that ZnS:Mn,Cu powder cell the blue emission is relatively much stronger. This may be due to the presence of more copper in the operating volume of this device. Also Howard et al. [29] have shown that the ratio of blue to manganese emission can increase with increasing voltage. In the present case the blue emission can be due to Cu centers which can diffuse from Cu_xS into the ZnS layer in structures containing ZnS:Mn- Cu_xS heterojunctions, thus creating effective luminescent centers. Figure 7.9 shows the brightness voltage characteristic of DC TFEL device with ZnS:Mn as active layer.

In order to obtain fundamental information about the material, DC conductance was measured in the sandwich structure with Al as front and back electrodes and also with SnO_2 -film-Al structure. Here, we assume the measured conductance to be related with bulk properties of the layers and not with contacts. Figure 7.10 shows the DC conductance as a function of $10^3/T$ for each film. It can

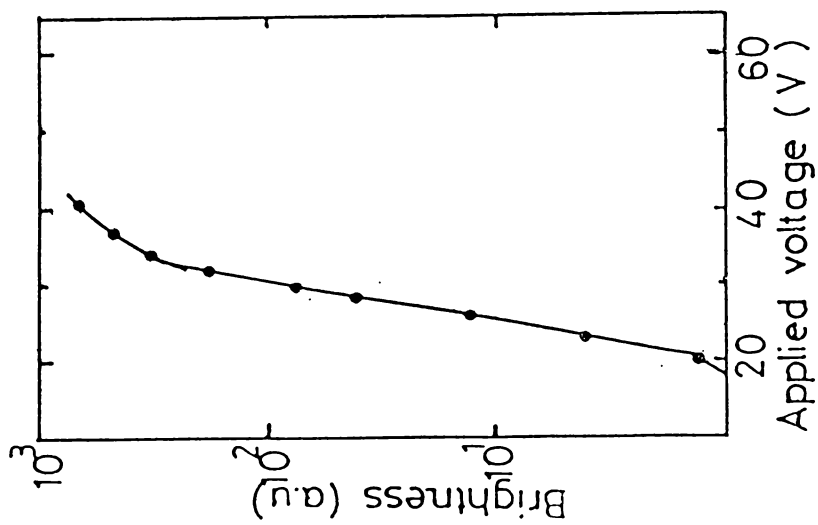


Fig.7.9. B-V characteristic of ZnS:Cu,Mn,C1 DC TFEL device.

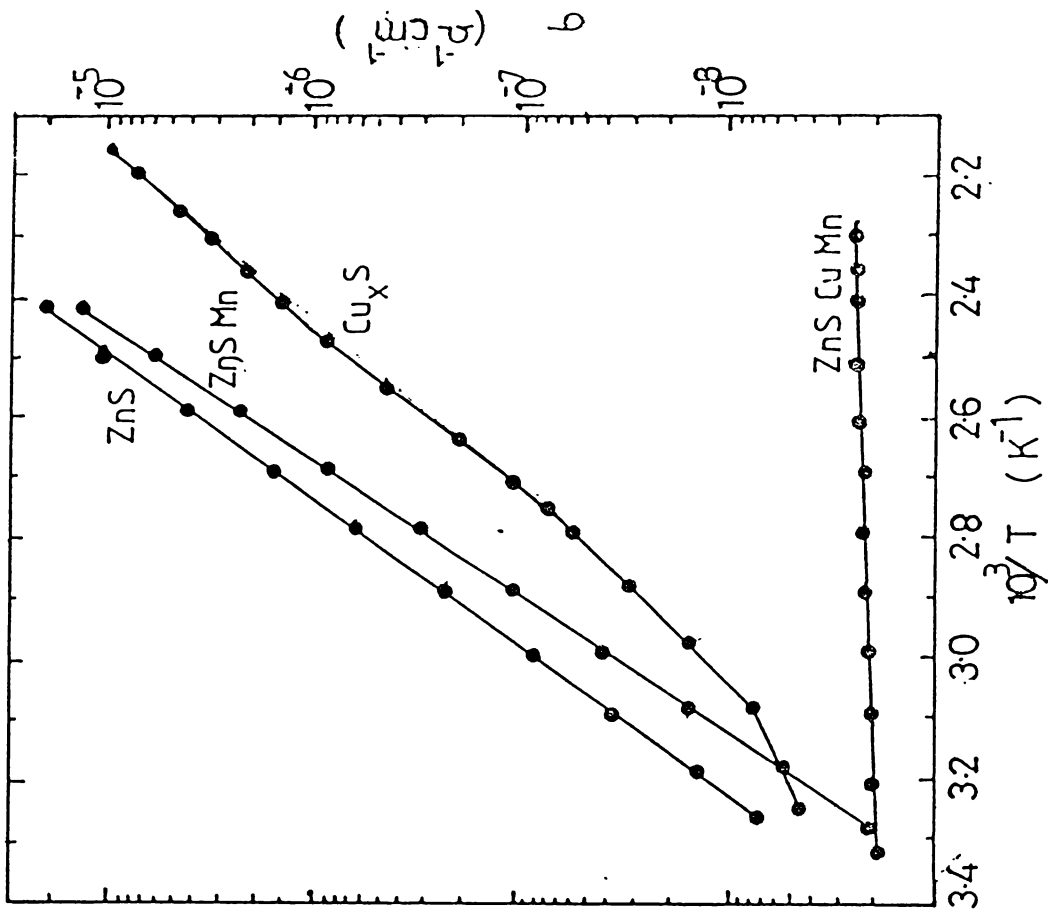


Fig.7.10. $\ln \sigma$ vs $10^3/T$

be seen that ZnS film has constant activation energy and the value of the activation energy is found to be 1.6 eV. The pure ZnS has band gap of 3.6 eV and the activation energy is given by the relation

$$\sigma = \sigma_0 \exp Eg/2kT$$

In the present case the observed activation energy may be due to defects or impurity levels within the band gap of ZnS and not due to band to band transition.

The ZnS:Mn has an activation energy of about 0.35 eV at low temperatures as temperature increases or exhibit higher activation energy of 1.33 eV. This may be due to the level created by Mn^{2+} levels in ZnS band gap. Tabei and Shinonoya [30] have reported that the energy of $2T_2$ state of Mn^{2+} ion is estimated to be 1.25 eV above the valence band and that of 2E state to be 0.40 eV. The present observation of activation energies, though deviate marginally, can also be attributed due to the presence of $2T_2$ and 2E levels of Mn^{2+} ions. The Cu_xS layer has an activation energy which increases with increase of temperature. The layer resulting after deposition of third layer i.e., ZnS:Mn and consequent annealing yeild a monotonous decrease in activation energy from about 0.028 eV at high

temperature, down to several meV. This indicate that neither intrinsic conduction nor conduction resulting from one localized imperfection level is the principal contributing factor for the conductivity.

Since simple crystalline conductivity does not seem to be applicable for the present electroluminescent structure, it can be considered the total layer to be amorphous ZnS doped with Mn and Cu. The high doping level may be the reason for the absence of long range ordering. The device after third step of preparation is considered to be single layer of ZnS:Mn,Cu,Cl, i.e., no Cu_xS layer exists. It is assumed to be dissolved into ZnS during the third step of production. There may also be crystalline phase in ZnS:Mn,Cu,Cl. If crystalline phases are present their resistance should be higher, and this will not contribute significantly to the conductivity. A possible conduction mechanism in amorphous semi conductors is variable range hopping near the fermi energy [31].

Figure 7.11 shows the current voltage characteristics of each layer while Figure 7.12 gives the variation of current with applied voltage for unformed sample, before and after aging. It can be seen that current of the aged

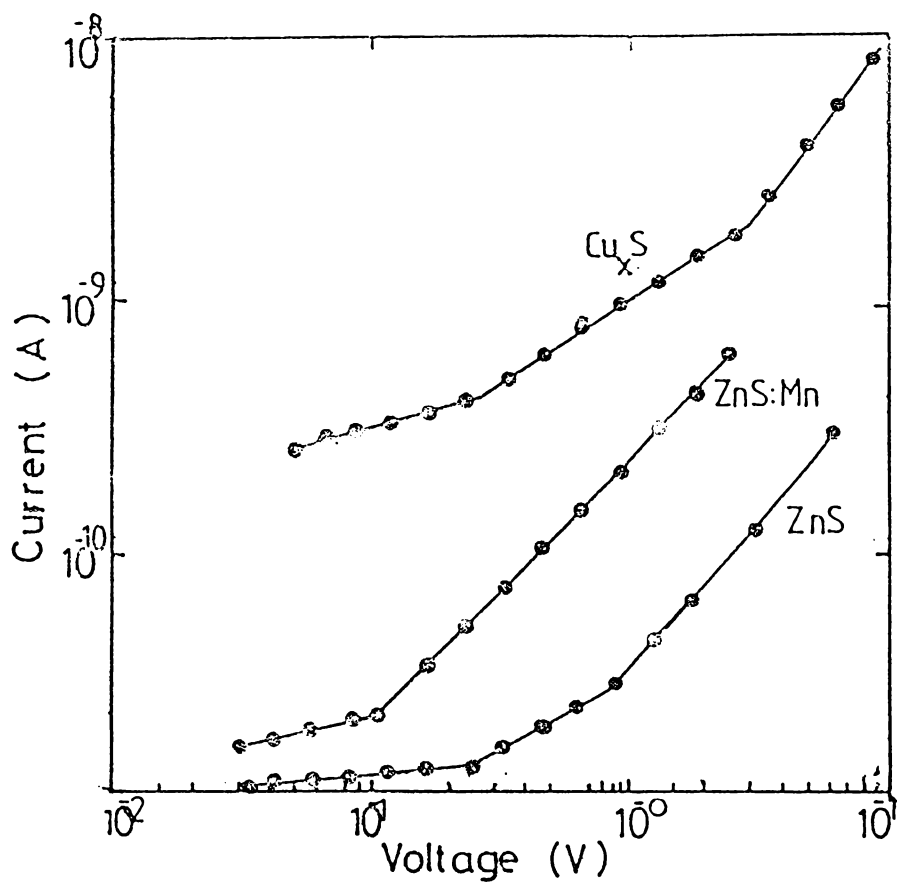


Fig.7.11. Current-voltage characteristics of various layers.

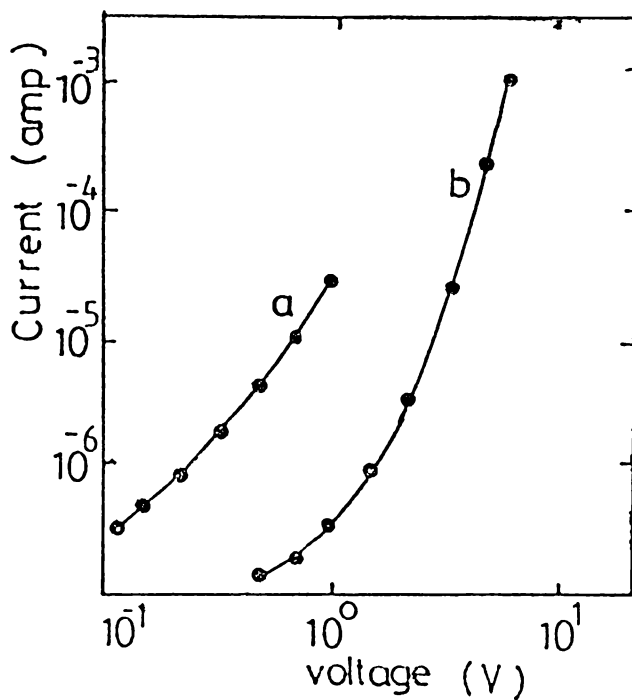


Fig.7.12. I-V characteristic of the (a) unformed, and (b) aged samples

sample is much smaller, but increase rapidly with voltage. The current does not follow any constant power function of voltage and it has got slope greater than 4. The characteristics are symmetric with polarity reversal. The conductivity is not supposed to be governed by the space charge region. After forming process is complete the device exhibit a current voltage relation $I \propto V^{1/2}$. The plot $\log I$ vs $V^{1/2}$ gives a straight line. This indicate that the current flow can be attributed to the simple Poole-Frenkel mechanism [32] governed by

$$I = AF \exp \left(\frac{BF^{1/2}}{KT} \right)$$

where F is the electric field strength. The decrease in current in the formed samples suggest formation or the existence of an insulating layer in series with the space charge region of the semiconductor. The decrease in current during aging is also due to this insulator layer, which increases in thickness under applied voltage. The blocking layer, i.e., insulating layer cannot be considered as aluminium oxide formed by oxidation since with Au electrodes also the device exhibit EL emission. Jchida's [33] studies reveal that the decrease in current is not only due to blocking layer between ZnS film and

metal electrode but the migration of Cu near the film surface may be a contributing factor. The Poole-Frenkel mechanism takes place both in amorphous as well as in crystalline films. So there is no evidence for an amorphous structure for the insulating layer. However, the sudden fall in current in the formed devices due to the formation of an insulating layer followed by the EL emission layer leads to a conclusion that insulating layer is crystalline. Moreover the observation of Soeya [34] indicates that regions of excess copper can enhance the crystallization. Thus in the present case also the forming and aging take place due to the growth of a crystalline phase of ZnS:Mn,Cu,Cl which is a field enhanced crystallization. Taking into account the migration of copper in ZnS [23] the crystallization can be considered to be accompanied by a decrease in Cu concentration in the crystalline region as observed by Uttcht et al. [35] in other types of amorphous compounds. This migration of Cu to the ZnS:Mn,Cl may be the reason for the blue emission in the observed spectrum.

7.6 DC Electroluminescence in rare earth doped ZnS thin films

Electroluminescent cells based on ZnS are a subject

of interest to many research workers. One of the more frequently used activators of ZnS is manganese, but the phenomena of laser action at low temperature in DC TFEL device with ZnS:Cu,Nd,Cl [18] has brought great attention to rare-earth doped ZnS DC TFEL devices. Moreover, rare earth doped ZnS thin film devices generally have emission in the entire visible spectrum [19].

The DC TFEL devices with ZnS:Cu,Pr,Cl; ZnS:Cu,Tb,Cl and ZnS:Cu,Sm,Cl were fabricated in the laboratory. For this the three step process adopted in the fabrication of ZnS:Cu,Mn,Cl devices is adopted, which is described in the previous section of this chapter. The ZnS with no activator is evaporated on thoroughly cleaned SnO₂ coated glass substrate kept at a substrate temperature of 120°C by electron beam gun. The ZnS films have a thickness of 0.2 μm. Then a Cu_xS layer is grown over this by chemical exchange of ZnS into Cu_xS. This can be achieved by dipping the ZnS film in hot (90°C) aqueous solution (.02 molar) of CuCl for about 5 to 15 seconds. Over this the ZnS:RE,Cl (RE = Pr,Tb,Sm) having a rare earth concentration of RE 3 wt % is evaporated (~ 1 to 2.5 μm) by electron beam gun. The ZnS:RE,Cl phosphor for evaporation was prepared in the laboratory by slurring technique and the usual firing

process described in Chapter-III. Evaporated aluminium forms the back electrode.

The electrical conduction mechanism and the forming process of these devices are same as those of ZnS:Cu,Mn,Cl devices and can be explained in the same lines for these devices. The EL emission spectra of RE doped ZnS films consisted of emission lines characteristic of transitions within the 4f shell of the triply-charged rare earth ions in the ZnS crystal field. Consequently various colours of electroluminescent emission were obtained by choosing different RE ions as luminescent centers. ZnS:Tb,Cl gives green emission ZnS:Pr,Cl yellow orange, while ZnS:Sm,Cl gives emission in the red region. Figure 7.13 shows the EL emission spectra of ZnS:Cu,Tb,Cl; ZnS:Cu,Pr,Cl and ZnS:Cu,Sm,Cl recorded at constant DC driving voltage. Figure 7.14 gives the brightness voltage characteristic of these devices. ZnS:Cu,Tb,Cl were found to give the brightest electroluminescence emission than the other two. The driving voltages were usually in the range 20 to 30 V and the devices drew current of only few milli amps. In comparison with the AC TFEL devices with same active layer, it is observed that the maximum

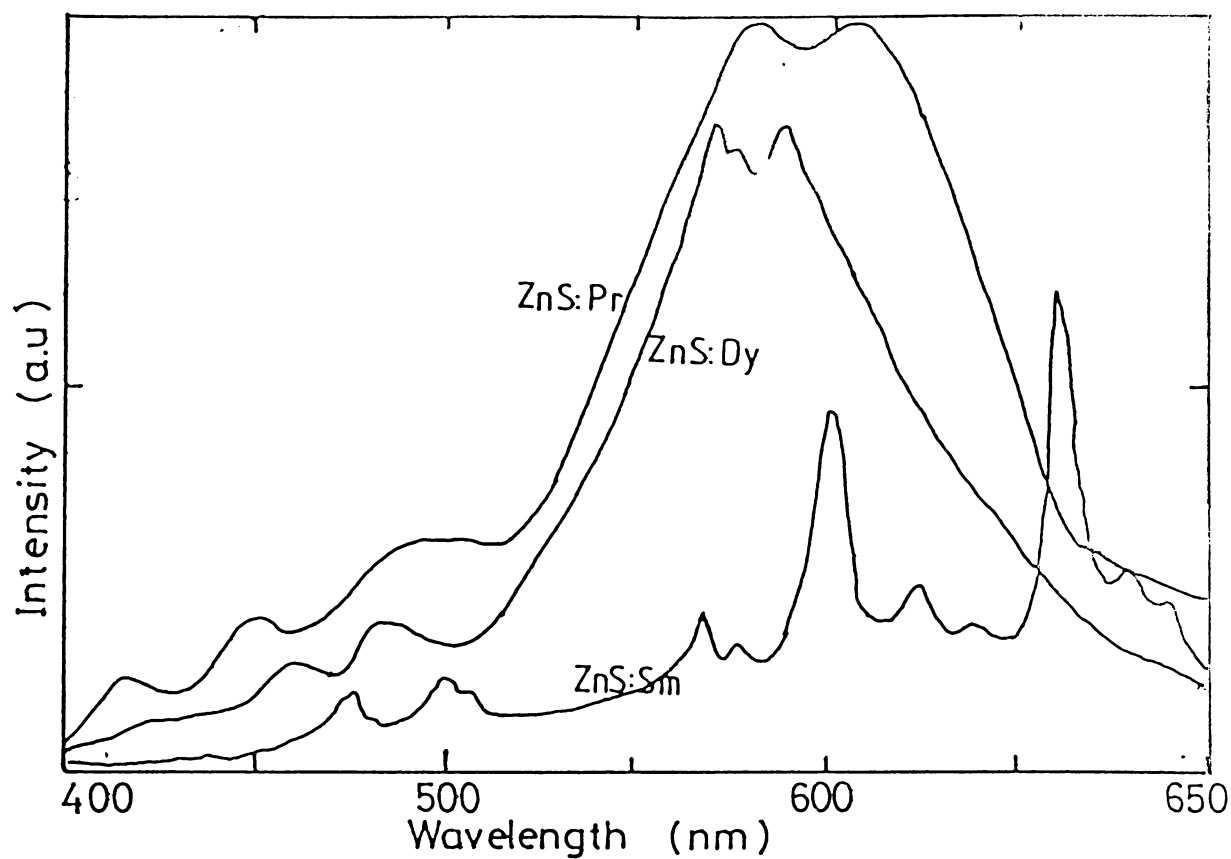


Fig.7.13. EL emission spectra of ZnS:Cu,RE,C1 DC TFEL devices.

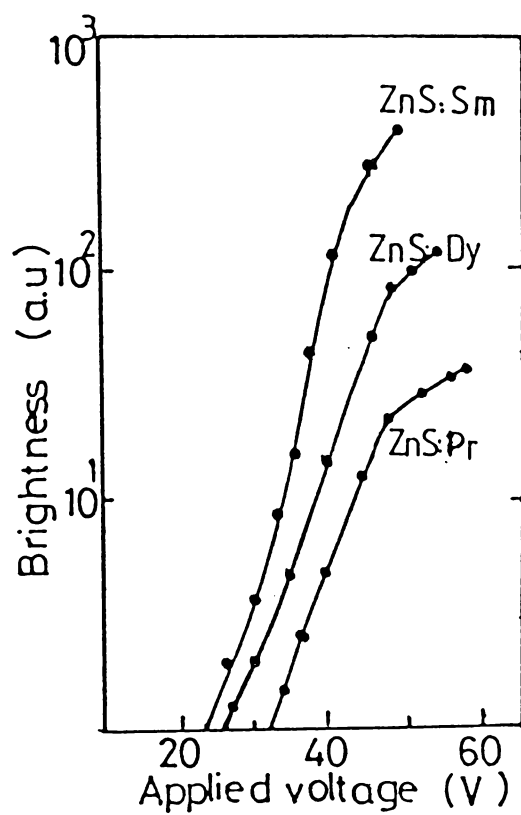


Fig.7.14. The B-V characteristics of ZnS:Cu,RE,C1 DC TFEL devices.

brightness attainable is less in the case of DC TFEL devices. However, for the same applied voltage DC TFEL has higher brightness than that of a AC TFEL devices. Also it is to be noted that the percentage of copper in the DC TFEL devices is critical. The higher dipping time, i.e., more copper ions in ZnS may cause conducting channel in the device and local burnout. This will affect the stability of the device. But in the present studies it is observed that DC TFEL cells prepared by dipping in CuCl solution for 5 to 10 seconds can operate for hours without any damage. The devices are sensitive to moisture, which may also cause local burn out. This can be overcome by proper protection layer coating. Usually a protective layer of SiO or MgF₂ films is given to the device to eliminate this problem.

REFERENCES

- [1] A Vecht; J.Cryst.Growth, 59(1982) 81.
- [2] M I Abdalla, J Thomas, A Brenac and J P Noblac,
IEEE Trans. on Electron Devices, ED 28(1981)
694.
- [3] A Vecht, N J Werring and P J F Smith; Brit.J.Appl.
Phys. (J.Phys.D), Ser 2 1(1968) 134.
- [4] A Vecht, N J Werring, A Ellis and P J F Smith;
Proc. IEEE, [7] 61(1973) 902.
- [5] A Vecht, M Waite, M H Higton and R Ellis; J.Lumin.,
24/25(1981) 917.
- [6] M Yoshiyama, Electron, 42(1969) 114.
- [7] Hiroshi Kawarada and Nobumasa Ohshima; Proc. IEEE,
[7] 61(1973) 907.
- [8] J M Blackmore, A F Cattell, K F Dexter, J Kirtan and
P Lloyd; J.Appl.Phys., 61(1987) 714.
- [9] F J Bryant and A Krier; Phys.Stat.Sol.(a),
81(1984) 681.
- [10] E Chimczak, R Czajka, M Bertrandt-Zytkowiak and
W S Gordon; Thin Solid Films, 76(1981) 349.

- [11] A Vecht, N J Werring, R Ellis and P J F Smith;
Brit.J.Appl.Phys. (J.Phys.D), Ser 2
2(1969) 953.
- [12] D May, Electronic Displays, 1981, Session 1.
- [13] M I Abdalla, A Godin and J P Noblanc,
J.Lumin, 18/19(1979) 473.
- [14] M I Abdalla, A Godin, A Brenac and J P Noblanc;
IEEE Trans., ED-28(1981) 689.
- [15] J G Simmons; DC conduction in thin films,
(M and B monographs, London, 1971)
- [16] A R Riben and D L Feucht; Sol.Stat.Electron,
9(1966) 1055.
- [17] A Vecht and N J Werring; J.Phys.D., 3(1970) 105.
- [18] G Z Zhong and F J Bryant; Solid State Communica-
tions, 39(1981) 907.
- [19] F J Bryant and A Krier; Phys.Stat.Sol. (a),
81(1984) 681.
- [20] S Szuba and W Polewska; Phys.Stat.Sol. (a),
71(1982) 65.
- [21] P Goldberg and J W Nickerson, J.Appl.Phys.,
34(1963) 7601.

- [22] W Uchida; Jpn. J.Appl.Phys., 12(1973) 670.
- [23] J L Plumb; Jpn. J.Appl.Phys., 10(1971) 326.
- [24] L C Burton and H M Windawi; J.Appl.Phys., 47(1976) 4621.
- [25] H E Gumlich, J. Lumin., 23(1981) 73.
- [26] T Miyata, S Nakagawa, H Hirayama, H Hasegawa and M Korenaga; Jpn.J.Appl.Phys., 9(1970) 615.
- [27] E Chimczak and J W Allen; J.Phys.D.Appl.Phys., 18(1985) 951.
- [28] M S Skolnick; J.Phys.D.Appl.Phys., 14(1981) 301.
- [29] W E Howard, O Sahni and P M Alt; J.Appl.Phys., 53(1982) 639.
- [30] M Tabei and S Shionoya; J.Lumin., 15(1977) 201.
- [31] N F Mott; J. Non-Crystalline Solids, 8/10(1972) 1.
- [32] M Burgelman; Thin Solid Films, 70(1980) 1.
- [33] W Uchida; Jpn.J.Appl.Phys., 7(1968) 378.
- [34] T Soeya, Jpn.J.Appl.Phys., 6(1967) 205.
- [35] R Uttcht, H Stevenson, C H Sie, J D Griener and K S Raghavan; J.Non-Crystalline Solids, 2(1970) 358.

Chapter-VIII

CONCLUDING REMARKS

Abstract:

This chapter gives the summary of the work presented in the previous chapters. The present status of EL display with special emphasis to AC TFEL devices is given in detail. It gives a concise review of the methods, modifications and the developments in the field of AC TFEL devices with reference to the literature since 1980. The various commercial products and its application are also described briefly. The chapter ends with survey of future possibility of EL display panels for various applications.

8.1 Summary of the work

Electroluminescence is very old and well advanced subject, but it still requires further improvements to enable one to use it for practical applications. The previous chapters of this thesis have dealt with some of the existing problems in electroluminescence and presented some successful and reproducible results obtained. As described in the initial two chapters we have now a fairly good idea of EL mechanism operative in ZnS phosphor systems, including the energy transport processes. The physics of AC TFEL devices, memory and non memory EL devices are also reasonably clear.

Among the work presented here, the preparation of white light emitting phosphor using ZnS:Cu,Pr,Cl phosphors is a major achievement because a single active layer can now give multicolour emission. The frequency dependent EL emission spectra of ZnS:Cu,Pr,Cl which makes it colour tunable by changing the excitation frequency also is a striking feature as far as phosphor development is concerned. The theoretical basis for this has been provided with Schön-Klasens

model together with resonant energy transfer from Cu to Pr ions. The mechanism behind the colour change in EL emission is clear in this context. One can also get a fairly good idea about energy transfer (or sensitized luminescence) from Cu/Ag to rare earth ions in ZnS host lattice.

One of the major problems in AC TFEL devices is the higher driving voltages which are not compatible with available IC's. This thesis describes the fabrication of low voltage operated (< 50 V) thin film EL devices. To achieve this AC TFEL devices in MISIM and MIS structure were fabricated with different insulating layer. It is observed that the dielectric properties of the insulating film is an important factor for low voltage operation. Also it demonstrates the frequency dependent threshold voltage for onset of emission in the devices having MgF_2 and Eu_2O_3 as insulators, and this effect is explained on the basis of frequency dependent loss tangent of insulator materials. The optimisation of the device, for low voltage, high brightness and stability in terms of insulator and active layer thickness is a very useful information for EL technologist. The dielectric properties of the insulating film is

closely related to device performance and a detailed study of the electrical, dielectric and optical properties gives a deeper understanding required for fabrication of TFEL devices.

The full colour display devices have not yet become a reality. The various emission colours obtained including the primary blue, green and red colours, developed using rare earth doped ZnS as active layer in AC TFEL devices, indicate the possibility of developing full colour display. The effect of halides and oxides on the emission spectra is also given here in this context. Some of the results using DC PEL and DC TFEL devices and fabrication techniques presented enable one to evaluate the major merits and demerits of different types of EL cells.

The following section gives a concise report of present status of thin film EL devices, its application for TV and computer screens and the future possibilities with TFEL devices.

3.2 Present status of thin film EL devices

The history of high field electroluminescence (EL) acts as a warning example of uncritical futuristic

expectations regarding the potentialities of this phenomenon without having sufficient material control and physical understanding of the underlying mechanisms. After the early discovery by Destriau [1] intense research efforts in the 1950s ended in complete disillusionment by the mid sixties due to poor life, brightness and efficiency of EL devices [2]. By the middle of seventies, however, the interest in various modifications of high field electroluminescence for display applications was again growing rapidly, stimulated by significant progress obtained in Japan with AC driven thin films [3], in Great Britain with DC driven powder cell [4] and with the occurrence of laser action in DC TFEL devices [5].

Eventhough there is noticable achievements in the DC TFEL and DC PEL devices, it seems that AC TFEL devices have made tremendous advancement and the achievements made are now viable as commercial products. During this decade the technology of AC TFEL has changed very much in materials, preparation and deposition techniques. The most widely used deposition method for preparation of EL phosphor films giving complete device structures is sputtering in its various modifications [6].

Yet another common method for thin film preparation is vacuum evaporation from resistance, electron beam, radio frequency or laser heated sources [7,8]. The film materials can be evaporated from single or multiple sources.

Sputtering and evaporation are physical processes. Chemical vapour deposition methods are of most recent origin. One novel method is MOCVD (Metal Organic Chemical Vapour Deposition) [9,10] in which the reactions of volatile organometallic compounds at atmospheric or reduced pressures are exploited. At the moment, however the MOCVD method is much more firmly established for preparation of III-V semiconductors than II-VI EL phosphors. One of the most successful growth methods used in the commercial production of AC TFEL devices is Atomic Layer Epitaxy (ALE) [11]. The preparation methods for EL thin films are critical and affect several of its important properties viz., crystal structure and orientation [12-14], the microstructure [12, 14-17], optical properties and smoothness of the film thickness over the whole device area [18,19].

The device performance is also dependent on the properties of insulating films. It has been observed that the driving voltage can be reduced by making use of insulators of high dielectric constant and breakdown

strength [20]. Various attempts were made to bring down the driving voltage for the device. The range of insulators is very wide and extends from amorphous oxides and nitrides (Al_2O_3 , Y_2O_3 , Sm_2O_3 , TiO_2 , SiO_2 , ZnO_2 , $\text{Al}_x\text{Ti}_y\text{O}_z$, Ta_2O_5 , $\text{Ta}_x\text{Ti}_y\text{O}_z$, BaTa_2O_6 , Si_3N_4 and SiAlON) to ferroelectric materials (SrTiO_3 , BaTiO_3 , PbTiO_3) [7, 21-24]. Low voltage operation has been achieved using different type of insulators [21-24] and threshold voltage for onset of emission has been brought down to 20 V by using BaTiO_3 ceramic sheet produced by mixing powder and binder followed by sintering [25]. Another noticeable report in respect of low voltage operation is on the ZnSe /Langmuir-Blodgett film MIS diodes which emit blue-white for a forward bias greater than 2 volts [26]. Black Pr-Mn oxide dielectric for AC TFEL which has high dielectric constant is used for low voltage operation and high contrast by Matsuoka et al. [32].

Though significant progress in structure and stability of the devices have been made, inspite of many efforts it seems impossible to find efficient EL phosphors other than ZnS . The properties of ZnS:Mn still serve as a yardstick for all other systems. Only the yellow emitting ZnS:Mn has a high luminescence

level as high as $10,000 \text{ Cd/m}^2$ and efficiency of 8 lm/W [27]. Extensive reviews and discussions of the physical characteristics of TFEL and the performance of ZnS:Mn have recently been published [28,29,30,31]. More than hundreds of papers have been published every year on the study to improve the ZnS:Mn AC TFEL devices. An excellent review on this aspect, viz., brightness saturation, hysteresis in luminescence, the dependence of brightness and efficiency on concentration of manganese, thickness dependence and aging effects are neatly presented in the review by M Leskela and M Tammenmaa [31].

A world wide interest exists in the development of multicolour thin film EL devices. The potential of rare earth ions to provide the basic three colours (blue, green and red) needed in a full colour device has led to intensive study of the doping of II-VI compounds with rare earths during past few years [33]. The rare earth ions were introduced into ZnS lattice by various methods, (i) by preparing RE doped ZnS, (ii) by evaporating rare earth compounds together with ZnS powder, (iii) by evaporating rare earth metals together with ZnS, (iv) by RF sputtering sintered pellets containing ZnS and a rare earth compound, (v) by epitaxial growth of ZnS and sublimating rare earth chelates [6, 33-36].

Early on, Kahng [37] observed that among rare earth halide doped ZnS, TbF_3 gave the highest (about 25 cd/m^2) brightness levels. The values with TbF_3 slowly increased and the highest value reported being 3400 cd/m^2 with efficiency 0.4 lm/W which was obtained with 5 KHz sinusoidal voltage [31,34]. The AC TFEL of SmF_3 in ZnS has been raised to 1000 cd/m^2 with 5 KHz , but that of TmF_3 remains below 10 cd/m^2 . Various attempts are still being undertaken to improve the brightness and efficiency. The brightness of TFEL structures strongly depends on the particular terbium compound used for doping. It is observed that F^- , Br^- , O^{2-} act favourably for Tb centers from suitable complexes but N^{3-} and H^- do not affect the Tb centers [35]. Other rare earths are also being investigated for the colour display.

Recent investigation on alkaline earth sulphides have revealed calcium sulphide (CaS) is a potential host material for highly efficient cathodoluminescent phosphors [38]. Vecht et al. [39] have reported that CaS:Ce powder type DC EL devices can compete with the best ZnS:Mn powder DC EL devices in brightness and efficiency. However, the first attempts to use alkaline earth sulphides (CaS, SrS, BaS) in AC TFEL devices were

those of Barrow et al. [40] with SrS:CeF₃ and Shanker et al. [4] with CaS:Ce. These materials has tendency towards thermal decomposition when subjected to conventional electron beam evaporation. A simultaneous sulphur coevaporation is therefore required [41]. Some physical properties of alkaline earth sulphides, i.e., CaS, SrS, BaS were compared with ZnS [42]. White light emission is achieved using single active layer ZnS:PrF₃ by Yoshida et al. [43] though the emission is very weak. The other significant development is the white light emission obtained by device structure combining patterned and stacked phosphors. The SrS:Ce,K blue green emission is filtered to separate blue and green emissions which are superimposed on the CaS:Eu red emission [44]. This has been achieved by other active layers such as SrS:Pr,K single layer and SrS:Ce,K|SrS:Eu stacked structure [45] and SrS:Ce|CaS:Eu [46,47]. Few theoretical models have been suggested to account the observed luminescence in alkaline earth sulphides [48-50].

Reports dealing with BaS host material are few in number [42], but it seems clear that it cannot compete with CaS and SrS as a host matrix. The other type of matrices mentioned in the literature are the solid solutions

of alkaline earth sulphides [42] and SrSe [51]. The above materials and in particular the white light emission from stacked structure have higher luminescence at 5 KHz excitation frequency. However, these devices show luminescence of 30 cd/m^2 at 60 KHz [45], which is only one third compared with the required luminescence level for practical EL panel applications. Still, the present developments and achievements clearly indicate the full colour EL panels will be viable as a commercial product within few years.

8.3 EL Flat Panel: applications

Flat panel displays will be giving CRT's very strong competition in applications that stress portability, power and compactness, although CRT's will continue to dominate wherever cost, colour and high resolution are the chief objectives. Three active flat-panel technologies are the electroluminescent, plasma-gas discharge and vacuum fluorescent techniques. TFEL displays are generally recognised as the most aesthetically pleasing of the flat-display technologies. A TFEL display is a light emitter, has crisply defined uniform luminance pixels, and has high contrast because of its low reflectivity yet specular

like surface. This surface functions go well in a contrast enhancing circular polarizer filter. The display appears most like a high-intensity CRT without unwanted high degree of phosphor reflectance and glare normally present in a CRT.

Many companies particularly in US and Japan and the US Army have developed and marketed EL display for various applications [52-55]. Right now they are monochrome displays.

A Tektronix Inc. spin-off, Planar systems Inc., of Beaverton, Oregon, (USA) is focussing on AC-thin film EL technology. For example its model EL 6648 m uses an EL panel that displays 80 characters by 25 lines on a 4-by-8 inch active area with resolution of 66.7 lines/in. Finlux Inc; Finland's Lohja Corporation has also contributed to EL technology. Sigmatron Nova, California, USA; is another display maker which has produced dark-field displays that can be read in sunlight and this packs 96 by 160 pixels into an active area 5.2 by 7.6 cm. In addition, the company is also developing full-colour display for avionics applications.

The TFEL displays have applications in almost all market segments. These displays can be found in MS-DOS-compatible laptop computers, specialized computers and terminals, medical equipment, test instrumentation, process-control instrumentation and a host of military hardware, and sunlight-legible avionic displays. This mix of applications has come in part because of the strong CRT like appearance of a TFEL display.

8.4 Future possibilities

The electroluminescent display- though very thin and truly solid state displays with a light weight, the cost is high due to the complexities in production, complexity in driving circuits due to high driving voltage, small range of allowed over voltage and small margin of fabrication tolerances. The EL flat panel which is now commercially available is only monochrome display. Many of the problems to be overcome are now being tackled by researchers in industry and R & D. Cherry Corporation is introducing a thick film, direct-current EL technology that promises much lower costs, than thin film EL display. The recent advances in matrix addressing system, in which incorporation of

additional components at each picture element represents the increase in complexity of driving circuits. The fabrication of TETs at present is not fully developed. But the recent progress with laser annealed polysilicon films performing nearly as well as conventional MOS FETs may result in breakthrough in the field of driving circuits. Also many advancement have been made to reduce the driving voltage of the EL devices.

The most striking and present interest of EL technologists is the full colour display. Full colour seems to be a success now for TFEL displays. Two colour TFEL prototypes have been produced by Planar Systems Inc. Exciting progress is also being made by Electronics Department of Tottori University. This group have developed two colour stacked phosphors embedded with filters to add third primary colour for the full colour spectrum. In the immediate future these technological problems will be solved then AC TFEL with its superior optical performance and suitable physical characteristics such as flatness and light weight will secure the major share of flat panel display market.

REFERENCES

- [1] G Destriau; J.Chem.Phys., 33(1936) 587.
- [2] H F Ivey; Advances in Electronics and Electron Physics, Electroluminescence and related effects, (Academic Press, New York, 1963).
- [3] T Inoguchi and S Mito; Topics in Applied Physics Vol. 17, Electroluminescence, Ed. J I Pankove, (Springer-Verlag, Berlin, Hedelberg, New York, 1977) p. 197.
- [4] A Vecht; J.Vac.Sci.Technol., 10(1973) 789.
- [5] G Z Zhong and F J Bryant, Solid State Commun., 39(1981) 907.
- [6] H Onishi, N Sakuma, K Ieyasu and Y Hamakawa; J.Electro.Chem.Soc., 130(1983) 2115.
- [7] M G Clark; Proc. 9th Int. Vacuum Congr. and 5th Int.Conf.Solid Surfaces, Madrid, 1983, p.499.
- [8] K L Chopra; Thin film phenomena, (Robert E. Krieger Publishing Co., New York, 1979) p.19.
- [9] P J Wright and B Cockayne; J.Cryst.Growth, 59(1982) 148.

- [10] P J Wright, B Cockayne, A F Cattell, P J Oean,
A D Pitt and G W Blackmore, *J.Cryst.Growth*,
59(1982) 155.
- [11] T Suntola, J Antson, A Pakkala and S Lindfors;
SID 80 Digest, 11(1980) 108.
- [12] V P Tanninen, M Oikkonen and T Tuomi; *Thin Solid
Films*, 109(1983) 283.
- [13] J A Lahtinen, A Lu, T Tuomi and M Tammenmaa;
J.Appl.Phys., 58(1985) 1851.
- [14] P J Oean; *Phys.Stat.Sol.*, A 81(1984) 625.
- [15] O Theis, H Oppalzer, G Ebbinghaus and S Schild;
J.Cryst.Growth, 63(1983)47.
- [16] M Oikkonen, M Blomberg, T Toumi and M Tammenmaa;
Thin Solid Films, 124(1985) 317.
- [17] D Theis; *Phys.Stat.Sol.*, A 81(1984) 647.
- [18] T R N Kutty; *Thin Solid Films*, 127(1985) 223.
- [19] J Ohwaki and O Kogure; *Jpn.J.Appl.Phys.*, 23(1984)
1649.
- [20] W E Howard; *Proc. SID*, 18(1977) 119.

- [21] J Ohwaki, H Kozawaguchi and B Tsujiyama;
Jpn.J.Appl.Phys., 22(1983) 1133.
- [22] H Kozawaguchi, B Tsujiyama, K Murase; Jpn.J.Appl.
Phys., 21(1982) 1028.
- [23] K Okamoto, Y Nasu and Y Hamakawa; IEEE Trans.
on Electron Devices ED 28(1981) 698.
- [24] Shin-Ichi Ohta, T Tadokoro, S Satou and M Yokoyama;
Thin Solid Films, 162(1988) 73.
- [25] H Nanto, T Minami, S Murakami and S Takata;
Thin Solid Films, 164(1988) 363.
- [26] Y L Hua, M C Petty, G G Roberts, M M Ahmad,
H M Yates, N J Manug and J O Williams;
Electron Lett., 23(1987) 231.
- [27] T Santola; SID 81 Digest, Los Angeles, (1981) p.20.
- [28] R Mach and G D Muller; Phys.Stata Sol., A 81
(1984) 609.
- [29] R Mach, G O Muller and G Shultz ; Phys.Stat.
Sol., A 81(1984) 723.
- [30] R Tornquist; J.Cryst.Growth, 72(1985) 538.
- [31] M Leskela and M Tammenmaa; Materials Chemistry and
Physics, 16(1987) 349.

- [32] T Matsuoka, J Kuwata, Y Fujita and A Abe;
J.Electrochem.Soc., Vol. 135(1988) 1836.
- [33] D C Krupka and D M Mahoney; J.Appl.Phys.,
43(1972) 2314.
- [34] H Kobayashi, S Tanaka, V Shanker, M Shiiki,
T Kunou, J Mita and H Sasakura; Phys.Stat.
Sol., A 88(1985) 713.
- [35] H Kobayashi, S Tanaka, T Kunou, M Shiiki and
H Sasakura; Proc. SID, 25/3(1984) 187.
- [36] A Mikami, T Ogura, K Tanaka, K Taniguchi,
M Yoshida and S Nakajima; J.Appl.Phys.,
61(1987) 3028.
- [37] D Kahng; Appl.Phys.Lett., 13(1968) 210.
- [38] W Lehmann; J.Lumin., 5(1972) 87.
- [39] A Vecht, M Waite, M H Highton and R Ellis;
J. Lumin., 24/25 (1981) 917.
- [40] W A Barrow, R E Coover and C W King;
SID, 84 Digest, (1984) 249.
- [41] V Shanker, S Tanaka, M Shiiki, H Deguchi,
H Kobayashi and H Sasakura; Appl.Phys.
Lett., 45(1984) 960.

- [42] S Tanaka, V Shanker, M Shiiki, H Deguchi and H Kobayashi; Proc. SID Digest, 26/4(1985) 255.
- [43] M Yoshida, K Tanaka, K Taniguchi, T Yamashita, Y Kakihara and T Inoguchi; SID,80 Digest, (1980) 106.
- [44] S Tanaka, Y Mikami, J Nishiura, S Ohshio, H Yoshiyama and H Kobayashi; Proc. of SID, 28/4 (1987) 357.
- [45] S Tanaka, H Yoshiyama, J Nishiura, S Ohshio, H Kawakami and H Kobayashi; Proc. of SID, 29/4 (1988) 305.
- [46] Y A Ono, M Fuyama, K Onisawa, K Taguchi and H Kawakami; J.Lumin., 40(1988) 796.
- [47] J Nishiura, S Ohshio, H Hawakami; Appl.Phys.Lett., 51(1987) 661.
- [48] R S Crandall; Appl.Phys.Lett., 50(1987) 641.
- [49] R S Crandall; Appl.Phys.Lett., 50(1987) 551.
- [50] V P Singh, D C Morton and M R Miller; IEEE Trans. on Electron Devices, ED 35(1988) 38.
- [51] Y Kageyama, K Kameyama and S Oseto; SID 86 Digest, (1986) p. 33.
- [52] A K Bindra; Electronics, 22(1984) p. 113.
- [53] A R Tebo; Laser focus/Electro-optics, March(1985) 46.
- [54] T Manuel; Electronics, 28(1987) p. 55.
- [55] E Schlam; Laser focus/Electro-optics, May(1988) p.155.